A HISTONE DEACETYLASE HOS3 ESTABLISHES CROSSLINK BETWEEN THE MORPHOGENESIS AND SPINDLE POSITIONING CHECKPOINTS

A Dissertation

Presented to the Faculty of the Graduate School

of Cornell University

In Partial Fulfillment of the Requirements for the Degree of

Doctor of Philosophy

by

Mengqiao Wang

January 2013

A HISTONE DEACETYLASE HOS3 ESTABLISHES CROSSLINK BETWEEN THE MORPHOGENESIS AND SPINDLE POSITIONING CHECKPOINTS

Mengqiao Wang, Ph.D.

Cornell University 2013

An increasing number of cellular activities are under the regulation of lysine acetylation. This post-translational modification (PTM) is reversibly catalyzed by histone acetyltransferases (HATs) and histone deacetylases (HDACs). Targeting these enzymes to different cellular compartments is instrumental in defining their substrates and functions *in vivo*. Here we showed that a *S. cerevisiae* HDAC Hos3 is asymmetrically targeted to the daughter side of the bud neck and to the daughter spindle pole body (SPB). Screening for mutants defective in targeting Hos3 to the bud neck identified septins and members of the morphogenesis checkpoint, pinpointing Hsl7 as the protein that recruits Hos3 to the bud neck.

When spindle orientation defect is present, Hos3 is loaded symmetrically onto both SPBs. Importantly, although the neck localization of Hos3 is dispensable for a number of cellular activities, it is required for the response of Hos3 to spindle misorientation. When symmetrically associated with both SPBs, Hos3 may function as a spindle position checkpoint (SPOC) component to inhibit mitotic exit. The results together reveal how a uniquely targeted HDAC Hos3 functions as crosslink between the morphogenesis checkpoint and the SPOC. On a more general perspective, this study substantiates an important role of lysine acetylation in monitoring spindle orientation and regulating the cell cycle.

BIOGRAPHICAL SKETCH

Mengqiao Wang was born in the City of Chengdu, Sichuan Province, PR China in 1984. His ancestry is from Yaan, Sichuan. After growing up in Chengdu as a kid and teenager, he became very interested in mathematics and natural sciences. Mengqiao graduated from Chengdu Foreign Languages School in 2002 and was among the top students of National College Entrance Examination in Sichuan Province that year. As a result, he was admitted to the University of Science and Technology of China (USTC) located in the City of Hefei, Anhui Province. After four years of industrious study, Mengqiao graduated with a Bachelor of Science degree from USTC in 2006. During his time in USTC, he was honorably awarded the Zhang Zhongzhi Memorial Scholarship. Mengqiao was then accepted into the Biochemistry, Molecular, and Cell Biology (BMCB) program at Cornell University. Starting from the summer of 2006, he moved to the United States to pursue graduate school. After a year of rotations, Mengqiao was accepted into the Collins lab and aimed to investigate a *S. cerevisiae* histone deacetylase Hos3 for his Ph.D. study. After working for five years in the Collins lab, he submitted his research results to a scientific journal for review. During his time at Cornell, Mengqiao was honorably awarded the Hsien Wu and Daisy Yen Wu Scholarship. He is planning to conduct postdoctoral research in the United States after completing graduate school at Cornell University.

Dedicated to

my late grandfather Ti-Chiang Wang (王體江) and late grandmother Tsai-Feng Peng (彭采蕸). Your spirits and blesses are with me everyday.

Also dedicated to

my father Xisheng Wang (王希胜) and mother Na Li (李娜).

I always love you and we are forever a family.

ACKNOWLEDGMENTS

Every story has an ending and so is graduate school. It is amazing how long I have stayed in graduate school (six years!) but it is also equally shocking how fast these years just flew by. My journey started in the summer of 2006 after I was honorably admitted into the Biochemsitry, Molecular, and Cell Biology (BMCB) program at Cornell University. My journey is expected to end in the summer of 2012 when I complete the requirements and graduate with a Ph.D. degree. This journey is once-in-a-life-time experience for me: with ups and with downs, with happiness and with stress, with hopes and with doubts, with the knowledge that some day I will finally complete graduate school and with the uncertainty when this “some day” is going to be. Now that this “some day” is truly going to be there, I looked back and realized that this “some day” would never make to a real day if I did not get the help I actually got from many people and institutes. Therefore, I couldn’t thank them enough.

First of all, I want to sincerely thank my Ph.D. advisor Dr. Ruth Collins. I had the fortune to join her lab after a year of rotations, and life spent in the Collins lab made the core of my graduate school training. At the beginning, I worked on a histone deacetylase (HDAC) Hos3 hypothesizing that this protein would function in the regulation of post-Golgi vesicle trafficking. It turned out that the hypothesis was wrong but Ruth was very kind and supportive in allowing me to continue studying Hos3 for its unknown functions. My independent research on Hos3 finally developed into my current Ph.D. project. During this process, Ruth used her funding, resources, and scientific insights in guiding me through all the difficulties and moving the project forward for more and more discoveries. Moreover, on a personal level, she is a devoted

scientist and critical thinker, for which I learned tremendously. She also cares about me and makes all her efforts in helping me achieve my goals. I truly appreciate all the wonderful things she did for me. I couldn't thank her enough and hope she will train more and more young scientists just as the way she did for me.

Next, I want to thank all the past and present members of the Collins lab I had the great fortune to overlap with. I thank Dr. Ian Berke since he initially introduced the idea of studying HDACs. I thank Dr. Peter Rahl for all his devoted training of me during my rotation. I thank Dr. Christopher Heger, Dr. Carol DeRegis, Dr. Catherine Chen, and Dr. David Cragun for all the support I had during my first two years in the Collins lab. Dr. Catherine Chen also provided me with a lot of invaluable assistance in my search for a postdoctoral position. I spent my later three years in the lab primarily with Dr. Duane Hoch and Dr. Fabio Rinaldi for whom I thank for teaching me to grow scientifically. I apologize for not being able to name every one of the Collins lab people due to space limit but they all have my very best wishes for whatever career they plan for the future.

My special committee members Dr. Scott Emr and Dr. Paul Soloway are instrumental in supervising my graduate school progress. Without them, I would not be able to push my project to this far. Besides their scientific excellence, Scott truly taught me about the appropriate attitudes of doing research through his unparalleled passion for science and Paul is the exact person who introduced me into the field of epigenetics and encouraged me ever since. I truly thank both of them. Dr. Maurine Linder, as my Department Chair, also looks after me for my scientific progress and career planning. I thank her a lot.

I always regard the BMCB program as my “home” at Cornell. I sincerely thank my Director of Graduate Studies Dr. Volker Vogt and Dr. Sylvia Lee. Volker always cares a lot about the program, acts like the father of BMCB students, and supports me in whatever way he could. He is just awesome. Sylvia also helped me as needed and she is a nice person. I thank Dr. Jefferey Roberts and Dr. Michael Goldberg for giving me the chance of a very enjoyable rotation in their labs. I also want to thank Diane Colf (BMCB) and Debbie Crane (Molecular Medicine) for countless assistance.

During my time at Cornell, Dr. Chris Stefan, Dr. Yading Ling, Dr. Zachary Via, Dr. Bong-Kwan Han, Kirk Donovan, and Lavanya Sayam all helped me with various experiments or equipments. The lab of Dr. Gary Whittaker is generous to share many resources with me.

I was honorably awarded the Hsien Wu and Daisy Yen Wu Scholarship from Cornell University. Dr. Hsien Wu is the father of biochemistry in China and I feel the unique scientific link between the scholarship and my Chinese heritage. Given such a prestigious scholarship named after him and his wife, I feel truly grateful and view it as lifetime pride.

Graduate school is never easy, and I admit there were times I thought I could not make through. The fact that I did conquer those setbacks is due to all of the support I gained from my friends at Cornell and elsewhere. Dr. Yading Ling, Victor Tse, Lu Huang, Yueting Zhang, Xinwei Wu, Mingxing Li, Dr. Kevin Tang, Dr. Qi Wang, Dr. Jun Cui, Dr. Yong Zhao, and many others I could not name due to space limit are the people who share my happiness and sorrow all the way through. I was very thankful to Yuji Shi who always encourages and supports me. I thank Si Yan a lot for the care and support, and you mean so much to me. On the boat of graduate school, all of them

make sure I stay onboard no matter how many waves come and go. Now I almost reach my destination and thus thank them from the bottom of my heart.

Finally, I want to thank my family most. Being the only kid of my parents, I enjoyed all their nonconditional love and support. However, being the only kid, I spent most of the past six years thousands of miles away from home on the other side of this planet. They sacrificed a lot for me in the hope of helping me to pursue my journey of life but never asked for anything in return. Not truly understanding what research I am working on, they always believe it is not only important for me but also beneficial for the larger society and humanity. It is because of them I come to this world and it is also because of them I get the encouragement to start my journey. As I grow up, I drift farther and farther away from home but there is always a beacon of family lighting in my heart to guide me through the unknown. Therefore, I did not get lost and I actually survived and thrived in the graduate school of Cornell University. I dedicate my efforts and achievements to my family. Dad and Mom, I thank you for everything! I love you forever!

TABLE OF CONTENTS

Biographical Sketch……(iv)

Dedication……..(v)

Acknowledgements……(vi)

Table of Contents……....(x)

List of Figures……...(xii)

List of Tables……...(xvi)

Chapter 1 Introduction……..……..1

Introduction……1

References……29

Chapter 2 Hos3 Is a Uniquely Targeted HDAC……...35

Introduction……...35

Materials and Methods……36

Results……..43

Discussion……78

References……80

Chapter 3 Screening of Mutants Defective in Hos3 Bud Neck Targeting…….82

Introduction……...82

Materials and Methods……84

Results……..88

Discussion……..108

References……110

Chapter 4 Hsl7 of the Morphogenesis Checkpoint Recruits Hos3 to the Bud Neck……...112

Introduction……112

Materials and Methods……...113

Results……119

Discussion……..164

References……166

Chapter 5 Neck-localization Facilitates Hos3 to Function as a Spindle Position Checkpoint (SPOC) Component……...168

Introduction……168

Materials and Methods……...169

Results……173

Discussion……..210

References……212

Chapter 6 Discussion of the Functions of Hos3 as an HDAC……..213

Introduction……213

Materials and Methods……...214

Discussion……..216

References……231

LIST OF FIGURES

Figure 1.1. Proteins can be regulated by various PTMs……3

Figure 1.2. Lysine acetylation as a reversible PTM……9

Figure 1.3. The cell cycle of budding yeast……...18

Figure 1.4. Assembly of proteins at the bud neck……21

Figure 1.5. Regulation of spindle orientation and mitotic exit…….25

Figure 2.1. Localization of HDACs in budding yeast……44

Figure 2.2. Unique targeting of Hos3……..48

Figure 2.3. Hos3 is asymmetrically targeted to the daughter side of the bud neck……..51

Figure 2.4. Hos3 is asymmetrically targeted to the daughter SPB in a cell-cycle-dependent manner……..54

Figure 2.5. Sequence analysis of Hos3……57

Figure 2.6. Sequence alignment of *A. aeolicus* AcuC1 and *S. cerevisiae* class I and II HDACs……..59

Figure 2.7. Chimera assay to test Hos3 HDAC activity *in vivo*……..63

Figure 2.8. Hos3 could deacetylate histones within the heterochromatin in the context of a chimera……..67

Figure 2.9. Mapping regions required for the unique targeting of Hos3……71

Figure 2.10. Localization features of certain Hos3 truncated alleles…….76

Figure 3.1. Hos3 neck localization is intact after nocodazole or latrunculin-B

treatment…….89
Figure 3.2. Hos3 colocalizes with septins……..91
Figure 3.3. Hos3 localization at the bud neck is dependent on septins…….94
Figure 3.4. A microscopy-based phenotypic screening for genes required for Hos3 neck targeting……101
Figure 3.5. Four genes are required for Hos3 neck targeting……..103
Figure 3.6. Hits from the screening are specific candidates…….106
Figure 4.1. Septins and the four hit proteins localize to the bud neck……120
Figure 4.2. The morphogenesis checkpoint prevents mitotic entry in the absence of budding…….124
Figure 4.3. Targeting Hos3 to the bud neck is upstream of CDK regulation……..129
Figure 4.4. Targeting Hos3 to the bud neck is downstream of Elm1 and Gin4……132
Figure 4.5. Reciprocal localization would reveal proteins that directly recruit Hos3 to the bud neck……..137
Figure 4.6. Reciprocal localization profile of Hos3 and its neck-targeting regulators……..140
Figure 4.7. Summary of the reciprocal localization profile……146
Figure 4.8. Neck-localized Hsl7 is required to recruit Hos3 to the bud neck……150
Figure 4.9. Hsl7 interacts with and recruits Hos3……...153

Figure 4.10. Hsl1 determines Hos3 asymmetry at the bud neck……156
Figure 4.11. Investigating the function of neck-localized Hos3 ……...160
Figure 5.1. Hos3 is loaded onto both SPBs in *dyn1*Δ cells with spindle misorientation……...174
Figure 5.2. Hos3 is loaded onto both SPBs when cells undergo spindle misorientation……...176
Figure 5.3. Hos3 fails to be loaded onto both SPBs in *hsl7*Δ cells in response to spindle orientation defect……...179
Figure 5.4. Known components of the SPOC are loaded onto both SPBs in response to spindle misorientation…….....181
Figure 5.5. Hos3 functions as an HDAC to arrest cells with misaligned spindle……...183
Figure 5.6. Overexpression leads to constitutive association of Hos3 with the SPBs……..186
Figure 5.7. Overexpression of the known SPOC components and Hos3 leads to cellular growth defect……..188
Figure 5.8. The known SPOC components and Hos3 are mutually dispensable for their overexpression effect……...191
Figure 5.9. The known SPOC components and Hos3 are mutually dispensable for their targeting onto the SPBs…….....193
Figure 5.10. Overexpression of Hos3 leads to cellular growth defect in *hsl7*Δ cells…….....195
Figure 5.11. Hos3 is degraded in a proteasome-dependent manner throughout

the cell cycle.....197

Figure 5.12. Two models for the mechanism of loading Hos3 onto the SPBs. 201

Figure 5.13. Overexpression leads to constitutive association of Hos3 with the SPBs.....204

Figure 5.14. Hos3(*N*Δ) does not cause cellular growth defect in the wild-type cells.....207

Figure 5.15. Loss of the NH_2-terminus renders Hos3 HDAC-inactive…….....209

Figure 6.1. Truncated Hos3 is likely imported into the mitochondria……..226

Figure 6.2. Localization of truncated Hos3 in mitochondria mutants……..229

LIST OF TABLES

Table 2.1. Yeast strains used in Chapter 2……40

Table 2.2. Plasmids used in Chapter 2……..41

Table 3.1. Yeast strains used in Chapter 3……86

Table 3.2. Plasmids used in Chapter 3……..……87

Table 3.3. List of genes included in the screening for defective targeting of Hos3 to the bud neck……99

Table 4.1. Yeast strains used in Chapter 4……116

Table 4.2. Plasmids used in Chapter 4……118

Table 5.1. Yeast strains used in Chapter 5……171

Table 5.2. Plasmids used in Chapter 5……172

Table 6.1. Yeast strains used in Chapter 6……215

Table 6.2. Plasmids used in Chapter 6……215

CHAPTER 1

INTRODUCTION

INTRODUCTION

Lysine acetylation as a post-translational modification

Cells are constituded of various types of biological components such as polynucleotides (DNA and RNA), proteins, lipids, metabolites, and small molecules. Their fine-tuned regulation within the cell is essential for appropriate cellular growth and adaptation. Proteins are synthesized as long chains of polypeptides. Apparently, whether a specific protein is synthesized or not is an instrumental cellular decision. Meanwhile, a lot of proteins are actively or conditionally turned over *in vivo* to finely adjust their homeostasis. Together, cells are under the constant regulation for their proteosome at transcriptional, post-trancriptional, translational, and degradational levels (Vogel and Marcotte, 2012).

However, synthesis and degradation of proteins are time- and energy-consuming processes. In comparison, post-translational modifications (PTMs) confer synthesized proteins with the addition or removal of various chemical groups or polypeptide moiety. Without drasticically changing the basic levels of proteins, PTMs happen relatively much faster (although depending on the kinetics of the responsible enzymes), require less energy input, are in most cases reversible, and could potentially crosstalk with each other. Many types

of PTMs have been discovered for proteins (Figure 1.1). These PTMs could each have significant consequence to the modified proteins. Protein phosphorylation is widely involved in cellular signaling. Upon ligand binding, membrane-anchored epidermal growth factor receptor (EGFR) dimerizes and activates its intrinsic kinase activity. As a result, the autophosphorylation of EGFR in its cytoplasmic portion initiates a series of downstream signaling events to trigger DNA synthesis and cell proliferation (Herbst, 2004). *N-alpha*-acetylation of proteins is regulated by the availability of acetyl-coenzyme A and confers cellular sensitivity to apoptotic signals (Yi et al., 2011). *N-epsilon*-acetylation, or better known as lysine acetylation since it modifies internal lysine residues, is commonly observed on chromatin modification proteins and metabolic enzymes suggesting a significant impact of lysine acetylation in gene expression and metabolic regulation (Yang and Seto, 2008). Amazingly, every enzyme involved in intermediate metabolism such as glycolysis, the urea cycle, and glycogen metabolism is acetylated in human liver tissue (Zhao et al., 2010). Similarly, approximately 90% of the enzymes participating in central metabolism are acetylated in prokaryotes *S. enterica* revealing an extensive role of lysine acetylation in metabolic control (Wang et al., 2010). With regards to protein methylation, either lysine or arginine can be methylated. Lysine can be methylated once, twice, or three times to end up as mono-, di-, or tri-methylated lysine. In comparison, arginine can be methylated once or twice. Histone tails could be dynamically modified by methylation as an important mechanism of transcriptional regulation (Paik et al., 2007).

Figure 1.1

PTM	Modified residue	Responsible enzymes
phosphorylation	serine, threonine, tyrosine	kinase; phosphatase
N-alpha-acetylation	Met^{ATG}	N-terminal acetyltransferase
N-epsilon-acetylation	lysine	histone acetyltransferase (HAT); histone deacetylase (HDAC)
methylation	lysine, arginine	methyltransferase; demethylase
ubiquitination	lysine	ubiquitin ligase; deubiquitinating enzyme (DUB)
SUMOylation	lysine	SUMO ligase; SUMO protease
palmitoylation	cysteine, serine, threonine	palmitoyl acyltransferase; palmitoyl thioesterase

Figure 1.1. Proteins can be regulated by various PTMs

A selected number of PTMs were respectively summarized for their preference towards modified residues and also for their responsible enzymes.

Ubiquitination, instead of adding a small chemical moiety to lysine, covalently links a 76-amino-acid polypetides called ubiquitin to lysine residues. Polyubiquitination through K48-linked ubiquitins targets proteins for proteolytic degradation, an instrumental mechanism to adjust protein homeostasis and conditionally clear unwanted proteins (Kerscher et al., 2006). Similar to ubiquitination, SUMOylation covalently adds a family of polypeptides (called SUMO proteins) and is revealed in diverse cellular processes such as gene expression and cell cycle control (Hay, 2005). Another PTM called palmitoylation acts predominantly on membrane proteins. Covalent attachment of palmitic acid to cysteines enhances the hydrophobicity of membrane proteins and thus contributes to their membrane association (Smotrys and Linder, 2004). Apart from these listed PTMs that are more commonly known and better studied, there are far more PTMs present and ready to be better characterized (eg. prenylation, acylation, neddylation, citrullination, succinylation, ADP-ribosylation, glycosylation etc.) (Walsh et al., 2005).

A protein can be modified by multiple PTMs thus providing these different PTMs the opportunity to crosstalk with each other. For example, lysine acetylation usually couples with arginine demethylation during the process of transcriptional activation (Jenuwein and Allis, 2001). Given that histone tails are diversely modified by various PTMs and each PTM could have its own impact, the exact output of all of these PTMs should undoubtedly be the combined effect of the crosstalk. Such “code” of crosstalk also applies to p53 (potentially to be phosphorylated, acetylated, ubiquitinated etc.) and

other proteins that are under the regulation of diverse PTMs (Yang and Seto, 2008). On another perspective, one residue could be modified by multiple PTMs but with regards to this particular residue, these PTMs are mutually exclusive. One such residue is lysine which can be methylated (mono-, di-, and tri-), acetylated, ubiquitinated, SUMOylated, biotinylated etc. When a defined lysine residue is modified by one PTM, the presence of this modification excludes the possibility for this lysine residue to undergo other PTMs. Such exclusion together with the crosstalk tremendously adds to the biological dimensions of the PTMs. Meanwhile, cells evolutionarily evolve to develop many recognition domains for certain PTMs. SH2 domain specifically recognizes phosphorylated-tyrosine (Pawson et al., 2001). The bromodomain and chromodomain respectively binds to acetylated-lysine and methylated-lysine (Mujtaba et al., 2007; Jacobs and Khorasanizadeh, 2002). As a result, proteins containing such recognition domains are ready to respond to the corresponding PTMs.

In accordance with the large number of proteins that are post-translationally modified and the complexity of these PTMs, a large number of genes in the genome from prokaryotes to eukaryotes encode enzymes responsible for the PTMs of the proteosome. As PTMs confer an efficient way to change protein property transiently and conditionally, such changes need to be reversed when the previous unmodified state is preferred. For example, when nutrients are available, upon ligand binding and receptor dimerization, EGFR becomes autophosphorylated to mediate downstream signaling events

(Herbst, 2004). However, once nutrients are significantly consumed, the environmental conditions and cellular states become unfavorable for cellular proliferation. This is executed through the dephosphorylation of phosphorylated EGFR by protein tyrosine phosphatases to antagonize the previous phosphorylation and thus suppress EGFR signaling (Tiganis, 2002). Therefore, the majority of the commonly known PTMs are reversible modifications. For proteins regulated by reversible PTMs, the post-translational modification status of each protein is a result of the dynamic balance between the forward modification and the reverse de-modification. Enzymes responsible for the listed PTMs are annotated (Figure 1.1).

Of the many PTMs, I am particularly interested in *N-epsilon*-acetylation, or lysine acetylation. As discussed, acetylation of the *epsilon*-amino group of lysine residues is a commonly observed PTM. Lysine acetylation could have many biological effects on the modified proteins. Upon lysine acetylation, the positive charge of the unmodified lysine becomes neutralized. This as a result could change the profile of protein-protein interactions or protein-DNA or RNA interactions. Moreover, acetylated lysine creates a docking site for proteins with defined motifs such as the bromodomains. Even more complicatedly, acetylation of certain lysine prevents other PTMs of this specific lysine residue and could allow itself to potentially crosstalk with other PTMs of the protein. As a consequence, lysine acetylation is an instrumental PTM of which the molecular details and the biological effects are yet to be fully understood.

Core histones were the first proteins discovered with lysine acetylation (Allfrey et al., 1964). A potential link between histone acetylation and activation of RNA synthesis was even noticed then (Allfrey et al., 1964). Besides histones, nonhistones were also discovered acetylated. Acetylation of alpha-tubulin significantly increases its stability (L'Hernault and Rosenbaum, 1985). Hepatocyte nuclear factor-4 (HNF-4), a member of the nuclear hormone receptor family, is acetylated at multiple sites within its nuclear localization motif, and such acetylation is crucial for the nuclear retention of HNF-4 (Soutoglou et al., 2000). As time goes by, an increasing number of proteins, the majority of them nuclear, were found acetylated (Dokmanovic et al., 2007). With the development of modern mass-spectrometry technology, identification of novel acetylated lysine sites and acetylated proteins has entered the proteomic-scale stage. In mammalian cells, 388 lysine acetylation sites were discovered in 195 proteins (Kim et al., 2006). In just three years, such numbers were increased by almost ten fold given that 3600 lysine acetylation sites were recognized in 1750 proteins (Choudhary et al., 2009). Since such proteomic studies are far from saturation of the whole acetylosome, it should be reasonably inferred that more acetylation sites and more acetylated proteins are to be discovered in the future. In summary, lysine acetylation is a widely present PTM *in vivo*.

Given that histones were the first and for a certain period of time the only proteins discovered to undergo lysine acetylation, the enzymes catalyzing the addition or removal of the acetyl group to or from the lysine residues are

named as histone acetyltransferases (HATs) and histone deacetylases (HDACs). HATs and HDACs antagonize each other functionally to execute the action of reversible lysine acetylation (Figure 1.2A). While lysine acetylation was discovered over four decades ago, the search for enzymes responsible for this reversible PTM was not successful until the mid-90s of the 20th century. The Allis group cloned the first histone acetyltransferase HAT A from *Tetrahymena* and found it has striking sequence homology to yeast transcriptional adaptor Gcn5 (Brownell et al., 1996). They also demonstrated that Gcn5 possesses HAT activity (Brownell et al., 1996). Meanwhile, the Schreiber group cloned a histone deacetylase catalytic subunit (HD1) from human Jurkat T cell library and discovered that it contains HDAC activity (Taunton et al., 1996). Moreover, HD1 displays significant sequence homology to yeast transcriptional repressor Rpd3, which has been confirmed as an HDAC itself (Taunton et al., 1996; Rundlett et al., 1996). With Gcn5 as the first HAT and Rpd3 as the first HDAC identified in *S. cerevisiae*, other HATs and HDACs have been revealed based on sequence homology. They together become members of the HAT family and the HDAC family proteins.

HDACs

In the scope of lysine acetylation, HDACs are particularly interesting not only because they are biologically essential to reverse the acetylation

Figure 1.2

A

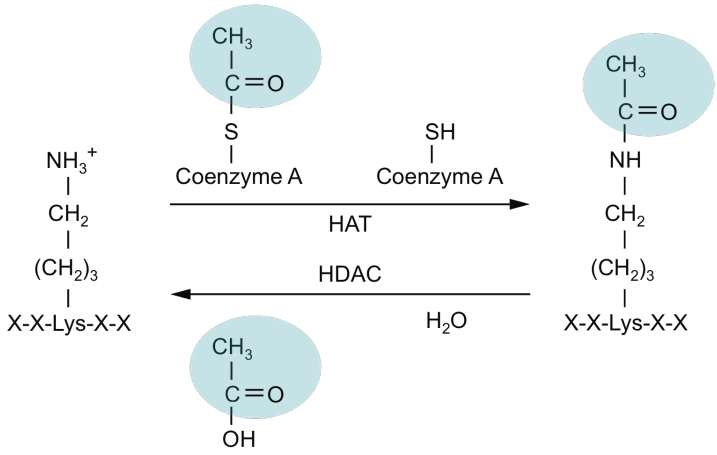

B

Class	HDAC	Essential	NAD+-dependent
I	Rpd3	No	No
I	Hos1	No	No
I	Hos2	No	No
II	Hda1	No	No
II	Hos3	No	No
III	Sir2	No	Yes
III	Hst1	No	Yes
III	Hst2	No	Yes
III	Hst3	No	Yes
III	Hst4	No	Yes

C

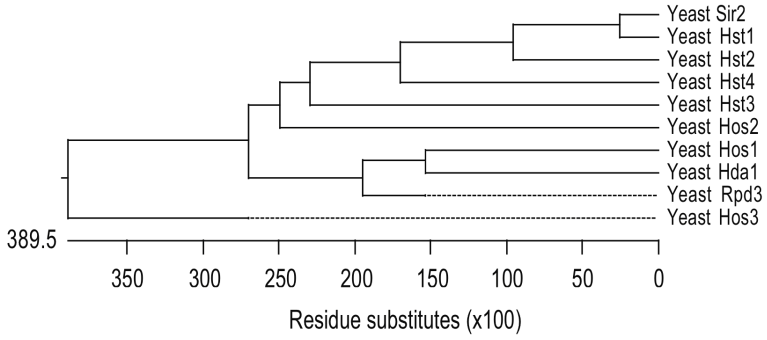

Figure 1.2. Lysine acetylation as a reversible PTM

A. Scheme depicts the reversible lysine acetylation and deacetylation. Acetylation of internal lysine residue is catalyzed by histone acetyltransferase (HAT) using an acetyl-moiety from acetyl-coenzyme A. Deacetylation of acetyl-lysine is catalyzed by histone deacetylase (HDAC) as a hydrolysis reaction to produce acetate as a byproduct.

B. Ten HDACs in *S. cerevisiae* are categorized into three classes. All of these HDACs are nonessential. In comparison to class I and II, class III Sir2-related HDACs are nicotinamide-adenine-dinucleotide (NAD^+)-dependent.

C. The amino acid sequences of all ten *S. cerevisiae* HDACs are aligned by Clustal-W and analyzed for phylogenetic tree by MegAlign. The coordinate represents the degree of residue substitution in sequence alignment.

modification, but more importantly because they are abnormally expressed or regulated in many human diseases such as neurodegeneration and cancers (Bolden et al., 2006). Therefore, reversible lysine acetylation plays important roles in the integrity of cellular activities, and accordingly the HDAC inhibitors are being actively tested as promising drugs for diseases related to the hypoacetylation of certain proteins caused by either dysfunction of the HAT or overexpression or overactivation of the HDAC (Bolden et al., 2006; Garber, 2007).

For the model organism of *S. cerevisiae*, a total of ten HDAC genes are categorized into three classes based on sequence homology and cofactor requirement: class I (*RPD3*, *HOS1*, and *HOS2*), class II (*HDA1* and *HOS3*), and class III (*SIR2*, *HST1*, *HST2*, *HST3*, and *HST4*) (Figure 1.2B) (Ekwall, 2005). All of these ten HDACs are nonessential. Class I and II HDACs catalyze lysine deacetylation through straightforward hydrolysis reaction while class III HDACs require nicotinamide-adenine-dinucleotide (NAD^+) as a cofactor for deacetylation. The ten HDACs are homologous and similar in their primary sequences (Figure 1.2C). Noticeably, in my sequence analysis, Hos1 is more related to Hda1 rather than Rpd3 (Figure 1.2C); in comparison, Hos1 was reported to be more homologous to Rpd3 than Hda1 (Ekwall, 2005). Such results likely reflect the minor difference in the algorithms of sequence analysis. The founding members of each class (*RPD3*, *HDA1*, and *SIR2*) have been extensively studied for their functions in processes such as gene expression, DNA damage response, and aging (Keogh et al., 2005; Robert et

al., 2011; Lin et al., 2000). However, little is known about the distribution and substrate specificity of the budding yeast HDACsome. It is imperative to investigate these questions and it is likely that such efforts could reveal novel roles of HDACs.

HDACs likely have a wide range of substrates

Reversible lysine acetylation could have many diverse biological functions. Histones are best studied and understood for their regulation by lysine acetylation. Acetylation of lysine residues within the histone tails neutralizes their positive charge and thus diminishes their electro-interaction with the negatively-charged phosphate groups of DNA backbones. As a result, the nucleosomes are less tightly packed and the relaxed state allows the transcriptional machinery to be appropriately assembled. Therefore, lysine acetylation is generally a transcriptional activation marker while lysine deacetylation is mainly a transcriptional repression marker (Shahbazian and Grunstein, 2007). However, given the complex regulation of histone tails, the exact biological consequence of the acetylation and deacetylation of each lysine is residue-specific (Shahbazian and Grunstein, 2007). Nevertheless, lysine acetylation of histones as crafted by the action of HATs and HDACs is a crucial part of the epigenetic regulation known as the histone code (Strahl and Allis, 2000).

As mentioned, a historical consequence of histones as the first

identified substrates of enzymes responsible for reversible lysine acetylation is that the acetyltransferases and deacetylases are termed as histone acetyltransferases (HATs) and histone deacetylases (HDACs). However, in recent years, there has been a growing appreciation of the presence of lysine acetylation and deacetylation in nonhistone proteins, both nuclear and nonnuclear, suggesting a much broader role of this PTM *in vivo* (Kim et al., 2006; Choudhary et al., 2009; Zhao et al., 2010). Accordingly, some researchers have proposed to change the names of HATs and HDACs to lysine acetyltransferases (KATs) and lysine deacetylases (KDACs) to better describe such enzymes. In this study, I chose to use the traditional terms of HATs and HDACs but it has to be emphasized again that the HATs and HDACs have a wide range of substrates not just limited to histones.

One prominent example of the acetylation of nonhistones is p53. This tumor suppressor protein is acetylated by coactivator CBP/p300 to markedly stimulate its DNA binding activity, while its deacetylation by an HDAC1-containing complex represses p53-mediated transcriptional activation (Gu and Roeder, 1997; Luo et al., 2000). Another example is that the lysine acetylation of alpha-tubulin stabilizes polymerized microtubules for less dynamics but more rigidity. Actually, alpha-tubulin could be acetylated by multiple HATs: by GCN5 through Myc-nick, a cytoplasmic truncated form of c-Myc, to induce cellular differentiation and by MEC-17 to facilitate neuron function as well as embryonic development (Conacci-Sorrell et al., 2010; Akella et al., 2010). Such studies have broadened our view of lysine acetylation, suggesting that

the assumption that individual HATs or HDACs have histones as their primary *in vivo* substrates may no longer hold validity. Indeed, an increasing number of nonhistones were discovered to be under the regulation of reversible lysine acetylation (Kim et al., 2006; Choudhary et al., 2009).

In comparison to the numerous acetyl-lysine sites identified in a large number of proteins, there are only a few HDAC-encoding genes within the genome (ten in *S. cerevisiae* and eighteen in *H. sapiens*). This implies that each HDAC may have a significant number of physiological substrates than previously thought. However, for the majority of the acetylated proteins identified so far, their relevant HDACs and the biological significance of the deacetylation events remain largely unknown. This raises the importance in investigating HDACs on a more comprehensive scale. Alternatively for clinical perspectives, the fact that any HDAC is likely to have a large number of biological substrates suggests that any HDAC inhibitor is likely to cause hyperacetylation of multiple substrates. Therefore, a better understanding of all HDACs is essential before the mechanism behind the tumor-suppression effects of HDAC inhibitors could be fully elucidated (Bolden et al., 2006).

Investigation of Hos3 as an HDAC

Given the large number of potential substrates, how is each HDAC paired with its particular group of substrates? Partitioning HDACs to different cellular compartments could be an important mechanism in defining their

physiological substrates and functions. In humans, HDAC6 is exclusively cytoplasmic and it deacetylates both alpha-tubulin and cortactin to respectively regulate microtubule stability and actin-dependent cell motility (Hubert et al., 2002; Zhang et al., 2007). HDAC6 also functions as an adaptor to target misfolded protein aggregates to the microtubule motor dynein, and the HDAC6 deacetylase activity is required for the aggresome formation (Kawaguchi et al., 2003). In *S. pombe*, three HDACs (Clr3, Clr6, and Hda1) have distinct subcellular localization and *in vivo* specificity (Bjerling et al., 2002). Where each HDAC is localized has not been fully investigated in *S. cerevisiae*, and I aim to address this question at the beginning of this study.

During my initial efforts to characterize the distribution of *S. cerevisiae* HDACs, I surprisingly discovered that a class II HDAC Hos3 is specifically targeted to the mother-bud neck and to a single focus in the daughter cell. Such unique targeting has never been reported for Hos3 or any HDACs. In addition to its interesting localization, Hos3 appears unique in several aspects. Unlike other HDACs that are functional only in the context of large complexes, Hos3 displays intrinsic deacetylase activity (Carmen et al., 1999). Deletion of *HOS3*, unlike deletion of other HDAC genes, results in little change in the global histone acetylation profile and causes no apparent phenotype (Robyr et al., 2002; Carmen et al., 1999). Contrary to Rpd3 and Hda1, Hos3 is relatively insensitive to a classic HDAC inhibitor tricostatin A (TSA) (Carmen et al., 1999). Upon oxidative stress, Hos3 is involved in mediating the induction of yeast apoptosis (Ahn et al., 2006). It is clear that Hos3 could function as an

HDAC capable of acting on histone tails *in vitro* (Carmen et al., 1999). Moreover, the catalytic domain of Hos3, when engineered to be targeted to the Sir complex sites, could replace Sir2 as a functional HDAC for heterochromatin establishment and maintenance, indicating that Hos3 possesses HDAC activity *in vivo* (Chou et al., 2008). Nevertheless, all of the above results provide fragmented pieces of information rather than a complete picture about Hos3. Most importantly, none of these studies ever looked at the localization of Hos3. Therefore, without noticing the unique targeting of Hos3, all previous studies mistakenly assumed that Hos3 as an HDAC able to act on histones should thus be a nuclear protein. Such failure to take the cellular distribution of Hos3 into consideration could potentially engage serious flaws into the interpretation of its authentic physiological substrates and functions, which remain largely undiscovered at the stage when this study began. I aim to investigate Hos3 as a uniquely targeted HDAC for its functions *in vivo*.

Implication of the involvement of Hos3 in the regulation of the cell cycle

Hos3 was found to localize to the bud neck and as a single focus in the daughter cell. Such distribution displays cell-cycle-dependent features. This potentially suggests a possible role of Hos3 in the regulation of the cell cycle.

Budding yeast cells grow in a polarized direction (Figure 1.3). Throughout the cell cycle, the nuclear envelope does not degrade so the whole nucleus is constantly within a membrane-wrapped compartment. At the

beginning of the cell cycle, G_1 cells are unbudded and there is only one spindle pole body (SPB), the yeast equivalent of the mammalian centrosomes which function as the microtubule organization centers (MTOCs) to nucleate both nuclear and cytoplasmic microtubules (Jaspersen and Winey, 2004). After DNA duplication in S phase, cells start budding in which a daughter cell grows from the mother cell. Then the sole SPB duplicates so that cells now possess two SPBs, one scheduled to stay in the mother cell and the other destined to segregate into the daughter cell. During these stages, the SPBs function to nucleate microtubules (both cytoplasmic microtubules to segregate the nucleus and the nuclear microtubules to facilitate the spindle assembly). As cells enter mitosis, the spindle elongates and the two SPBs are dragged toward the two opposite directions. Given that yeast cells have intrinsic polarity, the spindle needs to be aligned in parallel to the mother-daughter axis so that the nucleus would be segregated evenly between the mother and daughter cells. Thus a correct spindle orientation is required for the appropriate progression of the cell cycle. During this stage, the nuclear microtubules still facilitate the spindle with kinectochore microtubules bipolarly attaching to the kinectochores of chromosomes. By the end of metaphase, all chromosomes are correctly attached and the sister chromatids are bound together through cohesins. Later, the separase cleaves the cohesins to release the stable cohesion and thus allow sister chromatids to be pulled away from each other. The cytoplasmic microtubules are both attached to the SPBs and the cortical protein on the cell cortex. Movement by microtubule-

Figure 1.3

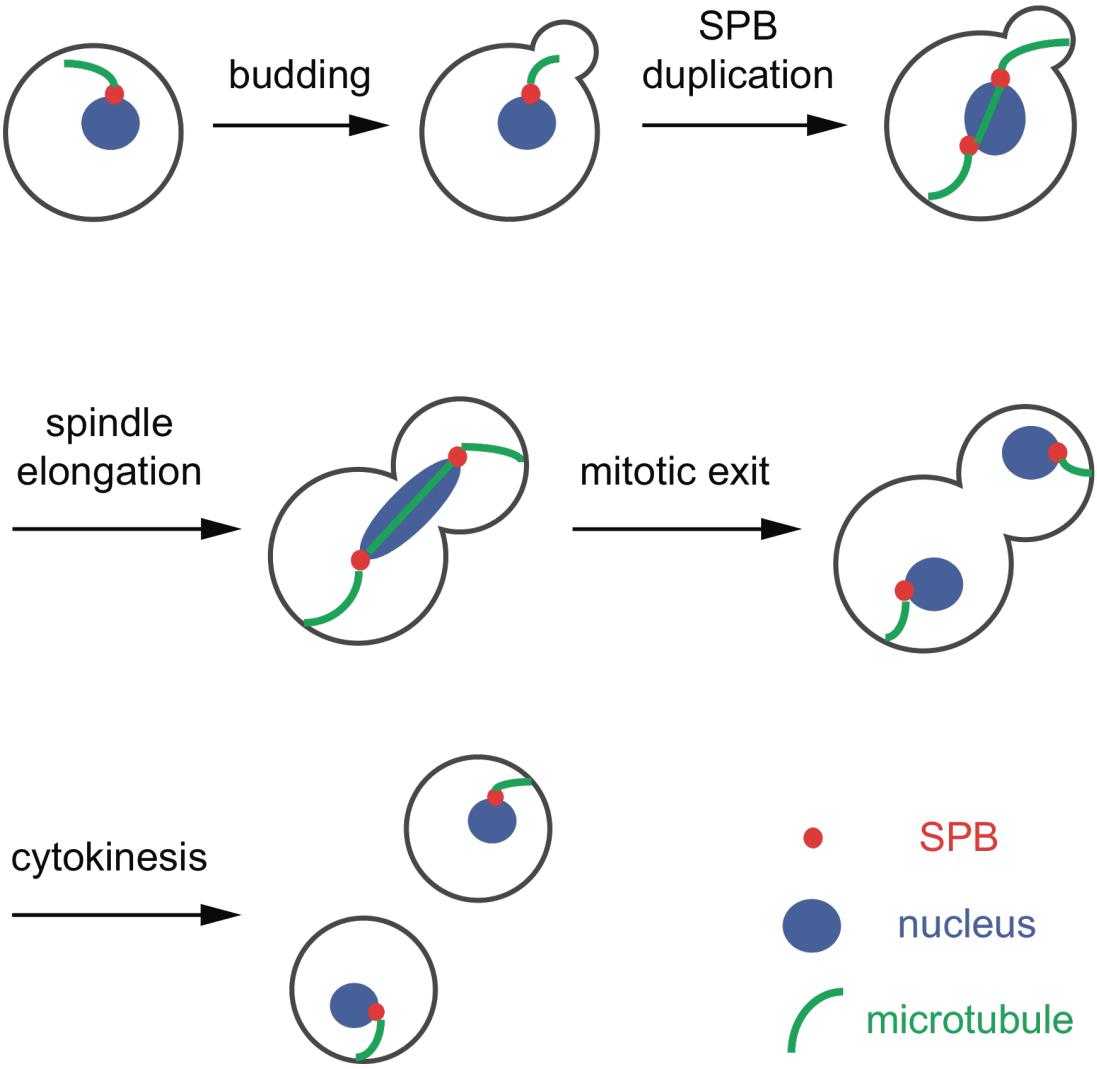

Figure 1.3. The cell cycle of budding yeast

Scheme depicts the morphology of budding yeast cells throughout the cell cycle. Major stages of “budding”, “SPB duplication”, “spindle elongation”, “mitotic exit”, and “cytokinesis” are shown.

dependent dynein motors pulls the SPBs repectively towards the mother and daughter cells. By mitotic exit, the nucleus divides into two new nucleuses respectively located in the mother and daughter cells. The last stage of the cell cycle is cytokinesis during which the mother and daughter cells, each inheriting one copy of the chromosomes, physically dissociate from each other and re-enter the next cell cycle.

Then how exactly could Hos3 be involved in the regulation of the cell cycle? The first landmark of Hos3 localization is the bud neck, a structural site connecting the mother and daughter cells. A certain number of proteins are bud-neck-associated (Cid et al., 2002). Particularly, a conserved family of proteins called septins form higher-order filaments and decorate the bud neck as 10 nm striations when analyzed by electron microscopy (Byers and Goetsch, 1976; Longtine et al., 1996). Given that septin filaments decorate the bud neck as lines of striations, they provide an effective diffusion barrier between the mother and daughter cells. Therefore, the proteins and lipids could not diffuse freely between the mother and the daughter cell cortexes, and their different composition and distribution is important for the asymmetrical cellular divison (Chant, 1999; Neumüller and Knoblich, 2009). Besides the role of diffusion barrier, septins also serve as scaffolds at the bud neck to recruit other bud-neck-associated proteins (Longtine et al., 1996; Oh and Bi, 2011). Septins are themselves membrane-associated (Bertin et al., 2011). In comparison, some bud neck proteins are membrane proteins while others localize to the bud neck due to interaction with other neck-associated

proteins rather than binding directly to the membranes (Gladfelter et al., 2001). Such facts result in a model in which septins function as the foundation for bud-neck-associated proteins to be assembled at the bud neck in a hierarchical manner (Figure 1.4). As expected, bud-neck-associated proteins localize as ring structures (Figure 1.4). Consistent with the role of septins as scaffolds at the bud neck, many neck proteins lose their bud neck localization in septin mutants (Gladfelter et al., 2001). It is important to discover if the neck localization of Hos3 is septins-dependent and which protein is responsible for the direct assembly of Hos3 at the bud neck.

A second unique targeting site for Hos3 is a single focus in the daughter cell. In comparison to the bud neck as a well-defined structure, many cellular machineries or structures could appear as a single focus. Such candidates include the SPBs, the endosomes, the post-Golgi trafficking vesicles, the autophagosome etc. It is essential to first reveal which of these compartments, if any, does the single focus of Hos3 within the daughter cell colocalize with. Such results would uncover the cellular site associated with this uniquely targeted single focus and thus suggest its potential biological roles. Given that all of the cellular structures mentioned above except the SPBs are generally present in multiples within the cell, they are unlikely to exclusively colocalize with the single focus of Hos3. In contrast, the SPBs are of one or two copies (before or after SPB duplication), and there is just one daughter SPB present within the daughter cell. Therefore, the daughter SPB appears as a possible marker for which the single foucs of Hos3 colocalizes

Figure 1.4

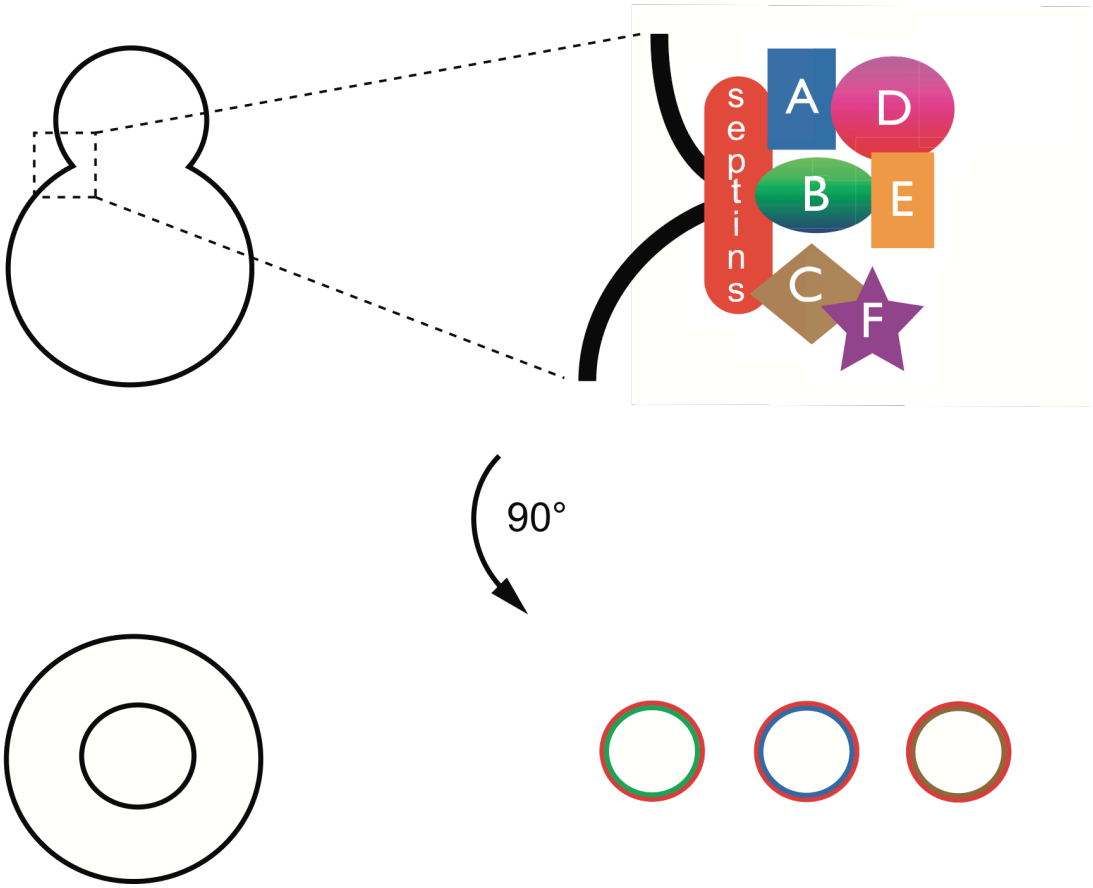

Figure 1.4. Assembly of proteins at the bud neck

An enlarged view of the bud neck demonstrates a hierarchical model for the assembly of bud-neck-associated proteins. Septins are directly bind plasma membranes at the bud neck. Septins then function as scaffolds to recruit protein A, protein B, and protein C. These neck-associated proteins further respectively assemble protein D, protein E, and protein F at the bud neck. A 90° rotation of the cell illustrates that septins and neck-associated proteins localize as ring structures at the bud neck.

with. Nevertheless, such hypotheses need to be tested and the results are instrumental in revealing the biological function relevant to such unique localization.

Regulation of motitic entry and mitotic exit

One of the fundamental questions of the cell cycle is how cells monitor the progression of each cell cycle stage. *S. cerevisiae* cells grow in an asymmetrical manner, and this raises an even more challenging question: how is the cell cycle progression linked to the polarized cellular morphology growth? Two important stages are mitotic entry and mitotic exit.

After DNA synthesis and cyclin activation, cells are ready to enter mitosis to elongate its spindle and prepare for chromosome segregation (Lindqvist et al., 2009). However, before mitotic entry, budding yeast cells have to first grow a bud. The budding event not only permits the growth of the daughter cell, but also defines the direction of the polarized growth as well as the orientation of the mother-daughter axis. Therefore, the morphogenesis and the mitotic entry have to be tightly coupled in the cell cycle (Sakchaisri et al., 2004). If budding somehow fails, mitotic entry should be temporarily prevented to allow cells extra time to adapt to stresses and re-grow a bud. Certain checkpoints are required to monitor and regulate the coupling of the morphogenesis and the mitotic entry.

Once the spindle has elongated and the chromosomes are bipolarly attached by kinectochore microtubules during metaphase, cells are ready to enter anaphase to divide the nucleus and exit mitosis. Given the presence of the asymmetrical cellular growth, the nuclear division has to be specifically orientated to allow for appropriate segregation of chromosomes. The spindle should be aligned in parallel to the mother-daughter axis (Figure 1.5). However, if the machinery involved in aligning the spindle becomes defective, the spindle could be misorientated so that it is certain degrees or even perpendicular to the mother-daughter axis (Figure 1.5). When such defects arise, mitotic exit should be temporarily prevented to allow cells extra time to adapt to stresses and re-align the spindle. If not, progression of the mitotic exit would result in an anucleate daughter cell and a bi-nucleate mother cell, causing a serious failure to evenly segregate the chromosomes (Figure 1.5). Certain checkpoints are required to monitor and regulate the coupling of the spindle orientation and the mitotic exit.

I am very interested in investigating if the potential involvement of uniquely targeted Hos3 in cell cycle control could be through its regulation of mitotic entry and mitotic exit.

Dynein pathway for positioning the spindle

The spindle needs to be correctly orientated for asymmetrical cell division in order to allow correct nuclear division and chromosome

Figure 1.5

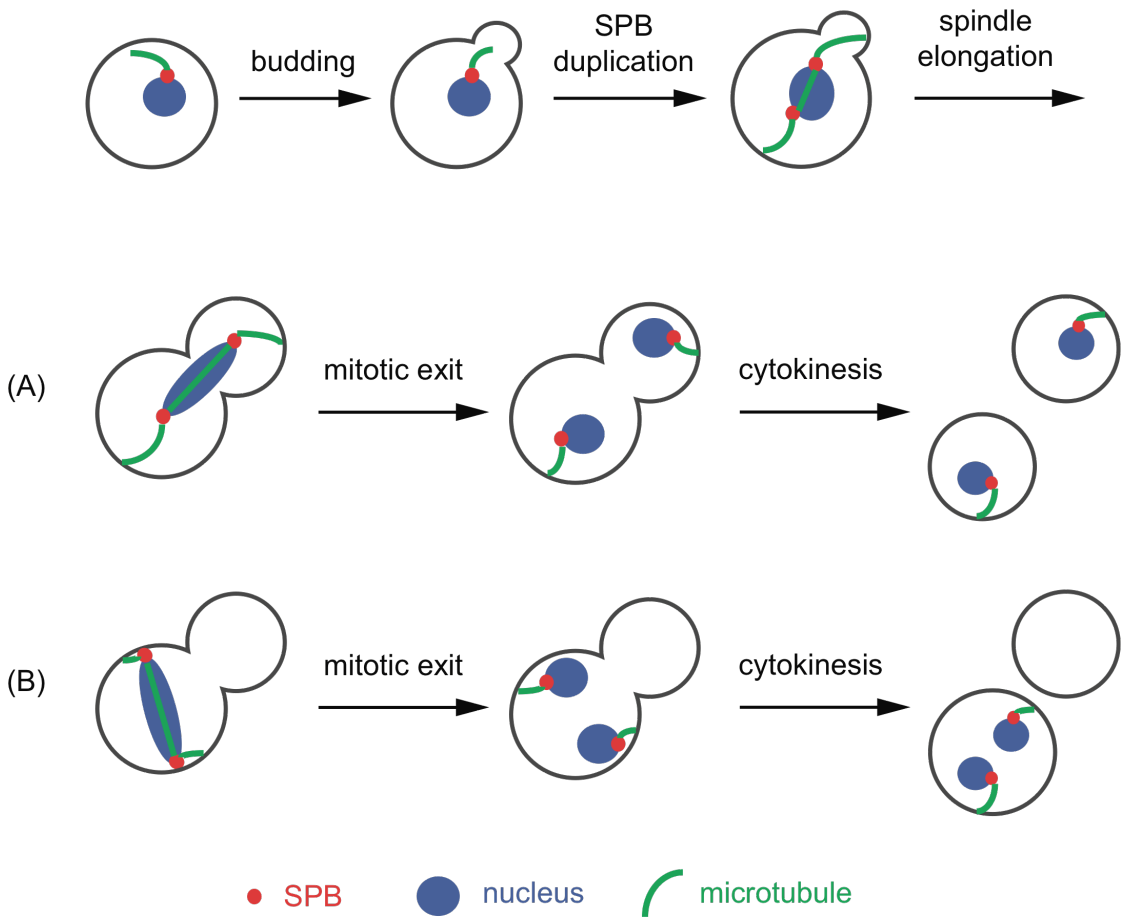
budding
SPB duplication
spindle elongation
(A)
mitotic exit
cytokinesis
(B)
mitotic exit
cytokinesis
SPB
nucleus
microtubule

Figure 1.5. Regulation of spindle orientation and mitotic exit

Scheme depicts the morphology of budding yeast cells throughout the cell cycle. Major stages of “budding”, “SPB duplication”, “spindle elongation”, “mitotic exit”, and “cytokinesis” are shown. Two conditions of spindle orientation are compared. (A) For cells adopting a correct spindle orientation in parallel to the mother-bud axis, the daughter SPB moves out of the mother cell and enters the daughter cell. As the nucleus is divided, cells exit mitosis. After cytokinesis, a mother cell and a daughter cell each inherit one set of chromosomes, and are ready to enter the next cell cycle. (B) For cells undergoing spindle misorientation in which the spindle is aligned almost perpendicular to the mother-bud axis, the daughter SPB does not get the opportunity to enter the daughter cell. Instead, both SPBs stay within the mother cell, and the cytoplasmic microtubules pull the two SPBs towards the opposite directions of the mother cell cortex. As the nucleus is divided, cells exit mitosis. After cytokinesis, the daughter cell becomes anucleate while the mother cell is bi-nucleate. The genetic materials are not correctly and evenly segregated between the two cells.

segregation (Siller and Doe, 2009). One important mechanism to achieve the alignment and positioning of mitotic spindle is the dynein pathway (Moore et al., 2009; Markus and Lee, 2011). Binding of Pac1 and dynactin to dynein motors triggers the dynein-dynactin complex to associate with the cortical anchor protein Num1 (Adames and Cooper, 2000; Lee et al., 2003). Since dynein is loaded onto the plus end of the cytoplasmic microtubules, the plus end is then anchored to the cell cortex. Meanwhile, the minus end of cytoplasmic microtubules is attached to the SPB destined to enter the daughter cell. Dynein motors walk towards the minus end thus generating pulling forces to drag the daughter SPB through the bud neck and into the daughter cell (Adames and Cooper, 2000). The microtubule-dependent dynein pathway is essential for correct spindle orientation so that mutants of this pathway display significantly large number of cells with misaligned spindle (Carminati and Stearns, 1997). It is interesting to test how this pathway might regulate Hos3 localization and its potential function in cell cycle control.

Oveview of the study

In this study, I reported the surprising discovery that Hos3 displays asymmetrical localization to the bud neck and to the daughter spindle pole body (SPB). Screening for mutants defective in targeting Hos3 to the bud neck identified septins and members of the morphogenesis checkpoint, pinpointing Hsl7 as the protein that recruits Hos3 to the bud neck. While Hos3 is

asymmetrically associated with the daughter SPB in a cell-cycle-dependent manner in wild-type cells, when spindle orientation defect is present in certain mutant cells, Hos3 is loaded symmetrically onto both SPBs. Importantly, although neck localization of Hos3 is dispensable for a number of cellular activities, it is required for the response of Hos3 to spindle misorientation. When symmetrically associated with both SPBs, Hos3 may function as a spindle position checkpoint (SPOC) component to inhibit mitotic exit. We also addressed the potential mechanism that confers Hos3 its unique association with the SPBs. The results together reveal how a uniquely targeted HDAC Hos3 functions as crosslink between the morphogenesis checkpoint and the SPOC. On a more general perspective, our study substantiates a role of lysine acetylation in monitoring spindle orientation and regulating mitotic exit.

REFERENCES

Adames, N. R., & Cooper, J. A. (2000). Microtubule interactions with the cell cortex causing nuclear movements in saccharomyces cerevisiae. *The Journal of Cell Biology, 149*(4), 863-874.

Ahn, S., Diaz, R. L., Grunstein, M., & Allis, C. D. (2006). Histone H2B deacetylation at lysine 11 is required for yeast apoptosis induced by phosphorylation of H2B at serine 10. *Molecular Cell, 24*(2), 211-220.

Akella, J. S., Wloga, D., Kim, J., Starostina, N. G., Lyons-Abbott, S., Morrissette, N. S., et al. (2010). MEC-17 is an α-tubulin acetyltransferase. *Nature, 467*(7312), 218-222.

Allfrey, V. G., Faulkner, R., & Mirsky, A. E. (1964). Acetylation and methylation of histones and their possible role in the regulation of RNA synthesis. *Proceedings of the National Academy of Sciences, 51*(5), 786-794.

Bertin, A., McMurray, M. A., Thai, L., Garcia III, G., Votin, V., Grob, P., et al. (2010). Phosphatidylinositol-4,5-bisphosphate promotes budding yeast septin filament assembly and organization. *Journal of Molecular Biology, 404*(4), 711-731.

Bjerling, P., Silverstein, R. A., Thon, G., Caudy, A., Grewal, S., & Ekwall, K. (2002). Functional divergence between histone deacetylases in fission yeast by distinct cellular localization and in vivo specificity. *Molecular and Cellular Biology, 22*(7), 2170-2181.

Bolden, J. E., Peart, M. J., & Johnstone, R. W. (2006). Anticancer activities of histone deacetylase inhibitors. *Nat Rev Drug Discov, 5*(9), 769-784.

Brownell, J. E., Zhou, J., Ranalli, T., Kobayashi, R., Edmondson, D. G., Roth, S. Y., et al. (1996). Tetrahymena histone acetyltransferase A: A homolog to yeast Gcn5p linking histone acetylation to gene activation. *Cell, 84*(6), 843-851.

Byers, B., & Goetsch, L. (1976). A highly ordered ring of membrane-associated filaments in budding yeast. *The Journal of Cell Biology, 69*(3), 717-721.

Carmen, A. A., Griffin, P. R., Calaycay, J. R., Rundlett, S. E., Suka, Y., & Grunstein, M. (1999). Yeast HOS3 forms a novel trichostatin A-insensitive homodimer with intrinsic histone deacetylase activity. *Proceedings of the National Academy of Sciences, 96*(22), 12356-12361.

Carminati, J. L., & Stearns, T. (1997). Microtubules orient the mitotic spindle in yeast through dynein-dependent interactions with the cell cortex. *The Journal of Cell Biology, 138*(3), 629-641.

Chant, J. (1999). Cell polarity in yeast. *Annual Review of Cell and Developmental Biology, 15*(1), 365-391.

Chou, C., Li, Y., & Gartenberg, M. R. (2008). Bypassing Sir2 and O-acetyl-ADP-ribose in transcriptional silencing. *Molecular Cell, 31*(5), 650-659.

Choudhary, C., Kumar, C., Gnad, F., Nielsen, M. L., Rehman, M., Walther, T. C., et al. (2009). Lysine acetylation targets protein complexes and co-regulates major cellular functions. *Science, 325*(5942), 834-840.

Cid, V. J., Jiménez, J., Molina, M., Sánchez, M., Nombela, C., & Thorner, J. W. (2002). Orchestrating the cell cycle in yeast: Sequential localization of key mitotic regulators at the spindle pole and the bud neck. *Microbiology, 148*(9), 2647-2659.

Conacci-Sorrell, M., Ngouenet, C., & Eisenman, R. N. (2010). Myc-nick: A cytoplasmic cleavage product of myc that promotes α-tubulin acetylation and cell differentiation. *Cell, 142*(3), 480-493.

Dokmanovic, M., Clarke, C., & Marks, P. A. (2007). Histone deacetylase inhibitors: Overview and perspectives. *Molecular Cancer Research, 5*(10), 981-989.

Ekwall, K. (2005). Genome-wide analysis of HDAC function. *Trends in Genetics, 21*(11), 608-615.

Garber, K. (2007). HDAC inhibitors overcome first hurdle. *Nat Biotech, 25*(1), 17-19.

Gladfelter, A. S., Pringle, J. R., & Lew, D. J. (2001). The septin cortex at the yeast mother–bud neck. *Current Opinion in Microbiology, 4*(6), 681-689.

Gu, W., & Roeder, R. G. (1997). Activation of p53 sequence-specific DNA binding by acetylation of the p53 C-terminal domain. *Cell, 90*(4), 595-606.

Hay, R. T. (2005). SUMO: A history of modification. *Molecular Cell, 18*(1), 1-12.

Herbst, R. S. (2004). Review of epidermal growth factor receptor biology. *International Journal of Radiation Oncology Biology Physics, 59*(2), S21-S26.

Hubbert, C., Guardiola, A., Shao, R., Kawaguchi, Y., Ito, A., Nixon, A., et al. (2002). HDAC6 is a microtubule-associated deacetylase. *Nature, 417*(6887), 455-458.

Jacobs, S. A., & Khorasanizadeh, S. (2002). Structure of HP1 chromodomain bound to a lysine 9-methylated histone H3 tail. *Science, 295*(5562), 2080-2083.

Jaspersen, S. L., & Winey, M. (2004). The budding yeast spindle pole body: structure, duplication, and function. *Annual Review of Cell and Developmental Biology, 20*(1), 1-28.

Jenuwein, T., & Allis, C. D. (2001). Translating the histone code. *Science, 293*(5532), 1074-1080.

Kawaguchi, Y., Kovacs, J. J., McLaurin, A., Vance, J. M., Ito, A., & Yao, T. (2003). The deacetylase HDAC6 regulates aggresome formation and cell viability in response to misfolded protein stress. *Cell, 115*(6), 727-738.

Keogh, M., Kurdistani, S. K., Morris, S. A., Ahn, S. H., Podolny, V., Collins, S. R., et al. (2005). Cotranscriptional Set2 methylation of histone H3 lysine 36 recruits a repressive Rpd3 complex. *Cell, 123*(4), 593-605.

Kerscher, O., Felberbaum, R., & Hochstrasser, M. (2006). Modification of proteins by ubiquitin and ubiquitin-like proteins. *Annual Review of Cell and Developmental Biology, 22*(1), 159-180.

Kim, S. C., Sprung, R., Chen, Y., Xu, Y., Ball, H., Pei, J., et al. (2006). Substrate and functional diversity of lysine acetylation revealed by a proteomics survey. *Molecular Cell, 23*(4), 607-618.

Lee, W., Oberle, J. R., & Cooper, J. A. (2003). The role of the lissencephaly protein Pac1 during nuclear migration in budding yeast. *The Journal of Cell Biology, 160*(3), 355-364.

L'Hernault, S. W., & Rosenbaum, J. L. (1985). Chlamydomonas .alpha.-tubulin is posttranslationally modified by acetylation on the .epsilon.-amino group of a lysine. *Biochemistry, 24*(2), 473-478.

Lin, S., Defossez, P., & Guarente, L. (2000). Requirement of NAD and SIR2 for life-span extension by calorie restriction in saccharomyces cerevisiae. *Science, 289*(5487), 2126-2128.

Lindqvist, A., Rodríguez-Bravo, V., & Medema, R. H. (2009). The decision to enter mitosis: Feedback and redundancy in the mitotic entry network. *The Journal of Cell Biology, 185*(2), 193-202.

Longtine, M. S., DeMarini, D. J., Valencik, M. L., Al-Awar, O., Fares, H., De Virgilio, C., et al. (1996). The septins: Roles in cytokinesis and other processes. *Current Opinion in Cell Biology, 8*(1), 106-119.

Luo, J., Su, F., Chen, D., Shiloh, A., & Gu, W. (2000). Deacetylation of p53 modulates its effect on cell growth and apoptosis. *Nature, 408*(6810), 377-381.

Markus, S. M., & Lee, W. (2011). Microtubule-dependent path to the cell cortex for cytoplasmic dynein in mitotic spindle orientation. *BioArchitecture, 1*(5), 209-215.

Moore, J. K., Stuchell-Brereton, M. D., & Cooper, J. A. (2009). Function of dynein in budding yeast: Mitotic spindle positioning in a polarized cell. *Cell Motility and the Cytoskeleton, 66*(8), 546-555.

Mujtaba, S., Zeng, L., & Zhou, M. (2007). Structure and acetyl-lysine recognition of the bromodomain. *Oncogene, 26*(37), 5521-5527.

Neumüller, R. A., & Knoblich, J. A. (2009). Dividing cellular asymmetry: Asymmetric cell division and its implications for stem cells and cancer. *Genes & Development, 23*(23), 2675-2699.

Oh, Y., & Bi, E. (2011). Septin structure and function in yeast and beyond. *Trends in Cell Biology, 21*(3), 141-148.

Paik, W. K., Paik, D. C., & Kim, S. (2007). Historical review: The field of protein methylation. *Trends in Biochemical Sciences, 32*(3), 146-152.

Pawson, T., Gish, G. D., & Nash, P. (2001). SH2 domains, interaction modules and cellular wiring. *Trends in Cell Biology, 11*(12), 504-511.

Robert, T., Vanoli, F., Chiolo, I., Shubassi, G., Bernstein, K. A., Rothstein, R., et al. (2011). HDACs link the DNA damage response, processing of double-strand breaks and autophagy. *Nature, 471*(7336), 74-79.

Robyr, D., Suka, Y., Xenarios, I., Kurdistani, S. K., Wang, A., Suka, N., et al. (2002). Microarray deacetylation maps determine genome-wide functions for yeast histone deacetylases. *Cell, 109*(4), 437-446.

Rundlett, S., Carmen, A., Kobayashi, R., Bavykin, S., Turner, B., & Grunstein, M. (1996). HDA1 and RPD3 are members of distinct yeast histone deacetylase complexes that regulate silencing and transcription. *Proceedings of the National Academy of Sciences, 93*(25), 14503-14508.

Sakchaisri, K., Asano, S., Yu, L., Shulewitz, M. J., Park, C. J., Park, J., et al. (2004). Coupling morphogenesis to mitotic entry. *Proceedings of the National Academy of Sciences, 101*(12), 4124-4129.

Shahbazian, M. D., & Grunstein, M. (2007). Functions of site-specific histone acetylation and deacetylation. *Annual Review of Biochemistry, 76*(1), 75-100.

Siller, K. H., & Doe, C. Q. (2009). Spindle orientation during asymmetric cell division. *Nature Cell Biology, 11*(4), 365-374.

Smotrys, J. E., & Linder, M. E. (2004). Palmitoylation of intracellular signaling proteins: regulation and function. *Annual Review of Biochemistry, 73*(1), 559-587.

Soutoglou, E., Katrakili, N., & Talianidis, I. (2000). Acetylation regulates transcription factor activity at multiple levels. *Molecular Cell, 5*(4) 745-751.

Strahl, B.,D., & Allis, C.,David. (2000). The language of covalent histone modifications. *Nature, 403*, 41-45.

Taunton, J., Hassig, C. A., & Schreiber, S. L. (1996). A mammalian histone deacetylase related to the yeast transcriptional regulator Rpd3p. *Science, 272*(5260), 408-411.

Tiganis, T. (2002). Protein tyrosine phosphatases: Dephosphorylating the epidermal growth factor receptor. *IUBMB Life, 53*(1), 3-14.

Vogel, C., & Marcotte, E. M. (2012). Insights into the regulation of protein abundance from proteomic and transcriptomic analyses. *Nature Reviews. Genetics, 13*(4), 227-232.

Walsh, C. T., Garneau-Tsodikova, S., & Gatto, G. J. (2005). Protein posttranslational modifications: The chemistry of proteome diversifications. *Angewandte Chemie International Edition, 44*(45), 7342-7372.

Wang, Q., Zhang, Y., Yang, C., Xiong, H., Lin, Y., Yao, J., et al. (2010). Acetylation of metabolic enzymes coordinates carbon source utilization and metabolic flux. *Science, 327*(5968), 1004-1007.

Yang, X., & Seto, E. (2008). Lysine acetylation: Codified crosstalk with other posttranslational modifications. *Molecular Cell, 31*(4), 449-461.

Yi, C., Pan, H., Seebacher, J., Jang, I., Hyberts, S., Heffron, G., et al. (2011). Metabolic regulation of protein N-alpha-acetylation by bcl-xL promotes cell survival. *Cell, 146*(4), 607-620.

Zhang, X., Yuan, Z., Zhang, Y., Yong, S., Salas-Burgos, A., Koomen, J., et al. (2007). HDAC6 modulates cell motility by altering the acetylation level of cortactin. *Molecular Cell, 27*(2), 197-213.

Zhao, S., Xu, W., Jiang, W., Yu, W., Lin, Y., Zhang, T., et al. (2010). Regulation of cellular metabolism by protein lysine acetylation. *Science, 327*(5968), 1000-1004.

CHAPTER 2

Hos3 Is a Uniquely Targeted HDAC

INTRODUCTION

Targeting proteins, particularly enzymes, to different cellular sites at specific stages of the cell cycle or in response to diverse physiological conditions is an important mechanism in directing where and when such proteins function. It has been reported that HDACs in model organisms such as *H. sapiens*, *C. elegans*, *A. arabidopsis* etc. could localize to different cellular sites *in vivo*. In *S. cerevisiae*, cellular distribution has been described for some but not all of its HDACs (Hoppe et al., 2002; Liu et al., 2012). We aimed to perform a comprehensive investigation of the localization of the *S. cerevisiae* HDACsome. We are particularly interested in discovering HDACs that display localization other than being exclusively nuclear. In other words, we are looking for if any HDACs display cytoplasmic localization or even unique targeting *in vivo*. Such HDACs, if existing, would likely play a role in cellular compartments other than the nucleus where HDACs are significantly involved in modifying histone acetylation status. The example of such cytoplasmical or even uniquely-targeted HDACs would be of high interest and importance to our understanding of reversible lysine deacetylation as a global PTM.

METHODS AND MATERIALS

Yeast Strains and Plasmids

All yeast strains were annotated as in Table 2.1. Null deletion strains were streaked from the Yeast Deletion Collection (Research Genetics) onto YPD+G418 plates (G418, Geneticin) to select for the *KanMX* marker. Each null strain was confirmed by preparing the genomic DNA of the strain as template and obtaining a PCR product using designed primers (the forward primer annealed to the genomic region about 300-500 base pairs upstream of the start codon, and the reverse primer annealed to a region within the *KanMX* cassette). The genomically-tagged Hos3::3GFP strain (RCY4582) was made by integrating a 306 3GFP plasmid into the C-terminal region of *HOS3*.

All plasmids were annotated as in Table 2.2. Plasmids were made by the "gap-repair" method. Basically, a linearized plasmid and DNA sequences of interest amplified through PCR were cotransformed into a wild-type strain and selected on minimal plates for the marker carried by the plasmid. The candidate strain was grown to mid- or late-log phase in minimal medium (if GFP or RFP was desgined as an insert, cells were also checked by fluorescence microscopy for signal). The plasmid was rescued from yeast cells and then transformed into competent bacteria cells. Finally the plasmid was purified from the bacteria and confirmed for correct gene insertion by either restrictive digestion or PCR amplification. For the cloning of Clr3-GFP (*CEN*) (RCB4774) and HDAC9-GFP (*CEN*) (RCB4775), the *S. pombe* genomic DNA

was kindly provided by the Pleiss lab and the *H. sapiens* cDNA was kindly provided by the Kraus lab.

Fluorescence Microscopy

Cells expressing GFP or RFP fusion proteins were grown to mid-log phase in synthetic minimal medium. Cells were then live imaged using an Eclipse E600 microscope (Nikon) through FITC (for GFP) or rhodamine (for RFP) channels. When both GFP and RFP were involved, we took the RFP image first followed by the GFP image. A series of z-stack sections (1.6 - 3 μm in total depth with a 0.2 μm step for each section) were imaged by IPLab (Scanalytics). Raw data were deconvolved and analyzed by AutoQuant X (Media Cybernetics). Fluorescence images shown are the max projections of three-dimensional images. A differential interference contrast (DIC) image was also taken for the cells. A scale bar of 5 μm was used.

Heterochromatin Chimera Assay

The Sir3-Hos3 chimeras were assayed for their capability to replace Sir2 as a functional HDAC for establishing and maintaining the heterochromatin. A copy of *URA3* reporter gene was cloned into the subtelomeric region of chromosome VII in *sir2*Δ (RCY4743) and *sir2*Δ *sir3*Δ (RCY4744) cells. These cells transformed with an empty vector or *CEN* vectors bearing the corresponding genes were assayed 1). for *URA3* reporter silencing by 10-serial dilution onto SCD-trp and SCD-trp + 0.1% 5-FOA (5-

FOA, 5-fluoroorotic acid) plates for incubation at 30°C, and 2). for mating efficiency by mating with a *MAT**a*** tester strain (RCY263) and replica onto the selective SD plates.

Transcription and expression of the *URA3* reporter confer cellular toxicity in the presence of 5-FOA. Cellular resistance to 5-FOA thus indicates efficient silencing of the *URA3* reporter within the subtelomeric region. The *sir2*Δ or *sir2*Δ *sir3*Δ assay strains and the *MAT**a*** tester strain were auxotrophic for certain non-overlapping amino acids. Therefore, growth after replica onto the selective SD plates reveals successful mating.

Dilution Assay

Cells were transformed with respective plasmids and grown to mid-log phase (OD_{600} ~ 0.6) in synthetic minimal media. After standardizing cell density by equalizing the OD_{600} value, equal amounts of cells (a total of 1 OD_{600}) were collected by centrifugation and resuspended in 200 μl double distilled water (ddH_2O). Cells were then serially diluted in a 96-well plate in ddH_2O and 6 μl resuspension from each well was applied onto the preferred plates for incubation at 30°C. Cellular growth was monitored for the next 2-4 days.

Immunoblotting

Cells were transformed with the plasmids of interest and grown to mid-log phase (OD_{600} ~ 0.6) in synthetic complete dropout media. After

standardizing cell density by equalizing the OD_{600} value, equal amounts of cells (a total of 10 OD_{600}) were collected by centrifugation and resuspended in TAz buffer (10 mM Tris, 10 mM sodium azide, pH 7.5) together with protease inhibitors (1 mM EDTA, 1 mM phenylmethylsulfonyl fluoride, 1 mM benzamidine, and 1 μg/ml pepstatin A). Cells were then subjected to multiple rounds (3-5 x 1min) of glass bead beating and checked for effective lysis under the microscope (over 90% of cells were lysed). After spinning down the total cellular lysates, the supernatant was mixed with SDS sample buffer and analyzed by SDS-PAGE. The protein gel was then electrophoretically transferred onto nitrocellulose membrane (Pall). The membrane was blocked with 5% defatted milk in TBST (10 mM Tris pH 7.5, 150 mM sodium chloride, and 0.1% Tween-20), and probed at room temperature with respective primary antibodies in TBST (dilution of 1:1000 - 1:5000) for 1h and with appropriate secondary antibodies in TBST (dilution of 1:5000) for 30min. An ECL kit (Pierce) was used to detect proteins of interest through the horseradish peroxidase (HRP) activity conjugated to the secondary antibodies. Antibodies used in this chapter were as following: α-HA (32-6700, Invitrogen) and α-tubulin (9280-0050G, AbD Serotec).

Table 2.1. Yeast strains used in Chapter 2

Strain	Genotype	Reference/Source
RCY239	*MAT*a *ura3-52 leu2-3,112*	This Study
RCY263	*MAT*a *ade6*	This Study
RCY3915	BY4742 *hos3Δ::KanMX4*	Research Genetics, Inc.
RCY4582	*MAT*α *ura3Δ0 leu2Δ0 his3Δ1 lys2Δ0 Hos3::3GFP-URA3*	This Study
RCY4743	W303-1B *adh4::URA3::C1-3A sir2Δ::KanMX*	CCC1 in Chou et al., 2008
RCY4744	W303-1B *adh4::URA3::C1-3A sir2Δ::KanMX sir3Δ::HIS3*	CCC12 in Chou et al., 2008

Table 2.2. Plasmids used in Chapter 2

Plasmid	Description	Reference/Source
pRC374	pRS314	Sikorski and Hieter, 1989.
pRC2601	pRS315 Rpb10-RFP	This Study
pRC3664	pRS316 Hos3-GFP	This Study
pRC3665	pRS316 Rpd3-GFP	This Study
pRC3674	pRS315 Img1-RFP	This Study
pRC4163	pRS316 Hst3-GFP	This Study
pRC4164	pRS316 Hst2-GFP	This Study
pRC4175	pRS316 Hos2-GFP	This Study
pRC4176	pRS316 Hst1-GFP	This Study
pRC4177	pRS316 Hst4-GFP	This Study
pRC4189	pRS316 Hda1-GFP	This Study
pRC4190	pRS316 Sir2-GFP	This Study
pRC4191	pRS316 Hos1-GFP	This Study
pRC4270	pRS426 Hos3-GFP	This Study
pRC4333	pRS315 Bni4-RFP	This Study
pRC4334	pRS315 Kcc4-RFP	This Study
pRC4418	pRS316 Hos3(1-443)-GFP	This Study
pRC4421	pRS316 Hos3(1-635)-GFP	This Study
pRC4447	pRS316 Hos3(1-487)-GFP	This Study
pRC4448	pRS316 Hos3(1-566)-GFP	This Study
pRC4450	pRS316 Hos3(40-697)-GFP	This Study
pRC4533	pRS316 GFP-Hos3	This Study
pRC4548	pRS316 Sir3-Hos3(2-549)-GFP	This Study
pRC4549	pRS316 Sir3-Hos3(2-697)-GFP	This Study
pRC4552	pRS315 Sir3-RFP	This Study
pRC4599	pRS316 $Hos3^{H196E, D231N}$-GFP	This Study
pRC4738	pRS314 Sir3-Hos3(2-697)	This Study
pRC4739	pRS314 Sir3-Hos3(2-697)-GFP	This Study
pRC4741	pRS316 Hos3(40-443)-GFP	This Study
pRC4747	pRS315 Hos3-3HA	This Study

pRC4750	pRS316 Hos3(1-39 + 444-697)-GFP	This Study
pRC5061	pRS315 Nup133-RFP	This Study
pRC4752	pRS314 Sir2	This Study
pRC4753	pRS314 Sir3	This Study
pRC4754	pRS314 Sir3-Hos3(2-549)	This Study
pRC4755	pRS314 Sir3-Hos3(2-549)-GFP	This Study
pRC4774	pRS316 Clr3-GFP	This Study
pRC4775	pRS316 HDAC9-GFP	This Study
pRC4815	pRS315 Hos3$^{H196E, D231N}$-3HA	This Study
pRC4823	pRS315 Hos3	This Study
pRC4837	pRS314 Sir3-Hos3(2-549)$^{H196E, D231N}$	This Study
pRC5060	pRS315 Tub4-RFP	This Study
pRC5159	pRS314 Sir3-Hos3(2-549)^{D233A}	This Study

RESULTS

Hos3 displays unique localization

A total of ten HDAC genes can be recognized in the *S. cerevisiae* genome. The localization of some of these HDACs has been reported (Hoppe et al., 2002; Liu et al., 2012). However, a comprehensive view of the cellular distribution of HDACs is still missing. We intended to address this issue by investigating the localization of all ten HDACs. Each HDAC gene is cloned into a single-copy *CEN* vector and is fused at its COOH-terminus with a copy of green fluorescent protein (GFP). Then we analyzed wild-type cells transformed with such HDAC-GFP-containing vectors by three-dimensional fluorescence microscopy. Using a RNA polymerase component Rpb10 fused with a copy of red fluorescent protein (RFP) as the nucleus marker, we discovered that HDACs display a wide diversity of *in vivo* localization (Figure 2.1). Among the ten HDACs, Rpd3, Hos1, and Hos2 are observed within both the nucleus and the cytoplasm; Hda1, Sir2, Hst1, Hst3, and Hst4 are exclusively in the nucleus; Hst2 is exclusively in the cytoplasm; and Hos3 displays a strikingly different distribution pattern compared to the other nine HDACs. With a selectively cytoplasmic localization pattern *in vivo*, Hos3 localizes to the mother-bud neck, to a single focus in the daughter cell, and weakly around the nucleus (Figure 2.1).

The localization pattern observed for Hos3-GFP is identical to that observed for NH_2-terminally tagged GFP-Hos3 (Figure 2.2A (i) and (ii)). Moreover, the cellular distribution is unchanged when three copies of GFP

Figure 2.1

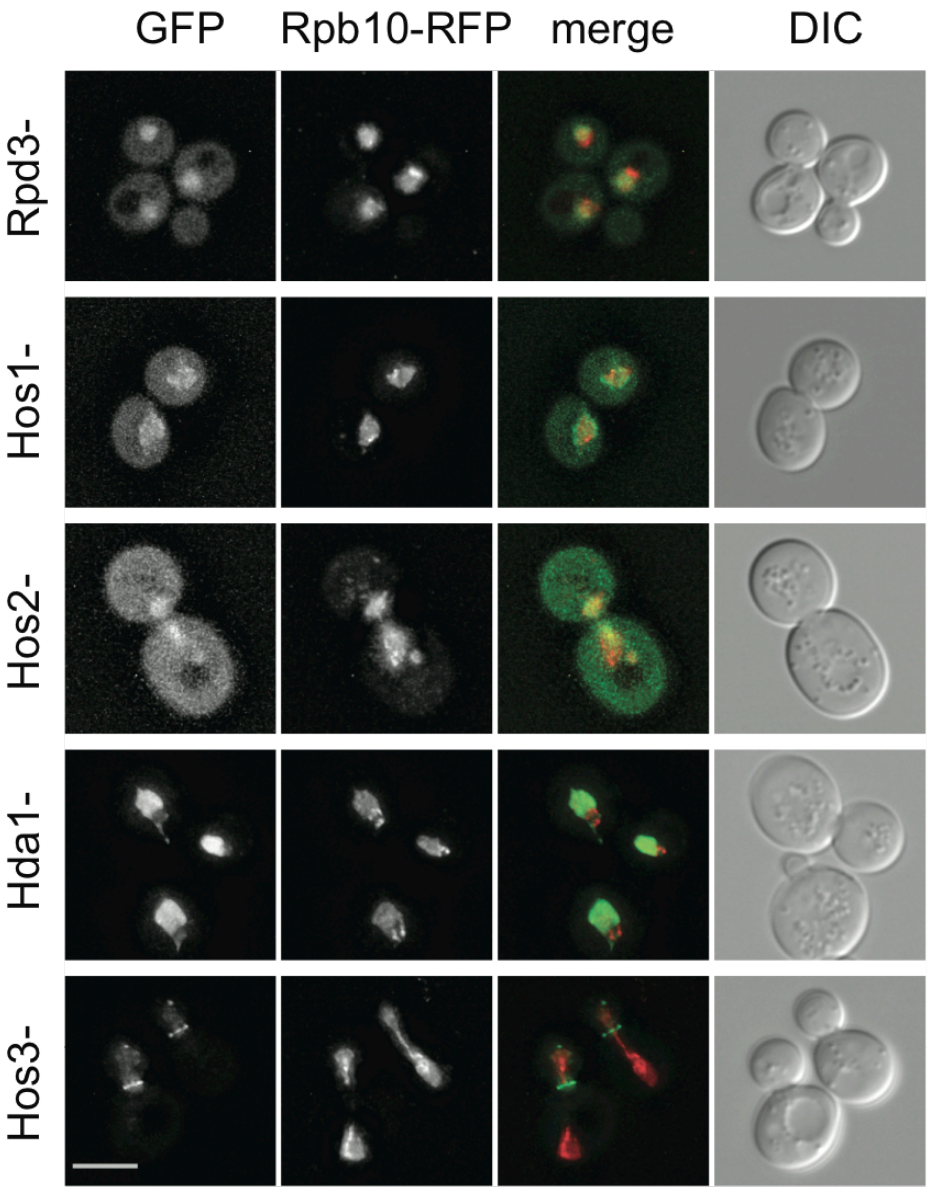

(to be continued)

Figure 2.1

(continued)

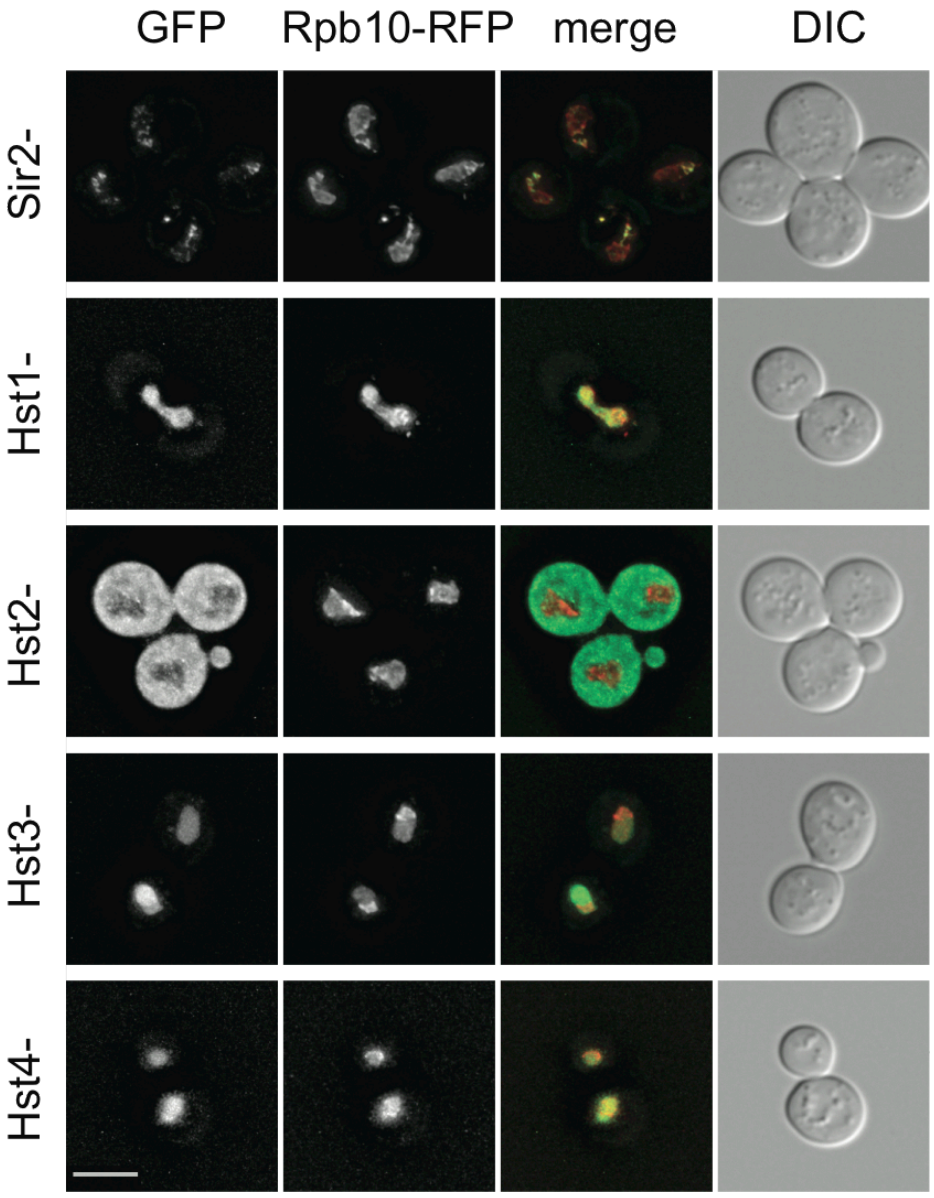

Figure 2.1. Localization of HDACs in budding yeast

Hos3 displays a unique localization pattern compared to other HDACs. All ten HDACs of *S. cerevisiae*, fused with GFP and expressed from a low-copy *CEN* vector, were imaged in wild-type cells coexpressing the nucleus reporter Rpb10-RFP (*CEN*). Scale bar, 5 μm.

are integrated into the genomic locus of *HOS3* so that endogenous Hos3 is COOH-terminally fused with 3GFP (Figure 2.2A (iii)). These data suggest that the unique localization observed for Hos3 reflects its authentic *in vivo* distribution.

Hos3 localizes asymmetrically to the bud neck and to the daughter spindle pole body (SPB)

The HDACs with the highest sequence alignment similarity to Hos3 in *S. pombe* is the single class II Clr3 and in *H. sapiens* is a class II HDAC9 (data not shown). When expressed ectopically in *S. cerevisiae*, neither Clr3 nor HDAC9 could localize to any of the cellular sites observed for Hos3, further arguing for the unique targeting of Hos3 (Figure 2.2B). Given that the bud neck of budding yeast is of an hourglass structure, Hos3 at the bud neck should form a ring. This is supported by the observation that Hos3 clearly displays a ring pattern at the bud neck when projected onto the X-Z dimension (Figure 2.2C).

The Hos3 ring at the mother-bud neck has two distinctive features. First, Hos3 localizes selectively to the daughter side of the bud neck (Figure 2.2A). A number of proteins have been observed to adopt asymmetrical localization at the bud neck (Cid et al., 2002). For example, Bni4 is a mother-side resident protein while Kcc4 is anchored to the daughter side (Kozubowski et al., 2005). Hos3 colocalizes with Kcc4 but not with Bni4 substantiating its

Figure 2.2

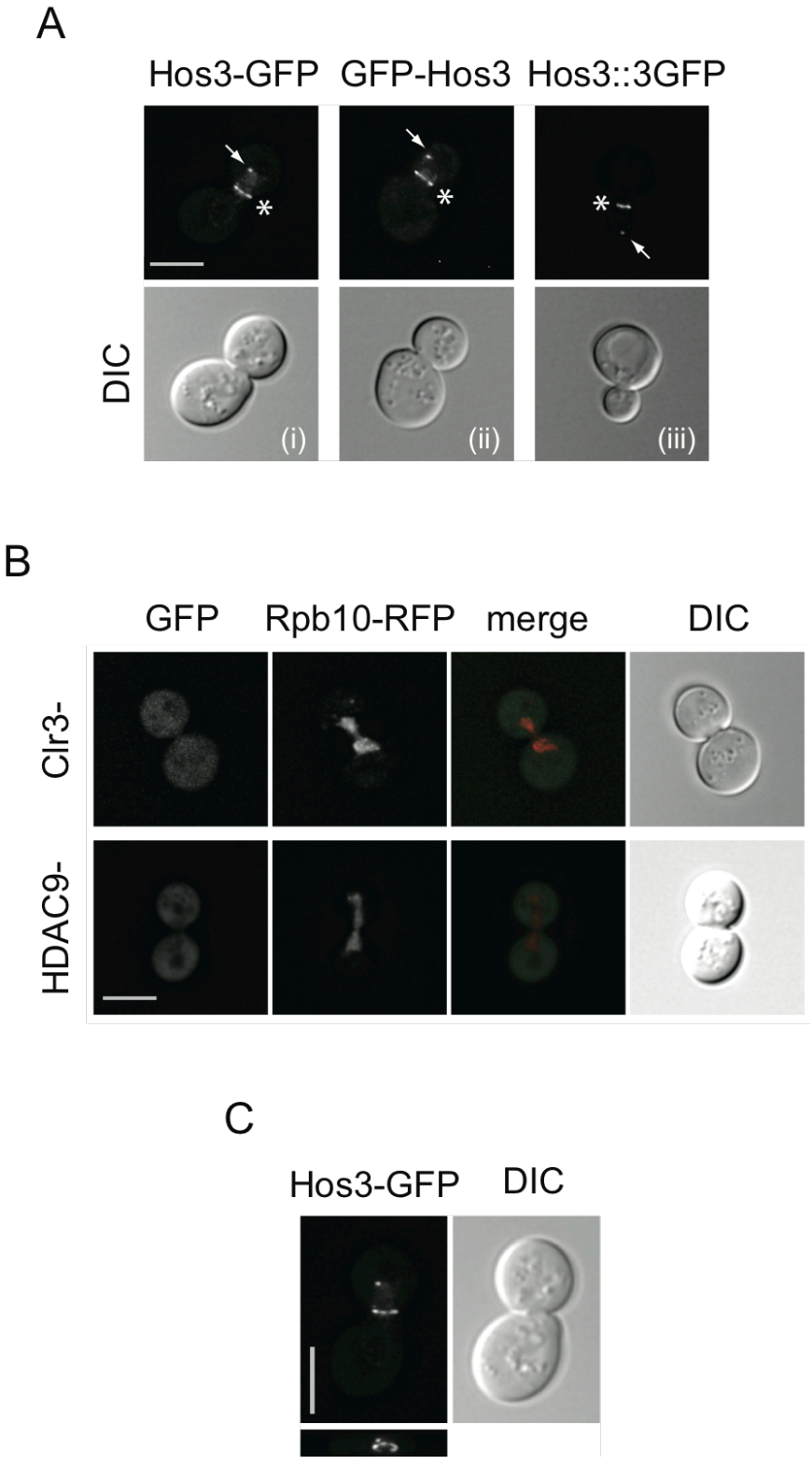
A
Hos3-GFP
GFP-Hos3
Hos3::3GFP
DIC
(i)
(ii)
(iii)
B
GFP
Rpb10-RFP
merge
DIC
Clr3-
HDAC9-
C
Hos3-GFP
DIC

Figure 2.2. Unique targeting of Hos3

(A) Wild-type cells transformed with a *CEN* vector bearing Hos3-GFP (i) or GFP-Hos3 (ii), or wild-type cells with endogenous Hos3 fused with three tandem copies of GFP (Hos3::3GFP) (iii) were analyzed by fluorescence microscopy. Asterisks denote Hos3 at the bud neck. Arrowheads point to the single Hos3 focus in the daughter cell. Scale bar, 5 μm.

(B) Wild-type cells transformed with a *CEN* vector bearing Clr3(*S. pombe*)-GFP or HDAC9(*H. sapiens*)-GFP and the nucleus reporter Rpb10-RFP (*CEN*) were analyzed by fluorescence microscopy. Scale bar, 5 μm.

(C) Cell in (A)(i) was rotated with the bud neck parallel to the horizontal axis. The image projection of the X-Z dimension was shown below. Scale bar, 5 μm.

asymmetric neck association (Figure 2.3A). The second feature is that association of Hos3 to the bud neck appears stable. We examined Hos3 neck localization in cells at different cell cycle stages. Upon the onset of budding, Hos3 is immediately targeted to the bud neck and then stays associated throughout the remaining cell cycle (Figure 2.3B). The asymmetrical Hos3 neck localization persists until cytokinesis during which the daughter-side Hos3 ring splits into two separate rings (Figure 2.3B). By the completion of mitosis, Hos3 dissociates from previous bud sites and is not maintained on the bud scars (data not shown). Interestingly, Hos3 does not associate with the mother side of the bud neck even when overexpressed, suggesting the asymmetry is not due to a lack of intrinsic affinity to the mother side but that the machinery that directs Hos3 to the bud neck is itself asymmetrical (Figure 2.3C).

The spindle pole bodies (SPBs) are the microtubule organization center (MTOC) in *S. cerevisiae* and function in instrumental processes such as spindle assembly, spindle alignment, and spindle segregation (Jaspersen and Winey, 2004). The observed Hos3 focus in the daughter cell colocalizes with the daughter SPB (Figure 2.4 (iv) and (v)). In comparison, Hos3 is not targeted to the mother SPB, revealing another pattern of asymmetry (Figure 2.4 (iv) and (v)). Interestingly, asymmetrical targeting of Hos3 onto the daughter SPB is cell-cycle-dependent (Figure 2.4). At early cell cycle stages, the sole SPB in the cell does not recruit Hos3 (Figure 2.4 (i) and (ii)). After SPB duplication, both SPBs positioned within the mother cell are still devoid of Hos3

Figure 2.3

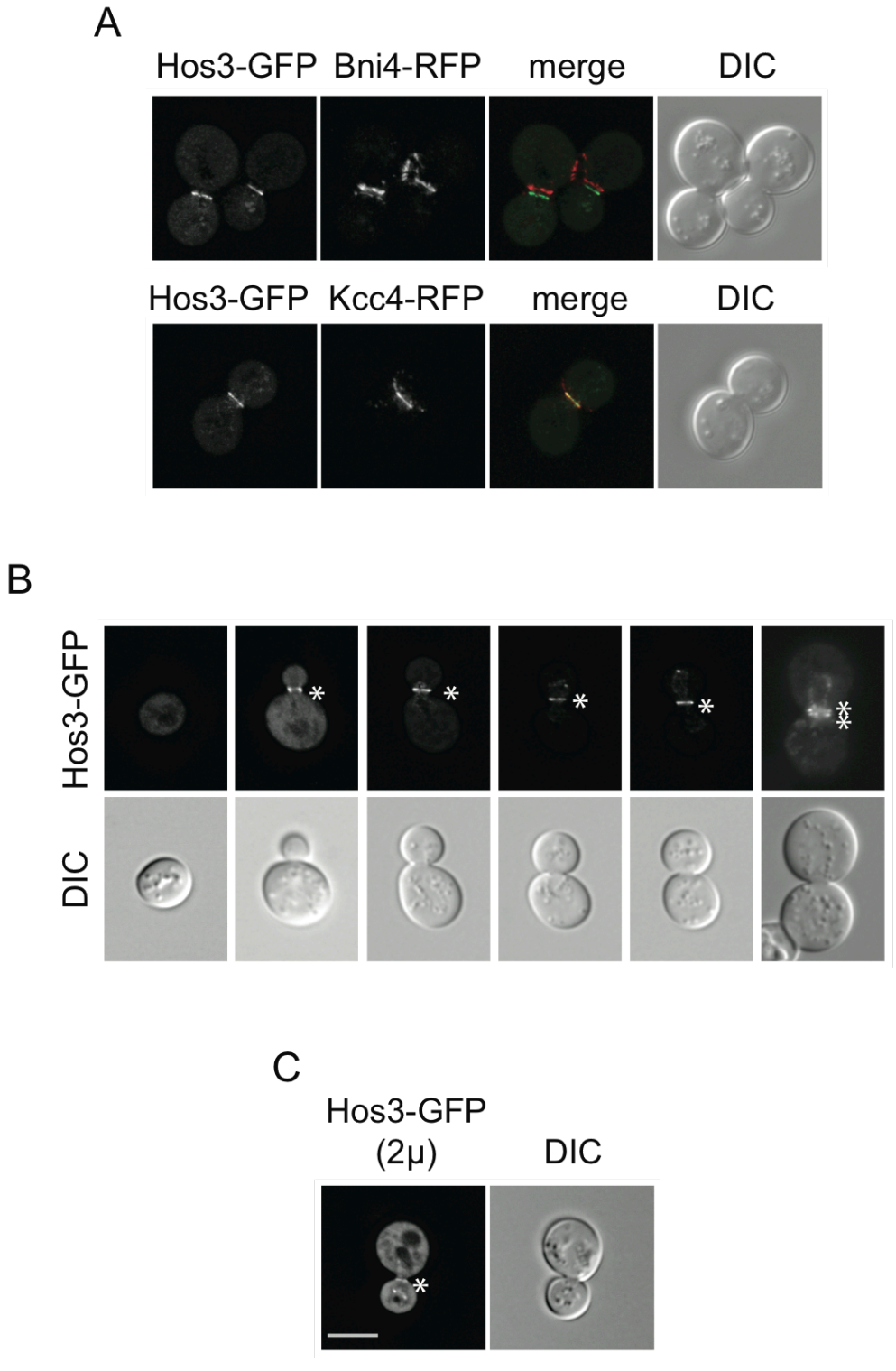
A
Hos3-GFP
Bni4-RFP
merge
DIC
Hos3-GFP
Kcc4-RFP
merge
DIC
B
Hos3-GFP
DIC
C
Hos3-GFP
(2μ)
DIC

Figure 2.3. Hos3 is asymmetrically targeted to the daughter side of the bud neck

(A) Hos3 localizes to the daughter side of the bud neck. Wild-type cells transformed with Hos3-GFP (*CEN*) and the mother-side neck reporter Bni4-RFP (*CEN*) or the daughter-side neck reporter Kcc4-RFP (*CEN*) were analyzed by fluorescence microscopy.

(B) Hos3 associates with the bud neck throughout the cell cycle. Hos3-GFP (*CEN*) was imaged in wild-type cells displaying a growing size of the bud. The images are rotated with the bud neck parallel to the horizontal axis. Asterisks denote Hos3 on the daughter side of the bud neck. During cytokinesis, the Hos3 ring splits into two rings thus giving to two asterisks with one on each side as annotation (the last image on the right).

(C) Overexpression of Hos3 does not break the asymmetry of its neck association. Wild-type cells transformed with a high-copy 2μ vector bearing Hos3-GFP was analyzed by fluorescence microscopy. Asterisk denotes Hos3 on the daughter side of the bud neck. Scale bar, 5 μm.

(Figure 2.4 (iii)). Hos3 is loaded onto the daughter SPB only after the designated daughter SPB partitions into the space of daughter cell (Figure 2.4 (iv) and (v)). Immediately after cytokinesis, Hos3 dissociates from the previous daughter SPB and both cells again appear Hos3-free for their sole SPB. Therefore, Hos3 is asymmetrically associated with the daughter SPB when the daughter SPB passes the bud neck and enters the daughter cell.

Hos3 as an HDAC

HDACs constitute a family of highly conserved enzymes. Sequence analysis of Hos3 reveals a single HDAC domain containing residues of 40-440, flanked by a short NH_2-terminus of 39 residues and a COOH-terminus of 257 residues (Figure 2.5A). No other motifs or domains could be identified apart from the catalytic HDAC domain. The crystal structure of a histone deacetylase homologue AcuC1, also called HDLP (histone deacetylase-like protein), from the hyperthermophilic bacterium *A. aeolicus* has been solved (Finnin et al., 1999). Its structure reveals a catalytic core that establishes the lysine deacetylation mechanism for class I and II HDACs (Finnin et al., 1999). After aligning the primary sequence of *A. aeolicus* AcuC1 to that of the five class I and II HDACs of *S. cerevisiae*, it becomes clear that these proteins share little homology except for a few highly conserved residues in the catalytic HDAC domain (Figure 2.6). This likely suggests that individual members of HDACs, while maintaining a conserved catalytic domain,

Figure 2.4

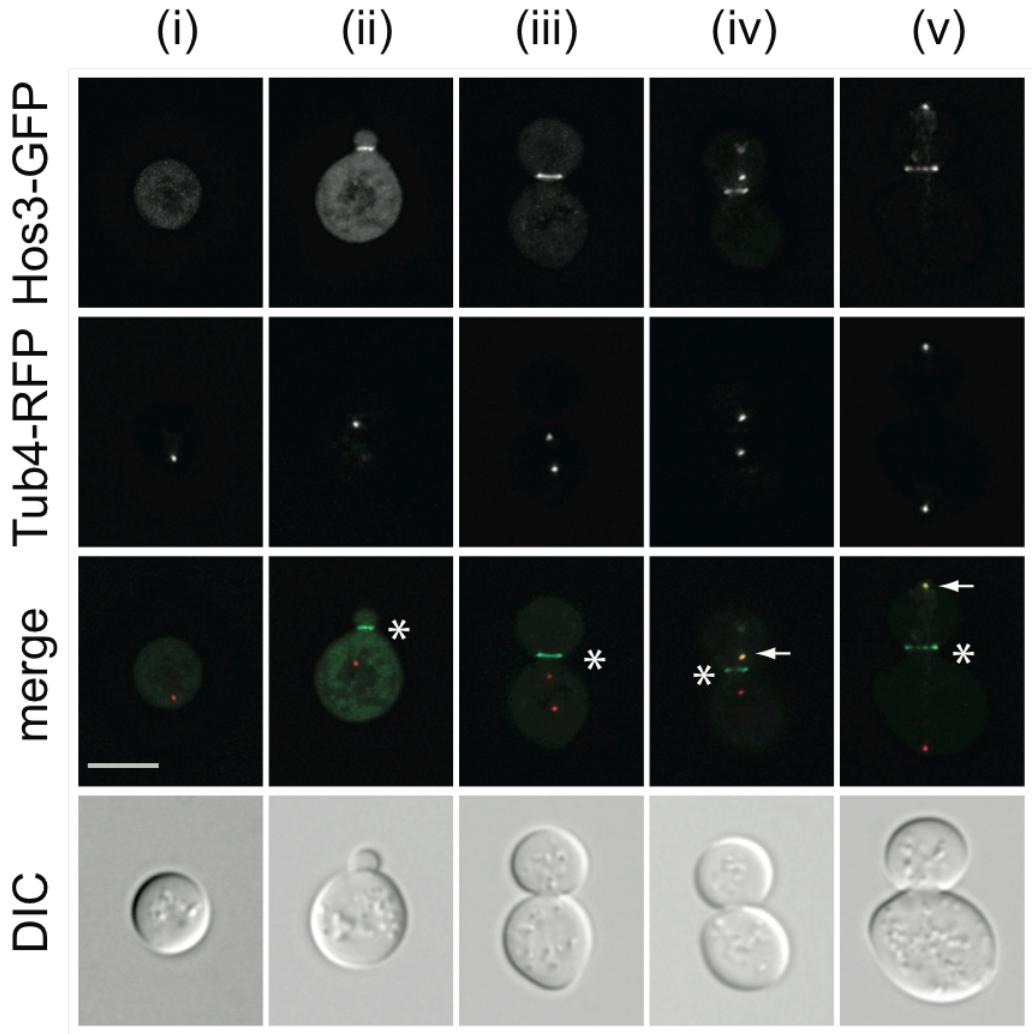

Figure 2.4. Hos3 is asymmetrically targeted to the daughter SPB in a cell-cycle-dependent manner

Wild-type cells transformed with Hos3-GFP (*CEN*) and the SPB marker Tub4-RFP (*CEN*) were analyzed by fluorescence microscopy. Cells at various cell cycle stages of (i) “unbudded”, (ii) “budding”, (iii) “post-SPB-duplication”, (iv) “spindle elongation”, and (v) “nuclear segregation”, are shown. The images are rotated with the bud neck parallel to the horizontal axis. Asterisks denote Hos3 on the daughter side of the bud neck. Arrowheads point to the daughter-SPB-associated Hos3. Scale bar, 5 μm.

evolutionarily diversify for residues outside the HDAC domain. The conserved residues are mainly located within the AcuC1 secondary structures of alpha helix α7, beta strands β5 and β6, and loops L3, L4, and L7 (Figure 2.6). Interestingly, although these conserved residues are scattered throughout the primary sequence of AcuC1, they are all spatially clustered in close proximity in the tertiary structure and are involved in the formation of the HDAC-like catalytic core (Figure 2.5B). Particularly, two charge-relay systems are required for the catalysis of lysine deacetylation by AcuC1 (Finnin et al., 1999). The first D166-H131 charge-relay pair is involved in coordinating an activated water molecule while the second D173-H132 charge-relay pair donates a proton to cleave the amide bond, yielding the acetate and the deacetylated lysine products (Finnin et al., 1999). AcuC1 also requires three residues (D168, H170, and D258) to stabilize a zinc ion for catalysis (Finnin et al., 1999).

Comparison of the primary sequences indicates that almost all residues required for the proposed AcuC1 catalytic mechanism are conserved in Hos3 (Figure 2.6 and 2.5B). The two charge-relay pairs of D166-H131 and D173-H132 of AcuC1 are respectively aligned to D231-H195 and D238-H196 of Hos3. For the three residues important for stabilizing the zinc iron, two are clearly conserved (AcuC1 D168 aligned to Hos3 D233, and AcuC1 H170 aligned to Hos3 H235) although no Hos3 counterpart to AcuC1 D258 could be identified from the primary sequence alignment. It is possible that the catalytic

Figure 2.5

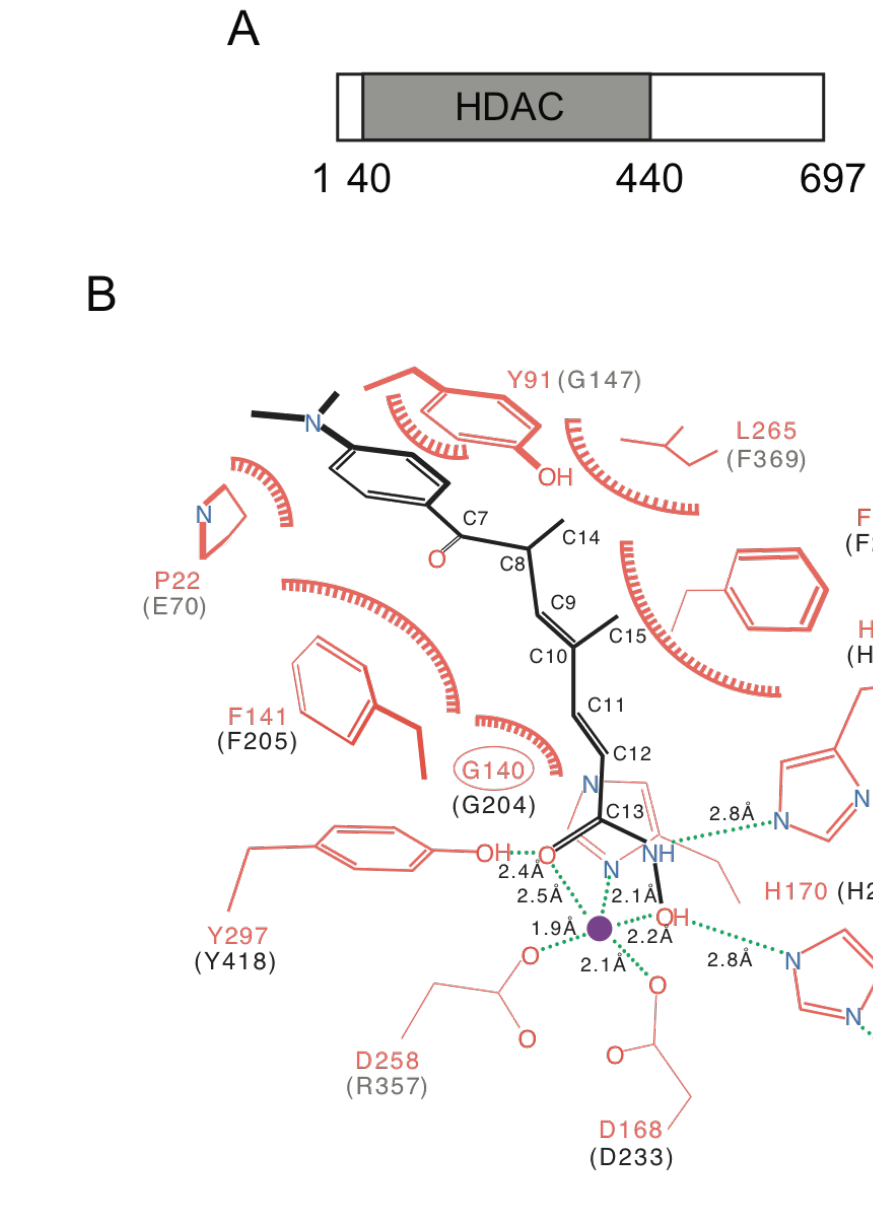
A
HDAC
1 40
440
697
B
Y91 (G147)
L265
(F369)
OH
N
C7
C14
O
C8
F198
(F291)
P22
(E70)
C9
C15
C10
H132
(H196)
C11
F141
(F205)
C12
G140
(G204)
N
C13
2.8Å
N
O
D173
(D238)
OH
O
2.4Å
N
NH
2.5Å
2.1Å
H170 (H235)
Y297
(Y418)
1.9Å
OH
2.2Å
2.1Å
2.8Å
N
O
O
H131
(H195)
D258
(R357)
O
O
N
O
D168
(D233)
D166
(D231)

Figure 2.5. Sequence analysis of Hos3

(A) The HDAC domain of Hos3 is comprised of residues 40-440.

(B) Potential catalytic core of Hos3. The schematic representation of AcuC1-TSA interactions is adapted and modified (Finnin et al., 1999). Hos3 residues aligned to the key catalytic residues of AcuC1 are adapted from Figure 2.6. TSA is in black and AcuC1 residues are labeled in red with their aligned counterparts in Hos3 in parentheses (conserved residues in black and non-conserved residues in gray). Thatched semi-circles indicate van der Waals contacts between hydrophobic protein residues and TSA. Hydrogen bonds are shown as green dashed lines.

Figure 2.6

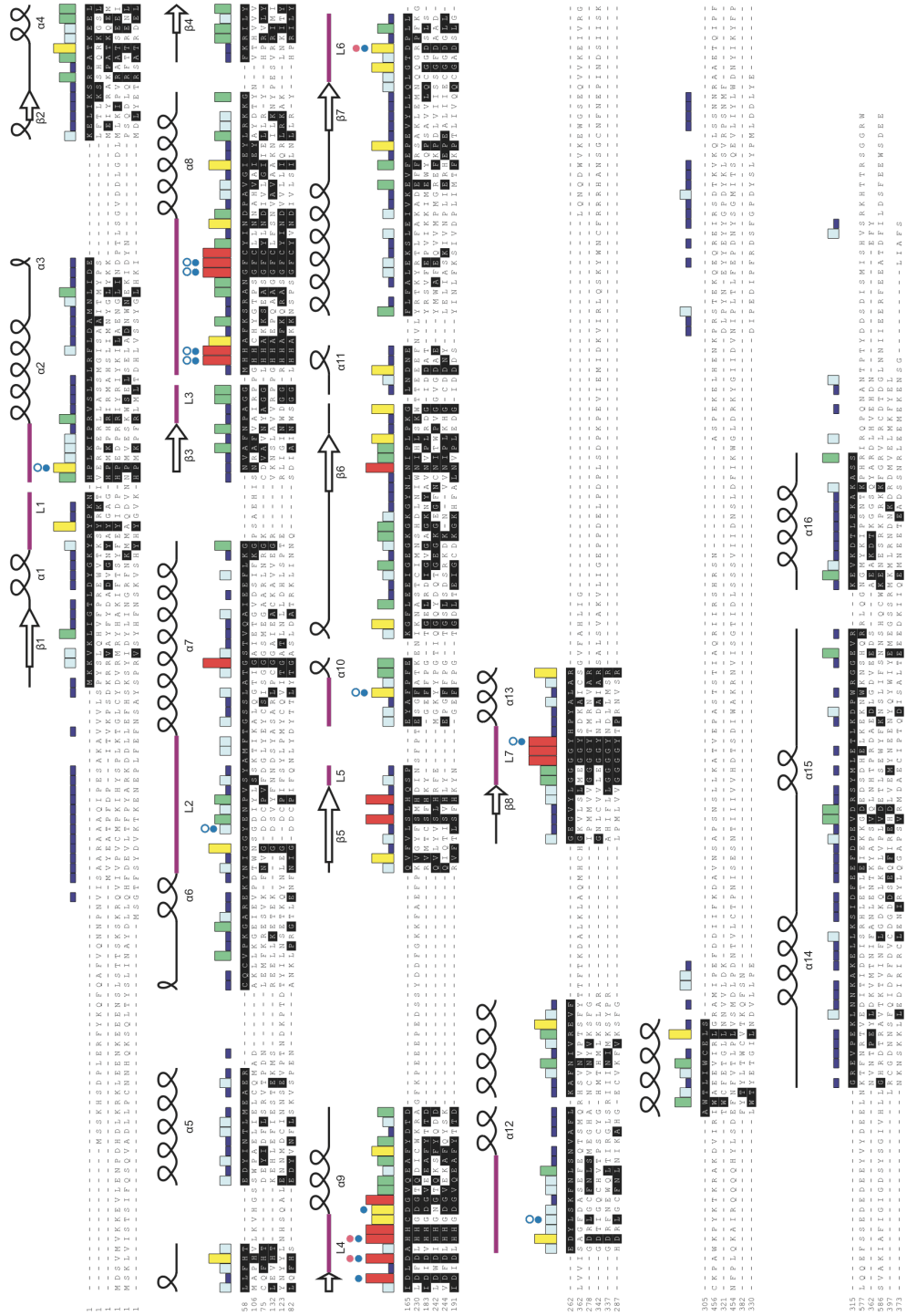
α1
β1
L1
α2
α3
β2
α4
β3
L3
α8
β4
α6
α7
L2
α5
α9
L4
α10
β5
L5
α11
β6
L6
β7
α12
α13
β8
L7
α14
α15
α16
low
high
conservation
alpha helix
beta strand
loop that forms the pocket
random coil
in contact with TSA
pocket residues
in contact with Zn2+

Figure 2.6. Sequence alignment of *A. aeolicus* AcuC1 and *S. cerevisiae* class I and II HDACs

The amino acid sequences of Hos3, Rpd3, Hda1, Hos1, and Hos2 were aligned with that of AcuC1 (accession no. NP_213698) by ClustalW. The AcuC1 primary sequence is shaded in black. HDAC residues identical to their aligned AcuC1 sequence are also highlighted in black. A summary for the accumulated degree of residue conservation bewteen HDACs and AcuC1 is coded by color bars. The secondary structure of AcuC1 is annotated above the corresponding primary sequence (Finnin et al., 1999). Specific residues of AcuC1 are annotated by circular markers (Finnin et al., 1999).

pocket of Hos3 is highly similar to but slightly different from that of AcuC1 so that another residue other than the aligned R357 of Hos3 functions to stabilize the zinc iron as D258 does for AcuC1. Therefore, we proposed that Hos3, like other class I and II HDACs, catalyzes lysine deacetylation in the similar mechanism adopted by AcuC1.

Noticeably, the crystal structure of AcuC1 was solved with the binding of a classic HDAC inhibitor TSA (Figure 2.5B). TSA inserts itself into the catalytic pocket of AcuC1 as a linear molecule (Figure 2.5B). For the aliphatic chain, while residues in contact with TSA at its hydroxamic acid group side are conserved (G140, F141, and F198), residues in contact with TSA at its dimethylamino-phenyl group side are not (P22, Y91, and L265) (Figure 2.5B and 2.6). This could possibly explain the previous observation that Hos3 is relatively insensitive to TSA: binding of TSA into the catalytic pocket of Hos3 is not as well stabilized as AcuC1 and other HDACs (Carmen et al., 1999).

Hos3 maintains HDAC activity *in vivo*

Affinity-purified Hos3 has been shown to be able to deacetylate acetylated histone peptides supporting its function as an HDAC *in vitro* (Carmen et al., 1999). However, it is yet to be determined if histones are the *in vivo* substrates of Hos3. Moreover, no other potential substrates have yet been reported for Hos3. Therefore, it remains an open question if Hos3

functions *in vivo* as an HDAC. This instrumental question needs to be addressed before we try to understand what Hos3 does *in vivo*.

With no authentic known *in vivo* substrates of Hos3 available, we noticed a clever chimera assay that utilizes Hos3 for the replacement of another HDAC Sir2 on the known substrates of histones. Establishment and maintenance of the heterochromatin, a strictly silenced region, is under transcriptional control. In *S. cerevisiae*, the Sir complex (Sir2, Sir3, and Sir4) is recruited to the appropriate regions within the genome, deacetylates the histones there, and thus represses the transcription of genes within this region (Rusche et al., 2003). On the molecular level, Sir3 functions as an adaptor to recruit Sir2 to the heterochromatin sites, and then Sir2 functions as the catalytic component to deacetylate the histones (Figure 2.7A). Therefore, either deletion of *SIR3* or *SIR2* results in the failure to establish and maintain the heterochromatin (Figure 2.7B). However, fusion of the heterologous HDAC Hos3 to the adaptor protein Sir3 would make a chimera of Sir3-Hos3 that gets recruited to the heterochromatin region by the Sir3 portion and deacetylate histones through the Hos3 portion (Figure 2.7C) (Chou et al., 2008). This chimera could then bypass endogenous Sir2 to reverse the heterochromatin defect. Therefore, this assay could be used for testing Hos3 *in vivo* HDAC activity in a chimera perspective.

The heterochromatin regions in *S. cerevisiae* are strictly silenced, allowing gene silencing in this region and as well efficient mating (Chou et al.,

Figure 2.7

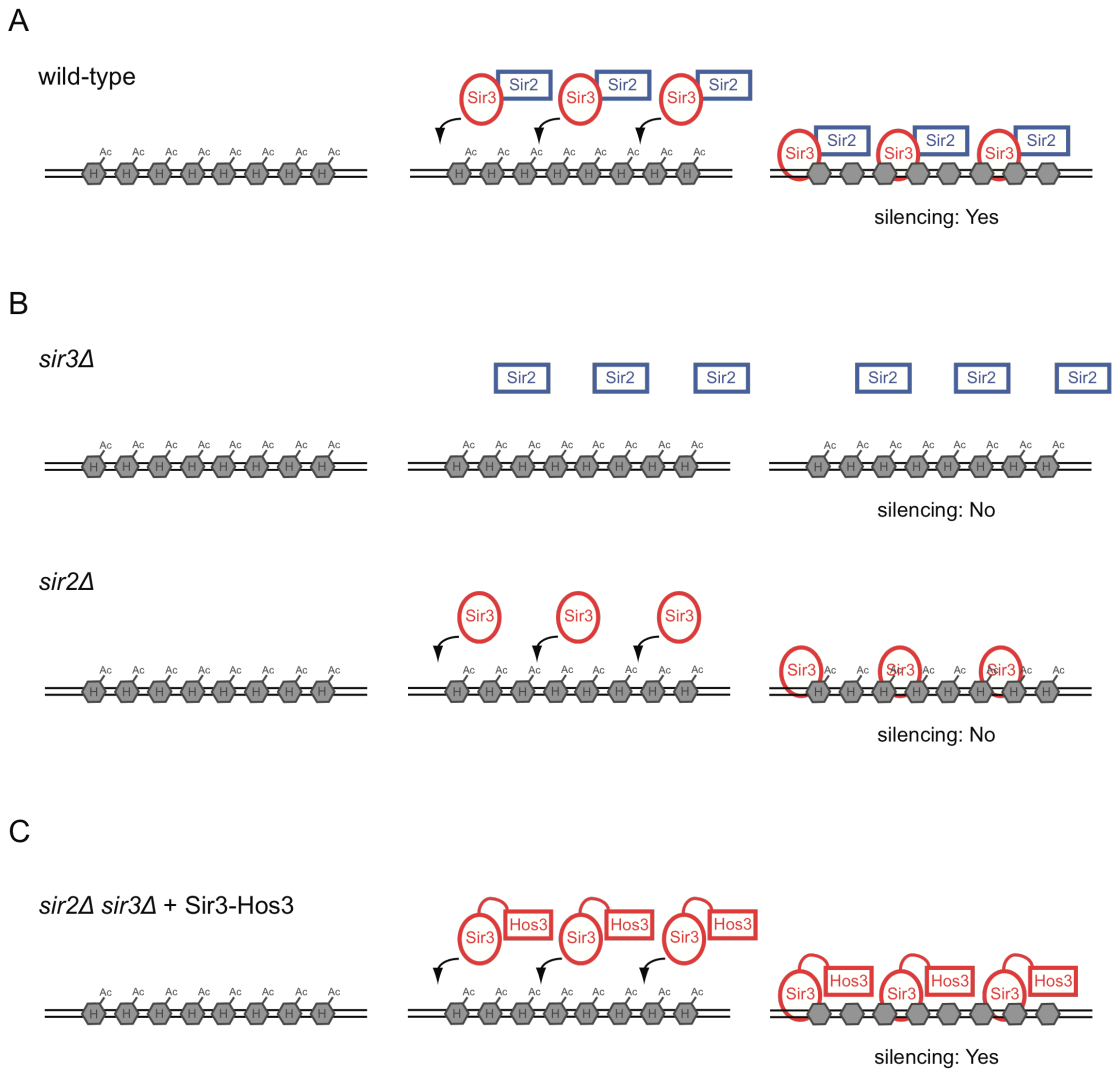
A
wild-type
Sir3
Sir2
silencing: Yes
B
sir3Δ
silencing: No
sir2Δ
silencing: No
C
sir2Δ sir3Δ + Sir3-Hos3
Hos3
silencing: Yes

Figure 2.7. Chimera assay to test Hos3 HDAC activity *in vivo*

Deacetylation of histones is required for establishing and maintaining heterochromatin regions.

(A) In wild-type cells, adaptor protein Sir3 recruits HDAC Sir2 to the heterochromatin sites. Sir2 then deacetylates histones and thus silences the region.

(B) In *sir3Δ* cells, HDAC Sir2 could not be targeted to the heterochromatin sites and consequently histones in these regions are still acetylated; in *sir2Δ* cells, adaptor protein Sir3 is targeted to the heterochromatin sites but lack of HDAC Sir2 renders the histones still acetylated. For both cell types, the region is not silenced.

(C) In *sir2Δ sir3Δ* cells, the absence of a functional Sir complex results in the failure to deacetylate histones within the heterochromatin regions. However, expression of a Sir3-Hos3 chimera would produce a fusion protein that gets recruited to the heterochromatin regions by the Sir3 portion and then deacetylates the histones through its Hos3 portion. Upon restoration of deacetylated histones, the Sir3-Hos3 chimera reverses the silencing defect.

2008). Therefore, in the absence of the adaptor protein Sir3 or of the HDAC Sir2, cells fail to silence a *URA3* reporter gene cloned into the subtelomeric region (a heterochromatin site), or to mate properly (Figure 2.8A 1st, 3rd and 4th rows) (Chou et al., 2008). However, fusion of the heterologous Hos3 with the adaptor protein Sir3 bypasses endogenous Sir3 or Sir2 to reverse the silencing or mating defect (Figure 2.8A 5th and 7th rows) (Chou et al., 2008). Therefore, Hos3 indeed functions *in vivo* as an HDAC.

Mutating conserved catalytic residues of the two charge-relay pairs (H196E, D231N) or of the residue required for zinc iron stabilization (D233A) renders the Sir3-Hos3 chimera unable to replace Sir2 and reverse the silencing or mating defects (Figure 2.8B and 2.8C). This suggests that both of these two mutations abolish Hos3 HDAC activity *in vivo*, thus supporting our previous hypothesis that Hos3 catalyzes lysine deacetylation in a similar mechanism as AcuC1.

Localization is important in defining where Hos3 functions

For the Sir3-Hos3 chimera assay, we made a very striking observation. In the case of two chimeras, Sir3-Hos3(2-549) but not Sir3-Hos3(2-697) could replace Sir2 as a functional HDAC (Figure 2.8A, 5th row vs. 6th row, 7th row vs. 8th row). Given that Hos3 HDAC domain contains residues of 40-440, both chimeras of Sir3-Hos3(2-549) and Sir3-Hos3(2-697) have the intact HDAC domain but completely differ in the apparent HDAC activity. We

investigated the localization of these two chimeras. The functional Sir3-Hos3(2-549) chimera is correctly targeted to the Sir complex sites, but the nonfunctional Sir3-Hos3(2-697) chimera is not (Figure 2.8D). Therefore, the reason Sir3-Hos3(2-697) appears nonfunctional in the chimera assay is most likely due to targeting rather than enzymatic defect. Therefore, localization of Hos3 is important in defining where it functions as an HDAC. Given its unique targeting to the bud neck and to the daughter SPB, Hos3 is likely to function as an HDAC at these specific sites. Together, the data suggest that Hos3 is an HDAC *in vivo* and the unique localization pattern likely reflects its action on non-nuclear targets.

Regions required for the unique targeting of Hos3

We tried to investigate the molecular determinants within Hos3 that is required for its unique targeting. Hos3 contains a single HDAC domain. Mutation of “H196E, D231N” abolishes Hos3 HDAC activity but loss of deacetylase activity does not perturb either the Hos3 protein level or its localization pattern (Figure 2.9A and 2.9B). Therefore, the HDAC activity is not involved in the unique targeting of Hos3.

We then performed serial truncations to map the regions essential for Hos3 localization (Figure 2.9C and 2.9D). As described earlier, Hos3 contains a core HDAC domain between residues 40 and 440, and neither the NH_2- nor

Figure 2.8

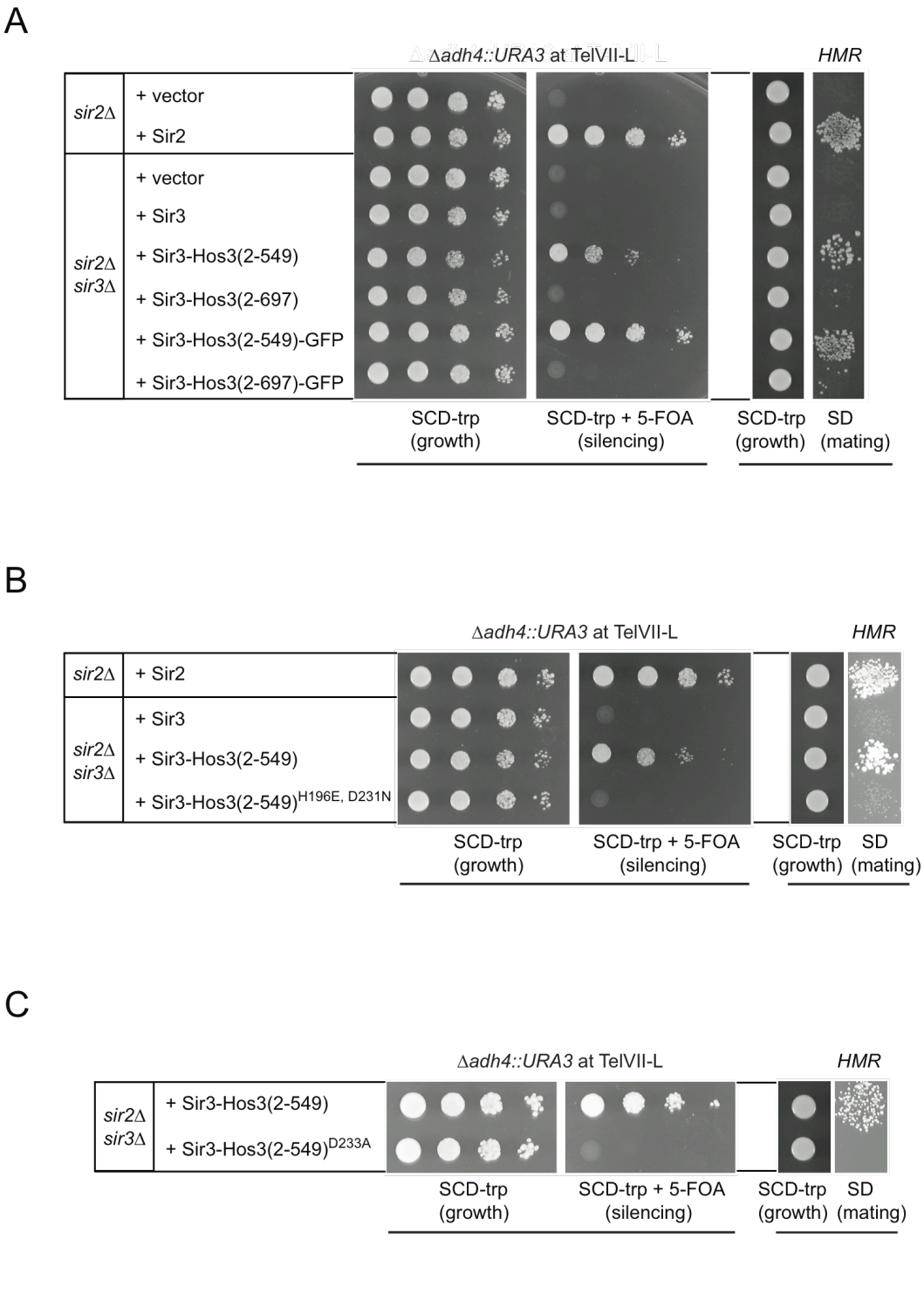
A
Δadh4::URA3 at TelVII-L
HMR
sir2Δ
+ vector
+ Sir2
sir2Δ sir3Δ
+ vector
+ Sir3
+ Sir3-Hos3(2-549)
+ Sir3-Hos3(2-697)
+ Sir3-Hos3(2-549)-GFP
+ Sir3-Hos3(2-697)-GFP
SCD-trp (growth)
SCD-trp + 5-FOA (silencing)
SCD-trp (growth)
SD (mating)
B
Δadh4::URA3 at TelVII-L
HMR
sir2Δ
+ Sir2
sir2Δ sir3Δ
+ Sir3
+ Sir3-Hos3(2-549)
+ Sir3-Hos3(2-549)H196E, D231N
SCD-trp (growth)
SCD-trp + 5-FOA (silencing)
SCD-trp (growth)
SD (mating)
C
Δadh4::URA3 at TelVII-L
HMR
sir2Δ sir3Δ
+ Sir3-Hos3(2-549)
+ Sir3-Hos3(2-549)D233A
SCD-trp (growth)
SCD-trp + 5-FOA (silencing)
SCD-trp (growth)
SD (mating)

Figure 2.8

D

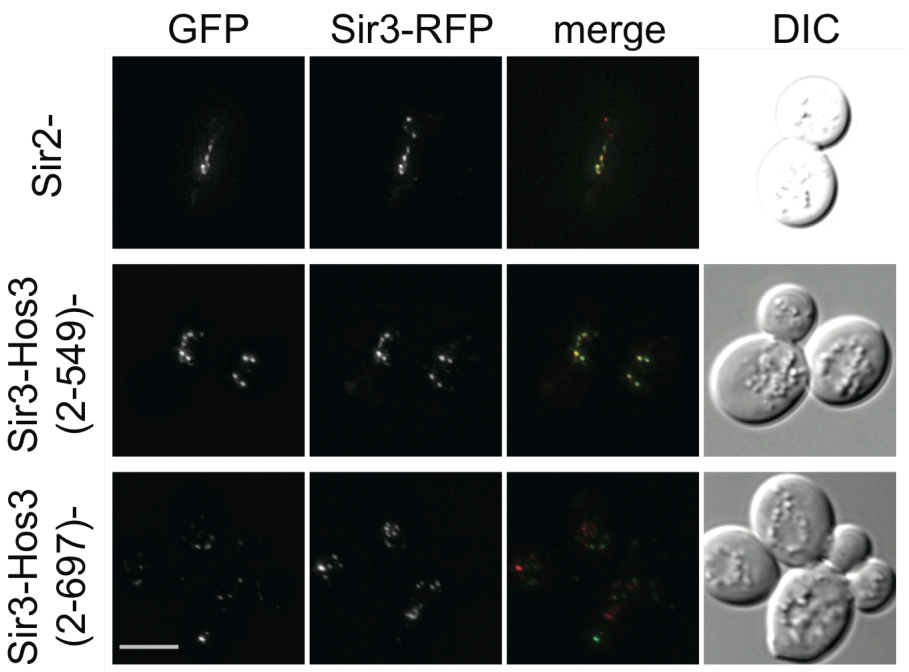

Figure 2.8. Hos3 could deacetylate histones within the heterochromatin in the context of a chimera

The Sir3-Hos3 chimeras are assayed for their capability to replace Sir2 as a functional HDAC within the heterochromatin.

(A) Two versions of Sir3-Hos3 chimeras, Sir3-Hos3(2-549) (also Sir3-Hos3(2-549)-GFP) and Sir3-Hos3(2-697) (also Sir3-Hos3(2-697)-GFP), (B) Sir3-Hos3(2-549) and a mutation version of Sir3-Hos3(2-549)$^{H196E,\ D231N}$, and (C) Sir3-Hos3(2-549) and a mutation version of Sir3-Hos3(2-549)^{D233A}, are respectively transformed into the assay strain and checked for their capability to replace Sir2 as a functional HDAC within the heterochromatin as described. (D) Targeting Sir3-Hos3 chimera to the Sir complex site correlates with its ability to function as an HDAC within the heterochromatin. Sir2-GFP (*CEN*), Sir3-Hos3(2-549)-GFP (*CEN*), and Sir3-Hos3(2-697)-GFP (*CEN*) were respectively imaged in wild-type cells coexpressing the Sir complex marker Sir3-RFP (*CEN*). Scale bar, 5 μm.

the COOH-terminal regions contain any distinguishable motifs or domains based on primary sequence (Figure 2.5A). We made truncation alleles of the COOH-terminal region of Hos3 about every 60 residues according to its secondary structure prediction (Figure 2.9C-E). Similar to full-length Hos3, Hos3(1-635), Hos3(1-566), and Hos3(1-487) all localize to the bud neck and to the daughter SPB (Figure 2.9D (i), (ii), and (iii)). Therefore, the very COOH-terminal residues of 488-697 are dispensable for Hos3 localization. However, deletion of the full COOH-terminus as Hos3(1-443), or Hos3(*C*Δ), abolishes the unique targeting of Hos3 (Figure 2.9D (iv)). This suggests that residues of 444-487 within the COOH-terminus are required for Hos3 localization. As a comparison, deletion of the full NH_2-terminus as Hos3(40-697), or Hos3(*N*Δ), maintains localization at the bud neck and the daughter SPB (Figure 2.9D (v)). Agreeing with the requirement of residues of 444-487, a combination deletion of both the NH_2- and the COOH-termini as Hos3(40-443), or Hos3(*N*Δ+*C*Δ), is mislocalized (Figure 2.9D (vi)). Then we deleted the HDAC domain to create a "HDAC-less" Hos3(1-39 + 444-697), or Hos3(*HDAC*Δ), and found that this construct loses the unique targeting (Figure 2.9D (vii)). Therefore, the HDAC domain also plays a role in Hos3 localization. Together, we mapped the region required for the unique targeting of Hos3 to residues from 40 to 487.

For our characterization of the truncated alleles of Hos3, we wanted to mention three additional features observed. First, Hos3(1-566) and Hos3(1-487), both maintaining the unique targeting, are enhanced for the "around-the-nucleus" signal which could even be weakly observed in full-length Hos3.

Figure 2.9

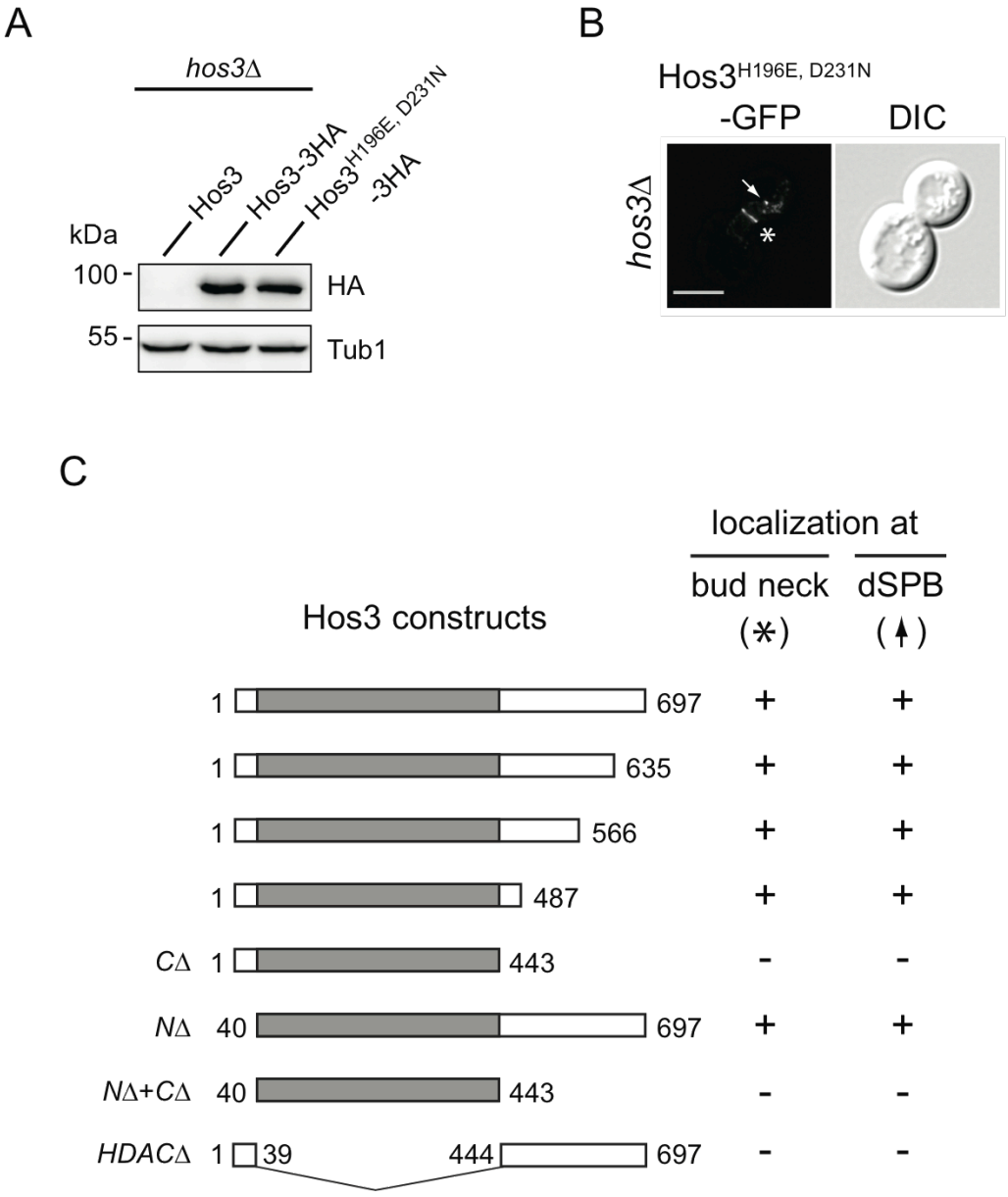
A
hos3Δ
Hos3
Hos3-3HA
Hos3H196E, D231N -3HA
kDa
100
HA
55
Tub1
B
Hos3H196E, D231N
-GFP
DIC
hos3Δ
C
Hos3 constructs
localization at
bud neck (*)
dSPB
1 697 + +
1 635 + +
1 566 + +
1 487 + +
CΔ 1 443 - -
NΔ 40 697 + +
NΔ+CΔ 40 443 - -
HDACΔ 1 39 444 697 - -

Figure 2.9

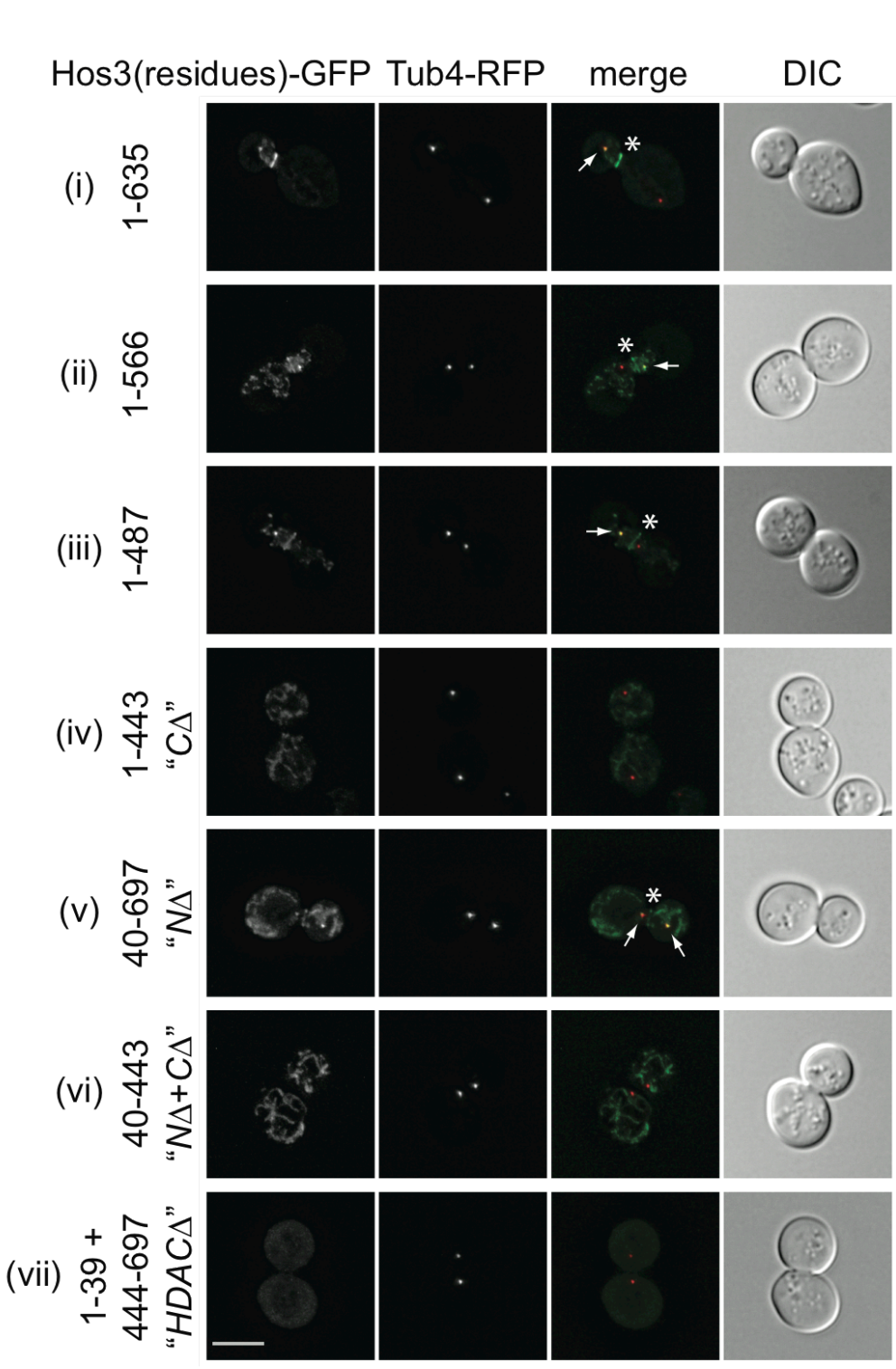
D
Hos3(residues)-GFP
Tub4-RFP
merge
DIC
(i) 1-635
(ii) 1-566
(iii) 1-487
(iv) 1-443 "CΔ"
(v) 40-697 "NΔ"
(vi) 40-443 "NΔ+CΔ"
(vii) 1-39 + 444-697 "HDACΔ"

Figure 2.9

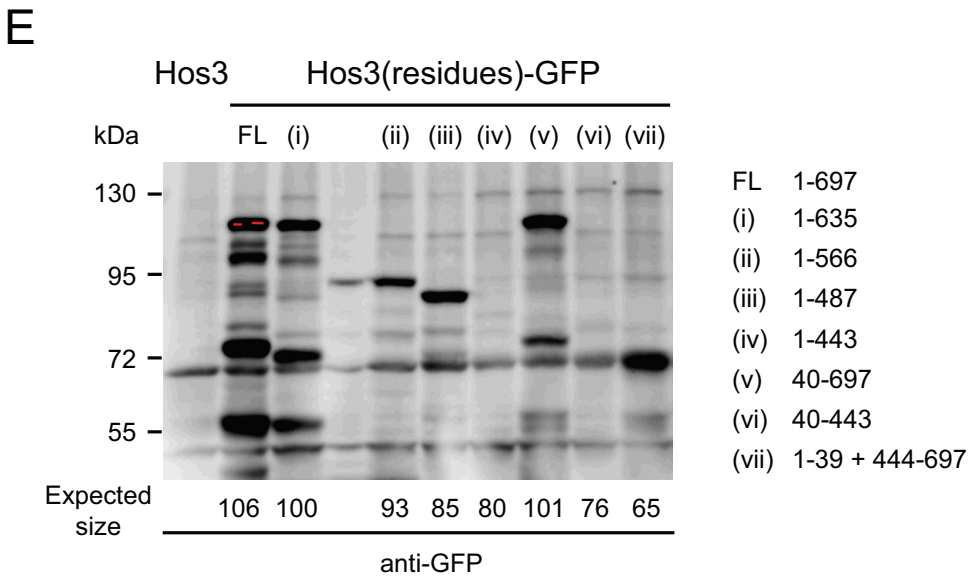

Figure 2.9. Mapping regions required for the unique targeting of Hos3

(A) Loss of HDAC activity does not alter Hos3 level. *hos3*Δ cells transformed with *CEN* vectors bearing Hos3, Hos3-3HA, and Hos3$^{H196E, D231N}$-3HA were grown to mid-log phase in SCD-leu medium and analyzed for Hos3 level by preparing the whole cell extracts for immunoblotting against HA tag. Tub1 was probed as loading control.

(B) Loss of HDAC activity does not change Hos3 localization. *hos3*Δ cells transformed with Hos3$^{H196E, D231N}$-GFP (*CEN*) were analyzed by fluorescence microscopy. Asterisk denotes Hos3$^{H196E, D231N}$ at the bud neck. Arrowhead points to Hos3$^{H196E, D231N}$ on the daughter SPB. Scale bar, 5 μm.

(C and D) Localization of truncated forms of Hos3.

(C) Systematically truncated versions of Hos3-GFP (*CEN*) are summarized for their capability to be targeted to the bud neck (asterisk) and to the daughter SPB (arrowhead).

(D) Wild-type cells transformed with systematically truncated versions of Hos3-GFP (*CEN*) and SPB reporter Tub4-RFP (*CEN*) were analyzed by fluorescence microscopy. Cells at a late cell cycle stage when the daughter SPB has entered the daughter cell are shown. Asterisks denote Hos3 at the bud neck. Arrowheads point to Hos3 at the daughter SPB. A second arrowhead (left) in Hos3(40-697) points to its association with the mother SPB (v). Scale bar, 5 μm.

(E) Wild-type cells transformed with untagged Hos3 (*CEN*) or systematically truncated versions of Hos3-GFP (*CEN*) were grown to mid-log phase in selective medium and analyzed by western blot using anti-GFP antibody. The alleles of (iv) 1-443 and (vi) 40-443 do not display apparent bands on the blot. This is possibly due to their degradation.

Such “around-the-nucleus” signal significantly colocalizes with the nuclear pore complex component Nup133, and thus raises a very interesting question if Hos3 could also function at the nuclear pore complex apart from its unique localization to the already-described bud neck and daughter SPB (Figure 2.10A). The second feature applies to Hos3(40-697), or Hos3(*N*Δ), in that this construct is targeted not only to the daughter SPB but also to the mother SPB (Figure 2.9D (v)). In another word, compared to the asymmetrical targeting to the daughter SPB for full-length Hos3, Hos3 lacking the short NH_2-terminus becomes constitutively and symmetrically associated with the SPBs. We are going to address this issue further in the later Chapter 5. Finally, Hos3(1-443), Hos3(40-697), and Hos3(40-443), constructs that lack either the COOH- or the NH_2- or both termini, all display a tubular structure not seen for full-length Hos3 (Figure 2.9D (iv), (v), and (vi)). Surprisingly, these tubules colocalize with the mitochondria marker (Figure 2.10B). This suggests that truncated forms of Hos3 could be specifically targeted to the mitochondria. While this observation is very interesting, for the following chapters we will mainly focus on Hos3 localization to the bud neck and to the daughter SPB. However, we will have a brief discussion of such mitochondria targeting of truncated Hos3 in the final Chapter 6.

Figure 2.10

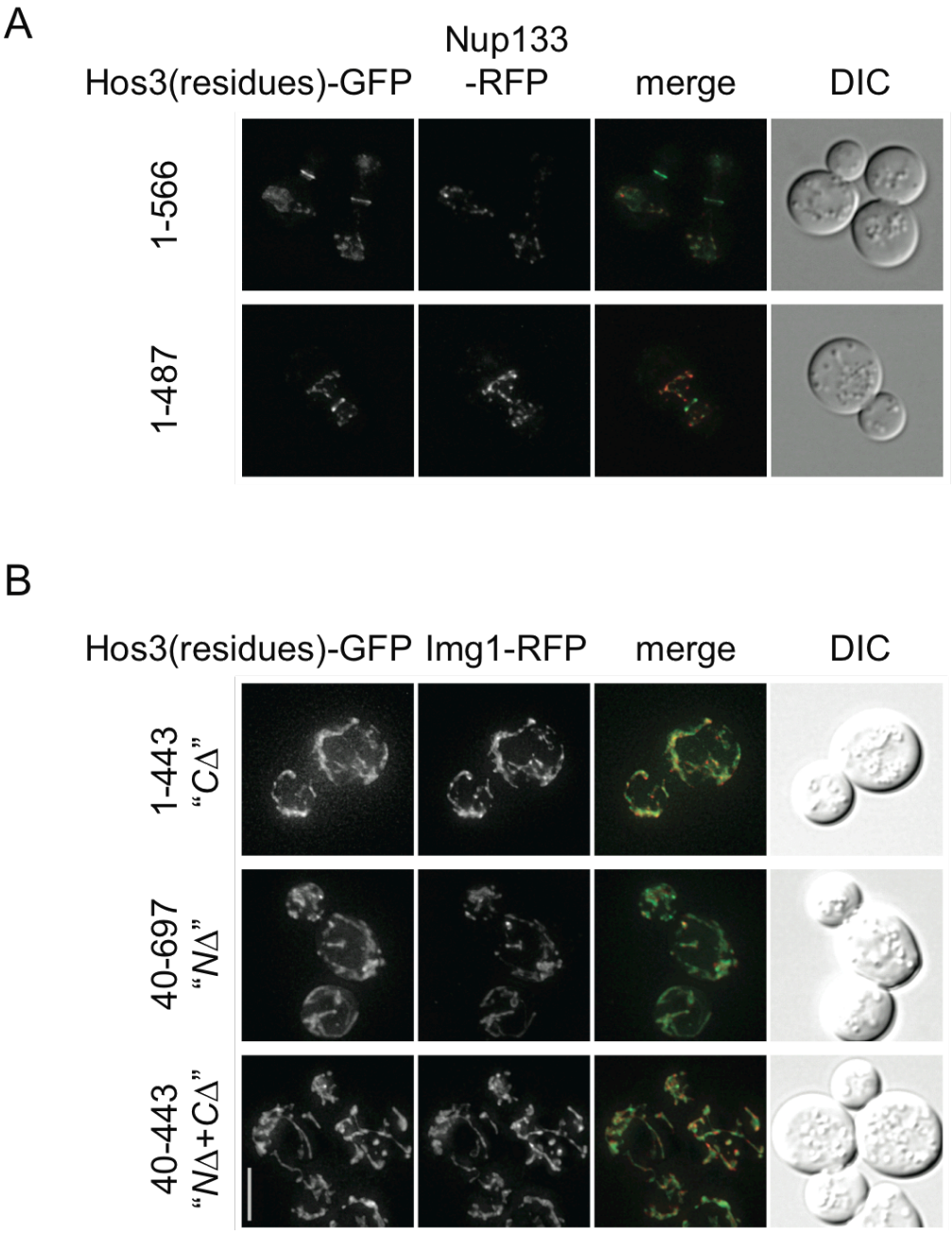
A
Hos3(residues)-GFP
Nup133
-RFP
merge
DIC
1-566
1-487
B
Hos3(residues)-GFP
Img1-RFP
merge
DIC
1-443
"CΔ"
40-697
"NΔ"
40-443
"NΔ+CΔ"

Figure 2.10. Localization features of certain Hos3 truncated alleles

(A) Wild-type cells transformed with Hos3(1-566)-GFP (*CEN*) or Hos3(1-487)-GFP (*CEN*) and the nuclear pore complex marker Nup133-RFP (*CEN*) were analyzed by fluorescence microscopy.

(B) Wild-type cells transformed with Hos3(1-443)-GFP (*CEN*), Hos3(40-697)-GFP (*CEN*), or Hos3(40-443)-GFP (*CEN*), and together with the mitochondria marker Img1-RFP (*CEN*) were analyzed by fluorescence microscopy. Scale bar, 5 μm.

DISCUSSION

Hos3 displays very unique targeting to a few defined cellular compartments within the cell. Of them, the bud neck is an hourglass region segregating and as well connecting the mother and daughter cells, and the SPBs are the MTOCs that polymerize mirotubules for the purpose of many spindle-related cellular activities. Such unique localization is important indication that Hos3 could play a very particular yet unknown role at these sites rather than act on histones. The unique targeting of Hos3 that we accidently discovered is what got us interested and thus determined to study this largely unknown HDAC.

Given that so little is known about Hos3, a few fundamental questions wait to be addressed. The chimera assay for heterochromatin establishment and maintenance serves to answer some of these questions. For example, Hos3 is uniquely targeted but is such unique localization important? Although the answer looks apparently to be yes, the absence of a clear phenotype of *hos3*Δ cells makes it hard to experimentally test. However, by fusing Hos3 to Sir3, we clearly showed that having an intact HDAC domain is insufficient for Hos3 to function in the replacement of Sir2. Targeting Hos3 to the heterochromatin region where the chimera is supposed to be is truly important in defining where Hos3 functions. Another important question the chimera assay demonstrates is that Hos3 is indeed an HDAC *in vivo*.

Finally, together with the help of the solved crystal structure of HDAC-like protein AcuC1, the chimera assay provides us with a platform to dissect

the catalytic mechanism of Hos3 as an enzyme and also reveals point-mutation alleles of HDAC-dead Hos3 that we'll use later to investigate the HDAC-activity-dependent functions of Hos3. Hos3 is conserved for almost all AcuC1 residues that are required for the proposed HDAC catalytic mechanism. Mutations of these conserved residues abolish Hos3 HDAC activity in the chimera assay. This suggests that despite the absence of a crystal structure, we could infer that Hos3 is very likely to function as an HDAC using the same catalytic mechanism as other class I and II HDACs. Notably, one residue required for stabilizing the zinc iron as well as a few residues predicted to be in contact with TSA are not conserved. This disparity suggests that despite a likely conserved catalytic core, a mild difference may exist in the pocket structure of Hos3 compared to AcuC1 and other class I and II HDACs. Such difference in structure could determine the substrate binding and specificity of Hos3.

It's surprising to find out that apart from being targeted to so many particular cellular sites, truncated forms of Hos3 could even localize to the mitochondria. It's not yet known if full-length Hos3 is cleaved and targeted to the mitochondria *in vivo* under certain conditions or stresses. Interestingly, mitochondria are highly enriched for acetyl-lysines in mammalian cells, and many of these acetylation sites are conserved in budding yeast (Kim et al., 2006). We will discuss the potential significance of the mitochondria targeting by truncated Hos3 in Chapter 6.

REFERENCES

Carmen, A. A., Griffin, P. R., Calaycay, J. R., Rundlett, S. E., Suka, Y., & Grunstein, M. (1999). Yeast HOS3 forms a novel trichostatin A-insensitive homodimer with intrinsic histone deacetylase activity. *Proceedings of the National Academy of Sciences, 96*(22), 12356-12361.

Chou, C., Li, Y., & Gartenberg, M. R. (2008). Bypassing Sir2 and O-acetyl-ADP-ribose in transcriptional silencing. *Molecular Cell, 31*(5), 650-659.

Cid, V. J., Jiménez, J., Molina, M., Sánchez, M., Nombela, C., & Thorner, J. W. (2002). Orchestrating the cell cycle in yeast: Sequential localization of key mitotic regulators at the spindle pole and the bud neck. *Microbiology, 148*(9), 2647-2659.

Finnin, M. S., Donigian, J. R., Cohen, A., Richon, V. M., Rifkind, R. A., Marks, P. A., et al. (1999). Structures of a histone deacetylase homologue bound to the TSA and SAHA inhibitors. *Nature, 401*(6749), 188-193.

Hoppe, G. J., Tanny, J. C., Rudner, A. D., Gerber, S. A., Danaie, S., Gygi, S. P., et al. (2002). Steps in assembly of silent chromatin in yeast: Sir3-independent binding of a Sir2/Sir4 complex to silencers and role for Sir2-dependent deacetylation. *Molecular and Cellular Biology, 22*(12), 4167-4180.

Jaspersen, S. L., & Winey, M. (2004). The budding yeast spindle pole body: structure, duplication, and function. *Annual Review of Cell and Developmental Biology, 20*(1), 1-28.

Kim, S. C., Sprung, R., Chen, Y., Xu, Y., Ball, H., Pei, J., et al. (2006). Substrate and functional diversity of lysine acetylation revealed by a proteomics survey. *Molecular Cell, 23*(4), 607-618.

Kozubowski, L., Larson, J. R., & Tatchell, K. (2005). Role of the septin ring in the asymmetric localization of proteins at the mother-bud neck in saccharomyces cerevisiae. *Molecular Biology of the Cell, 16*(8), 3455-3466.

Liu, I., Chiu, S., Lee, H., & Leu, J. (2012). The histone deacetylase Hos2 forms an Hsp42-dependent cytoplasmic granule in quiescent yeast cells. *Molecular Biology of the Cell, 23*(7), 1231-1242.

Rusche, L. N., Kirchmaier, A. L., & Rine, J. (2003). The establishment, inheritance, and function of silenced chromatin in *Saccharomyces cerevisiae*. *Annual Review of Biochemistry, 72*(1), 481-516.

Sikorski, R. S., & Hieter, P. (1989). A system of shuttle vectors and yeast host strains designed for efficient manipulation of DNA in saccharomyces cerevisiae. *Genetics, 122*(1), 19-27.

CHAPTER 3

Screening of Mutants Defective in Hos3 Bud Neck Targeting

INTRODUCTION

Hos3 is distinctively targeted to the bud neck and the daughter SPB. Given that *hos3Δ* cells display no apparent phenotype, we wanted to investigate how Hos3 is specifically targeted in order to better understand its physiological functions *in vivo*. In this chapter, we decided to first search for genes that are required for Hos3 bud neck targeting.

Specific targeting of proteins to various cellular sites is often partially or totally dependent on various self-assembled high-order structures. Three subcellular ultrastructures conserved in eukaryotes (from budding yeast to human) are 1). microtubules, 2). actins, and 3). septins. In budding yeast, microtubules are made from the polymerization of α- and β-tubulins and facilitate the formation of the spindle and the positioning of the nucleus; actins form patches and filaments which are important for diverse processes such as polarity establishment, endocytosis, and vesicle trafficking; septins form high-order filaments which are further assembled into an hourglass collar structure decorating the bud neck to serve both as a diffusion barrier and as a scaffold to recruit many neck-associated proteins (Huffaker et al., 1987; Oh and Bi, 2011). We aimed to examine if any of these ultrastructures are involved in

targeting Hos3 to the bud neck.

Moreover, Hos3 is a soluble protein and sequence analysis reveals no potential transmembrane or lipid-binding domains (Figure 2.5A). Therefore, Hos3 is unlikely to have direct physical interactions with the plasma membrane at the bud neck region. Instead, it is likely that some protein(s) recruit Hos3 to the bud neck, and these protein(s) are likely themselves neck proteins. Since many of the bud neck proteins are nonessential for cellular viability, we could potentially make use of the Yeast Deletion Collection to perform a screening of the genes required for Hos3 neck targeting. The identity of these genes, if successfully found, would be instrumental for our in-depth understanding of how and why Hos3 is recruited to the bud neck.

METHODS AND MATERIALS

Yeast Strains and Plasmids

All yeast strains were annotated as in Table 3.1. Manipulation of strains should be refered to *Materials and Methods* of Chapter 2. Double mutants were made by mating the two individual single mutants for a diploid and then selecting for the spore that bears double mutant markers. In the case where both single mutants were of the same marker, the candidate double mutant spore was prepared for its genomic DNA and confirmed for both markers by PCR amplification. We found that the *hsl7Δ* cells (*MAT*α) streaked from the Yeast Deletion Collection (Research Genetics) were incorrect since an Hsl7 ORF could be confirmed by PCR amplification from the genomic DNA of this strain. Therefore, we made an *hsl7Δ* strain (RCY4702) using homology-based recombination method to delete endogenous *HSL7* gene from the wild-type strain (Longtine et al., 1998b). Deletion of the *HSL7* gene was confirmed by PCR.

All plasmids were annotated as in Table 3.2. Construction of the plasmids should be refered to *Materials and Methods* of Chapter 2.

Microscopy-based Screening

A list of ~120 genes were identified as potential candidates that are required for Hos3 bud neck targeting. The corresponding null strain was streaked from the Yeast Deletion Collection (Research Genetics) onto YPD + G418 plates. Hos3-GFP (*CEN*) was transformed into each strain and analyzed

by fluorescence microscopy. For essential genes such as Cdc42 and Cdc24, a heat-sensitive allele strain was transformed with Hos3-GFP (*CEN*) and shifted to restrictive temperature (37°C) for 1h. Adjustment of the stage on the Z-dimension reveals the pattern of Hos3 at the bud neck of each strain. Strains with defective or absent Hos3 neck localization were scored as hits.

Fluorescence Microscopy

Methods of fluorescence microscopy were similar as described in the *Materials and Methods* of Chapter 2.

Immunoblotting

Methods of immunoblotting were similar as described in the *Materials and Methods* of Chapter 2.

Table 3.1. Yeast strains used in Chapter 3

Strain	Genotype	Reference/Source
RCY239	*MAT*a *ura3-52 leu2-3,112*	This Study
RCY4042	*MAT*α *ura3 leu2 cdc3-3*	M-12 from Mark Longtine
RCY4043	*MAT*α *ura3 leu2 met1 cdc11-6*	M-34 from Mark Longtine
RCY4044	*MAT*a *ura3 leu2 his3 cdc10-1*	M-195 from Mark Longtine
RCY4045	*MAT*a *ura3 leu2 his3 trp1 cdc12-6*	M-239 from Mark Longtine
RCY4564	BY4742 *shs1Δ::KanMX4*	Research Genetics, Inc.
RCY4565	BY4742 *cla4Δ::KanMX4*	Research Genetics, Inc.
RCY4568	BY4742 *elm1Δ::KanMX4*	Research Genetics, Inc.
RCY4570	BY4742 *gin4Δ::KanMX4*	Research Genetics, Inc.
RCY4607	BY4742 *kcc4Δ::KanMX4*	Research Genetics, Inc.
RCY4609	*MAT*a *ura3Δ0 leu2Δ0 his3Δ1 lys2Δ0 met15Δ0 hos3Δ::HIS3*	This Study
RCY4624	BY4742 *hsl1Δ::KanMX4*	Research Genetics, Inc.
RCY4656	*MAT*α *ura3Δ0 leu2Δ0 his3Δ1 lys2Δ0 elm1Δ::KanMX4 hos3Δ::HIS3*	This Study
RCY4658	*MAT*α *ura3Δ0 leu2Δ0 his3Δ1 lys2Δ0 met15Δ0 gin4Δ::KanMX4 hos3Δ::HIS3*	This Study
RCY4660	*MAT*α *ura3Δ0 leu2Δ0 his3Δ1 lys2Δ0 met15Δ0 hsl1Δ::KanMX4 hos3Δ::HIS3*	This Study
RCY4702	*MAT*α *ura3Δ0 leu2Δ0 his3Δ1 lys2Δ0 hsl7Δ::KanMX4*	This Study
RCY4721	*MAT*a *ura3Δ0 leu2Δ0 his3Δ1 lys2Δ0 hsl7Δ::KanMX4 hos3Δ::HIS3*	This Study

Table 3.2. Plasmids used in Chapter 3

Plasmid	Description	Reference/Source
pRC540	pRS315	Sikorski and Hieter, 1989.
pRC2601	pRS315 Rpb10-RFP	This Study
pRC3664	pRS316 Hos3-GFP	This Study
pRC4246	pRS315 Cdc12-RFP	This Study
pRC4266	pRS315 Cdc3-RFP	This Study
pRC4267	pRS315 Cdc10-RFP	This Study
pRC4268	pRS315 Cdc11-RFP	This Study
pRC4509	pRS315 Shs1-RFP	This Study
pRC4511	pRS315 Elm1	This Study
pRC4512	pRS315 Shs1	This Study
pRC4515	pRS315 Gin4	This Study
pRC4578	pRS317 Hsl1	This Study
pRC4678	pRS315 Hsl7	This Study
pRC4747	pRS315 Hos3-3HA	This Study

RESULTS

Septins but not microtubules or actin filaments are required for Hos3 bud neck localization

To test if microtubules or actin filaments are required for Hos3 neck localization, we treated wild-type cells expressing Hos3-GFP with nocodazole, a drug causing microtubule depolymerization, or with latrunculin-B, a drug causing actin filament depolymerization. As control, cells maintain intact Hos3 bud neck localization without any treatment or with the addition of DMSO (Figure 3.1 (i) and (ii)). Similarly, Hos3 still localizes as a full ring at the bud neck in the presence of nocodazole (Figure 3.1 (iii)) or of latrunculin-B (Figure 3.1 (iv)), suggesting these cytoskeletons are not involved in the assembly of Hos3 at the bud neck.

We next examined if septins are necessary for the bud neck localization of Hos3. Septins are composed of five subunits (four essential: Cdc3, Cdc10, Cdc11, and Cdc12; one nonessential: Shs1). These subunits assemble into high-order filaments and further form an hourglass structure at the bud neck, serving as a scaffold to recruit other proteins and as a diffusion barrier between the mother and daughter cells (Oh and Bi, 2011). Hos3 colocalizes with every subunit of the septins on the daughter side of the bud neck (Figure 3.2). Proper function of septins could be interrupted by two genetic approaches. First, temperature-sensitive alleles of essential septin genes confer conditional inactivation of septins. For example, for heat-sensitive septin mutants (*cdc3-3*, *cdc10-1*, *cdc11-6*, and *cdc12-6*), septins are functional

Figure 3.1

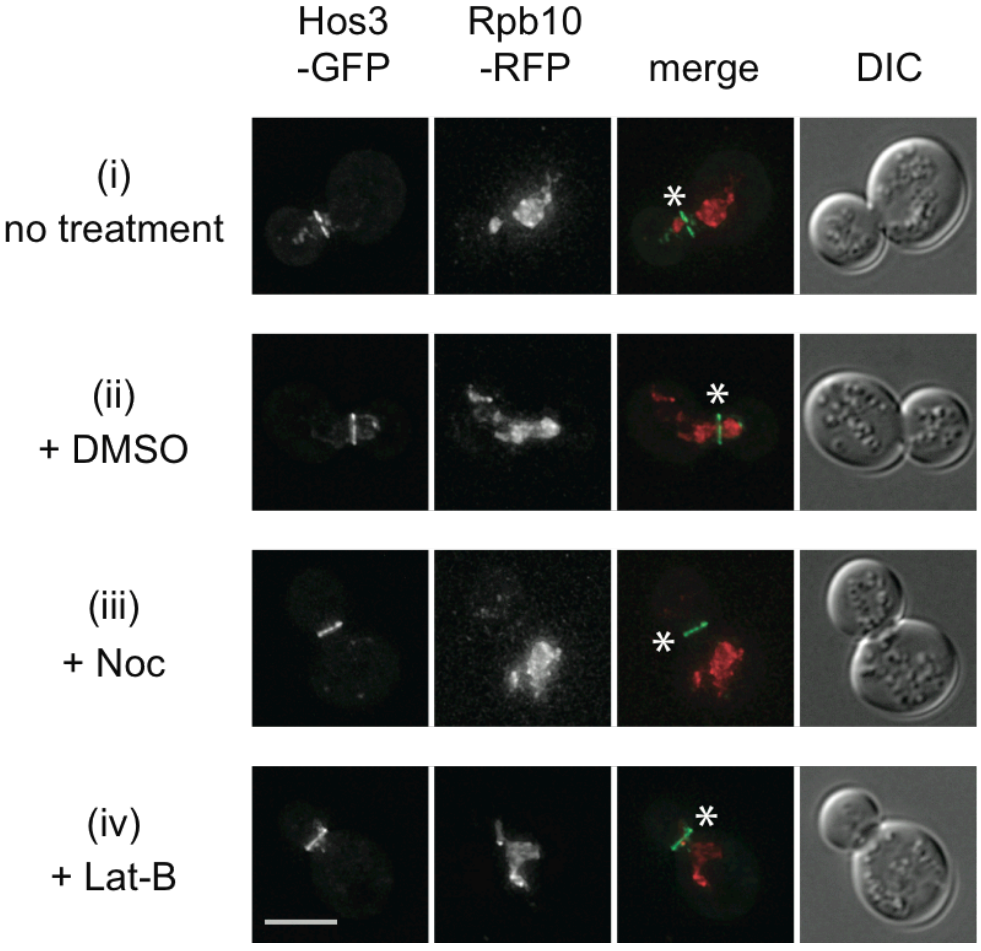
Hos3
-GFP
Rpb10
-RFP
merge
DIC
(i)
no treatment
(ii)
+ DMSO
(iii)
+ Noc
(iv)
+ Lat-B

Figure 3.1. Hos3 neck localization is intact after nocodazole or latrunculin-B treatment

Wild-type cells transformed with Hos3-GFP (*CEN*) and the nucleus marker Rpb10-RFP (*CEN*) were analyzed by fluorescence microscopy with no treatment (i) or with the addition of DMSO (ii) or of nocodazole (Noc) (iii) or of latrunculin-B (Lat-B) (iv). Cells were treated with DMSO for 2h, with Noc for 2.5h and with Lat-B for 3.5h. Asterisks denote Hos3 at the bud neck. Scale bar, 5 μm.

Figure 3.2

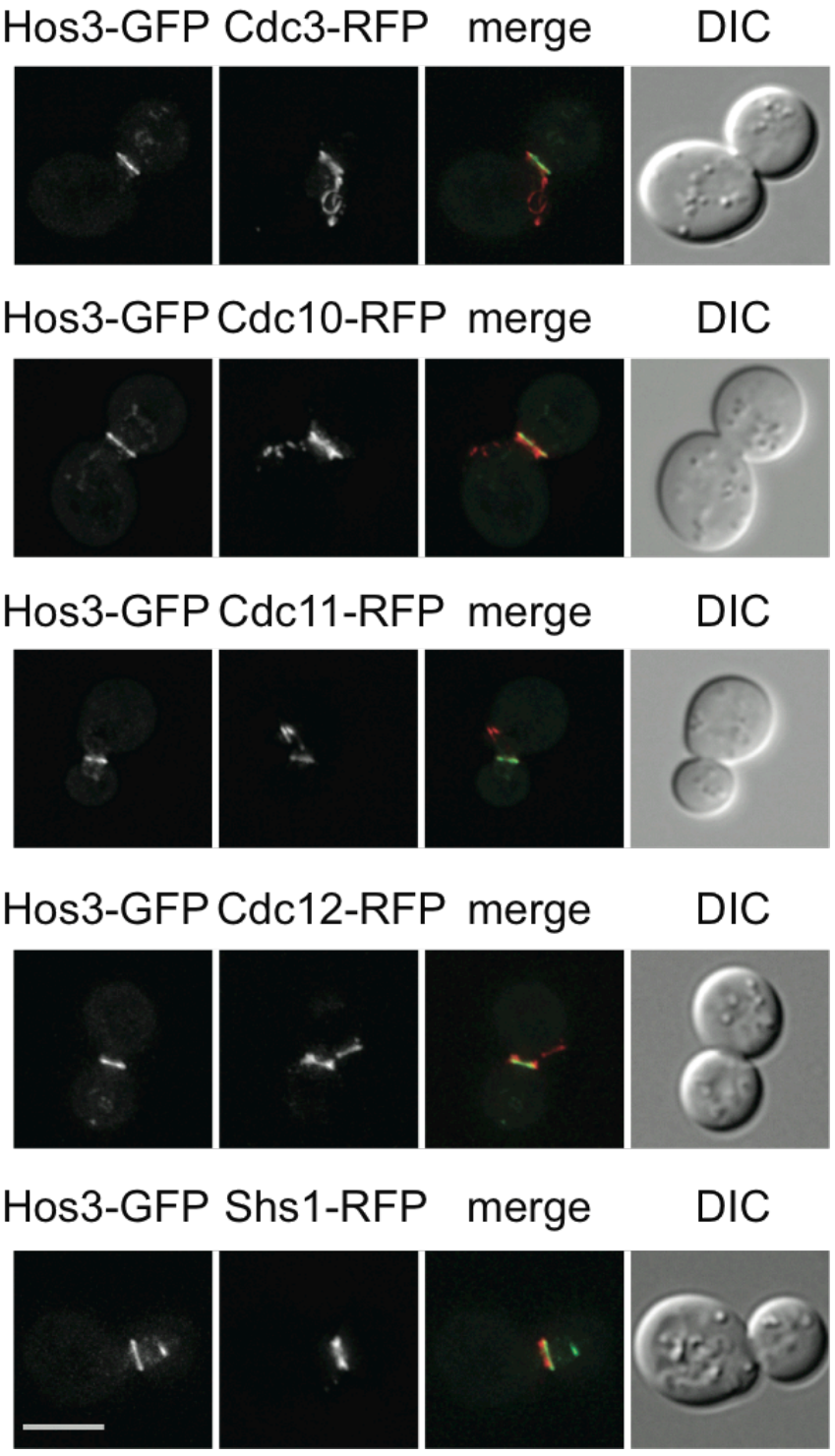
Hos3-GFP Cdc3-RFP merge DIC
Hos3-GFP Cdc10-RFP merge DIC
Hos3-GFP Cdc11-RFP merge DIC
Hos3-GFP Cdc12-RFP merge DIC
Hos3-GFP Shs1-RFP merge DIC

Figure 3.2. Hos3 colocalizes with septins

Wild-type cells respectively co-transformed with Hos3-GFP (*CEN*) and each septin subunit (Cdc3, Cdc10, Cdc11, Cdc12, and Shs1) fused with RFP (*CEN*) were analyzed by fluorescence microscopy. Scale bar, 5 μm.

at permissive temperature (room temperature, RT) but nonfunctional at restrictive temperature (37°C). As control, Hos3 maintains full-ring bud neck localization in wild-type cells at both permissive temperature (RT) and restrictive temperature (37°C) (Figure 3.3A). However, in the above heat-sensitive septin mutant cells, Hos3 is assembled as a full ring at the bud neck at permissive temperature (RT), but this localization is significantly interrupted at restrictive temperature (37°C) (Figure 3.3A). The defect of Hos3 bud neck localization could be mild as an incomplete defective ring, severe as a few puncta, or extreme as complete absence. Characterization of such features at both permissive temperature (RT) and restrictive temperature (37°C) reveals a maintenance of full-ring pattern in wild-type cells but a shift from full-ring to defective-ring or complete absence in septin mutants when septins are inactivated (Figure 3.3C). Alternatively, a second approach to interfere the function of septins is to delete the nonessential subunit Shs1. The *shs1Δ* cells, similar to heat-sensitive septin mutants at restrictive temperature, are defective in targeting Hos3 to the bud neck as a full ring and instead only a few puncta could be observed (Figure 3.3B). Such defect of Hos3 neck targeting could be fully restored by transforming a plasmid-borne Shs1 back into the *shs1Δ* cells (Figure 3.3B). The Hos3 localization at the bud neck in *shs1Δ* cells similarly displays a shift from full-ring to defective-ring or complete absence when septins are inactivated (Figure 3.3C).

Another method is available to chemically interrupt septin morphology and function. Treatment of tunicamycin (Tm), an inducer of endoplasmic

Figure 3.3

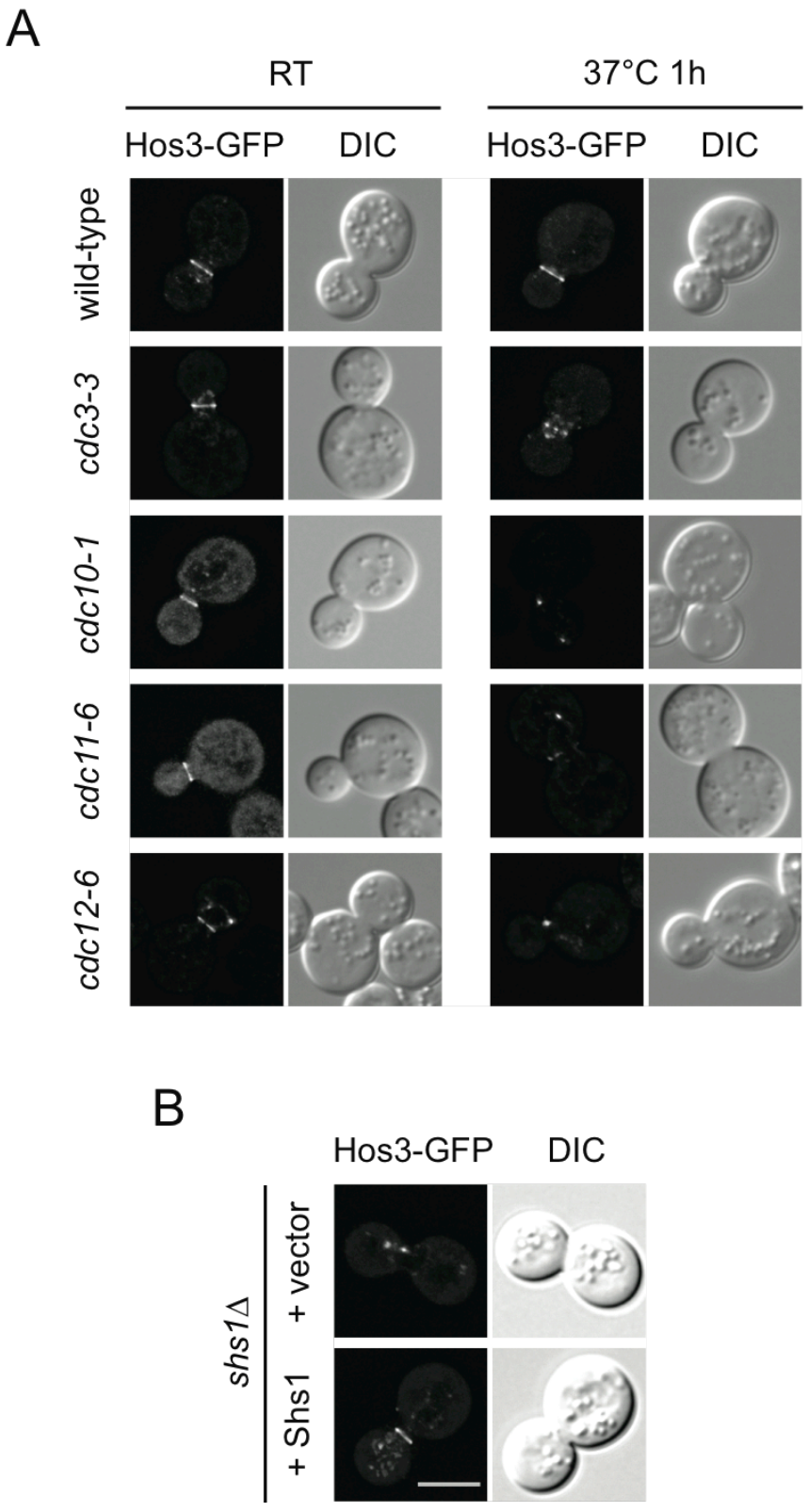
A
RT
37°C 1h
Hos3-GFP
DIC
Hos3-GFP
DIC
wild-type
cdc3-3
cdc10-1
cdc11-6
cdc12-6
B
Hos3-GFP
DIC
shs1Δ
+ vector
+ Shs1

Figure 3.3

C

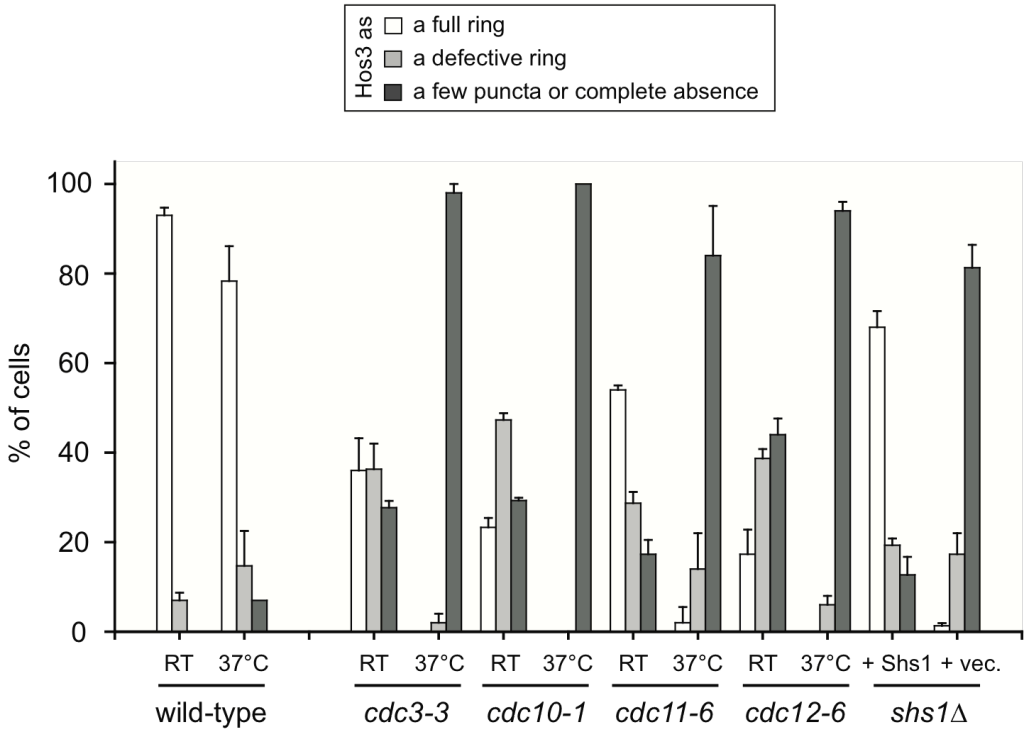
Hos3 as
a full ring
a defective ring
a few puncta or complete absence
% of cells
100
80
60
40
20
0
RT
37°C
wild-type
cdc3-3
cdc10-1
cdc11-6
cdc12-6
shs1Δ
+ Shs1
+ vec.

D

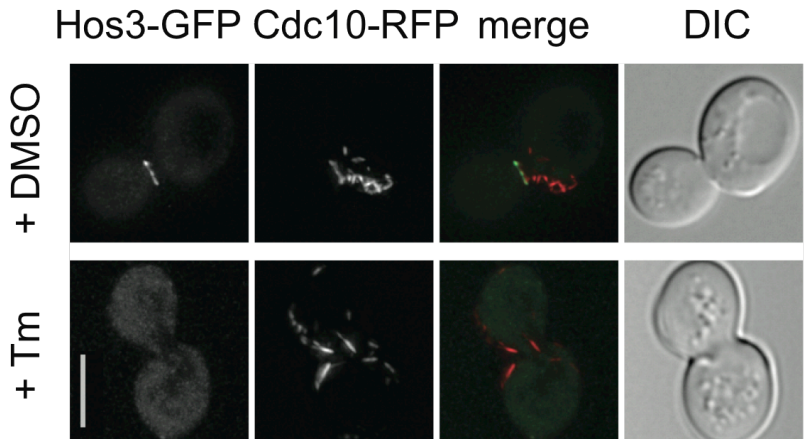
Hos3-GFP
Cdc10-RFP
merge
DIC
+ DMSO
+ Tm

Figure 3.3. Hos3 localization at the bud neck is dependent on septins

(A) Wild-type cells and heat-sensitive septin mutants (*cdc3-3*, *cdc10-1*, *cdc11-6*, and *cdc12-6*) were respectively transformed with Hos3-GFP (*CEN*), and then analyzed by fluorescence microscopy at permissive temperature (room temperature, RT) and after 1h shift to restrictive temperature (37°C).

(B) *shs1Δ* cells were transformed with Hos3-GFP (*CEN*) and cotransformed with either an empty vector or a *CEN* vector bearing Shs1. Cells were analyzed by fluorescence microscopy. Scale bar, 5 μm.

(C) The Z-serial adjustment of the microscope stage gave a 3-dimensional view of Hos3 localization at the bud neck. The neck pattern of Hos3 was characterized as 1). wild-type-like with Hos3 as a full ring, 2). mildly defective with Hos3 as an incomplete and defective ring, or 3). severely defective with Hos3 only as a few puncta or even as complete absence. Cells in (A) and (B) were scored into these three groups based on Hos3 bud neck pattern. A total of 100 cells were analyzed for each cell type at the defined conditions. Error bars, standard error of the mean (SEM).

(D) Wild-type cells transformed with Hos3-GFP (*CEN*) and septin marker Cdc10-RFP (*CEN*) were analyzed by fluorescence microscopy after 2h treatment at 30°C of dimethyl sulfoxide (DMSO) or 2 μg/ml tunicamycin (Tm). Scale bar, 5 μm.

reticulum (ER) stress, causes septin disassembly at the bud neck of budding yeast cells (Babour et al., 2010). As control, both septins and Hos3 maintain correct bud neck localization with addition of DMSO (Figure 3.3D top row). However, upon addition of Tm, septins become disassembled and quickly lose their bud neck association (Figure 3.3D bottom row). Accordingly, in the presence of Tm, Hos3 dissociates from the bud neck (Figure 3.3D bottom row). Septins apparently function upstream of the Hos3 assembly at the bud neck.

All of these results together demonstrate that localization of Hos3 at the bud neck is septin-dependent. This finding is consistent with the important role of septins as a scaffold to recruit other neck proteins to the bud neck.

Screening for mutants with defective Hos3 localization at the bud neck

It appears that although septins are necessary for Hos3 neck localization, they are unlikely the single determinant because septins are assembled as an hourglass structure (therefore decorating the daughter side, the middle, and the mother side of the bud neck) but Hos3 is only targeted to the daughter side of the bud neck (Figure 3.2). Therefore, we wanted to further expand our search of genes that are required for Hos3 neck localization. For such goals, we took a targeted approach and tried to screen for mutants with defective Hos3 neck localization. Given that the bud neck is a very defined local region, we reasoned that if any proteins other than septins are involved

in recruiting Hos3 to the bud neck, they are likely as well bud neck proteins (Figure 3.4A). Moreover, given that Hos3 is asymmetrically targeted to the daughter side of the bud neck and to the daughter SPB, this HDAC displays a clear feature of polarity (Figure 2.2A). Last but not least, the localization of Hos3 is under cell-cycle-dependent regulation (Figure 2.4). Therefore, out of the budding yeast genome, we picked out a pool of ~120 mutants covering genes critically involved in three types of cellular regulation: 1). bud neck assembly, 2). polarity establishment, and 3). cell-cycle control (Table 3.3) (Drees et al., 2001; Howell and Lew, 2012; Markus and Lee, 2011).

The majority of these genes are nonessential so we made use of their null mutants from the Yeast Deletion Collection. Alternatively, we used heat-sensitive allele for essential genes such as Cdc42 and Cdc24. For the screening, we transformed Hos3-GFP (*CEN*) into each mutant strain as a reporter and grew the cells for fluorescence microscopy analysis. Null mutants were directly tested while heat-sensitive mutants were analyzed after 2h shift to restrictive temperature (37°C). The microscope stage is capable of fine-tuned adjustment on the Z-dimension. Therefore, by visualizing cells through the FITC channel at a defined depth that reaches from the top surface to the bottom surface of the cell, we could characterize the localization of Hos3 at the bud neck. We adopted the similar categorization we previously used for studying Hos3 neck pattern in septin mutants (Figure 3.3C). We predicted that the majority of the mutant cells would behave as wild-type cells in which Hos3 is targeted as a full ring to the bud neck. However, we were interested in the

Table 3.3. List of genes included in the screening for defective targeting of Hos3 to the bud neck

Abp1, Ace2, Acf2, Acm1, Aip1, Arp1, Axl1, Axl2, Bem1, Bem2, Bem3, Bem4, Bcy1, Bfa1, Bik1, Bim1, Bni1, Bni4, Bnr1, Boi1, Boi2, Bub2, Bud2, Bud3, Bud4, Bud6, Bud8, Cap1, Cap2, Cdc24, Cdc26, Cdc42, Cdh1, Chs3, Chs4, Chs5, Cin8, Cka1, Cka2, Ckb1, Cla4, Cnm67, Cyk3, Dbf2, Dbf20, Dfg5, Dsk2, Dss4, Dyn1, Dyn2, Dyn3, Elm1, Fkh1, Fkh2, Gic1, Gic2, Gin4, Hof1, Hog1, Hsl1, Hsl7, Jnm1, Kar3, Kar9, Kcc4, Kin3, Kin4, Kip1, Kip2, Kip3, Lte1, Mih1, Mkk1, Mpc54, Msb1, Msb2, Msb3, Msb4, Mss4, Nap1, Ndl1, Nfi1, Nip100, Nis1, Num1, Pac1, Pac11, Pea2, Rad23, Rdi1, Rga1, Rga2, Rho2, Rho4, Rom1, Rom2, Rsr1, Rvs167, Sac6, Sac7, Sic1, Skg6, Skm1, Sla1, Slt2, Spa2, Spo21, Srv2, Sso1, Sso2, Ste20, Stt4, Swe1, Swi5, Syp1, Tos2, Tpm1, Tus1

For nonessential genes, a null mutant was used.

For essential genes, a heat-sensitive allele (*cdc24-2*, *cdc42-1*, *cdc42-118*) was assayed after 2h shift to restrictive temperature.

discovery of any mutants that fail to target Hos3 to the neck. The screening process is illustrated in the diagram (Figure 3.4B).

Ideally, if some proteins other than septins are indeed responsible for recruiting Hos3 to the bud neck and if they are fortunately included in our screening candidate list, we should expect two types of phenotypes (Figure 3.4B). For proteins that directly recruit Hos3 to the bud neck (eg. protein D in Figure 3.4A), their mutants (eg. *geneD*Δ) should be totally abolished for Hos3 neck localization (Figure 3.4B). In comparison, for proteins that indirectly recruit Hos3 to the bud neck (eg. protein A and protein E in Figure 3.4A), their mutants (eg. *geneA*Δ and *geneE*Δ) should be partially compromised for Hos3 neck targeting (Figure 3.4B).

Interestingly, out of the ~120 candidates, four null mutants were identified as hits from the screening: *hsl1*Δ, *hsl7*Δ, *elm1*Δ, and *gin4*Δ. Two of them fall into the first type of phenotype: Hos3 is completely absent from the bud neck in *hsl1*Δ and *hsl7*Δ cells, while the other two display the second type of phenotype: Hos3 is significantly but not completely compromised for neck targeting in *elm1*Δ and *gin4*Δ cells where Hos3 is observed as a few puncta at the neck (Figure 3.5A and 3.5B). Re-introduction of each deleted gene from a plasmid into these null mutants respectively restores Hos3 localization to the bud neck as a full ring (Figure 3.5A and 3.5B).

HSL1, *ELM1*, and *GIN4* all encode kinases; the product of *HSL7* is a protein arginine methyltransferase. The level of Hos3 is comparable between wild-type cells and the four hit mutants, arguing that the observed localization

Figure 3.4

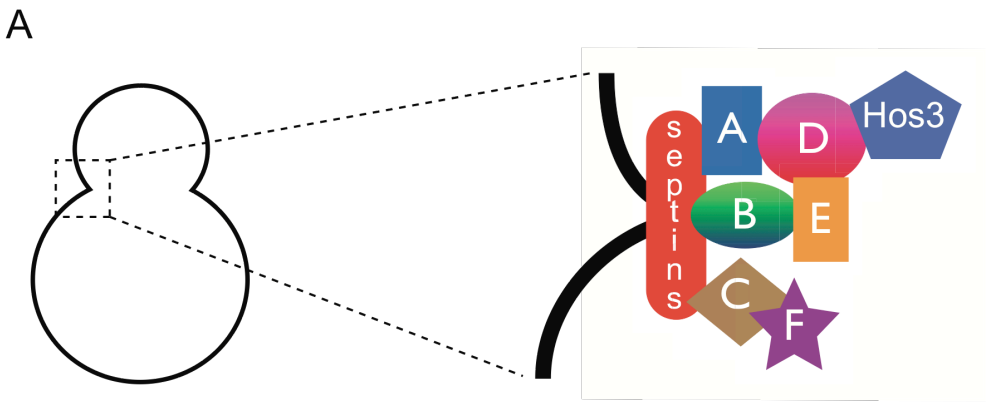

B

~ 6000 genes in *S. cerevisiae*

(~ 5000 are nonessential of which null mutants are available as a deletion collection;
~ 1000 are essential of which conditional mutants are available for some genes)

~ 120 genes encode proteins that are

(a). bud-neck-associated;
(b). required for establishment of cell polarity;
(c). cell cycle control.

mutant screening for Hos3 neck-localization pattern

(nonessential: *geneXΔ* + Hos3-GFP (*CEN*);
essential: heat-sensitive strain + Hos3-GFP (*CEN*) at restrictive temperature)

geneCΔ
geneFΔ

geneAΔ
geneEΔ

geneDΔ

Figure 3.4. A microscopy-based phenotypic screening for genes required for Hos3 neck targeting

(A) A proposed dissection of the assembly of proteins at the bud neck. The mother-bud neck of budding yeast is as an hourglass structure. Septins assemble into higher-order filaments and are associated with the plasma membrane to decorate the bud neck region. Septins function as a scaffold to recruit other proteins that are destined for the bud neck, and also as a diffusion barrier between the mother and daughter cells. Other proteins are then recruited to the bud neck in a hierarchal manner. For example, septins directly recruit proteins A, B, and C. Proteins B and C each respectively recruit protein E and F, while proteins A and E together recruit protein D. Protein D then targets Hos3 to the daughter side of the bud neck.

(B) The scheme of the strategy for screening mutants defective in Hos3 neck targeting. Fluorescence-microscopy-based screening reveals Hos3 at the bud neck as a full ring (*geneC*Δ, *geneF*Δ, etc.), as a partially defective ring (*geneA*Δ and *geneE*Δ), or as complete absence (*geneD*Δ).

Figure 3.5

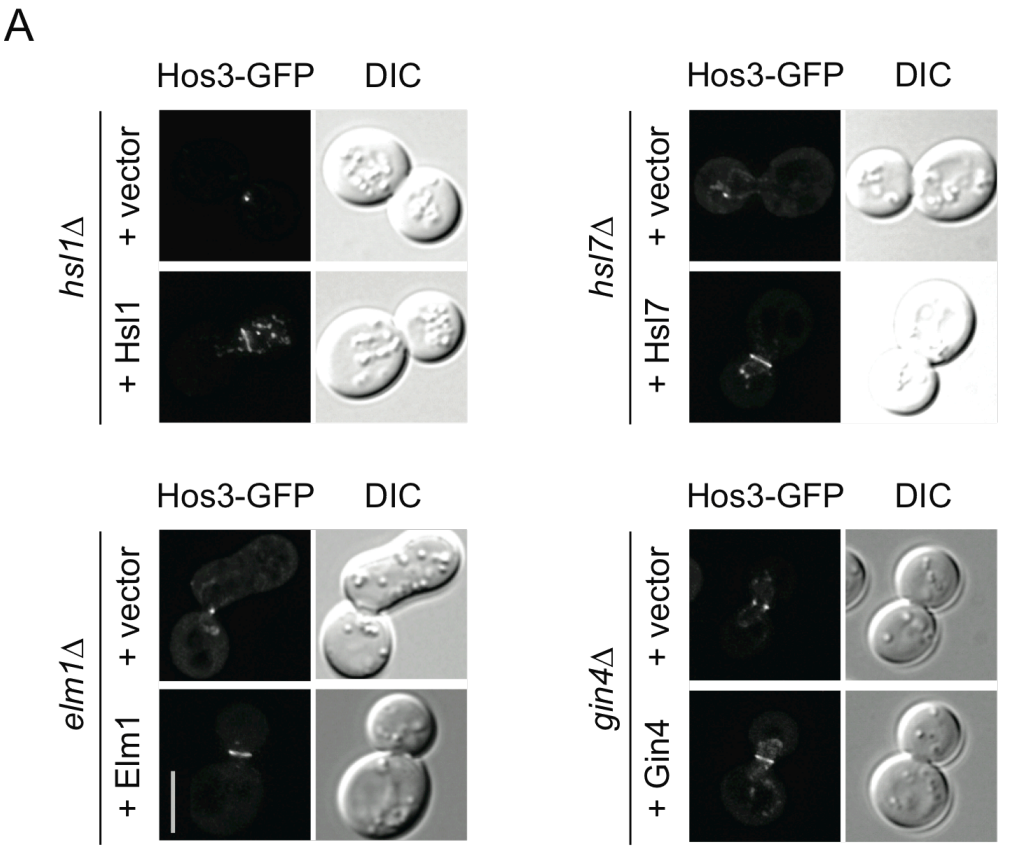
A
Hos3-GFP
DIC
hsl1Δ
+ vector
+ Hsl1
hsl7Δ
+ Hsl7
elm1Δ
+ Elm1
gin4Δ
+ Gin4
B
Hos3 as
a full ring
a defective ring
a few puncta or complete absence
% of cells
100
80
60
40
20
0
+vec.
+Hsl1
+Hsl7
+Elm1
+Gin4
hsl1Δ
hsl7Δ
elm1Δ
gin4Δ

Figure 3.5. Four genes are required for Hos3 neck targeting

(A) Screening identified four mutants deficient in Hos3 neck association. Hos3-GFP (*CEN*) was imaged in *hsl1*Δ, *hsl7*Δ, *elm1*Δ, and *gin4*Δ cells transformed with an empty vector or a *CEN* vector bearing a copy of the corresponding wild-type gene. Scale bar, 5 μm.

(B) Quantification of cells in (A) was performed as described in Figure 3.3C.

defect is not due to Hos3 downregulation (Figure 3.6A). Therefore, the hit proteins are likely to play a structural role in targeting Hos3 to the bud neck.

To validate how specific these hits are, we looked into the phenotype-negative candidates. In addition to the two hist of Hsl1 and Gin4, Kcc4 is a third member of the partially redundant Nim1-related kinases (Longtine et al., 1998a; Barral et al., 1999). However, deletion of *KCC4* does not cause Hos3 localization defect at the bud neck (Figure 3.7B). Likewise, Cla4 is a neck kinase and involved in septin filament assembly but Hos3 is intact as a full ring at the bud neck in *cla4*Δ cells (Figure 3.7C) (Versele and Thorner, 2004; Weiss et al., 2000). These data convince us that the four hits identified from the screening are highly specific regulators of Hos3 neck localization.

Figure 3.6

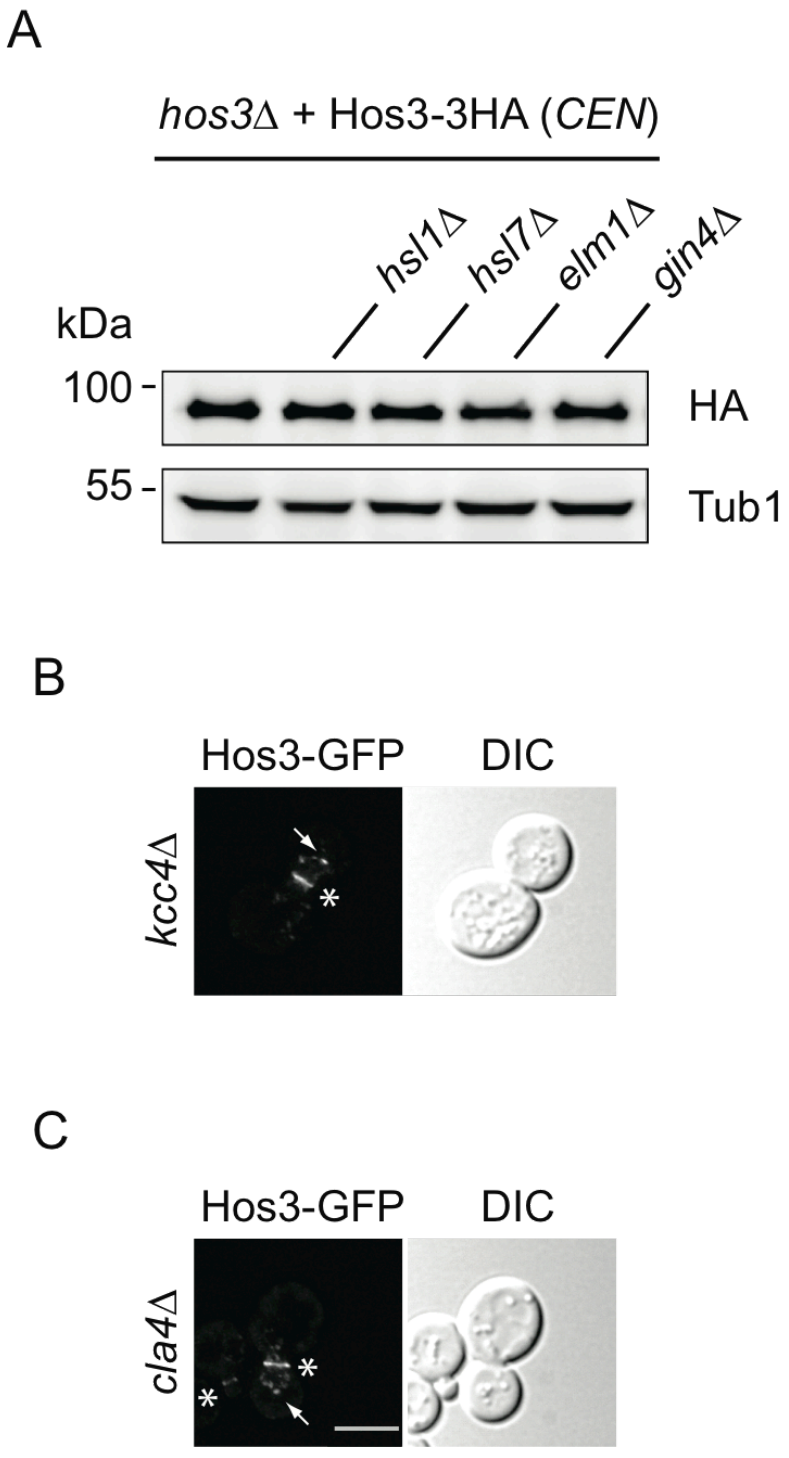
A
hos3Δ + Hos3-3HA (CEN)
hsl1Δ
hsl7Δ
elm1Δ
gin4Δ
kDa
100
55
HA
Tub1
B
Hos3-GFP
DIC
kcc4Δ
C
Hos3-GFP
DIC
cla4Δ

Figure 3.6. Hits from the screening are specific candidates

(A) Hos3 protein levels are unchanged in the mutant cells that mislocalize Hos3. A *CEN* vector bearing Hos3 fused with three tandem copies of HA tag, or Hos3-3HA (*CEN*), was respectively transformed into *hos3*Δ, *hsl1*Δ *hos3*Δ, *hsl7*Δ *hos3*Δ, *elm1*Δ *hos3*Δ, and *gin4*Δ *hos3*Δ cells. Hos3 levels in these cells were analyzed by preparing the whole cell extracts for immunoblotting against HA tag. Tub1 was used as loading control.

(B and C) Localization of Hos3-GFP (*CEN*) in *kcc4*Δ cells (B) or *cla4*Δ cells (C). Asterisks denote Hos3 at the bud neck. Arrowheads point to the daughter-SPB-associated Hos3. Scale bar, 5 μm.

DISCUSSION

Hos3 displays unique localization at the bud neck. The physiological functions of neck-anchored Hos3 are completely unknown. We reasoned that in order to solve this puzzle, the premier task is to understand how Hos3 is recruited to the bud neck in the first place. In such an effort to investigate the unknown mechanism to target Hos3 to the bud neck *in vivo*, we found septins as a scaffold complex are required. However, the direct link between Hos3 and its bud neck targeting is still missing. A screening of a selected pool of mutants identified four candidate genes (*HSL1*, *HSL7*, *ELM1*, and *GIN4*) that are required for Hos3 targeting to the bud neck. Therefore, septins and the proteins encoded by these four hit genes likely together direct the recruitment of Hos3 to the bud neck.

There is a degree of bud neck targeting defect as observed. Hos3 is completely absent from the bud neck in *hsl1*Δ and *hsl7*Δ cells. In comparison, while Hos3 localization to the bud neck is largely interrupted in septin mutant cells or *elm1*Δ and *gin4*Δ cells, Hos3 could still localize there as a few puncta. Septins are likely the scaffold and the hit genes are all reported to encode bud neck proteins so the role of septins in targeting Hos3 appears indirect. Given the nature of null mutation, it is reasonable to conclude that the effect of Elm1 and Gin4 should also be indirect. The defect phenotype as complete absence from the bud neck as observed in *hsl1*Δ and *hsl7*Δ cells clearly supports an assignment of a more direct role for them in targeting Hos3. Nevertheless, it

remains to be elucidated if one or both of Hsl1 and Hsl7 is directly involved in the recruitment of Hos3 to the bud neck.

Although our screening is of limited size therefore being noncomprehensive and biased, the fact that Hos3 is specifically targeted to the bud neck, a very defined local region of budding yeast cells, informs us that the proteins that are closely involved in targeting Hos3 are very likely to be bud neck proteins themselves. Therefore, by focusing on mutants of bud neck proteins, we exclude many genes that are not involved or at most indirectly involved in the regulation of Hos3 neck-targeting but at the same time keep an as inclusive as possible pool of highly likely candidates. As a result, we hold high confidence that the hit genes we identified from this screening would be very closely involved in targeting Hos3 to the bud neck.

REFERENCES

Babour, A., Bicknell, A. A., Tourtellotte, J., & Niwa, M. (2010). A surveillance pathway monitors the fitness of the endoplasmic reticulum to control its inheritance. *Cell, 142*(2), 256-269.

Barral, Y., Parra, M., Bidlingmaier, S., & Snyder, M. (1999). Nim1-related kinases coordinate cell cycle progression with the organization of the peripheral cytoskeleton in yeast. *Genes & Development, 13*(2), 176-187.

Drees, B. L., Sundin, B., Brazeau, E., Caviston, J. P., Chen, G., Guo, W., et al. (2001). A protein interaction map for cell polarity development. *The Journal of Cell Biology, 154*(3), 549-576.

Howell, A. S., & Lew, D. J. (2012). Morphogenesis and the cell cycle. *Genetics, 190*(1), 51-77.

Huffaker, T. C., Hoyt, M. A., & Botstein, D. (1987). Genetic analysis of the yeast cytoskeleton. *Annual Review of Genetics, 21*(1), 259-284.

Longtine, M. S., Fares, H., & Pringle, J. R. (1998). Role of the yeast Gin4p protein kinase in septin assembly and the relationship between septin assembly and septin function. *The Journal of Cell Biology, 143*(3), 719-736.

Longtine, M. S., Mckenzie III, A., Demarini, D. J., Shah, N. G., Wach, A., Brachat, A., et al. (1998). Additional modules for versatile and economical PCR-based gene deletion and modification in saccharomyces cerevisiae. *Yeast, 14*(10), 953-961.

Markus, S. M., & Lee, W. (2011). Microtubule-dependent path to the cell cortex for cytoplasmic dynein in mitotic spindle orientation. *BioArchitecture, 1*(5), 209-215.

Oh, Y., & Bi, E. (2011). Septin structure and function in yeast and beyond. *Trends in Cell Biology, 21*(3), 141-148.

Sikorski, R. S., & Hieter, P. (1989). A system of shuttle vectors and yeast host strains designed for efficient manipulation of DNA in saccharomyces cerevisiae. *Genetics, 122*(1), 19-27.

Versele, M., & Thorner, J. (2004). Septin collar formation in budding yeast requires GTP binding and direct phosphorylation by the PAK, Cla4. *The Journal of Cell Biology, 164*(5), 701-715.

Weiss, E. L., Bishop, A. C., Shokat, K. M., & Drubin, D. G. (2000). Chemical genetic analysis of the budding-yeast p21-activated kinase Cla4p. *Nature Cell Biology, 2*(10), 677-685.

CHAPTER 4.

Hsl7 of the Morphogenesis Checkpoint Recruits Hos3 to the Bud Neck

INTRODUCTION

Our previous results suggest that the association of Hos3 with the bud neck is under the control of the septins and the four hit proteins (Hsl1, Hsl7, Elm1, and Gin4). How do septins and these four hit proteins regulate Hos3 neck localization on the molecular level? The dissection of their relationship (epistasis, redundancy, independence etc.) is instrumental in revealing the underlining mechanism that targets Hos3 to the bud neck. For this purpose, we want to apply yeast genetics to build any potential pathway or genetic map in which septins and hit proteins are involved. The phenotype we tested is the neck-localization of Hos3. The goal is to narrow down the candidates (septins and four hit proteins) to the very few that are likely directly involved in targeting Hos3. Such efforts, if successful, would have two important implications. First, it helps us understand the molecular details of the intriguing bud neck association of this HDAC Hos3. Second, it would reveal the particular cellular activities Hos3 could potentially plays a role in and provide us with the appropriate mutant cells to focus on for the search of the physiological functions of Hos3.

METHODS AND MATERIALS

Yeast Strains and Plasmids

All yeast strains were annotated as in Table 4.1. Manipulation of the strains should be refered to *Materials and Methods* of Chapter 2 and 3.

All plasmids were annotated as in Table 4.2. Construction of the plasmids should be refered to *Materials and Methods* of Chapter 2 and 3.

Fluorescence Microscopy

Methods of fluorescence microscopy were similar as described in the *Materials and Methods* of Chapter 2.

Dilution Assay

Methods of dilution assy were similar as described in the *Materials and Methods* of Chapter 2.

Immunoblotting

Methods of immunoblotting were similar as described in the *Materials and Methods* of Chapter 2.

Immunoprecipitation

Genomically-tagged cells were grown to mid-log phase (OD_{600} ~ 0.6) in YPD medium. After standardizing cell density by equalizing the OD_{600} value, equal amounts of cells (a total of 10 OD_{600}) were collected by centrifugation

and resuspended in PBS buffer (137 mM sodium chloride, 2.7 mM potassium chloride, 10 mM sodium phosphate dibasic, 2 mM potassium phosphate monobasic, 0.1% Triton X-100, pH 7.4) together with protease inhibitors (1 mM EDTA, 1 mM phenylmethylsulfonyl fluoride, 1 mM benzamidine, and 1 μg/ml pepstatin A). Cells were then subjected to multiple rounds (3-5 x 1min) of glass bead beating and checked for effective lysis under the microscope (over 90% of cells were lysed). After spinning down the total cellular lysates, the supernatant was prepared for incubation with 30 μl pre-washed anti-HA agarose resin (Invitrogen) at 4°C for 4h with gentle rocking. The resins were then washed 3 times in 1 ml PBS buffer and eluted with SDS-PAGE sample buffer. After centrifugation of the resins, the supernatant was analyzed by immunoblotting for the detection of respective proteins. Antibodies used in this chapter were as following: α-HA (32-6700, Invitrogen) and α-Myc (SC-40, Santa Cruz).

Flow Cytometry

Cells were grown to mid-log phase (OD_{600} ~ 0.6) in YPD medium. Equal numbers of cells (a total of ~ 0.8 OD_{600}) were collected by centrifugation and fixed with 70% ethanol at 4°C for ~ 12-14h. Fixed cells were resuspended in 50 mM sodium citrate buffer (pH 7.4), sonicated at setting 30% for 15s (50% On-Off cycle) by a sonic dismembrator (Fisher Scientific), and incubated with 0.5 mg/ml RNAase at 50°C for 1h followed by with 1 mg/ml proteinase K at 50°C for 1h. After spinning down, cells were resuspended in 50 mM sodium

citrate buffer (pH 7.4) and stained with 16 μg/ml propidium iodide in dark at room temperature for 30min. Finally cells were subjected to analysis by a LSR II flow cytometer (Becton Dickinson).

Table 4.1. Yeast strains used in Chapter 4

Strain	Genotype	Reference/Source
W303-1A	*MAT*a *ura3-1 leu2-3,112 his3-11,15 trp1-1 can1-100 ade2-1*	This Study
W303-1B	*MAT*α *ura3-1 leu2-3,112 his3-11,15 trp1-1 can1-100 ade2-1*	This Study
BY4742	*MAT*α *ura3Δ0 leu2Δ0 his3Δ1 lys2Δ0*	Research Genetics, Inc.
RCY3915	BY4742 *hos3Δ::KanMX4*	Research Genetics, Inc.
RCY4564	BY4742 *shs1Δ::KanMX4*	Research Genetics, Inc.
RCY4568	BY4742 *elm1Δ::KanMX4*	Research Genetics, Inc.
RCY4570	BY4742 *gin4Δ::KanMX4*	Research Genetics, Inc.
RCY4624	BY4742 *hsl1Δ::KanMX4*	Research Genetics, Inc.
RCY4669	*MAT*a *ura3Δ0 leu2Δ0 his3Δ1 lys2Δ0 met15Δ0 elm1Δ::KanMX4 gin4Δ::KanMX4*	This Study
RCY4692	*MAT*a *ura3Δ0 leu2Δ0 his3Δ1 lys2Δ0 met15Δ0 Hsl7-13Myc::HIS3*	This Study
RCY4693	*MAT*α *ura3Δ0 leu2Δ0 his3Δ1 lys2Δ0 trp1 Hos3::3HA-HIS3*	This Study
RCY4696	BY4742 *swe1Δ::KanMX4*	Research Genetics, Inc.
RCY4702	*MAT*α *ura3Δ0 leu2Δ0 his3Δ1 lys2Δ0 hsl7Δ::KanMX4*	This Study
RCY4716	BY4742 *mih1Δ::KanMX4*	Research Genetics, Inc.
RCY4724	*MAT*a *ura3Δ0 leu2Δ0 his3Δ1 lys2Δ0 hsl1Δ::KanMX4 hsl7Δ::KanMX4*	This Study
RCY4725	*MAT*α *ura3Δ0 leu2Δ0 his3Δ1 lys2Δ0 elm1Δ::KanMX4 hsl7Δ::KanMX4*	This Study
RCY4727	*MAT*a *ura3Δ0 leu2Δ0 his3Δ1 lys2Δ0 elm1Δ::KanMX4 swe1Δ::KanMX4*	This Study
RCY4728	*MAT*a *ura3Δ0 leu2Δ0 his3Δ1 lys2Δ0 hsl7Δ::KanMX4 swe1Δ::KanMX4*	This Study
RCY4730	*MAT*a *ura3Δ0 leu2Δ0 his3Δ1 lys2Δ0 hsl1Δ::KanMX4 swe1Δ::KanMX4*	This Study

RCY4731	*MAT*a *ura3Δ0 leu2Δ0 his3Δ1 lys2Δ0 met15Δ0 shs1Δ::KanMX4 swe1Δ::KanMX4*	This Study
RCY4732	*MAT*a *ura3Δ0 leu2Δ0 his3Δ1 lys2Δ0 met15Δ0 gin4Δ::KanMX4 swe1Δ::KanMX4*	This Study
RCY4733	*MAT*α *ura3Δ0 leu2Δ0 his3Δ1 lys2Δ0 gin4Δ::KanMX4 hsl7Δ::KanMX4*	This Study
RCY4773	*MAT*α *ura3Δ0 leu2Δ0 his3Δ1 lys2Δ0 Hsl7-13Myc::HIS3 Hos3-3HA::HIS3*	This Study
RCY4889	*MATa ura3 leu2 his3 lys2 ade2*	YTH1636 in Turner et al., 2010.
RCY4890	*MATa ura3 leu2 his3 lys2 ade2 apc5^{CA}-PA::His5*	YTH1637 in Turner et al., 2010.
RCY4891	*MATa ura3 leu2 his3 lys2 ade2 hos3::KanMX6*	YTH2804 in Turner et al., 2010.
RCY4892	*MATa ura3 leu2 his3 lys2 ade2 apc5^{CA}-PA::His5 hos3::KanMX6*	YTH2806 in Turner et al., 2010.
RCY4896	W303-1A *hos3Δ::HIS3*	This Study
RCY4897	W303-1A *hsl7Δ::HIS3*	This Study
RCY4943	*MATa ura3 leu2 his3 lys2 ade2 apc5^{CA}-PA::His5 hsl7Δ::KanMX4*	This Study
RCY4947	*MATa ura3 leu2 his3 lys2 ade2 hsl7Δ::KanMX4*	This Study

Table 4.2. Plasmids used in Chapter 4

Plasmid	Description	Reference/Source
pRC380	pRS317	Sikorski and Boeke, 1991.
pRC2601	pRS315 Rpb10-RFP	This Study
pRC3664	pRS316 Hos3-GFP	This Study
pRC4267	pRS315 Cdc10-RFP	This Study
pRC4578	pRS317 Hsl1	This Study
pRC4579	pRS317 Hsl1^{K110R}	This Study
pRC4620	pRS315 Elm1-RFP	This Study
pRC4621	pRS315 Gin4-RFP	This Study
pRC4623	pRS315 Hsl1-RFP	This Study
pRC4624	pRS315 Hsl7-RFP	This Study
pRC4676	pRS316 Hos3$^{S47A, T201A, S533A, T671A}$-GFP	This Study
pRC4682	pRS317 Hsl7	This Study
pRC4707	pRS425 Elm1	This Study
pRC4708	pRS425 Gin4	This Study
pRC4751	pRS315 Gin4-Hsl7-RFP	This Study
pRC4762	pRS315 Sec2-Hsl7-RFP	This Study
pRC4839	pRS315 Sec2-RFP	This Study
pRC5060	pRS315 Tub4-RFP	This Study
pRC5071	pRS315 Hsl7^{K254E}-RFP	This Study

RESULTS

Hits from the screening are members of the morphogenesis checkpoint

Similar to septins, Hsl1, Hsl7, Elm1, and Gin4 all localize to the bud neck as a full ring (Figure 4.1). This supports the idea that these proteins function as structural components to recruit Hos3 to the bud neck. Intriguingly, we looked into the literature and found that the four hits from the screening are all members of a single signaling pathway – the morphogenesis checkpoint – that is critical for monitoring bud growth with regard to cell cycle progression (Lew, 2000; Blacketer et al., 1993; Longtine et al., 1998; Keaton and Lew, 2006).

Budding yeast cells grow and replicate in a highly polarized manner (Figure 4.2A). After accurate DNA duplication and cell cycle progression from S phase into G_2 phase, the machinery required for budding is recruited to the future bud site and promotes the growth of a bud. After budding, the nucleus is driven toward the bud neck and cells enter mitosis to allow for spindle elongation and segregation. Cells then exit mitosis and finally undergo cytokinesis, completing the reproduction process. Consequently, the genetic materials are evenly distributed in that the mother cell and the daughter cell each inherit one nucleus. Clearly, the mother-bud axis essentially defines the spatial direction of many cellular activities such as bud growth, exocytic vesicle trafficking, spindle orientation, and nuclear segregation. Therefore, the growth and presence of a bud is an instrumental incidence. However, certain environmental stresses such as heat or osmotic shock or certain intrinsic

Figure 4.1

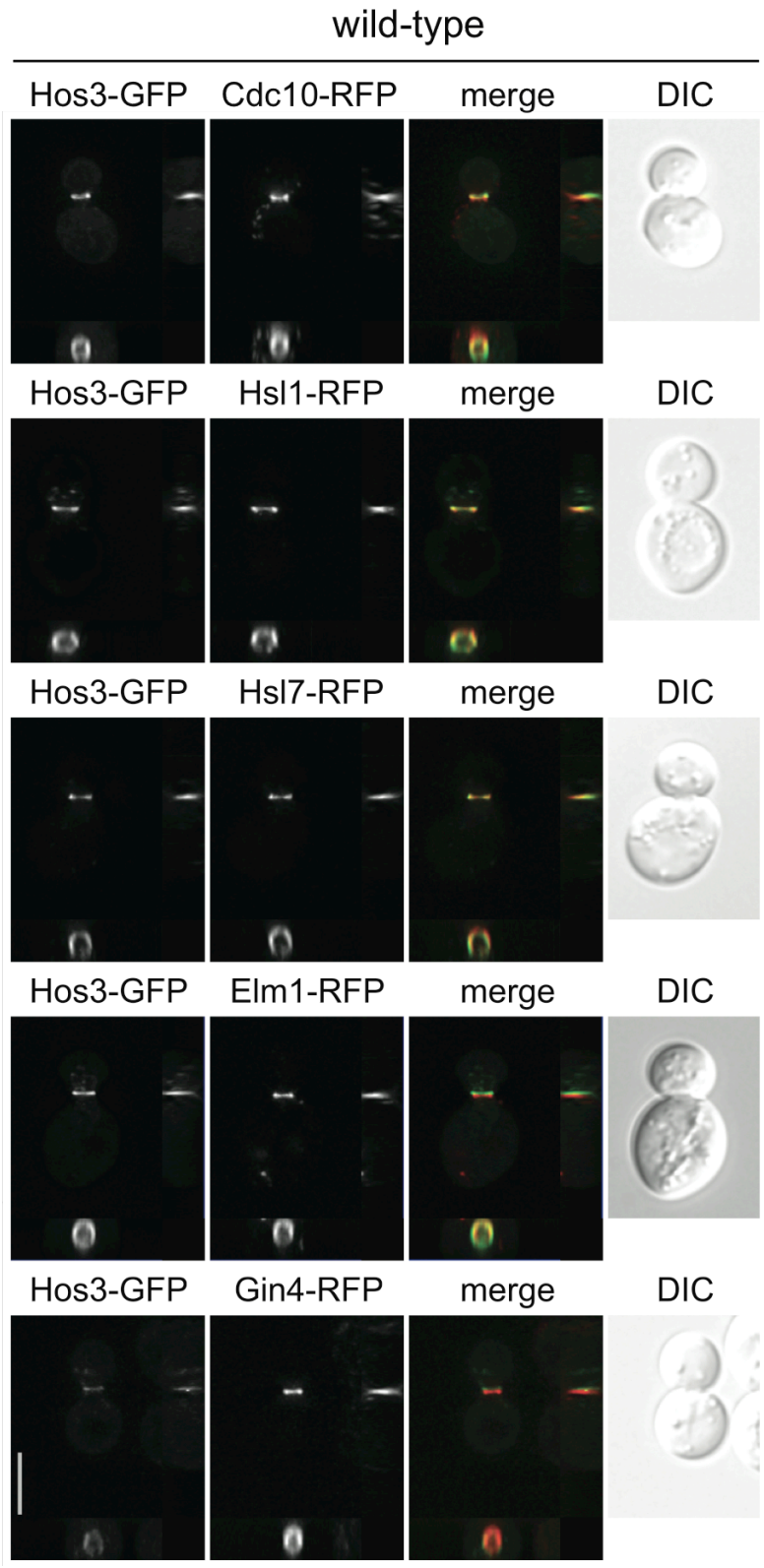
wild-type
Hos3-GFP
Cdc10-RFP
merge
DIC
Hos3-GFP
Hsl1-RFP
merge
DIC
Hos3-GFP
Hsl7-RFP
merge
DIC
Hos3-GFP
Elm1-RFP
merge
DIC
Hos3-GFP
Gin4-RFP
merge
DIC

Figure 4.1. Septins and the four hit proteins localize to the bud neck

Wild-type cells were cotransformed with Hos3-GFP (*CEN*) and Cdc10-RFP (*CEN*) or Hsl1-RFP (*CEN*) or Hsl7-RFP (*CEN*) or Elm1-RFP (*CEN*) or Gin4-RFP (*CEN*) respectively, and analyzed by fluorescence microscopy. Cdc10-RFP is used as the marker for septins. Images are rotated with the bud neck parallel to the horizontal axis. To illustrate the localization pattern at the bud neck, image projection on the XZ-dimension is displayed below and on the YZ-dimension is shown on the right. Scale bar, 5 μm.

stresses such as genetic mutations would interfere the machinery for polarized bud growth (Figure 4.2B). In such conditions, bud growth is significantly delayed. Given that the morphological growth and the nuclear segregation events are highly linked in budding yeast due to the mother-bud polarity, the cell cycle progression also needs to be delayed to prevent cells without budding from entering mitosis. The morphogenesis checkpoint is the machinery cells adopt to monitor such coordination between bud growth and mitotic entry. When cells grow a bud, the morphogenesis checkpoint becomes active in promoting mitotic entry and cell-cycle progression (Figure 4.2A). As a comparison, in the absence of a bud, the morphogenesis checkpoint is inactive so that cells are prevented from mitotic entry but instead triggered for a cell-cycle delay to allow extra time for adaptation to the stresses disallowing bud growth and finally re-growing a bud (Figure 4.2B). With the specific function of the morphogenesis checkpoint, cells are equipped intrinsically with a mechanism to allow mitotic entry only after successful bud growth. Under such elegant regulation, the morphological growth and the cell-cycle progression are tightly linked to approve accurate reproduction.

Therefore, if the morphogenesis checkpoint becomes nonfunctional, cells under stresses that delay or block bud growth will nevertheless still enter mitosis and ultimately result in becoming binucleate cells (Figure 4.2C). The morphogenesis checkpoint functions as a hierarchical signaling pathway on the molecular level (Figure 4.2D). Certain transient or sustained stresses inhibit bud growth. In such unbudded cells, the cyclin-dependent kinase (CDK)

Cdc28 undergoes an inhibitory Y19 phosphorylation by Swe1 kinase, a Wee1 homologue. This inhibitory tyrosine phosphorylation significantly reduces the activity of the CDK-cyclin complex and thus leads to a temporary G_2 delay for cells to adapt to the stresses and ideally re-grow a bud. The unbudded cells under stresses are devoid of a bud and accordingly of a bud neck. The absence of the bud neck renders septins and morphogenesis checkpoint members cytosolic (rather than bud-neck-associated) and thus inactive. The morphogenesis checkpoint is inactive in these unbudded cells. Therefore, cells do not enter mitosis but are arrested for a cell-cycle delay (Figure 4.2D (i)).

After re-adaptation or stress removal, cells then activate the bud growth machinery. Once budding resumes, formation of a bud accordingly results in the appearance of the structure of a bud neck. The bud neck then functions as the foundation for many bud neck proteins to be recruited. First, septins are assembled at the bud neck by binding to phosphoinositides, predominantly phosphatidylinositol 4-phosphate (PI(4)P) and phosphatidylinositol 5-phosphate (PI(5)P), at the plasma membrane (Casamayor et al., 2003). The assembled septins now serves as a scaffold for the sequential recruitment of other proteins of which targeting to the bud neck seems to be required for their activation. Particularly, Elm1 and Gin4 are recruited by the septins. One function possibly shared by Elm1 and Gin4 is to then correctly assemble Hsl1 at the bud neck. Neck-localized Hsl1 physically interacts with and recruits Hsl7. By this stage, the Hsl1-Hsl7 complex is bud-neck-associated, activated, and functions to direct the Swe1 kinase to ubiquitin-mediated and 26S-

Figure 4.2

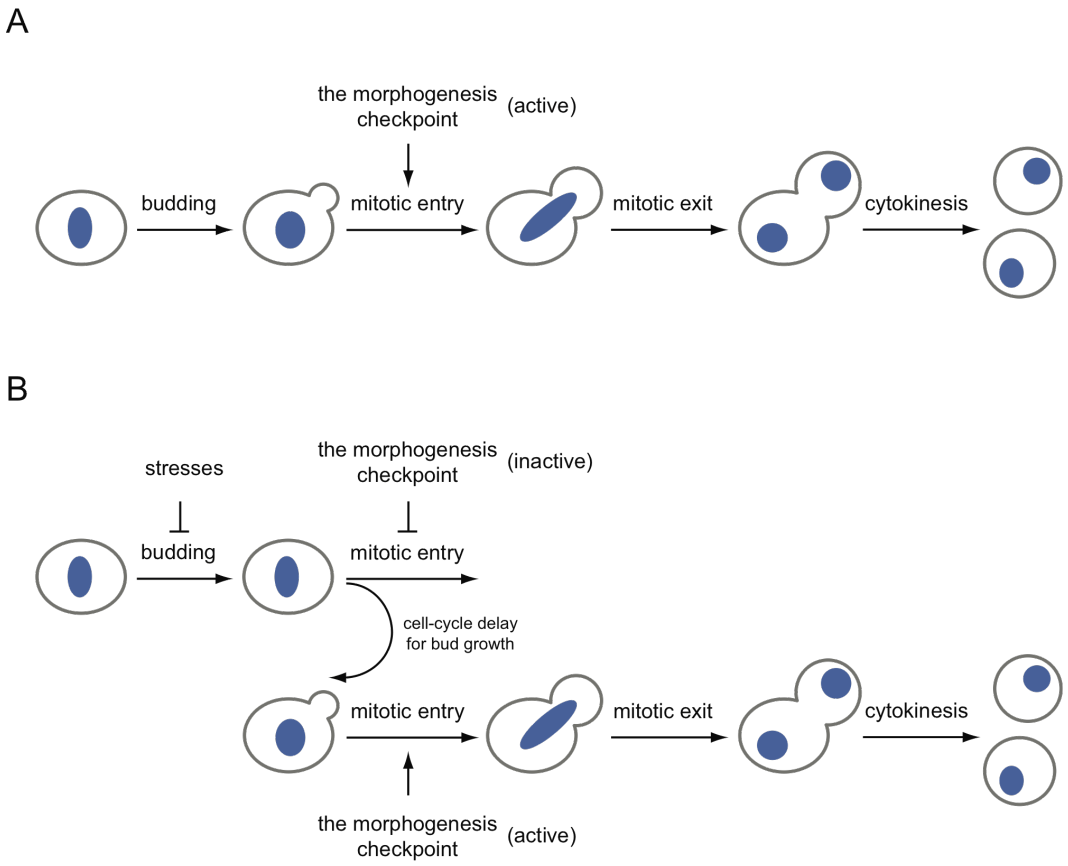
A
the morphogenesis checkpoint
(active)
budding
mitotic entry
mitotic exit
cytokinesis
B
stresses
the morphogenesis checkpoint
(inactive)
budding
mitotic entry
cell-cycle delay for bud growth
mitotic entry
mitotic exit
cytokinesis
the morphogenesis checkpoint
(active)
C
stresses
the morphogenesis checkpoint
budding
mitotic entry
mitotic exit

Figure 4.2

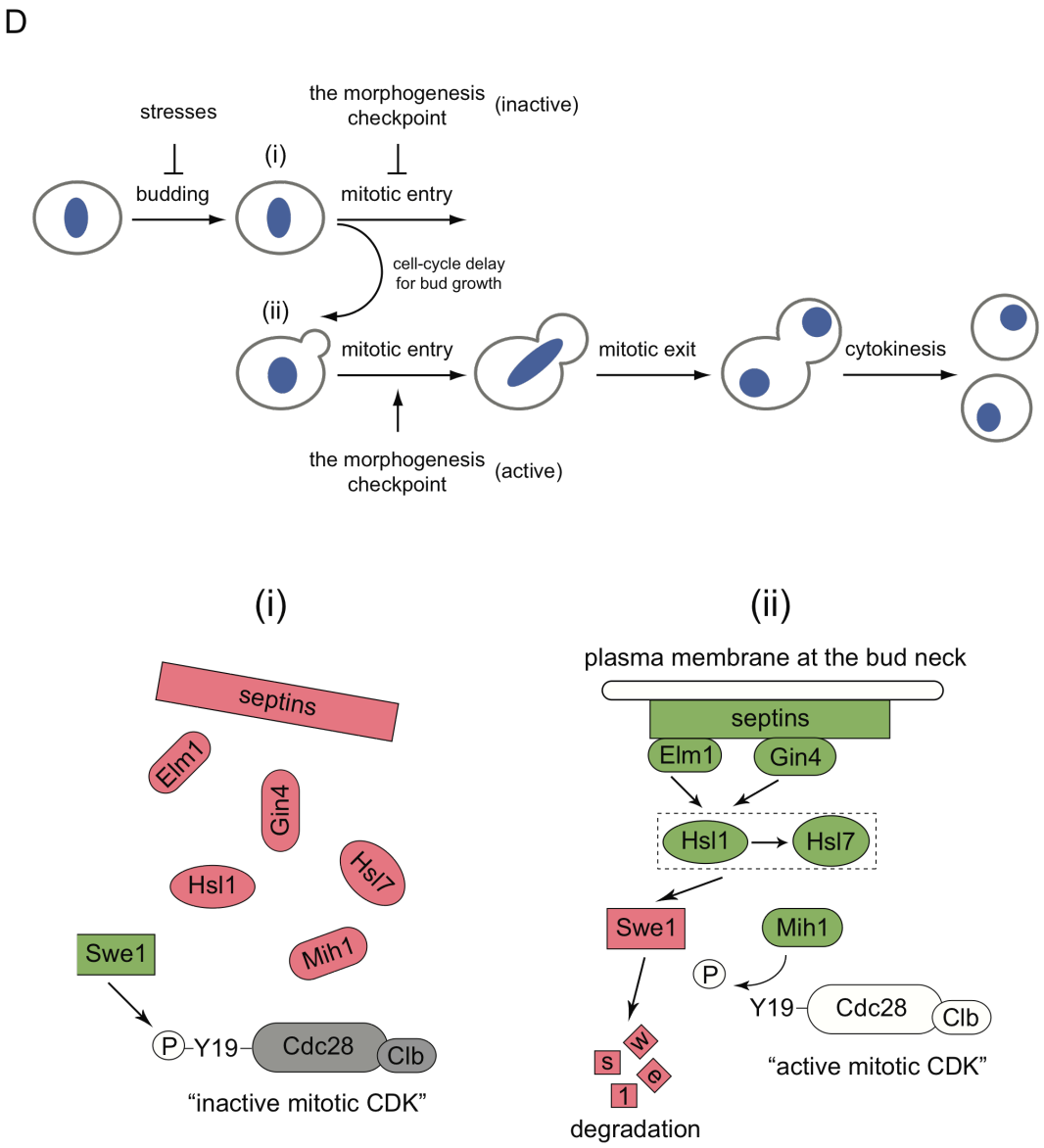
D
stresses
the morphogenesis checkpoint
(inactive)
budding
(i)
mitotic entry
cell-cycle delay for bud growth
(ii)
mitotic entry
mitotic exit
cytokinesis
the morphogenesis checkpoint
(active)
(i)
septins
Elm1
Gin4
Hsl1
Hsl7
Swe1
Mih1
P
Y19
Cdc28
Clb
"inactive mitotic CDK"
(ii)
plasma membrane at the bud neck
septins
Elm1
Gin4
Hsl1
Hsl7
Swe1
Mih1
P
Y19
Cdc28
Clb
"active mitotic CDK"
s
w
e
1
degradation

Figure 4.2. The morphogenesis checkpoint prevents mitotic entry in the absence of budding

Schematic illustration demonstrates the role of the morphogenesis checkpoint. The black circles denote yeast cells and the blue spheres denote the nucleus. (A) A typical cell cycle involves the sequential progression from an unbudded cell to two resulting cells each inheriting one set of genetic materials. In the presence of budding, active morphogenesis checkpoint allows mitotic entry. (B) Under certain environmental stresses such as heat or osmotic shock, or certain intrinsic stresses such as genetic mutations, cells fail to efficiently grow a bud. The morphogenesis checkpoint is not active and functions to prevent mitotic entry for such cells. The resulting cell-cycle delay allows cells extra time to readapt to the stresses so as to grow a bud and then re-enter the normal cell cycle to execute mitotic entry after reactivation of the morphogenesis checkpoint.

(C) When the morphogenesis checkpoint is nonfunctional, cells under stresses as described in (B) fail to grow a bud but nevertheless still enters mitosis. This finally results in binucleate cells given that the original unbudded cells have duplicated and segregated genetic materials but have not yet undergone cellular division.

(D) A mechanistic model of the morphogenesis checkpoint is illustrated for cells that fail to grow a bud (i) and cells that re-grow a bud (ii). For fill colors, red denotes “inactive” and green indicates “active”. The dashed box denotes the Hsl1-Hsl7 complex.

proteasome-dependent degradation. Meanwhile, the Mih1 phosphatase, a Cdc25 homologue, is activated to oppose the action of Swe1 kinase. As a consequence, Swe1 downregulation and Mih1 activation synergistically remove the inhibitory Y19 phosphorylation of Cdc28 and thus allow the active CDK-cyclin complex to propel cell-cycle progression into mitotic entry. The morphogenesis checkpoint is active in these rebudded cells. Therefore, after re-growing a bud, cells escape the cell-cycle delay and efficiently enter mitosis (Figure 4.2D (ii)).

Targeting Hos3 to the bud neck is upstream of CDK regulation

In order to understand how Hos3 is targeted to the bud neck by the morphogenesis checkpoint components, we wanted to map at which stage the bud neck localization of Hos3 is regulated. The signaling output of the morphogenesis checkpoint is the regulation of mitotic CDK activity through Swe1 and Mih1 (Figure 4.2D). Deletion of either *SWE1* or *MIH1* has no impact on Hos3 association with the bud neck (Figure 4.3A). This suggests that the regulation of Hos3 neck targeting is independent of Swe1 or Mih1. One hypothesis that the morphogenesis checkpoint components came out from the screening as hits could be that deletion of such genes result in inactive morphogenesis checkpoint and thus a sustained cell-cycle delay that causes Hos3 bud neck targeting defect. To address this issue, we noticed that the G_2 cell-cycle delay by the morphogenesis checkpoint is totally Swe1-dependent.

Therefore, deletion of *SWE1* abolishes the inhibitory phosphorylation of Cdc28 and thus removes the cell-cycle delay. Interestingly, deletion of *SWE1* in the septin or hit mutants does not restore Hos3 full-ring neck localization (Figure 4.3B, compared to Figure 3.3B and 3.5A). The result indicates that the cell-cycle delay due to the inactivation of the morphogenesis checkpoint is not responsible for the cellular defect to target Hos3 to the bud neck. Alternatively, we noticed that Hos3 is a potential Cdc28 substrate so it is possible that phosphorylation of Hos3 by Cdc28 is required for its neck localization (Holt et al., 2009). In this model, Cdc28 becomes inactive in the hit mutants and thus could not efficiently phosphorylate Hos3 to direct its neck localization. However, an allele of Hos3 with all four Cdc28 consensus sites mutated to alanine, Hos3$^{S47A,\ T201A,\ S533A,\ T671A}$, or Hos3(4A), mimics the non-phosphorylated form of Hos3 but displays wild-type-like pattern of localization (Figure 4.3C). This clearly demonstrates that the potential phosphorylation of Hos3 by Cdc28 is not involved in targeting Hos3 to the bud neck. Together, all of these data suggest that the targeting of Hos3 to the bud neck is upstream of the CDK regulation by the morphogenesis checkpoint.

Targeting Hos3 to the bud neck is downstream of Elm1 and Gin4

During our efforts in characterizing Hos3 bud neck localization in the hit mutants, we surprisingly noticed a rescue effect: an extra copy of plasmid-borne Hsl1 restores Hos3 as a full ring to the bud neck in *elm1*Δ or *gin4*Δ cells

Figure 4.3

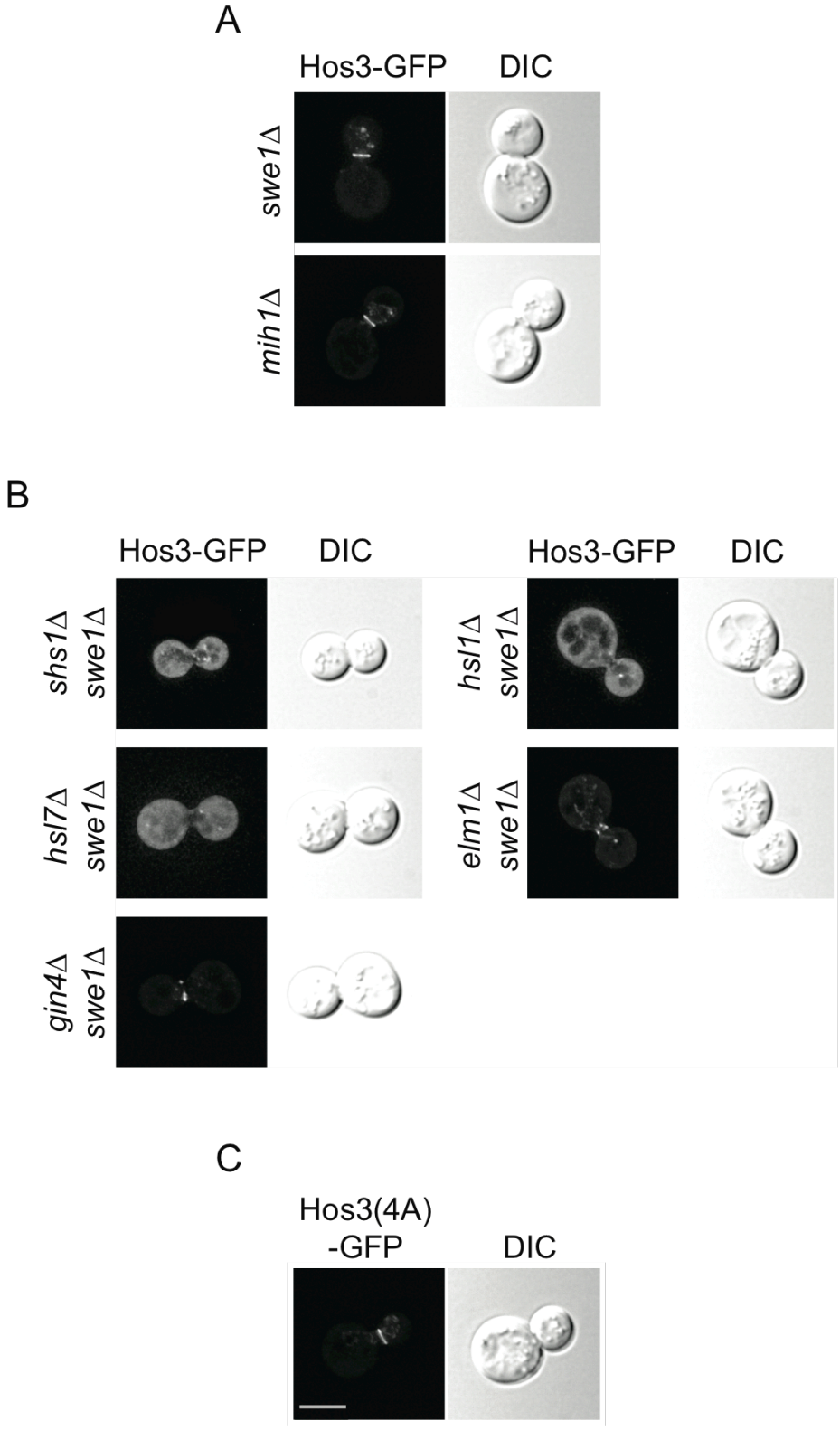
A
Hos3-GFP
DIC
swe1Δ
mih1Δ
B
Hos3-GFP
DIC
Hos3-GFP
DIC
shs1Δ swe1Δ
hsl1Δ swe1Δ
hsl7Δ swe1Δ
elm1Δ swe1Δ
gin4Δ swe1Δ
C
Hos3(4A)
-GFP
DIC

Figure 4.3. Targeting Hos3 to the bud neck is upstream of CDK regulation

(A) Localization of Hos3-GFP (*CEN*) in *swe1*Δ and *mih1*Δ cells.

(B) Hos3 neck defect in the septin or hit mutants is not caused by Swe1-dependent cell-cycle delay. The double mutant cells of *shs1*Δ *swe1*Δ, *hsl1*Δ *swe1*Δ, *hsl7*Δ *swe1*Δ, *elm1*Δ *swe1*Δ, and *gin4*Δ *swe1*Δ were respectively transformed with Hos3-GFP (*CEN*) and analyzed by fluorescence microscopy.

(C) Localization of Hos3$^{S47A,\ T201A,\ S533A,\ T671A}$-GFP (*CEN*), or Hos3(4A)-GFP, in wild-type cells. S47, T201, S533, and T671 of Hos3 are the four Cdc28 consensus sites (S/TPXK/R). Scale bar, 5 μm.

(Figure 4.4A, compared to Figure 3.5A). The similar effect is observed even in *elm1*Δ *gin4*Δ double mutant cells (Figure 4.4B). Given the model of the morphogenesis checkpoint, Elm1 and Gin4 functions upstream to activate and assemble Hsl1 to the bud neck (Figure 4.2D). We reasoned that Elm1 and Gin4 likely act in parallel to activate Hsl1 (Figure 4.2D). Supporting this hypothesis, overexpression of Gin4 in *elm1*Δ cells or of Elm1 in *gin4*Δ cells could not restore Hos3 neck localization suggesting Elm1 and Gin4 are unlikely to act within a single linear pathway (Figure 4.4C). Therefore, the loss of Hsl1 activation by upstream Elm1 in *elm1*Δ cells or by upstream Gin4 in *gin4*Δ cells or by both Elm1 and Gin4 in *elm1*Δ *gin4*Δ double mutant cells could be compensated by increasing the basal level of downstream Hsl1. Hsl1 activity over a threshold then enables the recruitment of Hos3 to the bud neck. Consistent with the requirement of Hsl1 kinase activity for targeting Hos3 to the bud neck, the rescue effect is dependent on Hsl1 as an active kinase. Kinase-dead Hsl1 fails to restore Hos3 neck localization in *elm1*Δ, *gin4*Δ, or *elm1*Δ *gin4*Δ cells (Figure 4.4D). This supports our analysis that Elm1 and Gin4 act upstream to activate Hsl1 and a threshold of Hsl1 activity is required for Hos3 bud neck localization.

Increased Hsl1 activity first restores Hsl1 itself to the bud neck in *elm1*Δ or *gin4*Δ cells (Figure 4.4E). Given that Hsl1 recruits Hsl7 to form a complex, Hsl7 is also restored to the bud neck under similar conditions (Figure 4.4F). These data combined indicate that as a consequence of increased Hsl1 activity in *elm1*Δ, *gin4*Δ, or *elm1*Δ *gin4*Δ cells, Hsl1, Hsl7, and Hos3 are all

Figure 4.4

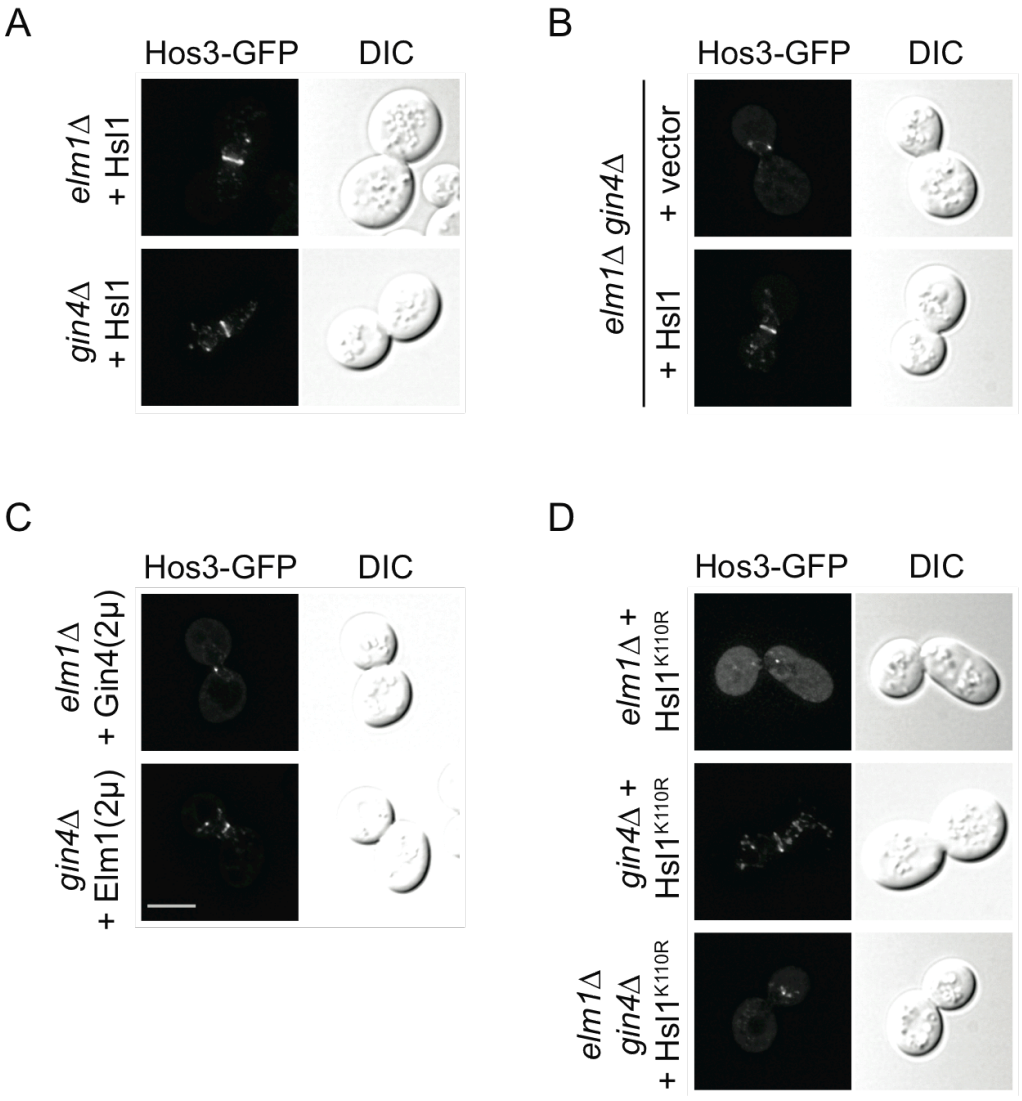
A
Hos3-GFP
DIC
elm1Δ + Hsl1
gin4Δ + Hsl1
B
Hos3-GFP
DIC
elm1Δ gin4Δ
+ vector
+ Hsl1
C
Hos3-GFP
DIC
elm1Δ + Gin4(2μ)
gin4Δ + Elm1(2μ)
D
Hos3-GFP
DIC
elm1Δ + Hsl1K110R
gin4Δ + Hsl1K110R
elm1Δ gin4Δ + Hsl1K110R

Figure 4.4

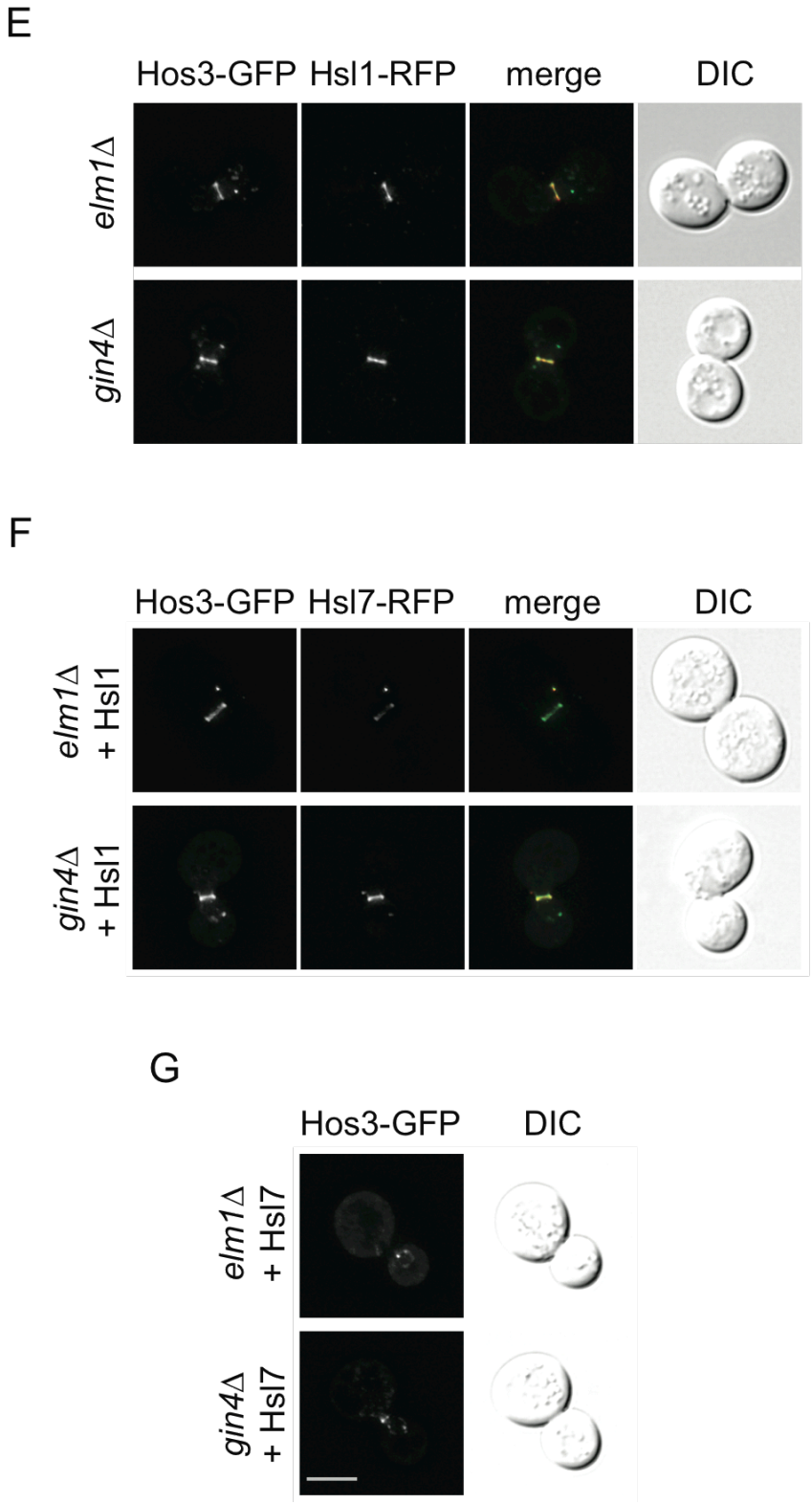
E
Hos3-GFP
Hsl1-RFP
merge
DIC
elm1Δ
gin4Δ
F
Hos3-GFP
Hsl7-RFP
merge
DIC
elm1Δ + Hsl1
gin4Δ + Hsl1
G
Hos3-GFP
DIC
elm1Δ + Hsl7
gin4Δ + Hsl7

Figure 4.4. Targeting Hos3 to the bud neck is downstream of Elm1 and Gin4

(A) Increasing the level of active Hsl1 rescues Hos3 to the bud neck. Hos3-GFP (*CEN*) was imaged in *elm1*Δ and *gin4*Δ cells transformed with a *CEN* vector bearing Hsl1.

(B) Hos3-GFP (*CEN*) was imaged in *elm1*Δ *gin4*Δ cells transformed with an empty vector or a *CEN* vector bearing Hsl1.

(C) Elm1 and Gin4 likely act in parallel pathways. Hos3-GFP (*CEN*) was imaged in *elm1*Δ cells transformed with a high-copy 2μ vector bearing Gin4 and *gin4*Δ cells transformed with a high-copy 2μ vector bearing Elm1. Scale bar, 5 μm.

(D) Kinase activity of Hsl1 is required for the rescue effect. Hos3-GFP (*CEN*) was imaged in *elm1*Δ, *gin4*Δ, and *elm1*Δ *gin4*Δ cells transformed with a *CEN* vector bearing kinase-dead $Hsl1^{K110R}$.

(E) Elevated level of Hsl1 restores both Hsl1 and Hos3 to the bud neck as a full ring. *elm1*Δ and *gin4*Δ cells transformed with Hos3-GFP (*CEN*) and Hsl1-RFP (*CEN*) were analyzed by fluorescence microscopy.

(F) Elevated level of Hsl1 restores both Hsl7 and Hos3 to the bud neck as a full ring. Hos3-GFP (*CEN*) and Hsl7-RFP (*CEN*) were co-imaged in *elm1*Δ and *gin4*Δ cells transformed with a *CEN* vector bearing Hsl1.

(G) Elevated level of Hsl7 does not restore Hos3 to the bud neck. Hos3-GFP (*CEN*) was imaged in *elm1*Δ and *gin4*Δ cells transformed with a *CEN* vector bearing Hsl7. Scale bar, 5 μm.

sequentially restored to the bud neck for full-ring localization. Thus, Hsl1 and Hsl7 are likely the proteins that recruit Hos3 to the bud neck while Elm1 and Gin4 act indirectly for Hos3 neck targeting through activating Hsl1. Therefore, the targeting of Hos3 to the bud neck is downstream of Elm1 and Gin4 actions.

The Hsl1-Hsl7 module targets Hos3 to the bud neck

The genetic data suggest that the recruitment of Hos3 to the bud neck is directly dependent on the Hsl1-Hsl7 module. We tried to investigate this issue from another perspective. In a sequentially hierarchical assembly system such as the bud neck, although proteins upstream of a candidate protein are all required for its localization, their epistatic relations determine that they could be differentiated for “direct vs. indirect” roles in targeting that specific downstream protein: the candidate protein should display highly correlated association with proteins that directly recruit it but somewhat different localization profile with proteins that indirectly recruit it. In the example of Hos3, when septins are nonfunctional, all downstream neck proteins should be absent from the bud neck (Figure 4.5 1st row); when protein A is absent, septins which is uspstream protein A should still be intact at the bud neck, and protein D could still be partially targeted by protein E which allows a defective pattern of both protein D and Hos3 at the bud neck (Figure 4.5 2nd row); when protein D is absent, Hos3 should also be completely absent from the bud neck

(Figure 4.5 4th row). By performing a comprehensive reciprocal localization study and comparing the neck pattern of the septins and the candidate proteins with that of Hos3 in the corresponding candidate mutants, we could evaluate the proteins that have the best the match of such reciprocal patterns to Hos3 as a way to discover the proteins that likely directly recruit Hos3 to the bud neck in an unbiased manner (Figure 4.5 protein D).

Based on this idea, we performed a reciprocal localization study. Previously we showed that regulators of Hos3 neck targeting (septins and the four hit proteins) all localize to the bud neck as a full ring in wild-type cells (Figure 4.1). We now look at the targeting of Hos3 and its regulators to the bud neck in septin and hit mutants (Figure 4.6). The patterns are recorded by being categorized into four groups defined by the degree the proteins are assembled at the bud neck as 1). complete absence (-), 2). a few puncta (+), 3). a defective and incomplete ring (++), and 4). a full ring (+++). A summary of these pairwise neck-localization comparison shows the pattern profile of each regulator protein with regard to that of Hos3 (Figure 4.7).

As expected, when we coexpress Hos3 and a regulator in that particular mutant, both the regulator and Hos3 localize as a full ring to the bud neck (Figure 4.7 diagonal boxes). We also confirm the previously described rescue effect of Hos3 to the bud neck in *elm1*Δ and *gin4*Δ cells by an extra copy of Hsl1 (Figure 4.6D second row, 4.6E second row, and 4.7). For the comparison of the pattern profile through the columns, Hsl7 display the best match to Hos3 (Figure 4.7). Moreover, Hsl7 colocalizes with Hos3 even when

Figure 4.5

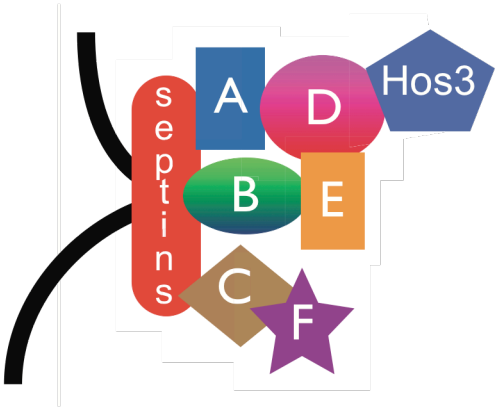

	protein					
	septins	A	B	D	E	Hos3
*septin*Δ	NA	–	–	–	–	–
*geneA*Δ	+++	NA	+++	+	+++	+
*geneB*Δ	+++	+++	NA	+	-	+
*geneD*Δ	+++	+++	+++	NA	+++	–
*geneE*Δ	+++	+++	+++	+	NA	+

Localization pattern at the bud neck
- −: absence
- +: a few puncta (< 50% of the full ring)
- ++: a defective ring (≥ 50% of the full ring)
- +++: a full ring
- NA: not available

Figure 4.5. Reciprocal localization would reveal proteins that directly recruit Hos3 to the bud neck

A model as described in Figure 3.4A reflects the sequential assembly of proteins to the bud neck region. In a theoretical reciprocal localization study, each component is deleted to assay if other proteins could still be targeted to the bud neck as in wild-type cells. Such data are recorded for each type of mutant cells in the rows. After completing such reciprocal localization study, the neck-localization of each protein throughout all the mutants is revealed by the patterns in the columns. The comparison of such patterns could reveal proteins (eg. protein D) that likely directly interact with a protein of interest (eg. Hos3).

the two proteins are defectively targeted to the bud neck, revealing a highly linked association (Figure 4.6A-E third rows). Additionally, Hsl1 also displays good pattern match to Hos3 with the exception in *hsl7*Δ cells (Figure 4.7). Other proteins (Cdc10 as septins, Elm1, and Gin4) display no pattern match to Hos3. Therefore, the results point to Hsl7 and Hsl1 as the likely proteins that directly recruit Hos3 to the bud neck, which is in agreement with the similar finding previously made from the genetic data.

In the reciprocal localization study, we noticed that Hsl1 and Hsl7, similar to Hos3, localize asymmetrically to the daughter side of the bud neck; in contrast, septins localize to both sides whereas Elm1 and Gin4 are associated to the middle of the bud neck (Figure 4.1). This again supports our finding that Hsl1 and Hsl7 likely directly recruit Hos3. Indeed, targeting of both Hsl1 and Hsl7 to the bud neck is largely abolished in *shs1*Δ, *elm1*Δ, and *gin4*Δ cells, suggesting that septins, Elm1, and Gin4 are required for Hos3 neck targeting likely because they function upstream to assemble the Hsl1-Hsl7 module at the bud neck (Figure 4.7).

Neck-localized Hsl7 is sufficient to recruit Hos3

Our data so far suggest that the recruitment of Hos3 to the bud neck is directly dependent on the Hsl1-Hsl7 module. Then we need to differentiate three mutually exclusive scenarios for the involvement of the Hsl1-Hsl7 module in Hos3 bud neck targeting: 1). Hsl1 alone, or 2). Hsl7 alone, or 3). Hsl1 and

Figure 4.6

A

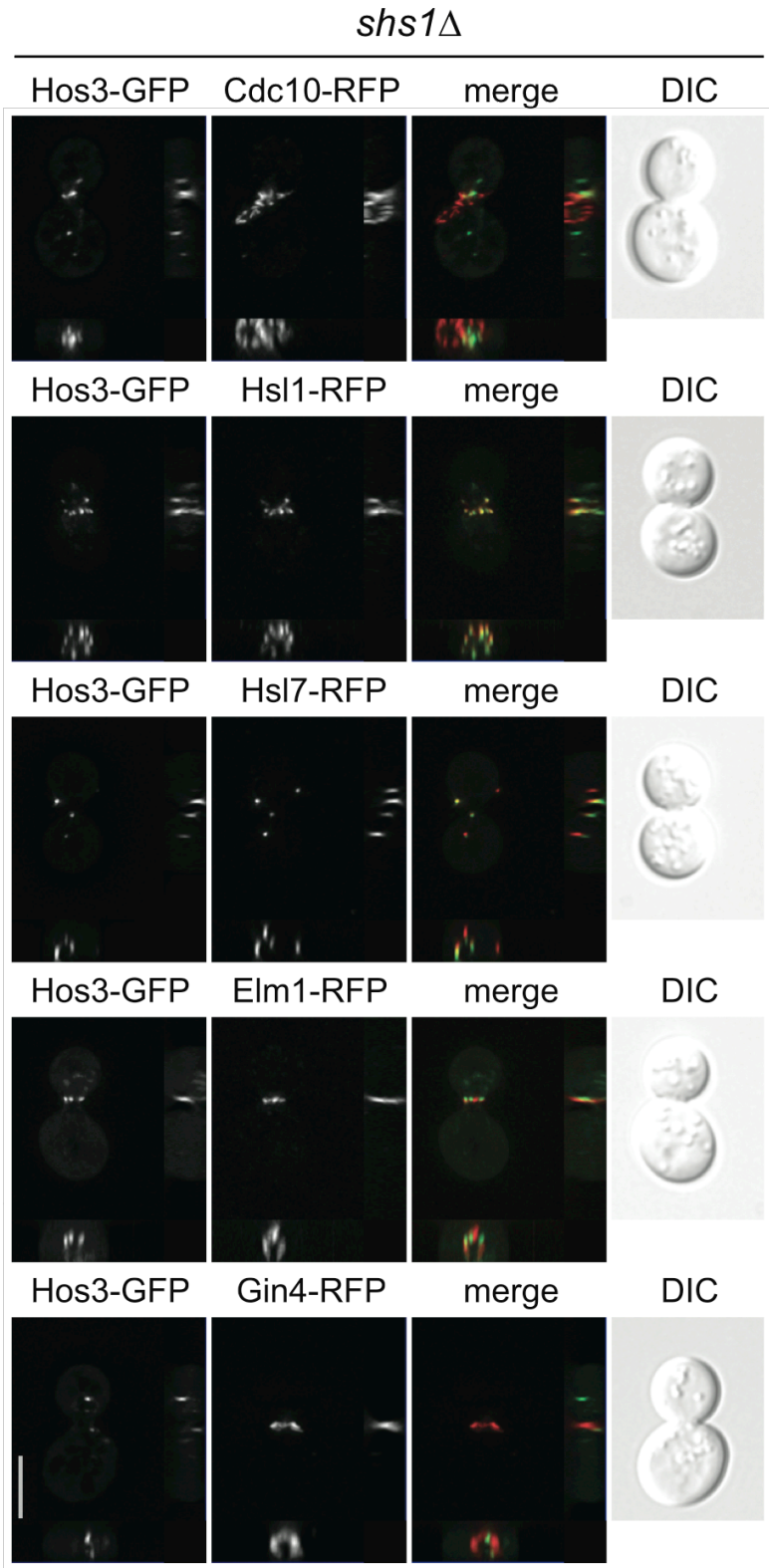
shs1Δ
Hos3-GFP
Cdc10-RFP
merge
DIC
Hos3-GFP
Hsl1-RFP
merge
DIC
Hos3-GFP
Hsl7-RFP
merge
DIC
Hos3-GFP
Elm1-RFP
merge
DIC
Hos3-GFP
Gin4-RFP
merge
DIC

Figure 4.6

B

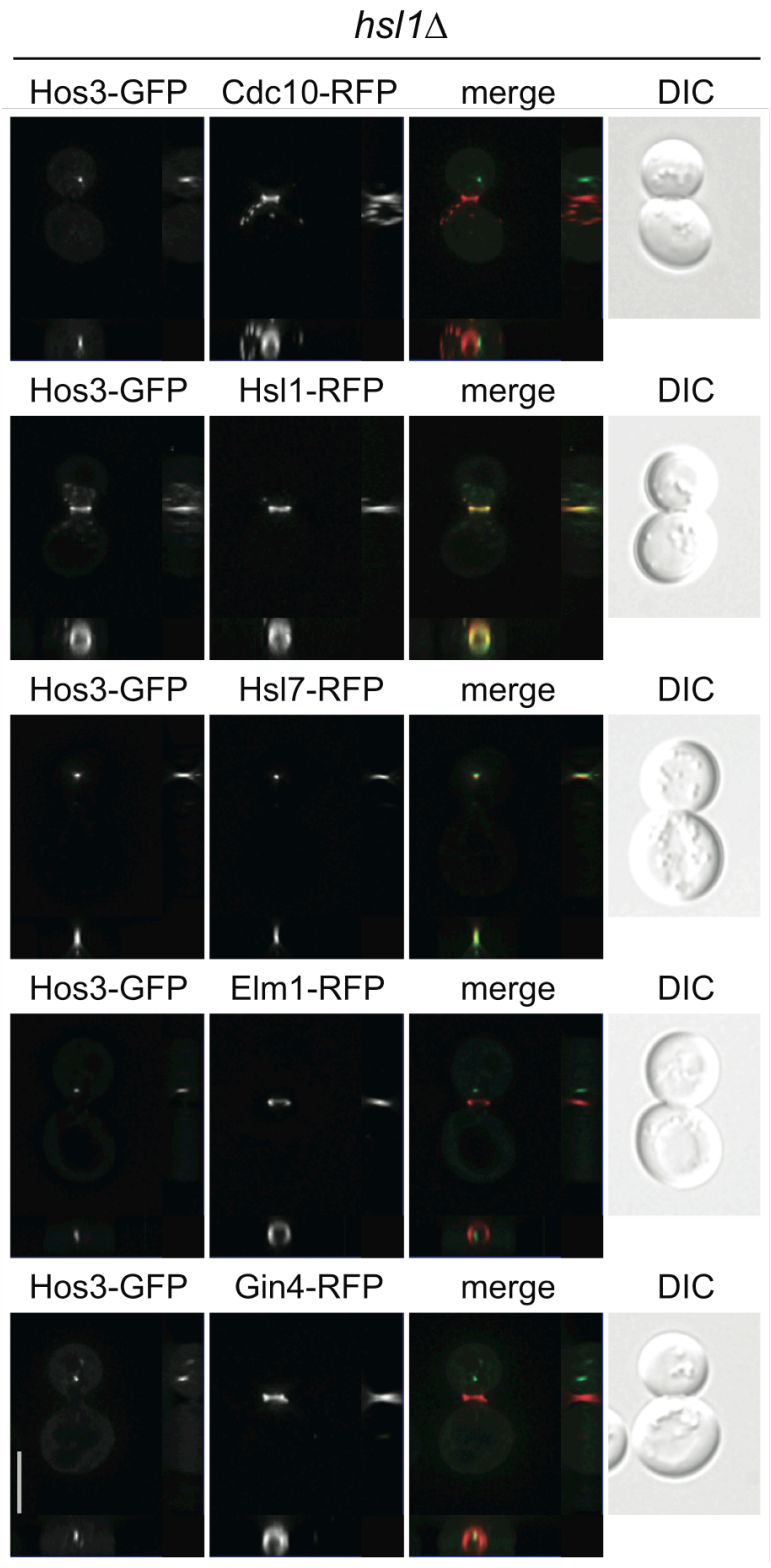
hsl1Δ
Hos3-GFP
Cdc10-RFP
merge
DIC
Hos3-GFP
Hsl1-RFP
merge
DIC
Hos3-GFP
Hsl7-RFP
merge
DIC
Hos3-GFP
Elm1-RFP
merge
DIC
Hos3-GFP
Gin4-RFP
merge
DIC

Figure 4.6

C

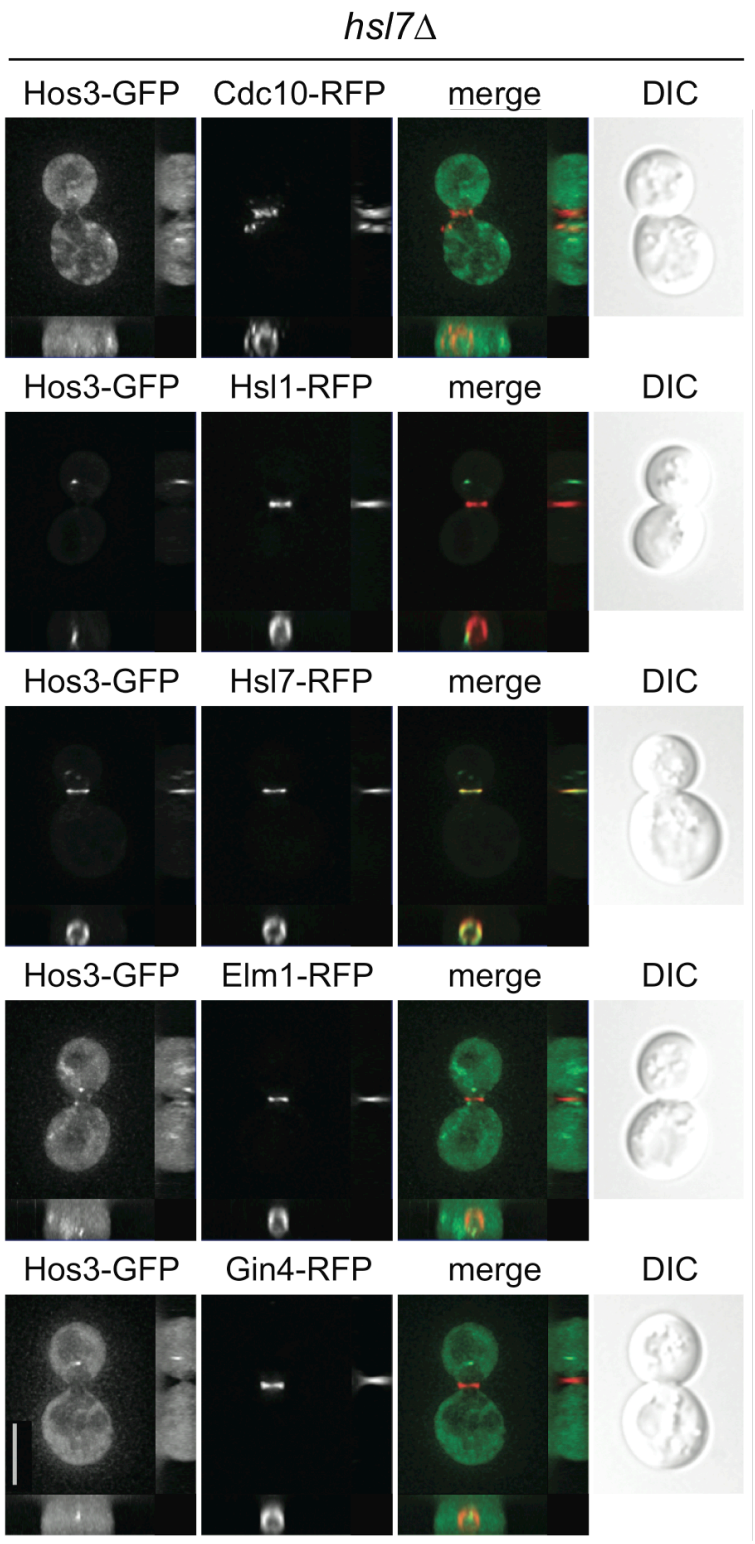
hsl7Δ
Hos3-GFP
Cdc10-RFP
merge
DIC
Hos3-GFP
Hsl1-RFP
merge
DIC
Hos3-GFP
Hsl7-RFP
merge
DIC
Hos3-GFP
Elm1-RFP
merge
DIC
Hos3-GFP
Gin4-RFP
merge
DIC

Figure 4.6

D

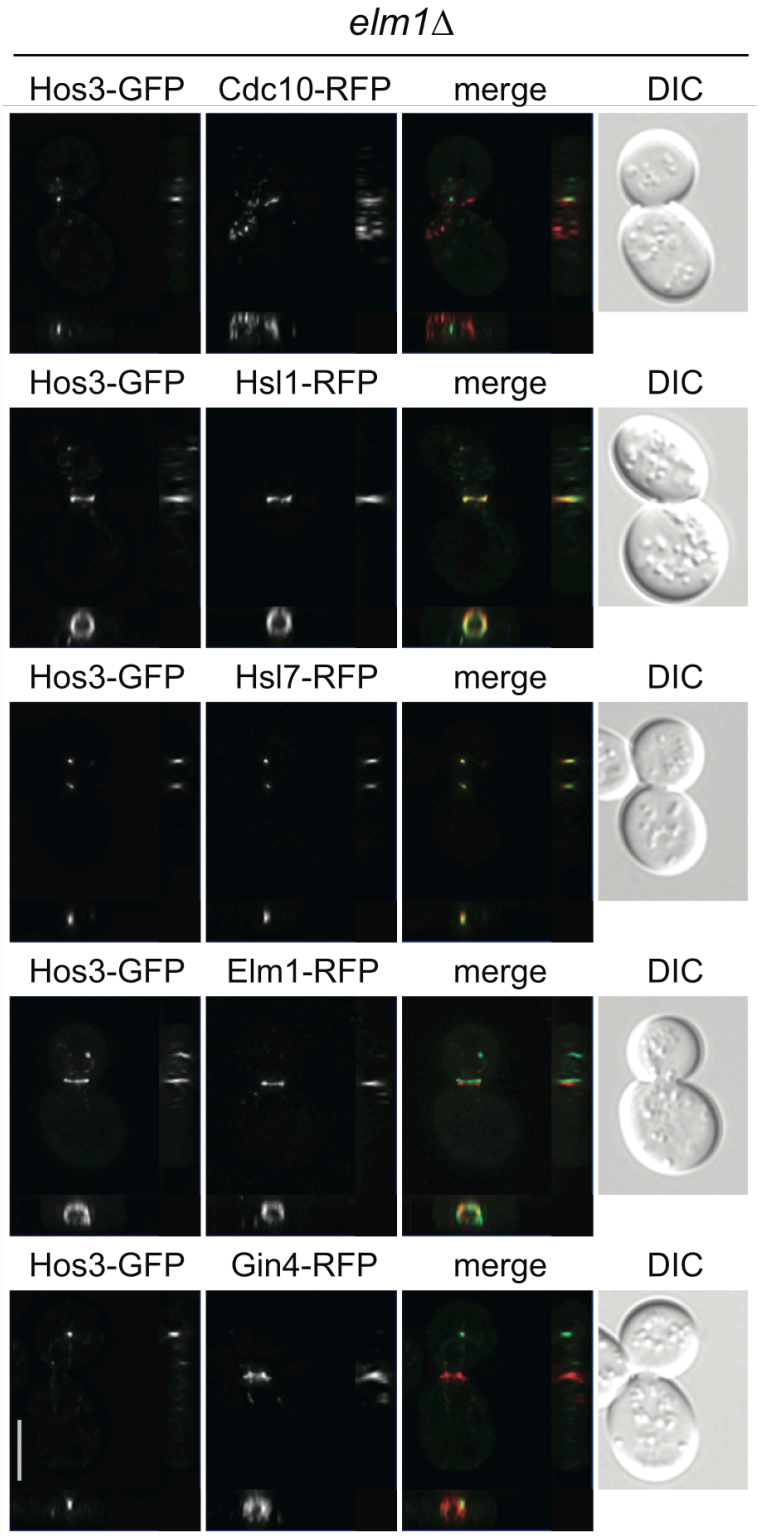
elm1Δ
Hos3-GFP
Cdc10-RFP
merge
DIC
Hos3-GFP
Hsl1-RFP
merge
DIC
Hos3-GFP
Hsl7-RFP
merge
DIC
Hos3-GFP
Elm1-RFP
merge
DIC
Hos3-GFP
Gin4-RFP
merge
DIC

Figure 4.6

E

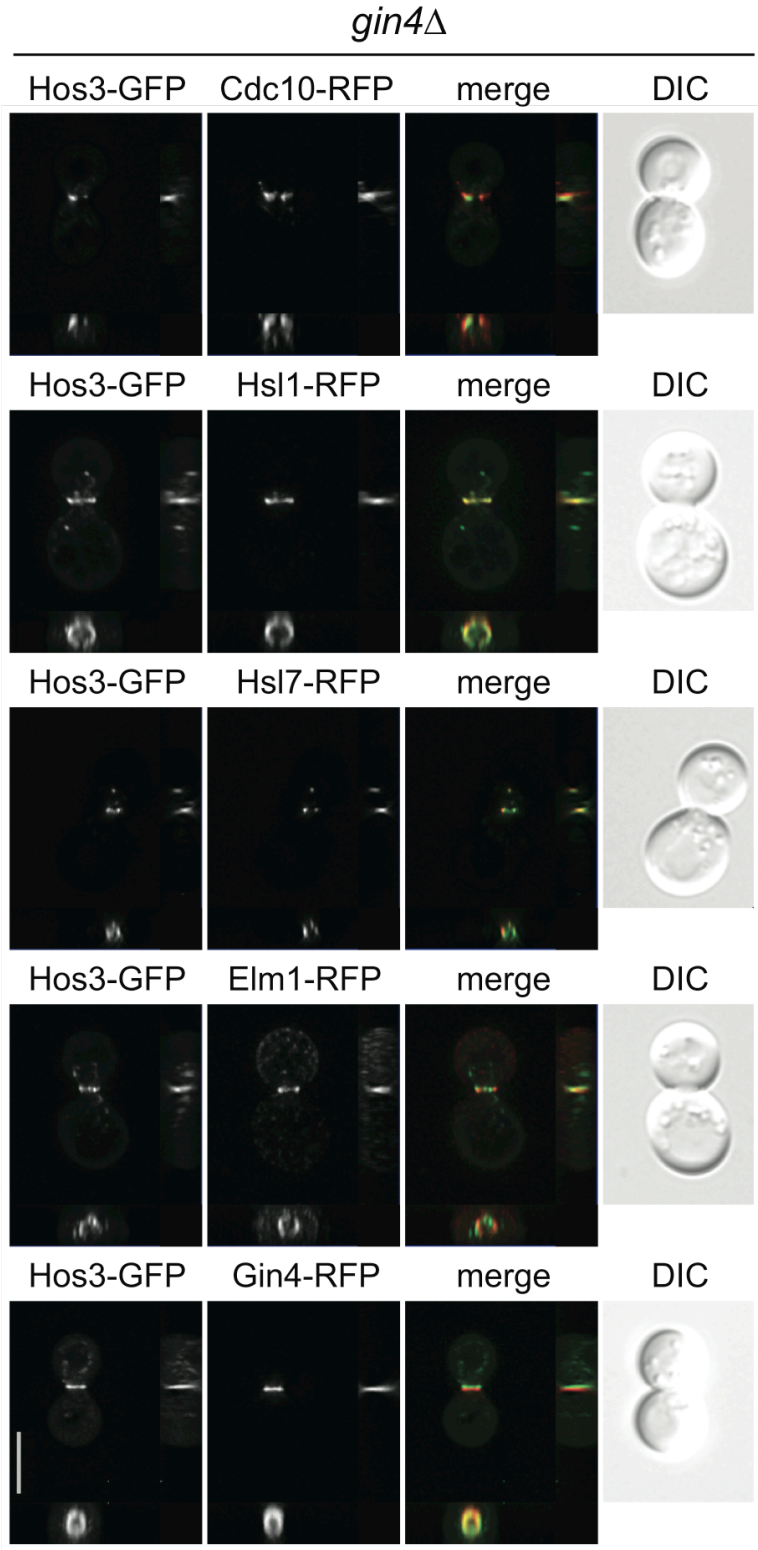
gin4Δ
Hos3-GFP
Cdc10-RFP
merge
DIC
Hos3-GFP
Hsl1-RFP
merge
DIC
Hos3-GFP
Hsl7-RFP
merge
DIC
Hos3-GFP
Elm1-RFP
merge
DIC
Hos3-GFP
Gin4-RFP
merge
DIC

Figure 4.6. Reciprocal localization profile of Hos3 and its neck-targeting regulators

*shs1*Δ (A), *hsl1*Δ (B), *hsl7*Δ (C), *elm1*Δ (D), and *gin4*Δ (E) cells were cotransformed with Hos3-GFP (*CEN*) and Cdc10-RFP (*CEN*) or Hsl1-RFP (*CEN*) or Hsl7-RFP (*CEN*) or Elm1-RFP (*CEN*) or Gin4-RFP (*CEN*) respectively, and analyzed by fluorescence microscopy. Cdc10-RFP is used as the marker for septins, and *shs1*Δ cells are used as septin mutants. Images are rotated with the bud neck parallel to the horizontal axis. To illustrate the localization pattern at the bud neck, image projection on the XZ-dimension is displayed below and on the YZ-dimension is shown on the right. Scale bar, 5 μm.

Figure 4.7

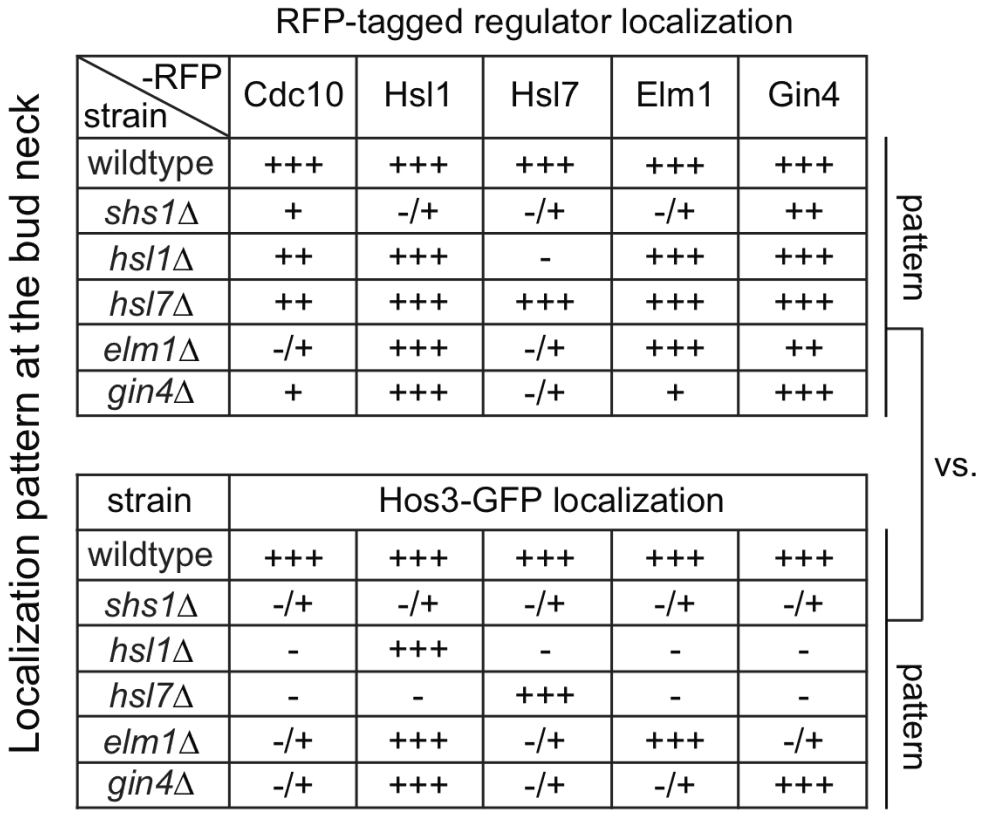

Localization pattern at the bud neck

−: absence

+: a few puncta (< 50% of the full ring)

++: a defective ring (≥ 50% of the full ring)

+++: a full ring

Figure 4.7. Summary of the reciprocal localization profile

Cells (Figure 4.1 and 4.6) were recorded for the neck patterns of Hos3 and its regulators. The top panel examines the neck localization of the RFP-tagged regulators in each strain of the cells tested. The bottom panel displays the neck localization of Hos3 assayed simultaneously in the corresponding cells. The localization pattern was characterized by one of four categories as indicated: -, absence from the bud neck; +, as a few puncta; ++, as a defective ring; +++, as a full ring.

Hsl7 together are responsible for the direct recruitment of Hos3 to the bud neck. We previously reported that Hsl1 displays good neck pattern match to Hos3 with the exception in *hsl7*Δ cells. In this case, with the absence of Hsl7, Hsl1 localizes as a full ring at the bud neck but is insufficient to target Hos3, thus arguing against the first scenario in which Hsl1 alone recruits Hos3 to the bud neck (Figure 4.6C 2nd row). Consistent with the other two scenarios in which Hsl7 is required, deletion of *HSL7* completely abolishes the rescue effect observed in *elm1*Δ and *gin4*Δ cells by overexpression of Hsl1 (Figure 4.8A, compared to Figure 4.4A). These results argue that Hsl7 is absolutely involved in Hos3 neck targeting.

We then tried to differentiate the remaining two scenarios of which the key difference is whether Hsl1 is required. However, since Hsl1 is required to recruit Hsl7, it becomes difficult to address if Hsl1 is directly targeting Hos3 or if Hsl1 is required only for targeting Hsl7, which is essential for directly targeting Hos3. In another word, we need to find out if the involvement of Hsl1 in Hos3 neck targeting is Hsl7-mediated. To achieve this purpose, we intentionally prevented the association between Hsl1 and Hsl7 by using an $Hsl7^{K254E}$ allele. The K254E mutation renders Hsl7 unable to bind to Hsl1 (Cid et al., 2001). Exogenous $Hsl7^{K254E}$ localizes weakly to the bud neck in the wild-type cells through dimerization with endogenous Hsl7, but is absent from the neck as the sole source in *hsl7*Δ cells (Figure 4.8B). Interestingly, while Hsl1 is correctly localized in *hsl7*Δ mutant, the inability of Hsl1 to associate with $Hsl7^{K254E}$ results in the similar failure to target Hos3 to the bud neck, leaving

Hos3 cytosolic (Figure 4.6C 2nd row and 4.8C). This suggests that Hsl1 likely functions in targeting Hos3 to the bud neck via its ability to recruit Hsl7. Assembly of Hsl7 at the bud neck by Hsl1 is a pre-requisite for Hos3 neck localization.

To better examine if Hsl1 plays a direct role in recruiting Hos3, we reasoned that since localization of Hsl7 to the bud neck is Hsl1-dependent, the key is to examine if targeting Hsl7 in an Hsl1-independent mechanism is sufficient to recruit Hos3 to the bud neck. To achieve such Hsl1-independent recruitment of Hsl7 to the bud neck, we created a chimera by fusing Hsl7 to the bud neck kinase Gin4. The Gin4-Hsl7 chimera localizes to the bud neck in both *hsl7*Δ and *hsl1*Δ cells (Figure 4.8D). Therefore, targeting the chimera to the bud neck is due to its Gin4 portion and thus independent of endogenous Hsl7 or Hsl1. The Hsl7 portion of the chimera is functional because the chimera rescues Hos3 to the bud neck as a full ring in *hsl7*Δ cells (Figure 4.8D top row). Most importantly, the Gin4-Hsl7 chimera is able to target Hos3 to the bud neck in *hsl1*Δ cells (Figure 4.8D bottom row). We previously showed that Hos3 is completely absent from the bud neck in *hsl1*Δ cells but now the neck-localized Gin4-Hsl7 chimera suppresses the neck-targeting defect of Hos3 in *hsl1*Δ cells (Figure 4.8D, compared to Figure 3.5A). Therefore, neck-localized Hsl7 alone is sufficient to recruit Hos3. The observation clearly suggests that Hsl1 is required for Hos3 neck localization due to its function in targeting and activating Hsl7 at the bud neck. Recruitment of Hsl7 in an Hsl1-independent manner is able to bypass this requirement.

Figure 4.8

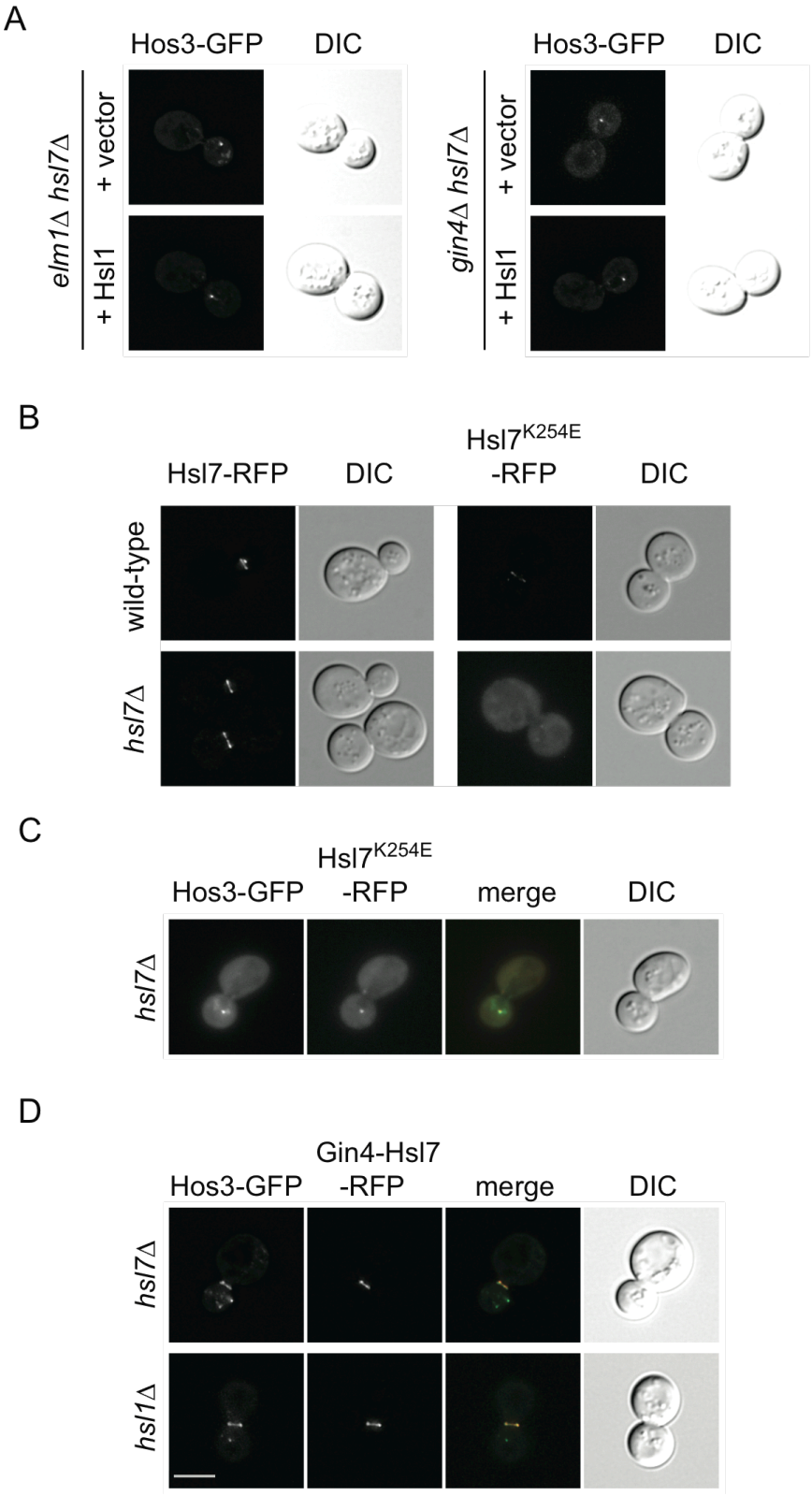
A
Hos3-GFP
DIC
Hos3-GFP
DIC
elm1Δ hsl7Δ
+ vector
+ Hsl1
gin4Δ hsl7Δ
+ vector
+ Hsl1
B
Hsl7-RFP
DIC
Hsl7K254E
-RFP
DIC
wild-type
hsl7Δ
C
Hsl7K254E
Hos3-GFP
-RFP
merge
DIC
hsl7Δ
D
Gin4-Hsl7
Hos3-GFP
-RFP
merge
DIC
hsl7Δ
hsl1Δ

Figure 4.8. Neck-localized Hsl7 is required to recruit Hos3 to the bud neck

(A) Rescue of Hos3 to the bud neck by increased level of active Hsl1 is dependent on Hsl7. Hos3-GFP (*CEN*) was imaged in *elm1*Δ *hsl7*Δ and *gin4*Δ *hsl7*Δ double mutant cells transformed with an empty vector or a *CEN* vector bearing Hsl1.

(B) Mutation of K254E interrupts Hsl7 interaction with Hsl1 thus abolishing its bud neck association. Hsl7-RFP (*CEN*) or $Hsl7^{K254E}$-RFP (*CEN*) was respectively imaged in wild-type and *hsl7*Δ cells.

(C) Failure to target Hsl7 to the bud neck abolishes Hos3 neck-localization. Hos3-GFP (*CEN*) and $Hsl7^{K254E}$-RFP (*CEN*) were co-imaged in *hsl7*Δ cells.

(D) Neck-localized Hsl7 bypasses Hsl1 for Hos3 neck targeting. *hsl7*Δ and *hsl1*Δ cells transformed with Hos3-GFP (*CEN*) and a chimera of Gin4-Hsl7-RFP (*CEN*) were analyzed by fluorescence microscopy. Scale bar, 5 μm.

Hsl7 interacts with and recruits Hos3

The above results strongly argue for a direct physical interaction between Hsl7 and Hos3 at the bud neck. We examined this possibility with two independent methods. First, we looked for the physical association between these two proteins. To assure the potential interaction is authentic rather than an artifact due to protein overexpression, we genomically tagged the *HOS3* gene and *HSL7* gene so that endogenous Hos3 is fused with 3 tandem copies of HA tag while endogenous Hsl7 is sued with 13 tandem copies of Myc tag. We were able to co-immunoprecipitate endogenous Hsl7 with endogenous Hos3 (Figure 4.9A). Given that both Hsl7 and Hos3 are of endogenous level in this experiment, the observed physical interaction between these two proteins reflect authentic *in vivo* interactions.

Indeed, the physical interaction between Hsl7 and Hos3 could be further confirmed *in vivo* by a second approach. Sec2, a guanine nucleotide exchange factor for Rab GTPase Sec4, is involved in the delivery of post-Golgi vesicles and localize to polarized secretory vesicles in the daughter cell (Figure 4.9B top row) (Walch-Solimena et al., 1997). We then made a chimera between Sec2 and Hsl7. In wild-type cells, endogenous Hsl7 recruits Hos3 to the bud neck and exogenous Sec2-Hsl7 chimera is sufficient to target Hos3 to the post-Golgi vesicles (Figure 4.9B bottom row). This observation strongly argues for the *in vivo* physical interaction between Hsl7 and Hos3, and also convincingly demonstrates that functional Hsl7 is sufficient to recruit Hos3 and direct Hos3 localization. As expected, deletion of *HSL7* or *HSL1* in cells

Figure 4.9

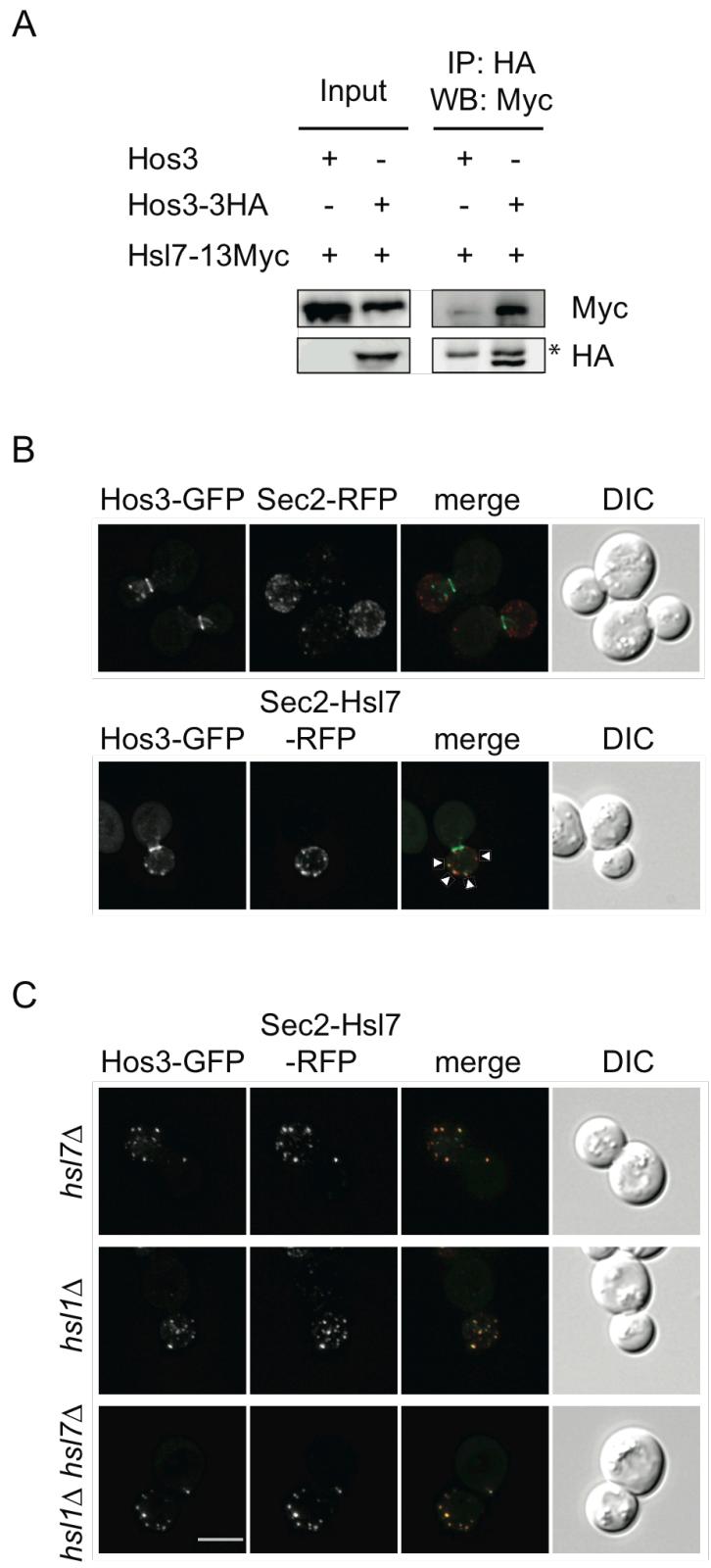
A
Input
IP: HA
WB: Myc
Hos3
Hos3-3HA
Hsl7-13Myc
Myc
* HA
B
Hos3-GFP
Sec2-RFP
merge
DIC
Sec2-Hsl7
-RFP
C
hsl7Δ
hsl1Δ
hsl1Δ hsl7Δ

Figure 4.9. Hsl7 interacts with and recruits Hos3

(A) Hos3 interacts with Hsl7. Cells, of which endogenous Hsl7 is fused with 13 copies of Myc tag and endogenous Hos3 is either untagged or fused with 3 copies of HA tag, were grown to mid-log phase in YPD medium and lysed for immunoprecipitation with anti-HA agarose resins. The resins were eluted with SDS-PAGE sample buffer and analyzed by immunoblotting against HA or Myc tag. Star denotes a non-specific band originating from resin-attached anti-HA antibodies.

(B and C) Hsl7 is sufficient to direct Hos3 localization. Hos3-GFP (*CEN*) and Sec2-RFP (*CEN*) were co-imaged in wild-type cells (B). Hos3-GFP (*CEN*) and a chimera of Sec2-Hsl7-RFP (*CEN*) were co-imaged in wild-type cells (B) or in *hsl7*Δ, *hsl1*Δ, and *hsl1*Δ *hsl7*Δ cells (C). Triangles in (B) indicate the sites of colocalization between Hos3-GFP and the exocytic vesicles marked with the Sec2-Hsl7-RFP chimera. Scale bar, 5 μm.

expressing the Sec2-Hsl7 chimera results in dissociation of Hos3 from the bud neck but not from the post-Golgi secretory vesicles (Figure 4.9C). In conclusion, Hsl7 physically interacts with and recruits Hos3 to the bud neck.

Hsl1 determines the asymmetry of Hos3 at the bud neck

Both Hsl1 and Hsl7 localize asymmetrically to the daughter side of the bud neck (Figure 4.1) (Barral et al., 1999; Shulewitz et al., 1999). Given the sequential recruitment of Hsl7 by Hsl1 and of Hos3 by Hsl7, Hsl1 establishes the asymmetry of the Hsl1-Hsl7-Hos3 module. Consistent with this notion, when Hsl1 is expressed from a low-copy plasmid instead from its genomic locus (a mild condition of overexpression), about 20% of the cells assemble Hsl1 symmetrically on both sides rather than asymmetrically on the daughter side of the bud neck (Figure 4.10A). This phenotype is likely due to the mild overexpression effect. Unlike the two split rings only seen at the end of cytokinesis, symmetrical localization of Hos3 to the bud neck under this condition appears right after budding and therefore could be observed in cells that are yet to segregate the nucleus (Figure 4.10B). Accordingly, when Hsl1 gets targeted symmetrically to both sides of the bud neck, so is Hos3 (Figure 4.10C). Given that Hsl7 is the adaptor between Hsl1 and Hos3, Hos3 completely loses its localization to both sides of the bud neck when *HSL7* is deleted (Figure 4.10D). All of these results suggest that while Hsl7 interacts with and recruits Hos3, Hsl1 determines the neck asymmetry of Hos3 through

Figure 4.10

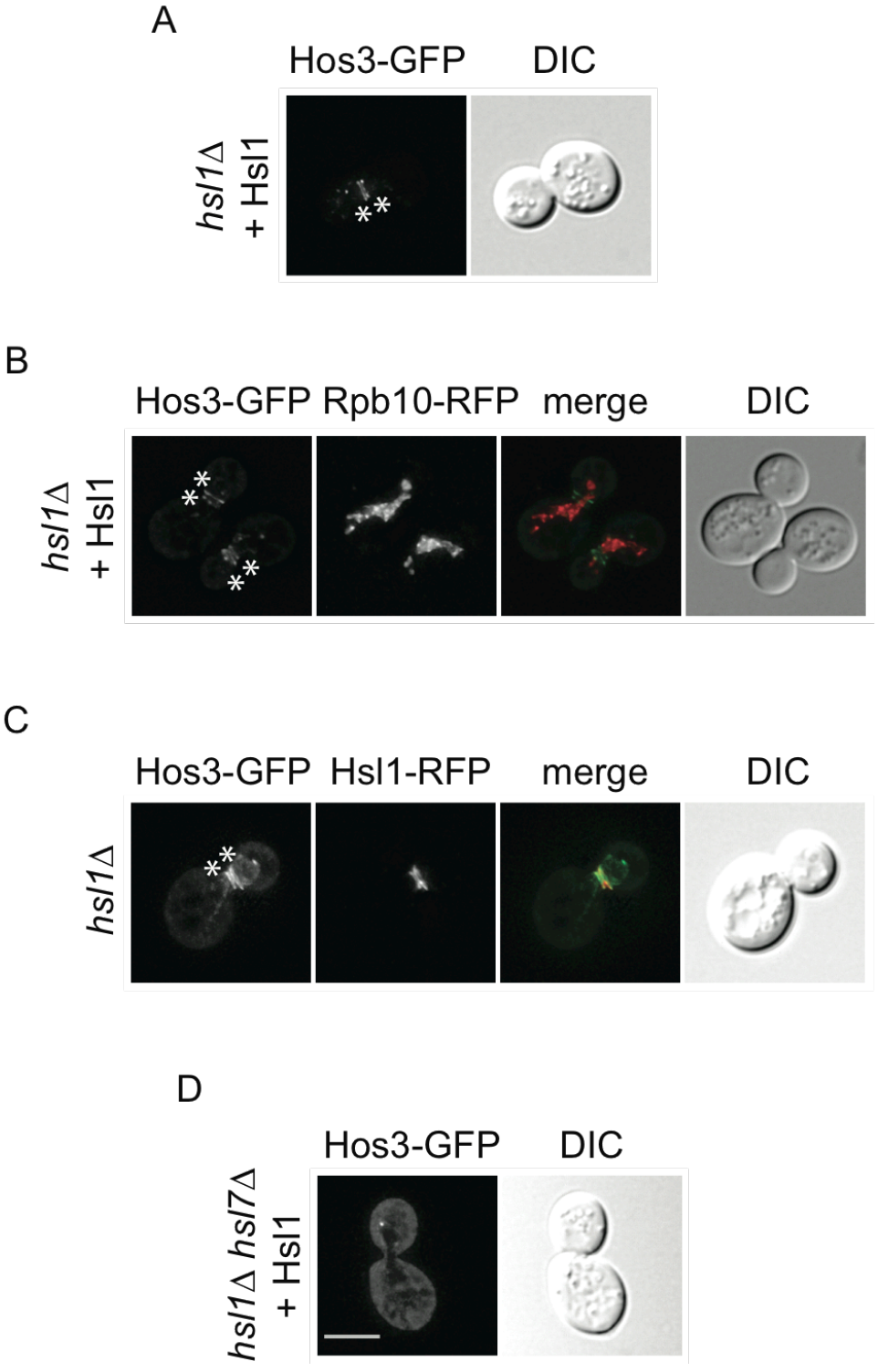
A
Hos3-GFP
DIC
hsl1Δ + Hsl1
B
Hos3-GFP
Rpb10-RFP
merge
DIC
hsl1Δ + Hsl1
C
Hos3-GFP
Hsl1-RFP
merge
DIC
hsl1Δ
D
Hos3-GFP
DIC
hsl1Δ hsl7Δ + Hsl1

Figure 4.10. Hsl1 determines Hos3 asymmetry at the bud neck

(A) Hos3-GFP (*CEN*) was imaged in *hsl1*Δ transformed with a *CEN* vector bearing Hsl1. Asterisks point to Hos3 on both sides of the bud neck. About 20% of the cells display this localization pattern.

(B) Hos3-GFP (*CEN*) and Rpb10-RFP (*CEN*) were co-imaged in *hsl1*Δ cells transformed with a *CEN* vector bearing Hsl1. Asterisks point to Hos3 on both sides of the bud neck.

(C) Hos3-GFP (*CEN*) and Hsl1-RFP (*CEN*) were co-imaged in *hsl1*Δ cells. Asterisks point to Hos3 on both sides of the bud neck.

(D) Hos3-GFP (*CEN*) was imaged in *hsl1*Δ *hsl7*Δ cells transformed with a *CEN* vector bearing Hsl1. Scale bar, 5 μm.

asymmetrically targeting itself and Hsl7 to the bud neck.

Neck-localization of Hos3 is dispensable for certain cellular activities

Having uncovered the mechanism that asymmetrically targets Hos3 to the bud neck, we sought to understand how this could impact the physiological functions of Hos3. Hos3 is not involved in assembling septins and the four hit proteins (Hsl1, Hsl7, Elm4, and Gin4) at the bud neck consistent with the finding that it acts downstream of the septins and the morphogenesis checkpoint (Figure 4.11A). We also observed no cytokinesis defect in *hos3*Δ cells (data not shown). Therefore, Hos3 does not appear to play an essential structural role at the bud neck.

We next examined if Hos3 could actually be a member of the morphogenesis checkpoint. Deletion of *HSL1* or *HSL7* inactivates the morphogenesis checkpoint and results in a G_2 delay as revealed by the analysis using flow cytometry, but *hos3*Δ cells are not enriched for the G_2/M subpopulation (Figure 4.11B). In a different W303 strain background, the G_2 delay of *hsl7*Δ cells is readily apparent from their elongated morphology and temperature sensitivity whereas *hos3*Δ cells display neither of these defects (Figure 4.11C and 4.11D). Therefore, while the morphogenesis checkpoint is important in targeting Hos3 to the bud neck, Hos3 does not appear to be a member of this signaling pathway.

Another attractive hypothesis could be that neck-localization is required

to load Hos3 onto the daughter SPB. However, despite being absent from the bue neck, Hos3 is correctly targeted onto the daughter SPB in *hsl7*Δ cells (Figure 4.11E). Finally, deletion of several HDAC genes including *HOS3* suppresses the temperature sensitivity of an $apc5^{CA}$ strain containing a mutation in the anaphase promoting complex (Turner et al., 2010). In contrast, deletion of *HSL7* fails to do so, indicating that neck-localization is dispensable for this Hos3-associated genetic interaction (Figure 4.11F).

Although we have, after considerable efforts, uncovered the molecular mechanism that asymmetrically targets Hos3 to the bud neck, it remains mysterious why Hos3 is targeted there. The neck localization of Hos3 seems dispensable for a number of cellular activites. The importance related to the unique targeting of Hos3 to the bud neck remains to be elucidated.

Figure 4.11

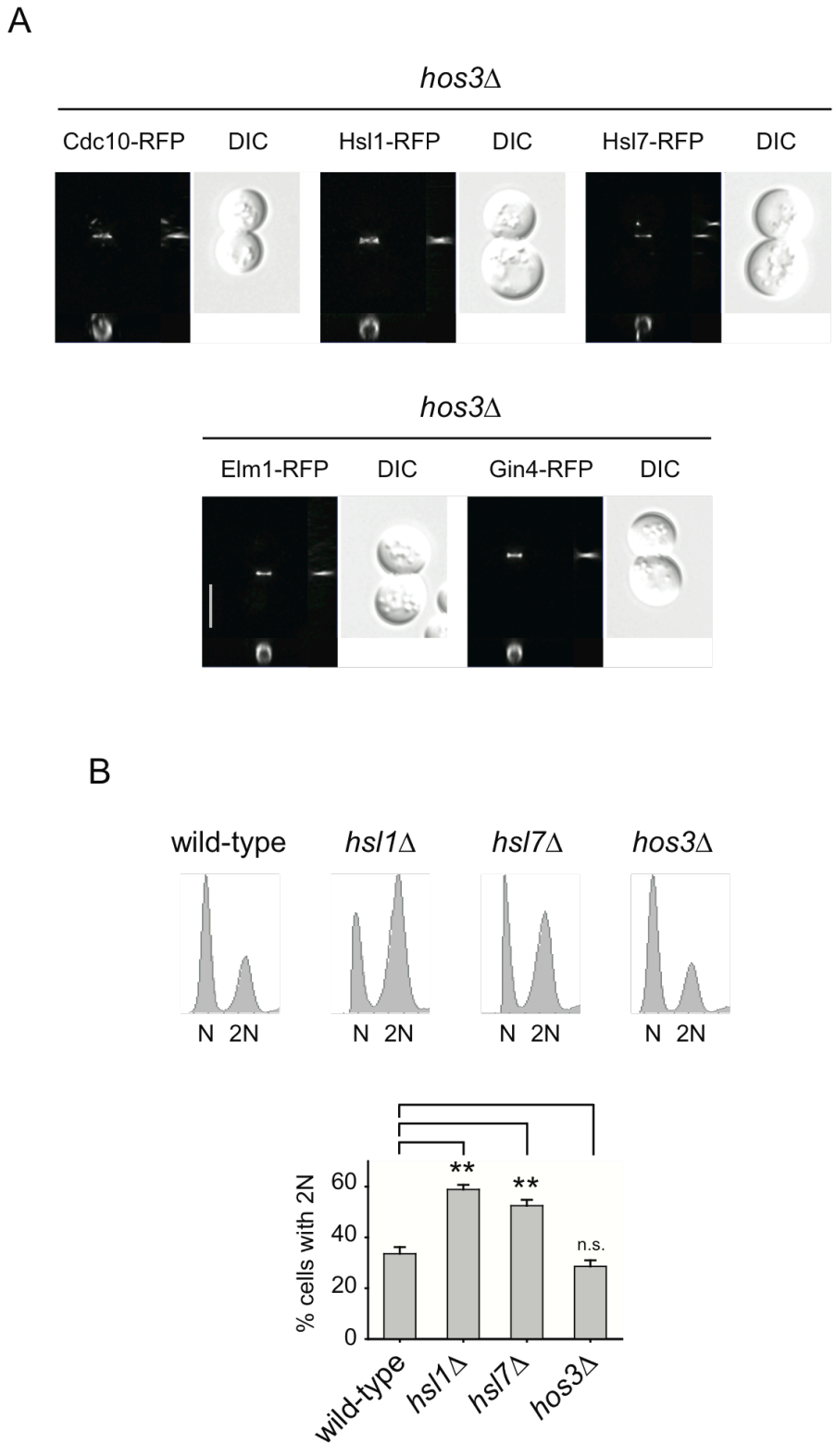
A
hos3Δ
Cdc10-RFP
DIC
Hsl1-RFP
DIC
Hsl7-RFP
DIC
hos3Δ
Elm1-RFP
DIC
Gin4-RFP
DIC
B
wild-type
hsl1Δ
hsl7Δ
hos3Δ
N 2N
N 2N
N 2N
N 2N
% cells with 2N
60
40
20
0
**
**
n.s.
wild-type
hsl1Δ
hsl7Δ
hos3Δ

Figure 4.11

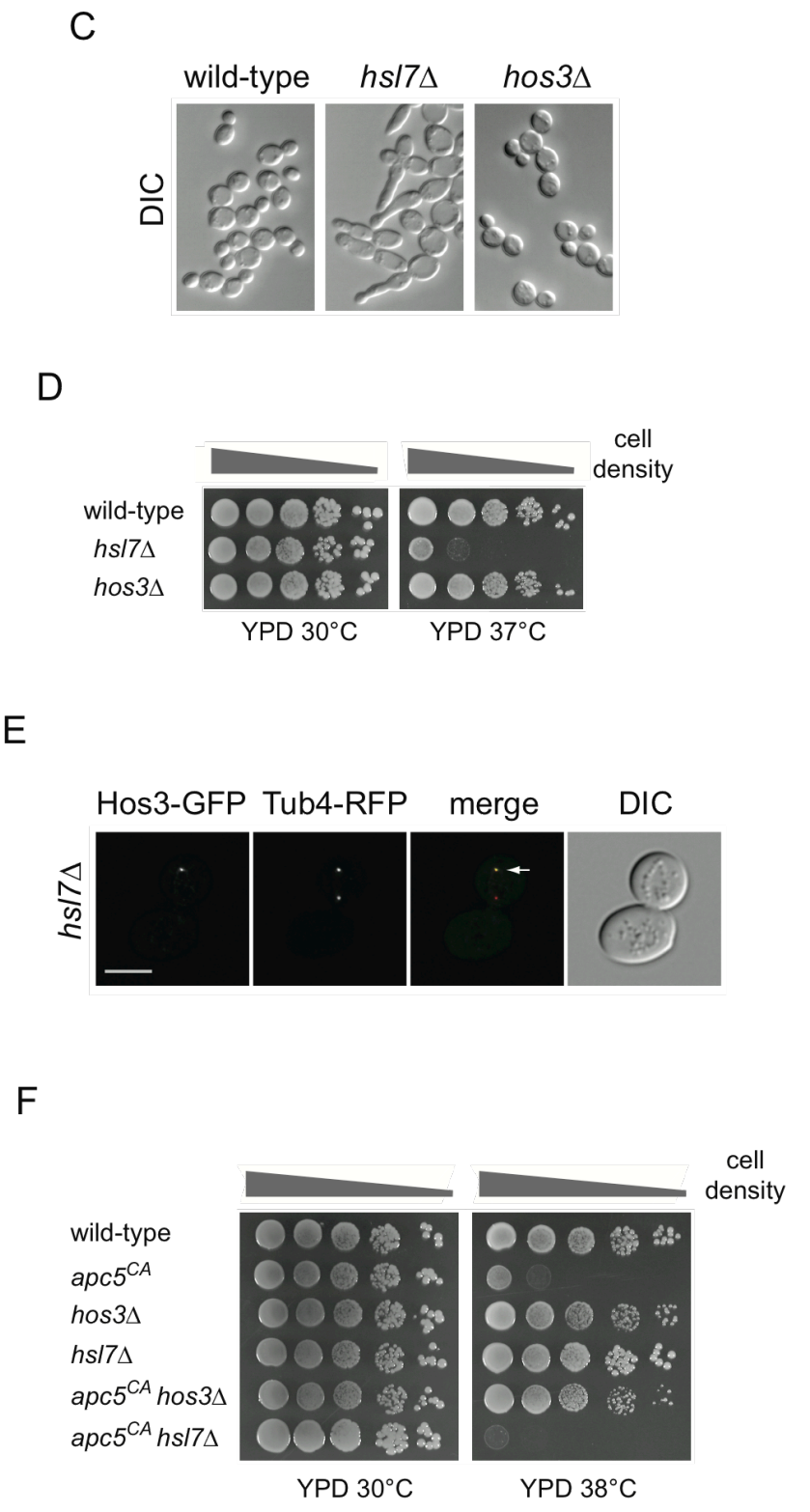
C
wild-type
hsl7Δ
hos3Δ
DIC
D
cell density
wild-type
hsl7Δ
hos3Δ
YPD 30°C
YPD 37°C
E
Hos3-GFP
Tub4-RFP
merge
DIC
hsl7Δ
F
cell density
wild-type
apc5CA
hos3Δ
hsl7Δ
apc5CA hos3Δ
apc5CA hsl7Δ
YPD 30°C
YPD 38°C

Figure 4.11. Investigating the function of neck-localized Hos3

(A) Hos3 is dispensable for assembling septins and hit proteins at the bud neck. Cdc10-RFP (*CEN*), Hsl1-RFP (*CEN*), Hsl7-RFP (*CEN*), Elm1-RFP (*CEN*), and Gin4-RFP (*CEN*) were respectively imaged in *hos3*Δ cells. Images are rotated with the bud neck parallel to the horizontal axis. To illustrate the localization pattern at the bud neck, image projection on the XZ-dimension is displayed below and on the YZ-dimension is shown on the right. Scale bar, 5 μm.

(B) Wild-type, *hsl1*Δ, *hsl7*Δ, and *hos3*Δ cells were grown to mid-log phase in YPD medium, stained with propidium iodide, and analyzed for DNA content by flow cytometry. Cells with 2N content of DNA reveal the G_2/M subpopulation. Data from three independent experiments were analyzed for statistics. Error bars represent SEM. For statistical significance by t-test, ** denotes "p value < 0.001"; n.s. denotes "not significant (p value > 0.05)".

(C and D) Wild-type, *hsl7*Δ, and *hos3*Δ cells of W303 background were grown to mid-log phase in YPD medium and analyzed by DIC microscopy (C) or by 10-serial dilution onto YPD plates for incubation at 30°C and 37°C (D).

(E) Neck-localization is dispensable for Hos3 association with the daughter SPB. Hos3-GFP (*CEN*) and the SPB marker Tub4-RFP (*CEN*) were co-imaged in *hsl7*Δ cells. Arrowhead points to the daughter-SPB-associated Hos3. Scale bar, 5 μm.

(F) Neck-localization is not involved in the genetic interaction between Hos3 and the $apc5^{CA}$ allele. Wild-type, $apc5^{CA}$, *hos3*Δ, *hsl7*Δ, $apc5^{CA}$ *hos3*Δ, and

apc5^{CA} *hsl7*Δ cells were grown to mid-log phase in YPD medium and analyzed by 10-serial dilution onto YPD plates for incubation at 30°C and 38°C.

DISCUSSION

We proposed the following model for targeting Hos3 to the bud neck: 1). septins function as the scaffold to recruit many bud neck proteins such as Elm1 and Gin4; 2). Elm1 and Gin4 are essential to target and activate Hsl1 at the daughter side of the bud neck; 3). Hsl1 interacts with Hsl7; 4). Hsl7 finally recruits Hos3 to the neck. In summary, Hsl1 establishes Hos3 asymmetry while Hsl7 recruits Hos3 to the bud neck. The genetic data truly supports the view of a hierarchal assembly of proteins at the bud neck.

First of all, although Hos3 targeting to the bud neck is regulated by the morphogenesis checkpoint, Hos3 does not appear a member of this signaling pathway. This raises a very interesting point in linking Hos3 function with the correct timing of mitotic entry. Although the exact physiological function of Hos3 remains unknown at this stage, whatever is its function would be regulated upstream by the morphogenesis checkpoint if this function requires targeting Hos3 to the bud neck. In such cases, logically, this unknown function of Hos3 should be active only after successful mitotic entry, which is monitored by the morphogenesis checkpoint. It also involves the unique action site of the bud neck. With all these analyses, it appears Hos3 should play a certain role in the regulation of the cell cycle.

The morphogenesis checkpoint is a clear linear pathway of which the output leads to the regulation of mitotic CDK activity with regards to the morphological condition of budding. Hsl7 is recruited to the bud neck by Hsl1, and then together with Hsl1 directs Swe1 for degradation as a way to promote

active mitotic CDK. Therefore, Hsl7 is at the very terminal end of this neck-associated signaling pathway. By having Hsl7 as the recruiter of Hos3, cells tightly link Hos3 neck-targeting to the regulation of mitotic entry. If cells adopt septins or other components (eg. Elm1, Gin4 etc.) of the morphogenesis checkpoint as the recruiter of Hos3 to the bud neck, even though Hos3 could still be efficiently targeted to the bud neck, the timing of its neck-targeting will be only remotely related to the regulation of mitotic entry since while these proteins recruit Hos3, their action in the morphogenesis checkpoint through downstream Hsl1 and Hsl7 is yet to be executed.

Finally, another beauty of the targeting machinery is that Hsl1 establishes the asymmetry of Hos3 at the bud neck. Such asymmetry would be lost if Hos3 was directly targeted to the bud neck by septins or Elm1 or Gin4. The polarity at the bud neck clearly has important implications for the yet unknown Hos3 functions as supported by the previous finding that localization is truly instrumental in defining where Hos3 acts as an HDAC. There must be a reason why the daughter side of the bud neck is preferred and chosen for Hos3.

REFERENCES

Barral, Y., Parra, M., Bidlingmaier, S., & Snyder, M. (1999). Nim1-related kinases coordinate cell cycle progression with the organization of the peripheral cytoskeleton in yeast. *Genes & Development, 13*(2), 176-187.

Blacketer, M. J., Koehler, C. M., Coats, S. G., Myers, A. M., & Madaule, P. (1993). Regulation of dimorphism in saccharomyces cerevisiae: Involvement of the novel protein kinase homolog Elm1p and protein phosphatase 2A. *Molecular and Cellular Biology, 13*(9), 5567-5581.

Casamayor, A., & Snyder, M. (2003). Molecular dissection of a yeast septin: Distinct domains are required for septin interaction, localization, and function. *Molecular and Cellular Biology, 23*(8), 2762-2777.

Cid, V. J., Shulewitz, M. J., McDonald, K. L., & Thorner, J. (2001). Dynamic localization of the Swe1 regulator Hsl7 during theSaccharomyces cerevisiae cell cycle. *Molecular Biology of the Cell, 12*(6), 1645-1669.

Holt, L. J., Tuch, B. B., Villén, J., Johnson, A. D., Gygi, S. P., & Morgan, D. O. (2009). Global analysis of Cdk1 substrate phosphorylation sites provides insights into evolution. *Science, 325*(5948), 1682-1686.

Keaton, M. A., & Lew, D. J. (2006). Eavesdropping on the cytoskeleton: Progress and controversy in the yeast morphogenesis checkpoint. *Current Opinion in Microbiology, 9*(6), 540-546.

Lew, D. J. (2000). Cell-cycle checkpoints that ensure coordination between nuclear and cytoplasmic events in saccharomyces cerevisiae. *Current Opinion in Genetics & Development, 10*(1), 47-53.

Longtine, M. S., Fares, H., & Pringle, J. R. (1998). Role of the yeast Gin4p protein kinase in septin assembly and the relationship between septin assembly and septin function. *The Journal of Cell Biology, 143*(3), 719-736.

Shulewitz, M. J., Inouye, C. J., & Thorner, J. (1999). Hsl7 localizes to a septin ring and serves as an adapter in a regulatory pathway that relieves tyrosine phosphorylation of Cdc28 protein kinase in Saccharomyces cerevisiae. *Molecular and Cellular Biology, 19*(10), 7123-7137.

Sikorski, R. S., & Boeke, J. D. (1991). [20] in vitro mutagenesis and plasmid shuffling: From cloned gene to mutant yeast. In G. R. F. Christine Guthrie (Ed.), *Methods in enzymology; guide to yeast genetics and molecular biology* (pp. 302-318) Academic Press.

Walch-Solimena, C., Collins, R. N., & Novick, P. J. (1997). Sec2p mediates nucleotide exchange on Sec4p and is involved in polarized delivery of post-golgi vesicles. *The Journal of Cell Biology, 137*(7), 1495-1509.

CHAPTER 5.

Neck-localization Facilitates Hos3 to Function as a Spindle Position Checkpoint (SPOC) Component

INTRODUCTION

Our previous efforts in the search for a physiological function of Hos3 related to its bud neck localization did not give a clear answer. This is likely because we purely focus on the neck-association itself. It comes to our mind that the previous characterization of Hos3 localization reveals two unique targeting sites: the bud neck and the daughter SPB. If the neck-localization of Hos3 is relevant to or even regulating the daughter-SPB-associated Hos3, we would not be able to discover the function of neck-localized Hos3 until we understand the function of the SPB-associated Hos3. Therefore, in this chapter we tried to focus on the other distinct aspect of Hos3 localization: its asymmetric association with the daughter SPB, to study why Hos3 is targeted to this particular site at the precise moment and what functions it plays. Then we wanted to go back and address the question if such SPB-targeting mechanism or SPB-associated functions of Hos3 are dependent on its bud neck localization. In such manner, we would have a better and more comprehensive understanding of Hos3 as a uniquely targeted HDAC.

METHODS AND MATERIALS

Yeast Strains and Plasmids

All yeast strains were annotated as in Table 5.1. Manipulation of the strains should be refered to *Materials and Methods* of Chapter 2 and 3.

All plasmids were annotated as in Table 5.2. Construction of the plasmids should be refered to *Materials and Methods* of Chapter 2 and 3.

Fluorescence Microscopy

Methods of fluorescence microscopy were similar as described in the *Materials and Methods* of Chapter 2.

Dilution Assay

Methods of dilution assy were similar as described in the *Materials and Methods* of Chapter 2.

SPOC Arrest vs. Bypass Assay

Cells were transformed with the SPB marker Tub4-RFP (*CEN*) and grown to early mid-log phase in minimal medium. Cells were then switched to 14°C for 20h and analyzed by fluorescence microcopy for “arrested” or “bypassed” spindle morphology. Cells containing aberrant spindle morphologies were categorized as either “arrested” (cells displaying misaligned spindle), or “bypassed” (cells containing a misaligned spindle

nevertheless exit mitosis thus giving rise to unbudded cells with 2 SPBs as well as cells with more than 2 SPBs when these unbudded cells start to grow).

Table 5.1. Yeast strains used in Chapter 5

Strain	Genotype	Reference/Source
BY4742	*MAT*α *ura3Δ0 leu2Δ0 his3Δ1 lys2Δ0*	Research Genetics, Inc.
RCY239	*MAT*a *ura3-52 leu2-3,112*	This Study
RCY4693	*MAT*α *ura3Δ0 leu2Δ0 his3Δ1 lys2Δ0 trp1 Hos3::3HA-HIS3*	This Study
RCY4702	*MAT*α *ura3Δ0 leu2Δ0 his3Δ1 lys2Δ0 hsl7Δ::KanMX4*	This Study
RCY4744	*W303-1B adh4::URA3::C1-3A sir2Δ::KanMX sir3Δ::HIS3*	CCC12 in Chou et al., 2008
RCY4749	*MAT*a *ura3Δ0 leu2Δ0 his3Δ1 met15Δ0 bar1Δ::HIS3 Hos3::3HA-HIS3*	This Study
RCY4875	RCY239 *rho*^{0}	This Study
RCY4904	BY4742 *dyn1Δ::KanMX4*	Research Genetics, Inc.
RCY4920	*MATa ura3Δ0 leu2Δ0 his3Δ1 met15Δ0 dyn1Δ::KanMX4 hos3Δ::HIS3*	This Study
RCY4922	BY4742 *kin4Δ::KanMX4*	Research Genetics, Inc.
RCY4932	*MATa ura3Δ0 leu2Δ0 his3Δ1 lys2Δ0 dyn1Δ::KanMX4 kin4Δ::KanMX4*	This Study
RCY4937	*MAT*α *ura3Δ0 leu2Δ0 his3Δ1 lys2Δ0 dyn1Δ::KanMX4 hsl7Δ::KanMX4*	This Study
RCY4939	BY4742 *nip100Δ::KanMX4*	Research Genetics, Inc.
RCY4940	BY4742 *bub2Δ::KanMX4*	Research Genetics, Inc.
RCY4941	BY4742 *bfa1Δ::KanMX4*	Research Genetics, Inc.
RCY4954	BY4742 *num1Δ::KanMX4*	Research Genetics, Inc.
RCY4955	BY4742 *arp1Δ::KanMX4*	Research Genetics, Inc.
RCY4956	BY4742 *jnm1Δ::KanMX4*	Research Genetics, Inc.
RCY4957	*MATa ura3Δ0 leu2Δ0 his3Δ dyn1Δ::KanMX4 bub2Δ::KanMX4*	This Study
RCY4958	*MATa ura3Δ0 leu2Δ0 his3Δ1 lys2Δ0 dyn1Δ::KanMX4 bfa1Δ::KanMX4*	This Study

Table 5.2. Plasmids used in Chapter 5

Plasmid	Description	Reference/Source
pRC374	pRS314	Sikorski and Hieter, 1989.
pRC540	pRS315	Sikorski and Hieter, 1989.
pRC1291	pRS426	Christianson et al., 1992.
pRC3664	pRS316 Hos3-GFP	This Study
pRC4270	pRS426 Hos3-GFP	This Study
pRC4450	pRS316 Hos3(40-697)-GFP	This Study
pRC4489	pRS426 P_{GAL10}-Hos3	This Study
pRC4596	316 Hos3	This Study
pRC4598	316 Hos3$^{H196E, D231N}$	This Study
pRC4753	pRS314 Sir3	This Study
pRC4754	pRS314 Sir3-Hos3(2-549)	This Study
pRC4837	pRS314 Sir3-Hos3(2-549)$^{H196E, D231N}$	This Study
pRC5060	pRS315 Tub4-RFP	This Study
pRC5078	pRS314 Sir3-Hos3(40-549)	This Study
pRC5079	pRS314 Sir3-Hos3(40-549)$^{H196E, D231N}$	This Study
pRC5163	pRS426 P_{GAL10}-Kin4	This Study
pRC5165	pRS426 P_{GAL10}- Hos3$^{H196E, D231N}$	This Study
pRC5178	pRS426 P_{GAL10}-Bub2	This Study
pRC5179	pRS426 P_{GAL10}-Bfa1	This Study
pRC5270	pRS316 Bub2-GFP	This Study
pRC5271	pRS316 Bfa1-GFP	This Study
pRC5272	pRS316 Kin4-GFP	This Study

RESULTS

Loading of Hos3 onto both SPBs in response to spindle misorientation

To understand Hos3 function further, we decided to focus on the other distinct aspect of Hos3 localization, namely its asymmetric association with the daughter SPB (Figure 2.4). A selective association with the daughter SPB suggests that Hos3 could discriminate between the two SPBs respectively positioned in the mother and daughter cells. The SPBs functions as the MTOCs in budding yeast and organize cytoplasmic microtubules which together with motor proteins are instrumental for positioning and segregating the nucleus (Jaspersen and Winey, 2004). Loss of the cytoplasmic dynein heavy chain Dyn1 causes misaligned spindles in a significant number of cells (Li et al., 1993). In such cells, the misaligned spindle is in an orientation perpendicular to rather than in parallel with the mother-bud axis. Interestingly, Hos3 is loaded onto both SPBs in *dyn1*Δ cells with misaligned spindle (Figure 5.1(i)). In comparison, as seen in wild-type cells, Hos3 is still asymmetrically and cell-cycle-dependently targeted onto the daughter SPB in the fraction of *dyn1*Δ cells with a well-aligned spindle (Figure 5.1 (ii) and (iii)). This suggests that the loading of Hos3 onto both SPBs is as a result of spindle orientation defect caused by the lack of dynein motor. Besides dynein, the dynactin complex and the cortical protein Num1 are also essential for pulling cytoplasmic microtubules so as to position the nucleus (Heil-Chapdelaine et al., 2000). Loss of dynactin components (Arp1, Jnm1, and Nip100) or the cortical protein Num1 similarly results in a significant number of cells with

Figure 5.1

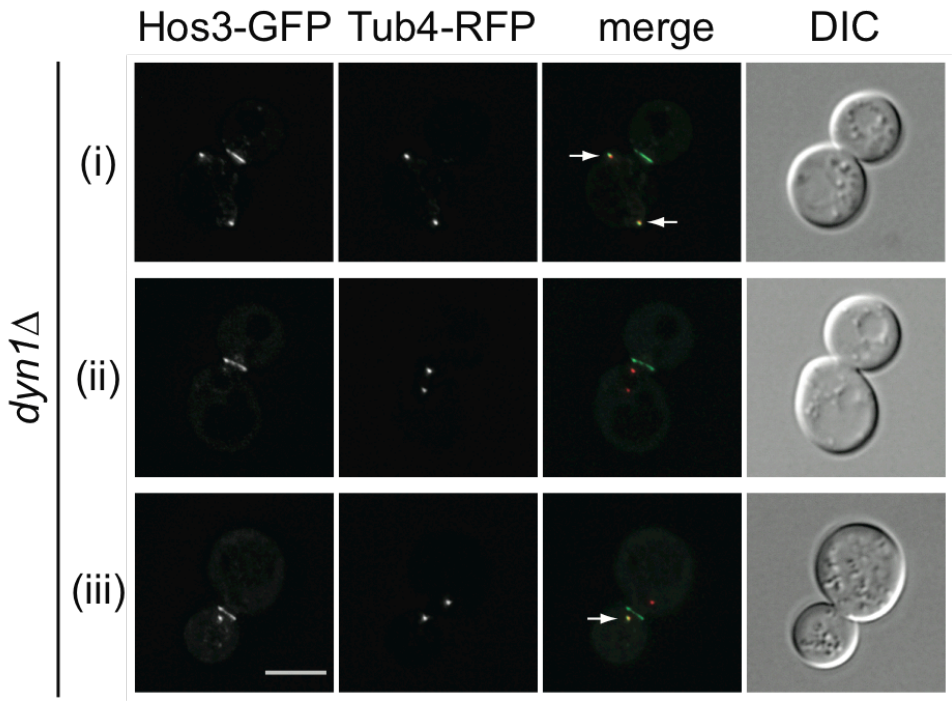

Figure 5.1. Hos3 is loaded onto both SPBs in *dyn1*Δ cells with spindle misorientation

Hos3-GFP (*CEN*) and the SPB marker Tub4-RFP (*CEN*) were co-imaged in *dyn1*Δ cells. Shown are cells with misaligned spindle as (i), or with spindles that are normally aligned as (ii) and (iii). Arrowheads point to Hos3 on both SPBs (i) or on the daughter SPB (iii). Scale bar, 5 μm.

misaligned spindle (Figure 5.2A). In such cells, Hos3 is targeted onto both SPBs (Figure 5.2A). Furthermore, treatment of nocodazole causes microtubule depolymerization and thus renders the spindle to collapse. As a result, the two SPBs stay close due to a lack of tension and appear as a single focus when markered with the SPB component Tub4. This single focus likely contains both SPBs that could not be differentiated from each other due to their close proximity. In these nocodazole-treated cells, Hos3 is targeted to the single focus suggesting that in these spindle-collapsed cells that fail to align the nucleus, Hos3 responds by being loaded onto likely both SPBs (Figure 5.2B). These data together indicate that Hos3 is normally asymmetrically localized to the daughter SPB but can be symmetrically loaded onto both SPBs in response to spindle orientation defect.

Neck-localization is required for loading Hos3 onto both SPBs in response to spindle orientation defect

We previously showed that neck-localization is dispensable for a few cellular activities. Given the unique targeting of Hos3 to both the bud neck and the SPB, we wondered if the neck-targeting of Hos3 is required for its response to spindle misorientation. Deletion of *HSL7* abolishes Hos3 association with the bud neck in *dyn1*Δ cells, and interestingly, *dyn1*Δ *hsl7*Δ cells with misaligned spindle become unable to efficiently load Hos3 onto both SPBs (Figure 5.3A and 5.3B). In the presence of spindle orientation defect,

Figure 5.2

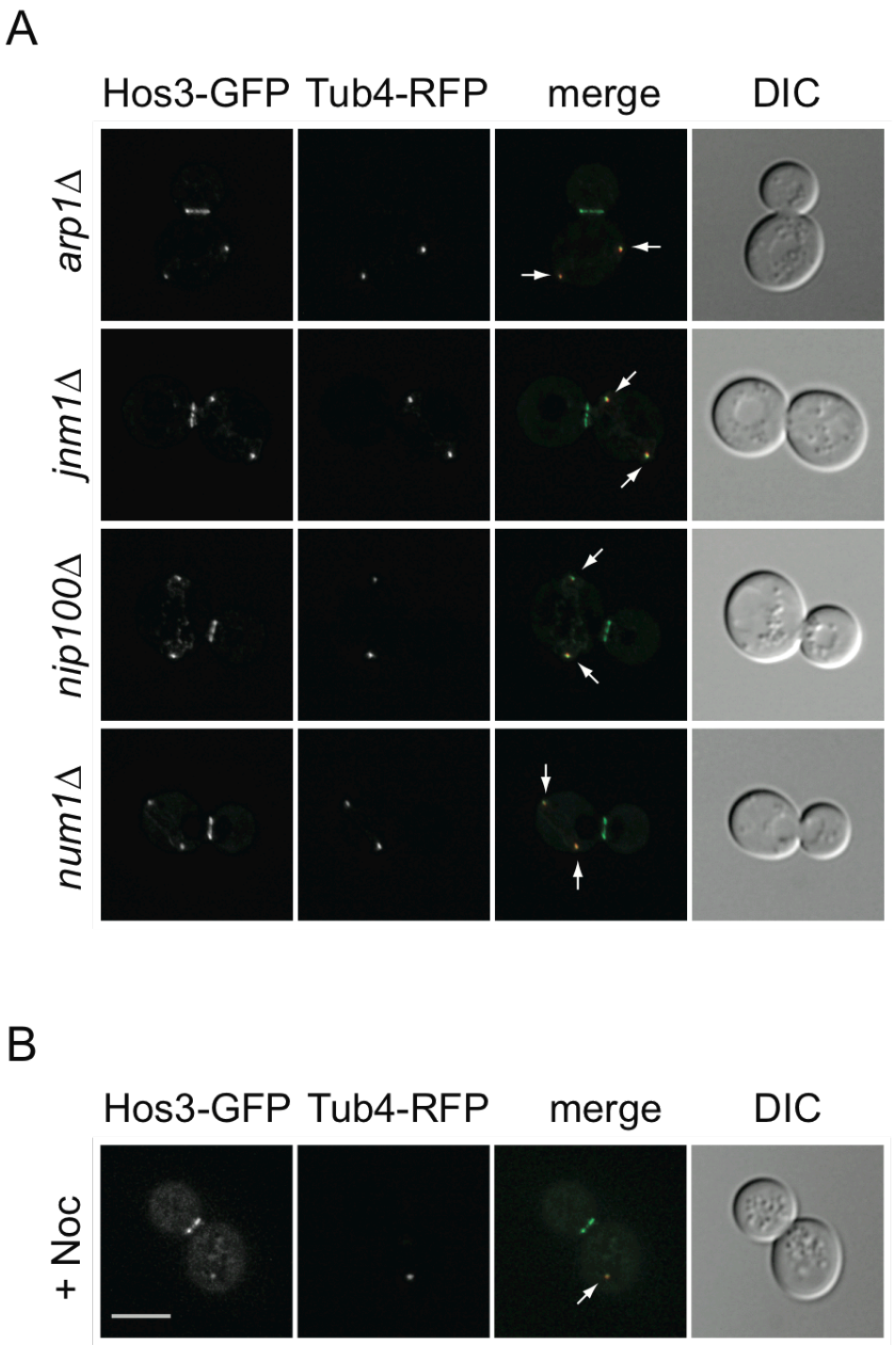
A
Hos3-GFP
Tub4-RFP
merge
DIC
arp1Δ
jnm1Δ
nip100Δ
num1Δ
B
Hos3-GFP
Tub4-RFP
merge
DIC
+ Noc

Figure 5.2. Hos3 is loaded onto both SPBs when cells undergo spindle misorientation

(A) Hos3-GFP (*CEN*) and the SPB marker Tub4-RFP (*CEN*) were co-imaged in *arp1*Δ, *jnm1*Δ, *nip100*Δ, and *num1*Δ cells. Shown are cells with misaligned spindle. Arrowheads point to Hos3 on both SPBs.

(B) Wild-type cells transformed with Hos3-GFP (*CEN*) and the SPB marker Tub4-RFP (*CEN*) were treated with 40 μg/ml nocodazole (Noc) for 3h at 30°C and then analyzed by fluorescence microscopy. Due to microtubule depolymerization, the spindle collapsed and the two SPBs remained close appearing as a single focus. Arrowhead points to Hos3 targeted to the single focus lablled by the SPB marker Tub4-RFP. Scale bar, 5 μm.

about half of the cell population fail to load Hos3 onto any SPB while association of Hos3 with only one SPB is observed in about 20% of the cells. This suggests that upon spindle orientation defect, neck-localized Hos3 serves as a pre-requisite for the cellular response by loading Hos3 onto both SPBs. Given that Hos3 has a low level of cytosolic distribution and there is clear spatial distance between the bud neck and the SPBs for cells with misaligned spindle, we reasoned that the fraction of Hos3 that gets loaded onto the SPBs is from its cytosolic pool. Therefore, neck-localized Hos3 somehow signals to cytosolic Hos3 so that cytosolic Hos3 could be loaded onto both SPBs in response to spindle orientation defect. It should be noted that although Hos3 is absent from the bud neck in all *dyn1*Δ *hsl7*Δ cells with misaligned spindle, still about 30% of such cells have Hos3 loaded onto both SPBs, suggesting that while neck-localization is significant for regulating Hos3 response to the spindle misorientation, some other unknown mechanism(s) should exist to regulate the same process although to a lesser extent.

Hos3 is a Novel Component of the Spindle Position Checkpoint

At least three other proteins (Bub2, Bfa1, and Kin4) were known to be recruited to both SPBs in cells with misaligned spindle (D'Aquino et al., 2005; Pereira and Schiebel, 2005; Figure 5.4). Bub2 and Bfa1 together act as a two-component GTPase-activating protein (GAP) that negatively regulates Tem1 GTPase, a key regulator of the mitotic exit network (MEN) (Bardin and Amon,

Figure 5.3

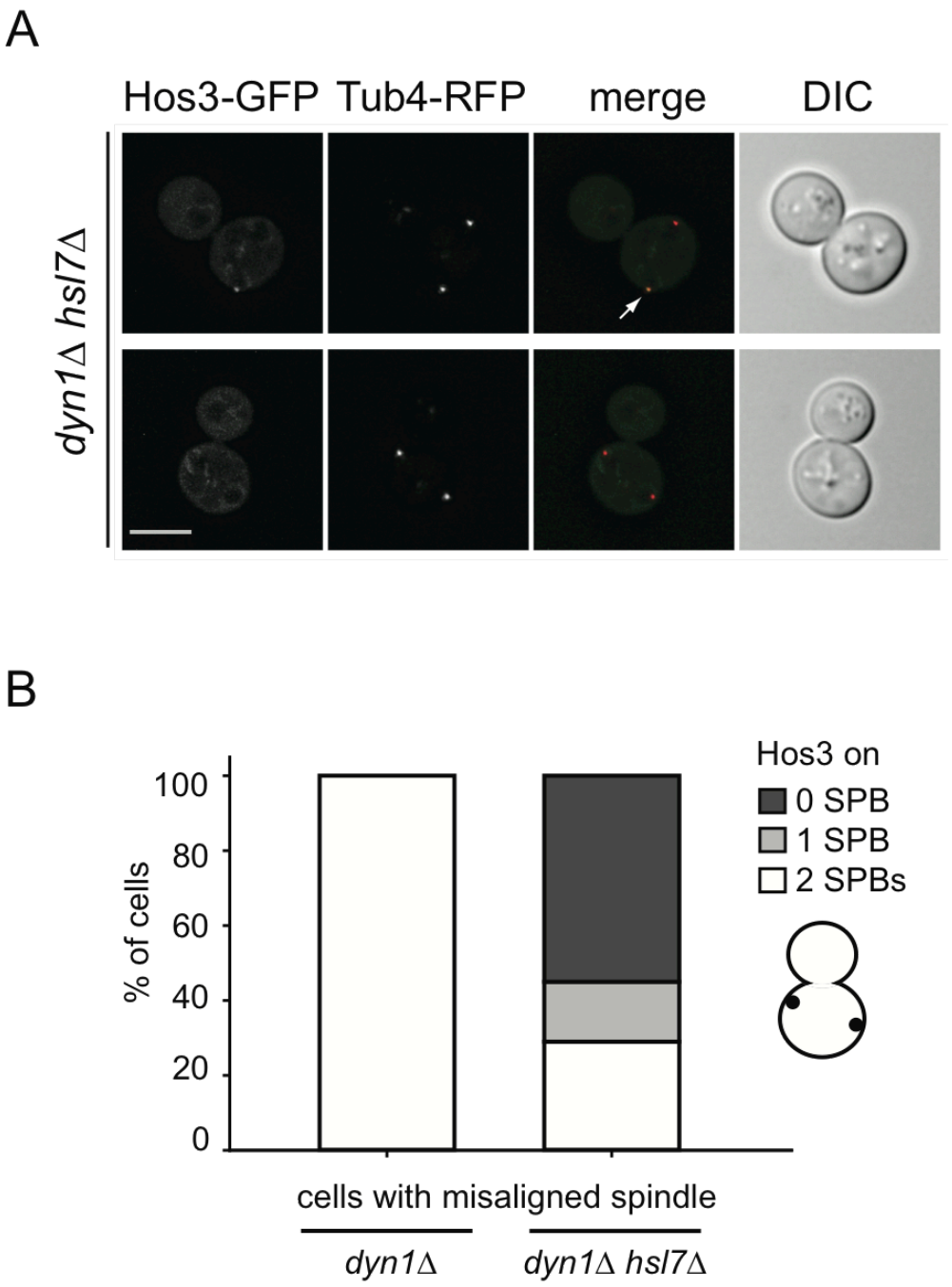
A
Hos3-GFP
Tub4-RFP
merge
DIC
dyn1Δ hsl7Δ
B
Hos3 on
0 SPB
1 SPB
2 SPBs
% of cells
100
80
60
40
20
0
cells with misaligned spindle
dyn1Δ
dyn1Δ hsl7Δ

Figure 5.3. Hos3 fails to be loaded onto both SPBs in *hsl7*Δ cells with spindle orientation defect

(A) Neck-targeting is required for the loading of Hos3 onto both SPBs in response to spindle misorientation. Hos3-GFP (*CEN*) and the SPB marker Tub4-RFP (*CEN*) were co-imaged in *dyn1*Δ *hsl7*Δ cells. Shown are cells with misaligned spindle that load Hos3 onto only one or none of the two SPBs. Arrowhead points to Hos3 on one SPB. Scale bar, 5 μm.

(B) Quantification of cells with misaligned spindle in (A) and Figure 5.1(i). Cells were categorized into three groups based on association of Hos3 with none, only one, or both of the two SPBs. A total number of 100 cells with misaligned spindle were analyzed for each strain.

Figure 5.4

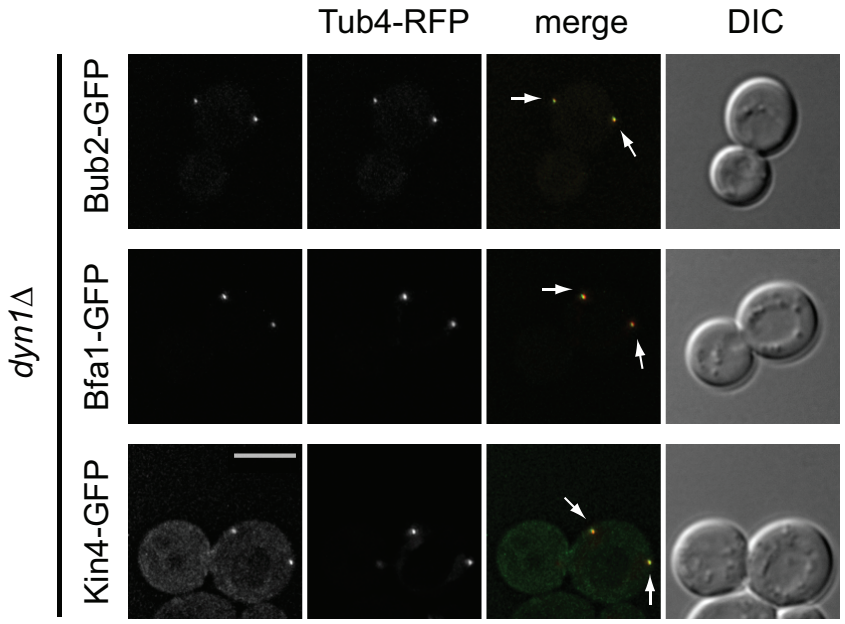

Figure 5.4. Known components of the SPOC are loaded onto both SPBs in response to spindle misorientation

*dyn1*Δ cells transformed with Bub2-GFP (*CEN*) or Bfa1-GFP (*CEN*) or Kin4-GFP (*CEN*) and the SPB marker Tub4-RFP (*CEN*) were analyzed by fluorescence microscopy. Scale bar, 5 μm.

2001). Kin4 functions as another negative regulator of the MEN through phosphorylating Bfa1 and preventing its inactivation by Cdc5 polo-like kinase (D'Aquino et al., 2005; Pereira and Schiebel, 2005; Maekawa et al., 2007). These three proteins are all members of the spindle position checkpoint (SPOC) that monitors spindle orientation before committing the cell to mitotic exit (Caydasi et al., 2010a). The SPOC inhibits the activation of the MEN until the mitotic spindle is aligned properly along the mother-bud axis; when the spindle is misaligned, the SPOC causes cells to arrest at anaphase (Caydasi et al., 2010a).

In response to spindle misorientation, SPOC members are loaded onto both SPBs to inhibit Tem1 activation and thus act as a stop signal for the MEN (D'Aquino et al., 2005; Pereira and Schiebel, 2005). Given its similar SPB-association feature, we asked if Hos3 could function as a SPOC component. Inactivation of the SPOC through loss of Bub2, Bfa1, or Kin4 causes *dyn1*Δ cells arrested with misaligned spindle to nevertheless exit mitosis so the cell population is reduced for "arrested" but increased for "bypassed" spindle morphology (D'Aquino et al., 2005). Similarly, upon loss of Hos3, *dyn1*Δ cells with misaligned spindle were defective in mitotic arrest and thus enriched for the "bypassed" subpopulation (Figure 5.5A). Interestingly, *dyn1*Δ *hsl7*Δ cells were also compromised for the SPOC, consistent with the requirement of neck-localized Hos3 to facilitate the response to spindle misalignment (Figure 5.4A). In *dyn1*Δ *hos3*Δ cells, a plasmid-based wild-type Hos3 restores the population to the "arrested" spindle morphology but the HDAC-dead allele of

Figure 5.5

A

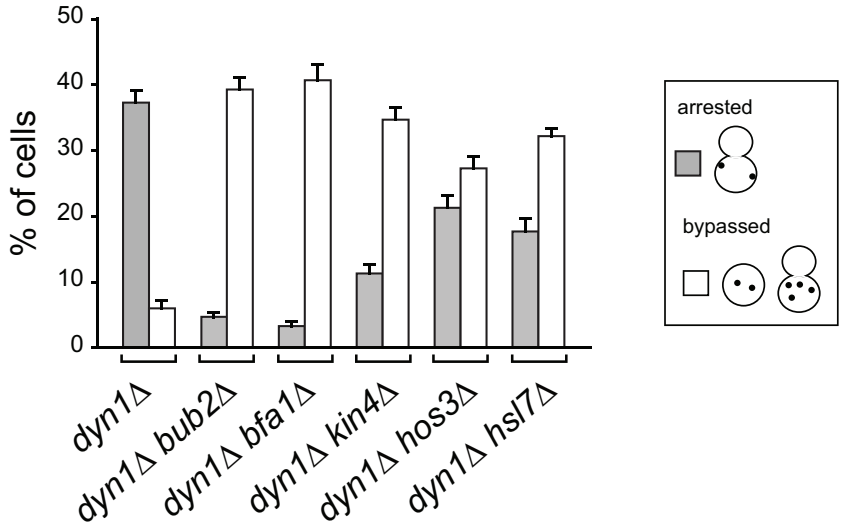
50
40
30
20
10
0
% of cells
arrested
bypassed
dyn1Δ
dyn1Δ bub2Δ
dyn1Δ bfa1Δ
dyn1Δ kin4Δ
dyn1Δ hos3Δ
dyn1Δ hsl7Δ

B

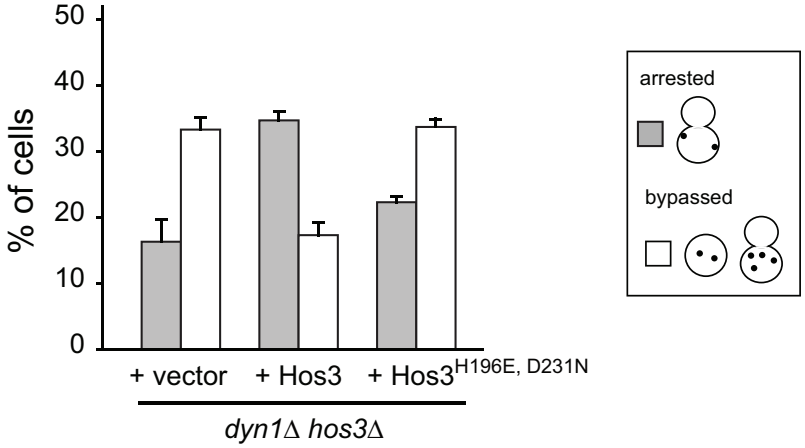
50
40
30
20
10
0
% of cells
arrested
bypassed
+ vector
+ Hos3
+ Hos3H196E, D231N
dyn1Δ hos3Δ

Figure 5.5. Hos3 functions as an HDAC to arrest cells with misaligned spindle

(A) *dyn1*Δ, *dyn1*Δ *bub2*Δ, *dyn1*Δ *bfa1*Δ, *dyn1*Δ *kin4*Δ, *dyn1*Δ *hos3*Δ, and *dyn1*Δ *hsl7*Δ cells, transformed with the SPB marker Tub4-RFP (*CEN*), were grown to early mid-log phase in minimal medium, switched to 14°C for 20h and analyzed by fluorescence microcopy for "arrested" or "bypassed" spindle morphology. A total of 100 cells were analyzed for each strain. Cells containing aberrant spindle morphologies were categorized as either "arrested": cells are arrested with misaligned spindle, or "bypassed": cells containing a misaligned spindle nevertheless exit mitosis thus giving rise to unbudded cells with 2 SPBs as well as cells with more than 2 SPBs when these unbudded cells start to grow.

(B) *dyn1*Δ *hos3*Δ cells transformed with the SPB marker Tub4-RFP (*CEN*) and co-transformed with an empty vector, Hos3 (*CEN*), or Hos3$^{H196E,\ D231N}$ (*CEN*) were analyzed as in (A).

Hos3$^{H196E, D231N}$ renders cells bypassing the mitotic arrest similar to the vector control (Figure 5.5B). Therefore, the HDAC activity is required for Hos3 to function in the SPOC. These data suggest that upon spindle misorientation, Hos3 is loaded onto both SPBs to deacetylate potential substrate(s) and inhibit mitotic exit.

Spindle misorientation activates the SPOC through loading its components onto both SPBs. Consequently, for cells with well-aligned spindle, constitutive association of SPOC components with both SPBs would still inhibit mitotic exit. Indeed, when overexpressed, Bub2 mildly inhibits cellular growth while Bfa1 or Kin4 causes lethality (Figure 5.7A) (D'Aquino et al., 2005; Ro et al., 2002). Compared to the cell-cycle-dependent asymmetrical targeting to the daughter SPB when expressed at low level from a low-copy plasmid, Hos3 could be constitutively associated with the SPBs when overexpressed at high level from a high-copy plasmid (Figure 5.6). In such cells, Hos3 is always associated with the SPBs and after SPB duplication, Hos3 is symmetrically loaded onto both SPBs. Overexpression of Hos3 similarly leads to cellular growth defect likely due to mitotic exit delay as overexpression of Bub2, Bfa1, or Kin4 does, agreeing with its proposed role as a SPOC component (Figure 5.7A). This property is critically dependent on the HDAC activity of Hos3 as overexpression of HDAC-dead Hos3$^{H196E, D231N}$ does not inhibit cellular growth (Figure 5.7B). Taken together, these data suggest that Hos3 functions as a SPOC component.

While exactly how Hos3 functions in the SPOC remains largely

Figure 5.6

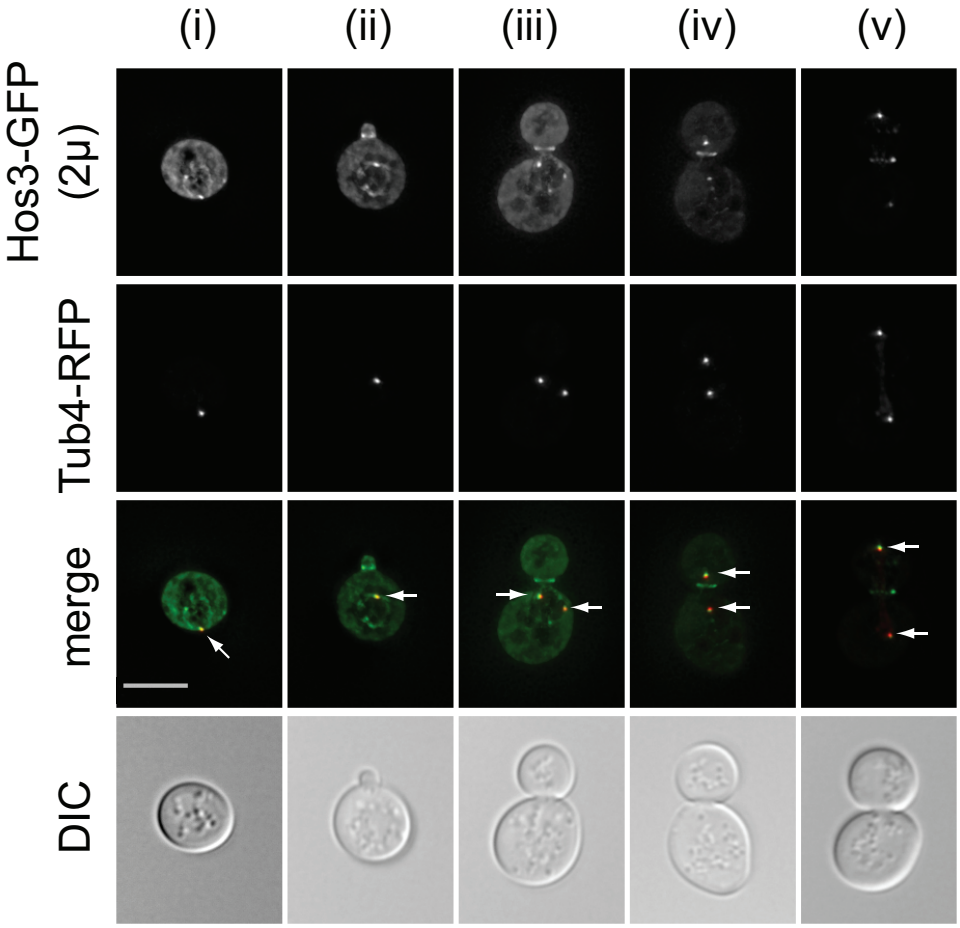

Figure 5.6. Overexpression leads to constitutive association of Hos3 with the SPBs

Wild-type cells transformed with a high-copy 2μ vector bearing Hos3-GFP and the SPB marker Tub4-RFP (*CEN*) were analyzed by fluorescence microscopy. Cells at various cell cycle stages of (i) “unbudded”, (ii) “budding”, (iii) “post-SPB-duplication”, (iv) “spindle elongation”, and (v) “nuclear segregation”, are shown. The images are rotated with the bud neck parallel to the horizontal axis. Arrowheads point to SPB-associated Hos3. Scale bar, 5 μm.

Figure 5.7

A

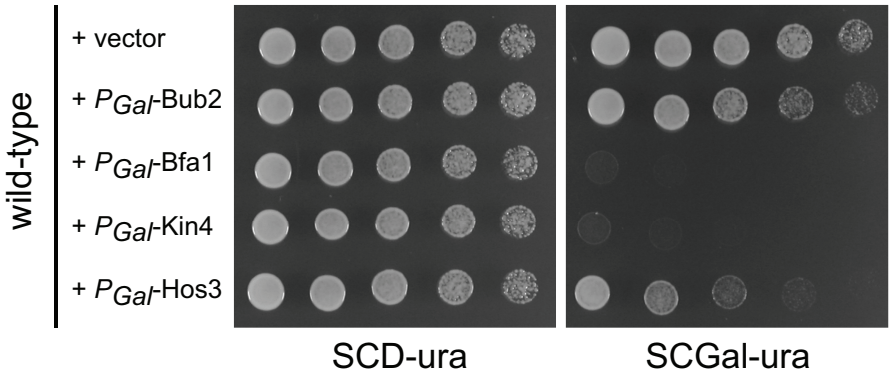
wild-type
+ vector
+ P_{Gal}-Bub2
+ P_{Gal}-Bfa1
+ P_{Gal}-Kin4
+ P_{Gal}-Hos3
SCD-ura
SCGal-ura

B

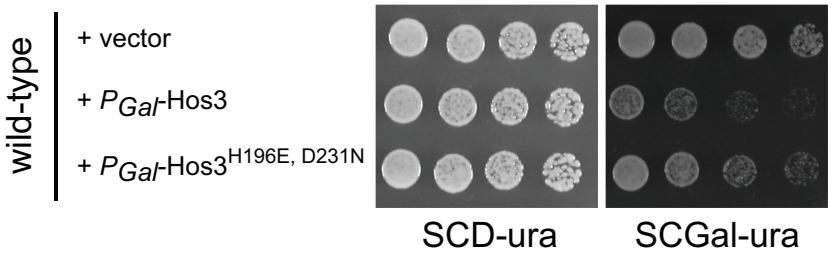
wild-type
+ vector
+ P_{Gal}-Hos3
+ P_{Gal}-Hos3$^{H196E, D231N}$
SCD-ura
SCGal-ura

Figure 5.7. Overexpression of the known SPOC components and Hos3 leads to cellular growth defect

(A) Wild-type cells, transformed with an empty vector or 2μ vectors bearing Bub2, Bfa1, Kin4, and Hos3 all driven under a galactose-inducible promoter, were grown to mid-log phase in synthetic raffinose medium (-ura) and analyzed by 3-serial dilution onto SCD-ura and SCGal-ura plates for incubation at 30°C. Gal: galactose.

(B) Wild-type cells, transformed with an empty vector or 2μ vectors bearing Hos3 and Hos3$^{H196E, D231N}$ both driven under a galactose-inducible promoter, were analyzed as in (A).

unknown, Hos3 seems to be dispensable for the known SPOC components as *hos3*Δ cells overexpressing such SPOC genes still display growth defect (Figure 5.8A, compared to Figure 5.7A). Conversely, mutant cells of the known SPOC components are still compromised for cellular growth when overexpressing Hos3, arguing they are not required for Hos3 to function in the SPOC (Figure 5.8B, compared to Figure 5.7A). When we checked the localization of such proteins, all of them are efficiently loaded onto both SPBs in the respective mutants with misaligned spindles (Figure 5.9). Therefore, Hos3 is not required for the association of the known SPOC components (Bub2, Bfa1, and Kin4) with the SPBs, and neither are they involved in targeting Hos3 onto the SPBs. This is consistent with the overexpression effect we observed (Figure 5.8). It appears that Hos3 may act in parallel with the known SPOC components.

We showed that neck-localized Hsl7 is important for effectively loading Hos3 onto both SPBs in cells with misaligned spindles. We asked if overexpression of Hos3 in *hsl7*Δ cells could cause a cellular growth defect. The result suggests that this is the case (Figure 5.10). This is likely because overexpression of Hos3 similarly targets Hos3 constitutively onto the SPBs in *hsl7*Δ cells as observed in the wildtype cells (Figure 5.6).

Figure 5.8

A

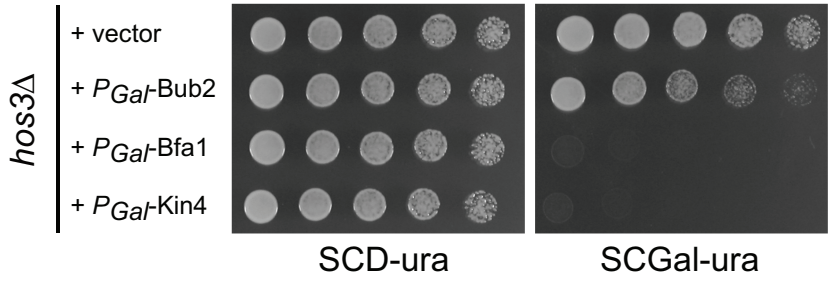
hos3Δ
+ vector
+ P_{Gal}-Bub2
+ P_{Gal}-Bfa1
+ P_{Gal}-Kin4
SCD-ura
SCGal-ura

B

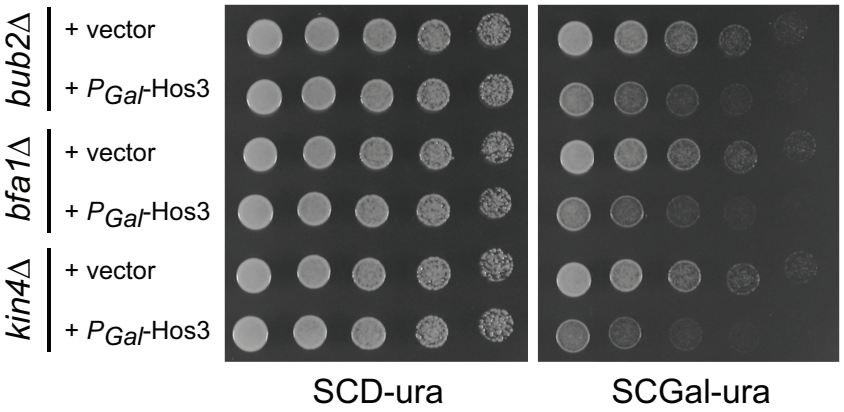
bub2Δ
+ vector
+ P_{Gal}-Hos3
bfa1Δ
+ vector
+ P_{Gal}-Hos3
kin4Δ
+ vector
+ P_{Gal}-Hos3
SCD-ura
SCGal-ura

Figure 5.8. The known SPOC components and Hos3 are mutually dispensable for their overexpression effect

(A) *hos3*Δ cells, transformed with an empty vector or 2μ vectors bearing Bub2, Bfa1, and Kin4 all driven under a galactose-inducible promoter, were grown to mid-log phase in synthetic raffinose medium (-ura) and analyzed by 3-serial dilution onto SCD-ura and SCGal-ura plates for incubation at 30°C. Gal: galactose.

(B) *bub2*Δ, *bfa1*Δ, and *kin4*Δ cells, respectively transformed with an empty vector or a 2μ vector bearing Hos3 driven under a galactose-inducible promoter, were analyzed as in (A).

Figure 5.9

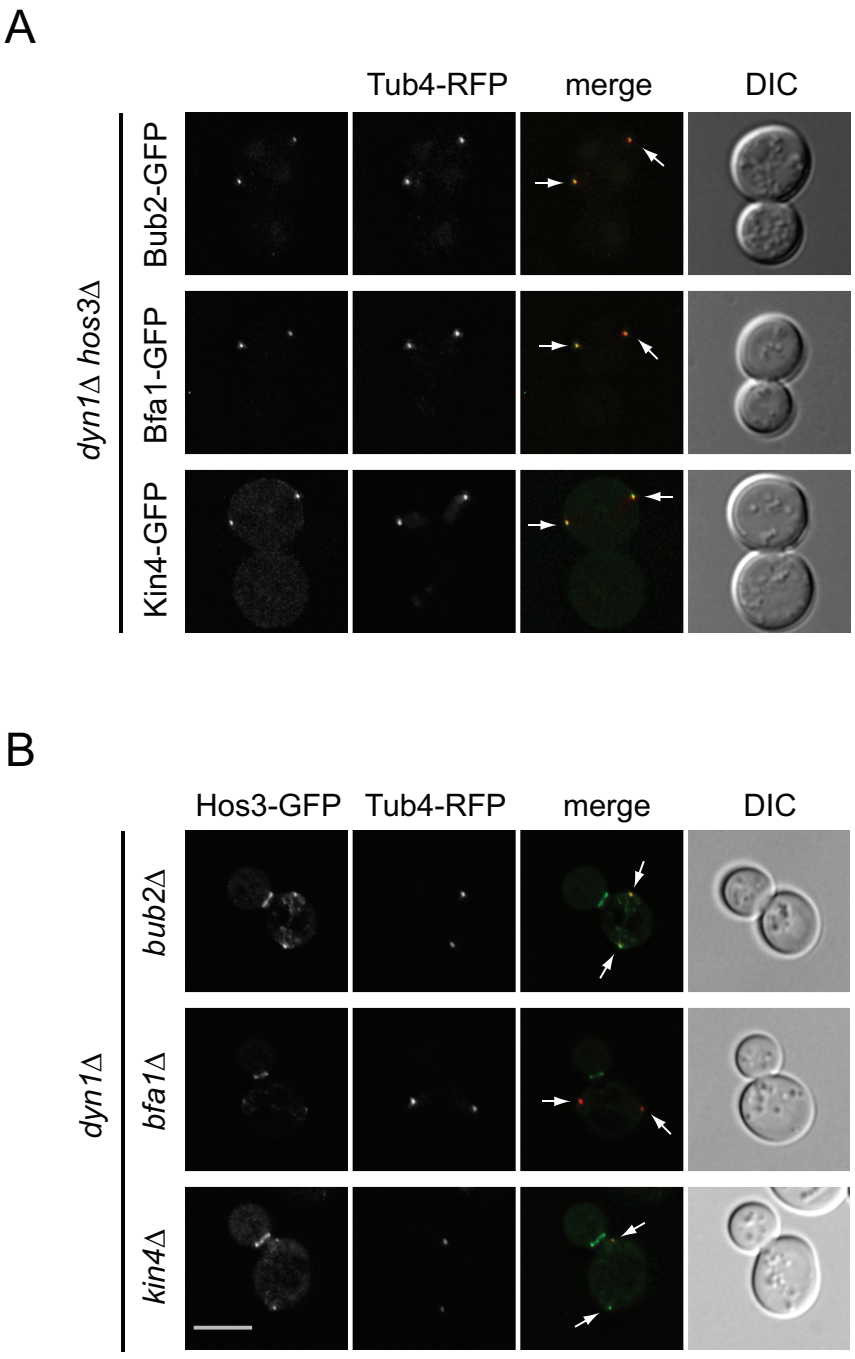
A
Tub4-RFP
merge
DIC
dyn1Δ hos3Δ
Bub2-GFP
Bfa1-GFP
Kin4-GFP
B
Hos3-GFP
Tub4-RFP
merge
DIC
dyn1Δ
bub2Δ
bfa1Δ
kin4Δ

Figure 5.9. The known SPOC components and Hos3 are mutually dispensable for their targeting onto the SPBs

(A) *dyn1*Δ *hos3*Δ cells, transformed with Bub2-GFP (*CEN*) or Bfa1-GFP (*CEN*) or Kin4-GFP (*CEN*), and with the SPB reporter Tub4-RFP (*CEN*), were analyzed by fluorescence microscopy. Shown are cells with misaligned spindle. Arrowheads point to Hos3 on both SPBs.

(B) *dyn1*Δ *bub2*Δ, *dyn1*Δ *bfa1*Δ, and *dyn1*Δ *kin4*Δ cells, were respectively transformed with Hos3-GFP (*CEN*) and Tub4-RFP (*CEN*) were analyzed by fluorescence microscopy. Shown are cells with misaligned spindle. Arrowheads point to Hos3 on both SPBs. Scale bar, 5 μm.

Figure 5.10

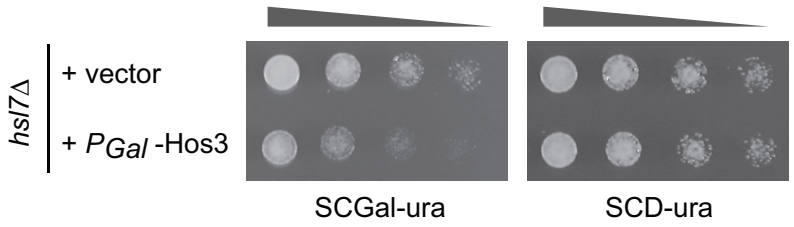

Figure 5.10. Overexpression of Hos3 leads to cellular growth defect in *hsl7*Δ cells

*hsl7*Δ cells, transformed with an empty vector or 2μ vectors bearing Hos3 driven under a galactose-inducible promoter, were grown to mid-log phase in synthetic raffinose medium (-ura) and analyzed by 3-serial dilution onto SCD-ura and SCGal-ura plates for incubation at 30°C. Gal: galactose.

Mechanism to target Hos3 onto the SPBs

The mechanism(s) underlying the conditional targeting of SPOC components onto both SPBs remain largely ambiguous. We sought to understand this question from the perspective of Hos3. The observation that overexpression constitutively targets Hos3 onto the SPBs throughout the cell cycle has three important implications (Figure 5.6, compared to Figure 2.4). First, an efficient regulation conferring asymmetrical SPB pattern for Hos3 is critically dependent upon its protein homeostasis. If the cellular levels of Hos3 are high beyond a threshold, Hos3 is unable to asymmetrically associate with the daughter SPB. Therefore, Hos3 level needs to be well regulated. Upon the inhibition of protein synthesis by cycloheximide, endogenous Hos3 is quickly turned over (with a half-life of ~ 48min) (Figure 5.10A). Addition of MG132, an inhibitor of the 26S proteasome, completely blocks Hos3 degradation revealing Hos3 is turned over in a proteasome-dependent manner (Figure 5.10B). Such proteasome-dependent turnover of endogenous Hos3 could be observed when cells were arrested at G_1 phase by alpha factor or at S phase by hydroxyurea or at G_2/M phase by nocodazole, suggesting Hos3 is actively turned over throughout the cell cycle (Figure 5.10C and 5.10D). These data demonstrate that Hos3 level is finely regulated *in vivo* to allow the asymmetrical association of Hos3 with the daughter SPB.

The second implication is that although the protein that directly recruits Hos3 to the SPBs remains unknown, it is probably a *bona fide* SPB

Figure 5.11

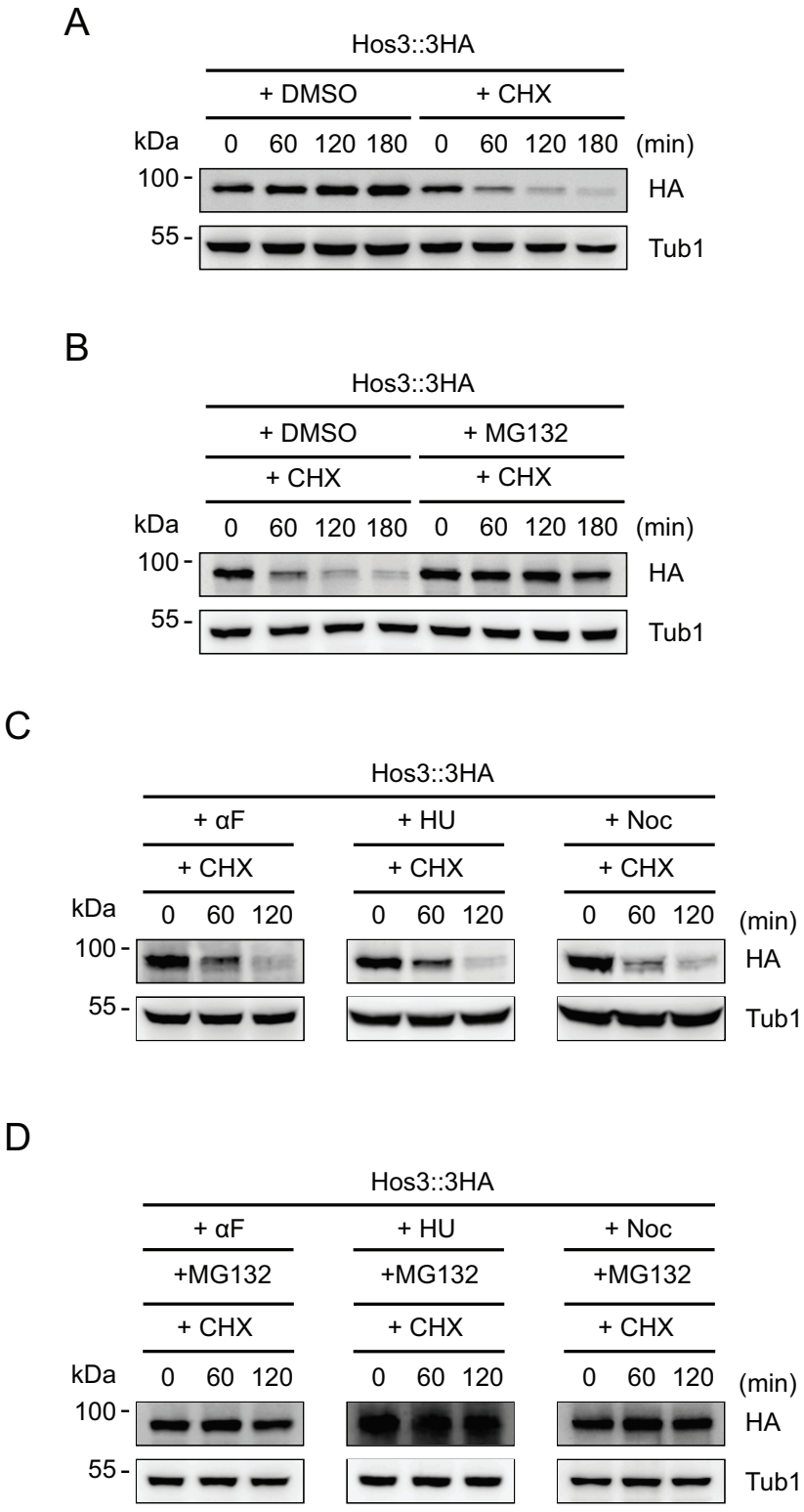
A
Hos3::3HA
+ DMSO
+ CHX
kDa
0 60 120 180 0 60 120 180 (min)
100 -
HA
55 -
Tub1
B
Hos3::3HA
+ DMSO
+ MG132
+ CHX
+ CHX
kDa
0 60 120 180 0 60 120 180 (min)
100 -
HA
55 -
Tub1
C
Hos3::3HA
+ αF
+ HU
+ Noc
+ CHX
+ CHX
+ CHX
kDa
0 60 120 0 60 120 0 60 120 (min)
100 -
HA
55 -
Tub1
D
Hos3::3HA
+ αF
+ HU
+ Noc
+MG132
+MG132
+MG132
+ CHX
+ CHX
+ CHX
kDa
0 60 120 0 60 120 0 60 120 (min)
100 -
HA
55 -
Tub1

Figure 5.11. Hos3 is degraded in a proteasome-dependent manner throughout the cell cycle

(A) Hos3 is turned over *in vivo*. Cells with endogenous Hos3 fused with 3 tandem copies of HA tag were grown to mid-log phase in YPD medium at 30°C and treated with DMSO or 50 μg/ml cycloheximide (CHX) at time point 0. Equal aliquots of cells were collected every 60min and assayed for Hos3 level by preparing the whole cell extracts for immunoblotting against the HA tag. Tub1 was used as loading control.

(B) Inhibition of the 26S proteasome by MG132 blocks Hos3 degradation *in vivo*. Cells in (A) were grown and pre-treated with DMSO or 75 μM MG132 for 30min as described in Liu et al., 2007. Cells were then treated with 50 μg/ml CHX and assayed as in (A).

(C) Hos3 is degraded throughout the cell cycle. Cells with endogenous Hos3 fused with 3 tandem copies of HA tag were arrested at G_1 phase with 0.1 μg/ml α-factor (αF), at S phase with 15 mg/ml hydroxyurea (HU) treatment, or at G_2/M phase with 15 μg/ml nocodazole (Noc) treatment. All cell-cycle arrest treatments were imposed for 3h at 30°C. *bar1*Δ cells were used in the αF treatment for higher arrest efficiency. Efficient cell cycle arrest was validated by both cellular morphology check and flow cytometry analysis (data not shown). The arrested cells were then treated with 50 μg/ml CHX and assayed as in (A).

(D) Hos3 is degraded throughout the cell cycle in a proteasome-dependent manner. Cells in (C) were grown as described in Liu et al., 2007, arrested with

αF, HU, or Noc as in (C), and pre-treated with 75 μM MG132 for 30min to inhibit the 26S proteasome. Cells were then treated with 50 μg/ml CHX and assayed as in (A).

component as Hos3 is capable of being recruited onto both SPBs (Figure 5.1, 5.6, and 5.12A).

As the third implication, the paradox that the “unknown recruiter” of Hos3 is constantly associated with the SPBs but Hos3 is loaded only onto the daughter SPB at a later cell cycle stage clearly suggests that there exists a mechanism to differentiate between the mother cell and the daughter cell. In theory, two alternative models could establish the asymmetrical association of Hos3 with the daughter SPB. One hypothetic model baed on a proposed daughter-cell-bound activation zone (Figure 5.12B). Based on this model, the “unknown recruiter” needs to be activated within the daughter cell to allow Hos3 association. Therefore, Hos3 is not loaded when SPBs are still in the mother cell but loaded onto the daughter SPB once it is located within the daughter cell. An alternative model based on a proposed mother-cell-bound inhibition zone could equally explain the SPB-association features of Hos3 (Figure 5.12C). Based on this model, an inhibitory zone exclusively within the mother cell inhibits the interaction between the “unknown recruiter” and Hos3, thus preventing Hos3 loading when the SPBs are still in the mother cell. As the daughter SPB passes the bud neck and enters the daughter cell during anaphase, it escapes from the inhibitory zone and thus allows for the “unknown recruiter” to load Hos3. For both models, in the presence of spindle orientation defect, neck-localized Hos3 in an unknown mechanism signals to cytosolic Hos3 for it to bypass the regulation (activation zone in Figure 5.12B

Figure 5.12

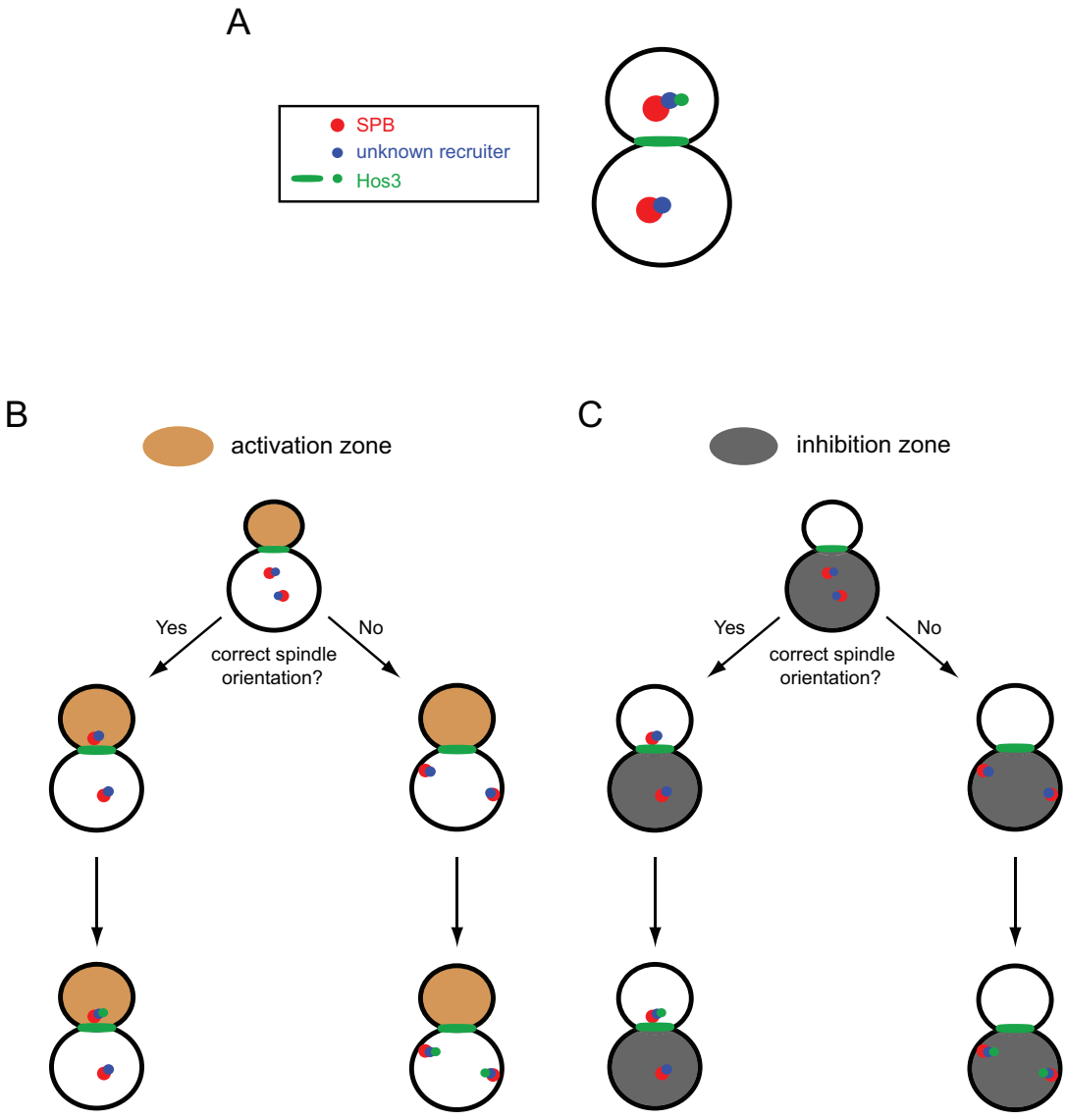
A
SPB
unknown recruiter
Hos3
B
activation zone
Yes
No
correct spindle orientation?
C
inhibition zone
Yes
No
correct spindle orientation?

Figure 5.12. Two models for the mechanism of loading Hos3 onto the SPBs

(A) A proposed SPB component functions as the “unknown recruiter” that directly recruits Hos3 to the daughter SPB in wild-type cells.

(B) Model #1: an activation zone is exclusively within the daughter cell. For cells with correct spindle orientation, as the daughter SPB enters the daughter cell, the SPB component capable of Hos3 association becomes activated and thus recruits Hos3. For cells with spindle misorientation, neck-localized Hos3 in an unknown mechanism signals to cytosolic Hos3 for it to bypass the activation zone and thus allow being recruited by the SPB component to both SPBs.

(C) Model #2: an inhibition zone is exclusively within the mother cell. For cells with correct spindle orientation, as the daughter SPB enters the daughter cell, the SPB component capable of Hos3 association escapes from the inhibition zone and thus recruits Hos3. For cells with spindle misorientation, neck-localized Hos3 in an unknown mechanism signals to cytosolic Hos3 for it to bypass the inhibition zone and thus allow being recruited by the SPB component to both SPBs.

or inihibition zone in Figure 5.12C) and thus allow being recruited by the "unknown recruiter" to both SPBs to function in the SPOC.

Future work is needed to investigate if one of these two competing models is correct to establish the SPB asymmetry of Hos3, and if so, the molecular details of this particular regulatory model.

The NH_2-terminus of Hos3 plays important roles in its asymmetrical association with the daughter SPB

Although the molecular determinants for the SPB asymmetry of Hos3 remains largely unknown, we found that its NH_2-terminus is important for such association feature. To be recruited asymmetrically to the daughter SPB in wildtype cells, Hos3 requires its short NH_2-terminus (amino acids of 1-39). A construct with deletion of amino acids 1-39, Hos3(*NΔ*), still localizes to the bud neck but becomes constitutively associated with the SPBs throughout the cell cycle (Figure 5.13A compared to Figure 5.13B). This result suggests that the NH_2-terminus of Hos3 is required for its asymmetrical SPB association pattern. More specifically, the fact that Hos3(*NΔ*) displays constant association with the SPBs argues that Hos3 has intrinsic ability to associate with the SPB but the NH_2-terminus places Hos3 under the cell-cycle-dependent regulation to establish an asymmetrical SPB association pattern. Without this region, Hos3(*NΔ*) no longer responds to this regulatory mechanism, and Hos3 is constitutively and symmetrically targeted onto the SPBs.

Figure 5.13

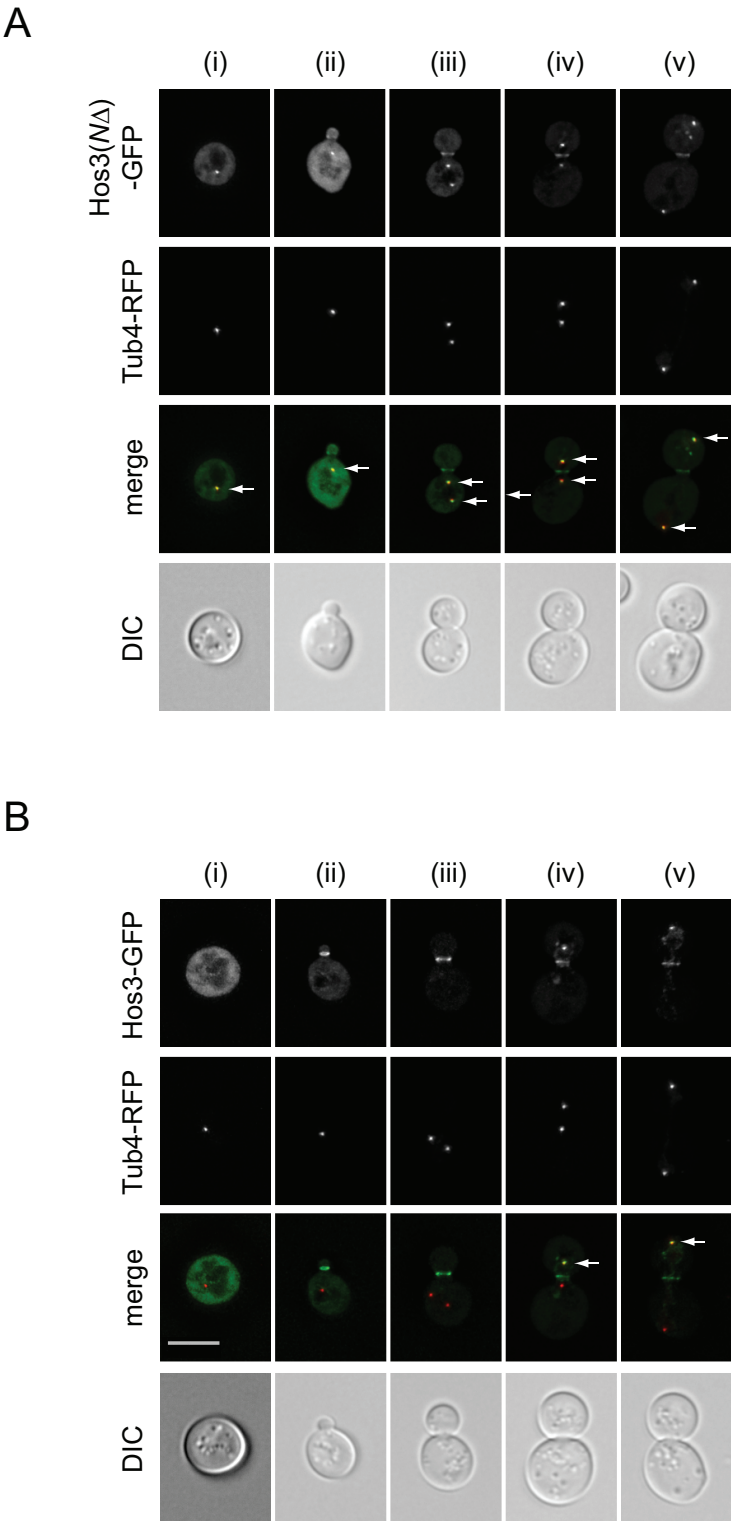
A
(i)
(ii)
(iii)
(iv)
(v)
Hos3(NΔ)-GFP
Tub4-RFP
merge
DIC
B
(i)
(ii)
(iii)
(iv)
(v)
Hos3-GFP
Tub4-RFP
merge
DIC

Figure 5.13. Overexpression leads to constitutive association of Hos3 with the SPBs

Localization of Hos3(*N*Δ)-GFP (*CEN*) (A) or Hos3-GFP (*CEN*) (B) was analyzed in wildtype *rho*^{0} cells coexpressing Tub4-RFP (*CEN*). Images are edited as in Figure 1E. Arrowheads point to Hos3(*N*Δ) constitutively on the SPBs (A), or full-length Hos3 on the daughter SPB (B). Scale bar, 5 μm.

Given that Hos3(*NΔ*) displays the striking different SPB-association feature compared to the full-length Hos3 (Figure 5.13), if our model in which the symmetrical targeting of Hos3 onto both SPBs after anaphase mediates a cell cycle inhibition is correct, Hos3(*NΔ*) should cause a delay in mitotic exit for the wild-type cells even though these cells do not have any spindle orientation defect at all.

I used the wild-type *rho0* strain rather than the wild-type strain to eliminate the mitochondria signal of Hos3(*NΔ*) (Figure 2.10B). The result was initially surprising in that Hos3(*NΔ*) does not cause a cellular growth defect compared to Hos3 (Figure 5.14). However, in a second thought, the above hypothesis is valid only on the condition of an important but not yet tested assumption: Hos3(*NΔ*) is a functional HDAC as Hos3. We showed that by fusing Sir3 with Hos3(40-549), an allele lacking the NH_2-terminus, the chimera (Sir3-Hos3(40-549)) is targeted to the Sir complex sites just as Sir3-Hos3(2-549) is (Figure 5.15A compared to Figure 2.8D). The ability of Sir3-Hos3(40-549) to be targeted to the Sir complex sites allows us to test the function of this chimera using the silencing and mating assays (Figure 5.15B).

The result shows that Sir3-Hos3(2-549) is a functional thus active HDAC but Sir3-Hos3(40-549) is nonfunctional and thus should be an inactive HDAC (Sir3-Hos3(40-549) behaves like HDAC-dead Sir3-Hos3(40-549)$^{H196E, D231N}$). Therefore, deletion of the N-terminus abolishes the HDAC activity of Hos3. We showed that the involvement of Hos3 in regulating spindle

Figure 5.14

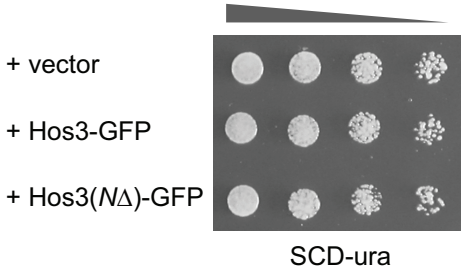

Figure 5.14. Hos3(*N*Δ) does not cause cellular growth defect in the wild-type cells

Wild-type *rho0* cells, transformed with an empty vector or a *CEN* vector bearing Hos3-GFP or Hos3(*N*Δ)-GFP, were grown to mid-log phase in the selective medium and analyzed by 3-serial dilution onto SCD-ura plates for incubation at 30°C.

misorientation is dependent on its HDAC activity (Figure 5.5B and 5.7B). Consequently, the result becomes understandable in that although Hos3(*NΔ*) is symmetrically targeted to the SPBs, it fails to arrest the cell cycle by being an inactive HDAC.

Therefore, at least two conditions are required of Hos3 to function in the SPOC: 1). Hos3 becomes symmetrically loaded onto both SPBs in telophase cells, and 2). Hos3 maintains HDAC activity. This model would be best tested if an allele that meets both of these conditions could be found in the future and used in the relevant assays. Nevertheless, the above experiment with the Hos3(*NΔ*) allele does not argue against our model, and it further supports our discovery that the function of Hos3 in the SPOC is dependent on its HDAC activity.

Figure 5.15

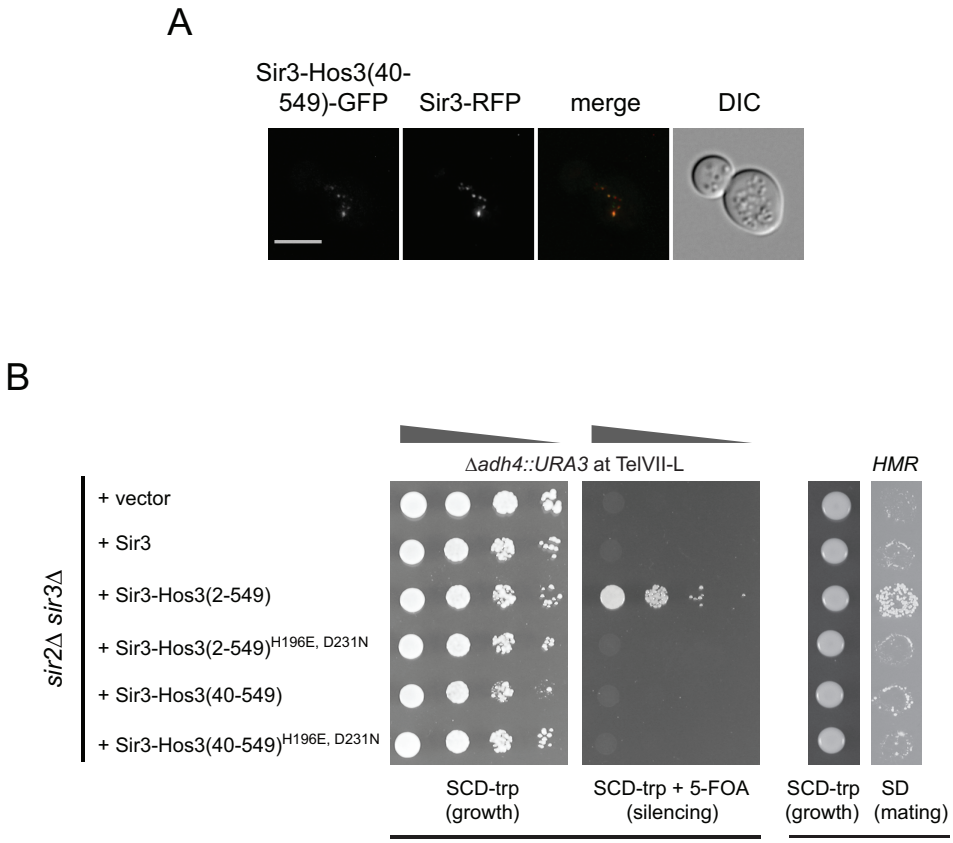

Figure 5.15. Loss of the NH_2-terminus renders Hos3 HDAC-inactive

(A) Wild-type cells, transformed with Sir3-Hos3(40-549)-GFP (*CEN*) and Sir3-RFP (*CEN*), were analyzed by fluorescence microscopy. Scale bar, 5 μm.

(B) *sir2Δ sir3Δ* cells were respectively transformed with the described vectors and analyzed by the silencing ad mating assays as in Figure 2.8.

DISCUSSION

Although we did not nail down the protein that recruits Hos3 to the daughter SPB as we did in Hsl7 for its recruitment of Hos3 to the bud neck, our study did reveal a group of mutants displaying the surprising phenotype: in comparison to the cell-cycle-dependent and asymmetrical association with the daughter SPB, Hos3 is symmetrically loaded onto both SPBs in cells with spindle orientation defect. Such finding finally points to the correct aspects of cell biology we should focus on for the search of Hos3 functions: spindle orientation and mitotic control.

Hos3 functions as a SPOC component to prevent mitotic exit in cells with spindle misorientation. Therefore, Hos3 acts like a checkpoint protein. It is not functioning until the checkpoint it is involved in (in this case the SPOC) has been appropriately activated. This also likely explains the observation that *hos3*Δ cells displays little phenotype: the role of Hos3 could be readily revealed only within the context that renders cells under active SPOC regulation. Therefore, *hos3*Δ cells would display a phenotype only with the *dyn1*Δ background.

Importantly the role of Hos3 in the SPOC requires Hos3 bud neck localization. One likely model would be that Hos3 at the bud neck functions as a “sensor” to monitor spindle orientation so that cells could properly decide if Hos3 would be loaded onto both SPBs or not. It is still unknown how spindle orientation defect could be spatially sensed by neck-localized Hos3. However, the daughter side of the bud neck serves as a critical landmark because as the

daughter SPB passes the neck, correct spindle orientation is defined and the MEN is activated. Given that Hos3 is likely loaded from its cytosolic pool onto both SPBs in the SPOC response, another unresolved issue is how neck-localized Hos3 would signal the spindle orientation defect to cytosolic Hos3. It should also be noted that while all *hsl7*Δ cells lack Hos3 neck localization, roughly 30% of the arrested population still load Hos3 onto both SPBs. Therefore, while Hos3 neck-targeting efficiently facilitates its SPOC response, other mechanism(s) are also involved. Detailed discussion of Hos3 functioning as an HDAC in the SPOC is included in the following Chapter 6.

REFERENCES

Caydasi, A., Ibrahim, B., & Pereira, G. (2010). Monitoring spindle orientation: Spindle position checkpoint in charge. *Cell Division, 5*(1), 28.

Christianson, T. W., Sikorski, R. S., Dante, M., Shero, J. H., & Hieter, P. (1992). Multifunctional yeast high-copy-number shuttle vectors. *Gene, 110*(1), 119-122.

D'Aquino, K. E., Monje-Casas, F., Paulson, J., Reiser, V., Charles, G. M., Lai, L., et al. (2005). The protein kinase Kin4 inhibits exit from mitosis in response to spindle position defects. *Molecular Cell, 19*(2), 223-234.

Heil-Chapdelaine, R. A., Oberle, J. R., & Cooper, J. A. (2000). The cortical protein Num1p is essential for dynein-dependent interactions of microtubules with the cortex. *The Journal of Cell Biology, 151*(6), 1337-1344.

Jaspersen, S. L., & Winey, M. (2004). The budding yeast spindle pole body: structure, duplication, and function. *Annual Review of Cell and Developmental Biology, 20*(1), 1-28.

Li, Y. Y., Yeh, E., Hays, T., & Bloom, K. (1993). Disruption of mitotic spindle orientation in a yeast dynein mutant. *Proceedings of the National Academy of Sciences, 90*(21), 10096-10100.

Maekawa, H., Priest, C., Lechner, J., Pereira, G., & Schiebel, E. (2007). The yeast centrosome translates the positional information of the anaphase spindle into a cell cycle signal. *The Journal of Cell Biology, 179*(3), 423-436.

Pereira, G., & Schiebel, E. (2005). Kin4 kinase delays mitotic exit in response to spindle alignment defects. *Molecular Cell, 19*(2), 209-221.

Ro, H., Song, S., & Lee, K. S. (2002). Bfa1 can regulate Tem1 function independently of Bub2 in the mitotic exit network of saccharomyces cerevisiae. *Proceedings of the National Academy of Sciences, 99*(8), 5436-5441.

Sikorski, R. S., & Hieter, P. (1989). A system of shuttle vectors and yeast host strains designed for efficient manipulation of DNA in saccharomyces cerevisiae. *Genetics, 122*(1), 19-27.

CHAPTER 6.

Discussion of the Functions of Hos3 as an HDAC

INTRODUCTION

We have made a certain number of important discoveries about the unknown HDAC Hos3. Such knowledge together suggests a well-orchestrated mechanism by targeting Hos3 to the unique cellular compartmetns at the appropriate physiological conditions and thus allowing Hos3 to function in the SPOC as neede. In this chapter, we aimed to discuss about the details how Hos3 achieves such extraordinary regulation as a checkpoint protein. Moreover, we would also briefly comment with regard to the surprising observation in Chapter 2 that certain truncated forms of Hos3 are targeted to the mitochondria. We hope by integrating all the information we have gathered so far for Hos3, we would have a better understanding of this HDAC from just the interesting localization observed at the beginning of Chapter 2 to the stage where we could finally be able to at least partially answer the core question of our study as how and why Hos3 is uniquely targeted to those cellular sites.

METHODS AND MATERIALS

Yeast Strains and Plasmids

All yeast strains were annotated as in Table 6.1. Manipulation of the strains should be refered to *Materials and Methods* of Chapter 2 and 3. The wild-type *rho0* strain (RCY4875) was made by treating the wild-type strain by two rounds of growth in synthetic complete medium + 25 μg/ml ethidium bromide (EtBr) followed by streaking onto YPD plates to islate colonies. The resulting candidate *rho0* strain was confirmed by respiration check: 1). failure of growth on YPGlycerol plate, 2). ability to grow on YPGlycerol plate after mating to a wild-type strain, and 3). failure of growth on YPGlycerol plate after mating to a *rho0* tester strain.

All plasmids were annotated as in Table 6.2. Construction of the plasmids should be refered to *Materials and Methods* of Chapter 2 and 3.

Fluorescence Microscopy

Methods of fluorescence microscopy were similar as described in the *Materials and Methods* of Chapter 2.

Dilution Assay

Methods of dilution assy were similar as described in the *Materials and Methods* of Chapter 2.

Table 6.1. Yeast strains used in Chapter 6

Strain	Genotype	Reference/Source
RCY239	*MAT*a *ura3-52 leu2-3,112*	This Study
RCY4866	BY4742 *mdm12Δ::KanMX4*	Research Genetics, Inc.
RCY4867	BY4742 *dnm1Δ::KanMX4*	Research Genetics, Inc.
RCY4868	BY4742 *fzo1Δ::KanMX4*	Research Genetics, Inc.
RCY4875	RCY239 *rho*^{0}	This Study

Table 6.2. Plasmids used in Chapter 6

Plasmid	Description	Reference/Source
pRC3674	pRS315 Img1-RFP	This Study
pRC4418	pRS316 Hos3(1-443)-GFP	This Study
pRC4450	pRS316 Hos3(40-697)-GFP	This Study
pRC4741	pRS316 Hos3(40-443)-GFP	This Study

DISCUSSION

How is Hos3 recruited to the bud neck?

Our results suggest that the Hos3 association with the bud neck is under the control of the morphogenesis checkpoint. During our initial screening to identify mutants defective in Hos3 bud neck localization, we discovered that Hos3 remains cytosolic in mutants that fail to grow a bud via defects in either bud site selection or Cdc42 polarization (data not shown). Therefore, budding is the pre-requisite for Hos3 to be targeted to the bud neck. After budding, the septin ring is required for Hos3 neck localization consistent with the role of septins as the scaffold for the recruitment of many bud-neck-associated proteins. Addition of nocodazole or latrunculin-B had no effect on Hos3 bud neck pattern. This could be explained by the discovery that the downstream outputs of Cdc42, a key GTPase for the budding machinery, are largely independent of either microtubules or actin filaments (Lew, 2012).

As previously described, we discovered a morphogenesis-checkpoint-based mechanism in targeting Hos3 to the bud neck: 1). septins function as the scaffold to recruit many bud neck proteins such as Elm1 and Gin4; 2). Elm1 and Gin4 are essential to target and activate Hsl1 at the daughter side of the bud neck; 3). Hsl1 interacts with Hsl7; 4). Hsl7 finally recruits Hos3 to the neck. In summary, Hsl1 establishes Hos3 asymmetry whereas Hsl7 recruits Hos3 to the bud neck. It is a sequential process of hierarchal assembly of proteins at the bud neck.

Why the morphogenesis checkpoint?

Although the morphogenesis checkpoint regulates Hos3 neck targeting, Hos3 is not a component of this checkpoint that regulates mitotic CDK activity. This raises the question of why the cell utilizes the morphogenesis checkpoint to recruit Hos3 to the bud neck? One suggestion may be that such targeting machinery allows Hos3 to establish its SPOC response capability only at the appropriate phase of the cell cycle. Anaphase spindle elongation and orientation are monitored before mitotic exit but after mitotic entry. Therefore, the SPOC functions between these two critical cell cycle landmarks. Since the morphogenesis checkpoint regulates mitotic entry, a neck-localized-Hsl7-dependent targeting of Hos3 guarantees Hos3 neck association only after the cell successfully enters the mitosis. Thus after being targeted to the neck by Hsl1, Hsl7 likely plays two parallel functions: (i) to direct Swe1 for degradation, and (ii) to recruit Hos3 to the bud neck so that Hos3 is ready to function in the SPOC. In this manner, the involvement of the morphogenesis checkpoint allows Hos3 neck targeting only after appropriate mitotic entry, and from this moment on until mitotic exit, neck-localized Hos3 monitors spindle orientation as a component of the SPOC.

A second rationale for cells to make use of the morphogenesis checkpoint to recruit Hos3 to the bud neck would be that such targeting machinery directs Hos3 to a spatially appropriate cellular site for monitoring spindle orientation. Given that the Hsl1-Hsl7 module is asymmetrically neck-associated, the asymmetry of Hsl7 explains the asymmetry of Hos3. The

daughter side of the bud neck, where Hos3 is targeted, serves as a critical landmark for spindle alignment. A mother-bud axis exists upon polarity establishment until cytokinesis. As the cells go through anaphase, the spindle elongates and the cytoplasmic microtubules pull the daughter SPB towards the daughter cell. Once this machinery moves the daughter SPB through the bud neck and into the nascent daughter cell, a correct spindle orientation is achieved. On the contrary, if the daughter SPB is mistakenly moved towards the cortex of the mother cell due to defects in the microtubule-dependent dynein pathway, the daughter SPB does not pass through the bud neck and remains within the mother cell, resulting in a spindle orientation defect. Hos3 makes use of the morphogenesis checkpoint in order to be targeted to a convenient site for monitoring spindle orientation.

Hos3 as crosstalk between the morphogenesis checkpoint and the SPOC?

Our data establish that Hos3 displays localization that is highly distinctive among known HDACs and tightly regulated in coordination with the cell cycle. The appropriate temporal regulation of the cell cycle guarantees correct division and inheritance between dividing cells.

After DNA replication and cellular growth, when to enter and then when to exit mitosis are key decisions for cells. The morphogenesis checkpoint regulates mitotic entry by modulating mitotic CDK activity. A variety of different

physiological signals impact the operation of the morphogenesis checkpoint. In the presence of conditions that delayed bud formation, cells are delayed for a longer G_2 of the cell cycle through action of the morphogenesis checkpoint to allow mitotic entry only after cells re-adapt and grow a bud. The action of the morphogenesis checkpoint ensures that nuclear division only happens after budding.

On another perspective, after budding and nuclear replication, the two nuclei need to be segregated in parallel to the mother-bud axis into the mother and daughter cells respectively. This process of spindle positioning is significantly dependent on the microtubule-dynein pathway and is monitored by the SPOC. Upon correct spindle elongation and positioning, the MEN activates mitotic exit. The SPOC monitors this status by inhibiting MEN in case of spindle misorientation, ensuring that cells only exit mitosis after the spindle is correctly elongated and aligned.

Given its unique localization features in response to the action of the morphogenesis checkpoint and the SPOC, one hypothesis would be that Hos3 could directly facilitate crosstalk between these two checkpoints. There is a precedent for such crosstalk. Elm1, the morphogenesis checkpoint member localized to the bud neck, facilitates the activation of the SPOC kinase Kin4. In order to function correctly in the SPOC, Kin4 needs to be phosphorylated by Elm1 (Caydasi et al., 2010; Moore et al., 2010). It suggests that the SPOC would be readily activated only by an intact and active morphogenesis checkpoint. This provides a counterpart to the example of Hos3. Both Elm1

and Hos3 are recruited to the bud neck under the control of the morphogenesis checkpoint. Elm is itself a morphogenesis checkpoint member but not a SPOC member; Hos3 is a SPOC component but not a member of the morphogenesis checkpoint. However, both Elm1 and Hos3 are somehow involved in both checkpoints. Therefore, the two checkpoints are coordinated to facilitate an overall progression of consecutive events during the cell cycle.

Hos3 functions as a SPOC component

A key feature shared among SPOC components is that they display cell-cycle-dependent and asymmetrical association with the SPB in unperturbed anaphase cells, but are recruited simultaneously onto both SPBs in response to spindle misalignment. For example, the Bub2-Bfa1 complex, like Hos3, is only seen on the daughter SPB, while Kin4 transiently localizes to the mother SPB (Pereira et al., 2000; Pereira and Schiebel, 2005; this study). The fact that Hos3 shares these key SPOC targeting features prompted us to ask if Hos3 is also a member of the SPOC. Two additional experiments suggest that Hos3 does indeed function as a SPOC component. First, *dyn1*Δ *hos3*Δ cells display a shift to the "bypassed" spindle morphology compared to *hos3*Δ cells. This is likely a result of *dyn1*Δ *hos3*Δ cells with misaligned spindle defective in mitotic arrest in a manner similar to the deletion of known SPOC components in *dyn1*Δ *bub2*Δ, *dyn1*Δ *bfa1*Δ, and *dyn1*Δ *kin4*Δ cells. Second, overexpression is able to constitutively associate Hos3 with the SPBs in wild-

type cells. Accordingly, overexpression of Hos3 significantly reduces cellular fitness presumably via an inappropriate delay of mitotic exit in the population of anaphase cells of which both SPBs are symmetrically loaded with Hos3. Similar effect is also observed when the known SPOC components are constitutively overexpressed. Therefore, we conclude that Hos3 is a novel component of the SPOC.

Regulation of the SPOC components through their targeting onto the SPBs

Electron micrographs show that both Bub2 and Bfa1 are deposited onto the cytoplasmic side of the SPB (Daum et al., 2000), and it is reasonable to assume that the same applies to Hos3. We favor a model in which an unknown outer-plaque SPB component physically recruits Hos3 to the SPB and this “unknown recruiter”, as a *de novo* SPB component, is constitutively associated with both SPBs. This raises the puzzling question of how Hos3 is selectively loaded onto the daughter SPB only when the daughter SPB enters the daughter cell. Given the spatial compartmentation of the mother and daughter cells, one could envision two competing models. Either there is an inhibitory zone exclusively within the mother cell to inhibit the interaction between Hos3 and the SPB, thus preventing Hos3 loading when the SPBs are still within the mother cell but allowing Hos3 loading when the daughter SPB escapes the inihibition zone, or alternatively, there is an activation zone

exclusively within the daughter cell that activates the interaction between Hos3 and its “unknown recruiter” so that Hos3 is loaded only when the daughter SPB enters the activation zone. It remains to be elucidated if one of these models is correct and if so the underlying molecular mechanism.

Since the cytosol is connected between the mother and emerging daughter cells, one possible mechanism to establish such compartment-specific zone is via proteins localized asymmetrically to the mother or daughter cell cortex. Interestingly, the SPOC component Kin4 localizes to the mother cell cortex throughout the cell cycle and was proposed to establish a mother-cell-restricted inhibitory zone for the MEN (Chan and Amon, 2009). In the presence of spindle misorientation, in addition to the SPOC response by SPB-associated Kin4, the inhibitory zone by the mother-cell-cortex-associated Kin4 further prevents MEN activation by excluding Tem1 from binding to both SPBs within the mother cell. As a comparison, in anaphase cells with normal spindles, Tem1 is loaded onto the daughter SPB to be readily activated as the daughter cell is devoid of the Kin4-based inhibitory zone (Chan and Amon, 2009). While Kin4 is not involved in establishing Hos3 SPB asymmetry, the proposed zone model for selectively targeting Hos3 onto the SPBs might also apply to Bub2 and Bfa1, which display similar SPB-association features as Hos3.

A key question for future studies is uncovering the identity of the “unknown recruiter” that physically interats with and recruits Hos3 to the SPBs. A large-scale screening of endogenous protein-protein interactions identified

an association between Hos3 and a SPB component Cdc31 (Krogan et al., 2006). Therefore, Cdc31 is a potential candidate as the “unknown recruiter” for Hos3 but it remains to be shown if this interaction is aunthentic and direct.

An expansive view of HDACs

Finally, does our discovery for the novel function of Hos3 indicate a broader view of HDACs? We showed that the HDAC activity is not required for Hos3 localization but is essential for its SPOC function. HDAC-dead Hos3$^{H196E, D231N}$ failed to efficiently arrest anaphase cells with misaligned spindle, nor could it inhibit the cellular fitness when overexpressed in wild-type cells. These results lead to a novel role of reversible lysine acetylation in the regulation of mitosis.

Could HDACs play similar roles in other organisms? While certain members of the morphogenesis checkpoint and the SPOC have clear homologues in other organisms (eg. Hsl7 as the homologue of human PRMT5; Bub2/Bfa1 as the homologue of fission yeast Cdc16/Byr4) (Lee et al., 2000; Li, 1999), how asymmetrical cell division is regulated and monitored in higher eukaryotes is still largely an open question. Both budding yeast and mammals use a microtubule-based system as the driving force to separate the SPBs/centrosomes (Pereira and Yamashita, 2011). Even more interestingly, the two SPBs in budding yeast and the two centrosomes in multicellular organisms display similar features of specified asymmetry. In budding yeast,

the mother cell retains the newly duplicated SPB while the daughter cell inherits the old SPB (Hotz et al., 2012; Pereira et al., 2001). In *Drosophila* male germline stem cells, the differentiating cell retains the daughter centrosome while the mother centrosome is inherited by the cell that retains stem cell identity (Yamashita et al., 2007).

Given the highly conserved regulation of spindle orientation, if the spindle is not correctly aligned with respect to the polarity determining factors and mitosis still persists, the outcome in budding yeast would be binucleate mother cells and anucleate daughter cells. Similarly, the outcome in mammalian cells results in aneuploidy, which drastically induces genomic instability and is a hallmark of systematic diseases such as cancer (Pellman, 2007; Rajagopalan and Lengauer, 2004; Sen, 2000; Sheltzer et al., 2011). These considerations suggest the existence of a mechanism functionally equivalent to the SPOC in budding yeast to act as a surveillance checkpoint to monitor spindle orientation in multicellular organisms. Indeed, a similar checkpoint named the centrosome orientation checkpoint (COC) has been found in *Drosophila* which activates a mitotic delay if the centrosomes are not properly oriented (Cheng et al., 2008). The interesting difference between the SPOC and the COC is that in budding yeast, the cell cycle is arrested by the SPOC prior to mitotic exit, but in contrast, in *Drosophila*, the cell cycle is arrested by the COC before commitment to mitosis, which is the stage of the cell cycle monitored by the morphogenesis checkpoint in budding yeast. It is intriguing to imagine if higher organisms have adopted and even evolutionarily

developed a checkpoint that incorporates both the morphogenesis checkpoint and the SPOC to monitor spindle orientation and assure asymmetric cell division. It is even more intriguing to speculate if such checkpoints in higher organisms could make use of any HDACs in the similar manner as our discoveries of Hos3 do in the morphogenesis checkpoint and the SPOC in budding yeast cells.

Truncated forms of Hos3 are likely imported into the mitochondria

With regard to our observation in Chapter 2 that certain truncated forms of Hos3 are targeted to the mitochondria, we aimed to test how this could happen. Interestingly, in wild-type *rho*^{0} strain that lacks mitochondria DNA and fails to respire, Hos3(*C*Δ) and Hos3(*N*Δ) completely lose their mitochondria localization while targeting of Hos3(*N*Δ+*C*Δ) to the mitochondria is severely reduced (Figure 6.1). Deficiency in respiration results in a reduction of the electrochemical potential across the mitochondria inner membrane, which is the driving force for mitochondrial import (Rehling et al., 2004). The “import” model predicts that localization of truncated Hos3 to the mitochondria is indirectly dependent on respiration. We tested this by using *dnm1*Δ, *fzo1*Δ, and *mdm12*Δ mutants that display sharply different mitochondrial morphology (“inter-connected nets”, “fragmented punctae”, and “large spheres”) respectively compared to wild-type cells (“tubules”) (Otsuga et al., 1998;

Figure 6.1

A

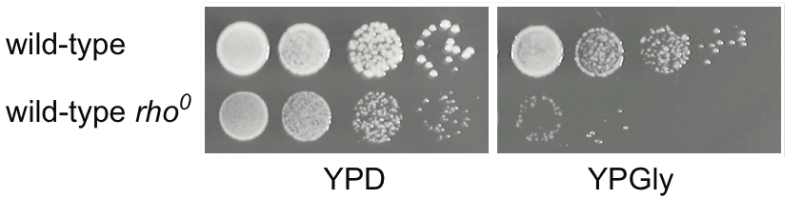
wild-type
wild-type rho0
YPD
YPGly

B

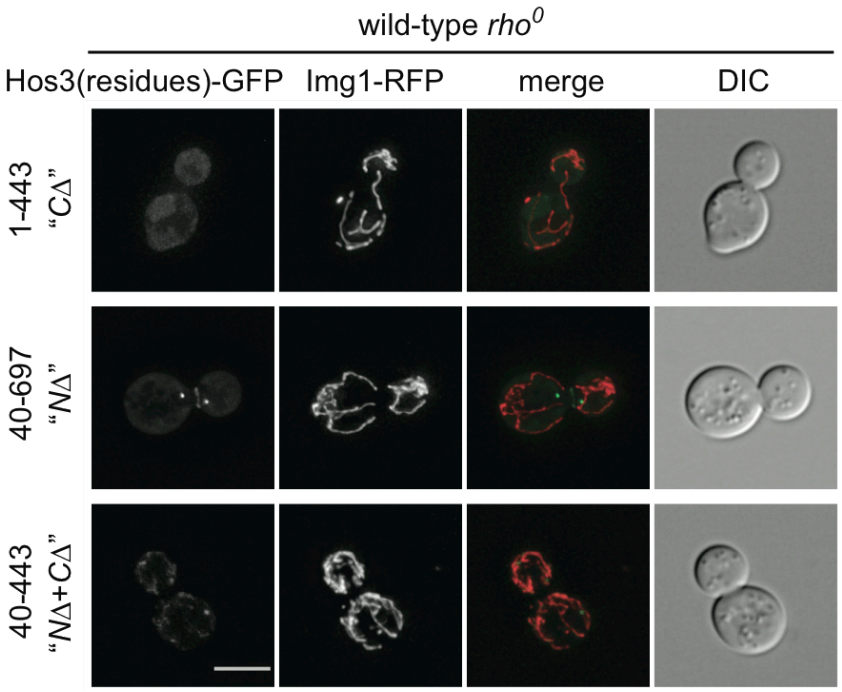
wild-type rho0
Hos3(residues)-GFP
Img1-RFP
merge
DIC
1-443 "CΔ"
40-697 "NΔ"
40-443 "NΔ+CΔ"

Figure 6.1. Truncated Hos3 is likely imported into the mitochondria

(A) Respiration capability of wild-type and wild-type *rho*^{0} cells. Cells were grown to mid-log phase in YPD medium and assayed by 10-serial dilution onto YPD and YPGly plates for incubation at 30°C. Gly: glycerol.

(B) Truncated forms (*C*Δ, *N*Δ, and *N*Δ+*C*Δ) of Hos3-GFP (*CEN*) were imaged in wild-type *rho*^{0} cells coexpressing the mitochondria marker Img1-RFP (*CEN*). Scale bar, 5 μm.

Rapaport et al., 1998; Berger et al., 1997; Okamoto and Shaw, 2005). Indeed, Hos3(*C*Δ) and Hos3(*N*Δ) are targeted to the mitochondria in the respiration-capable *dnm1*Δ cells, but not in the respiration-deficient *fzo1*Δ or *mdm12*Δ cells (Figure 6.2). The data suggest that the HDAC domain of Hos3 may contain a mitochondrial import signal that is normally buried in the full-length form but exposed in the truncated forms to guide their import into the mitochondria. While we currently do not understand the function of these mitochondria-targeted truncated forms of Hos3, it is intriguing if Hos3 could be cleaved *in vivo* and imported into the mitochondria under certain stresses or conditions to deacetylate the pool of substrates there. This remains an open and interesting question to be addressed in the future.

Interestingly, there does seem to be a potential role of Hos3 to function in the mitochondria. While there are mitochondria-localized HDACs in higher organisms such as class II HDAC7 and class III SIRT3, SIRT4 and SIRT5 in humans, no HDAC in budding yeast is specifically targeted to the mitochondria except truncated Hos3 (Bakin and Jung, 2004; Onyango et al., 2002; Michishita et al., 2005; Figure 2.1 and 2.10). Upon oxidative stress, Hos3 was reported to mediate the deacetylation of H2BK11 to induce yeast apoptosis (Ahn et al., 2006). Moreover, a number of mitochondria genes (*AIM43*, *ETR1*, and *ISU1*) genetically interact with *HOS3* (Lin et al., 2008). Consequently, all of these results point to Hos3 as an HDAC for a possible role in the mitochondria.

Figure 6.2

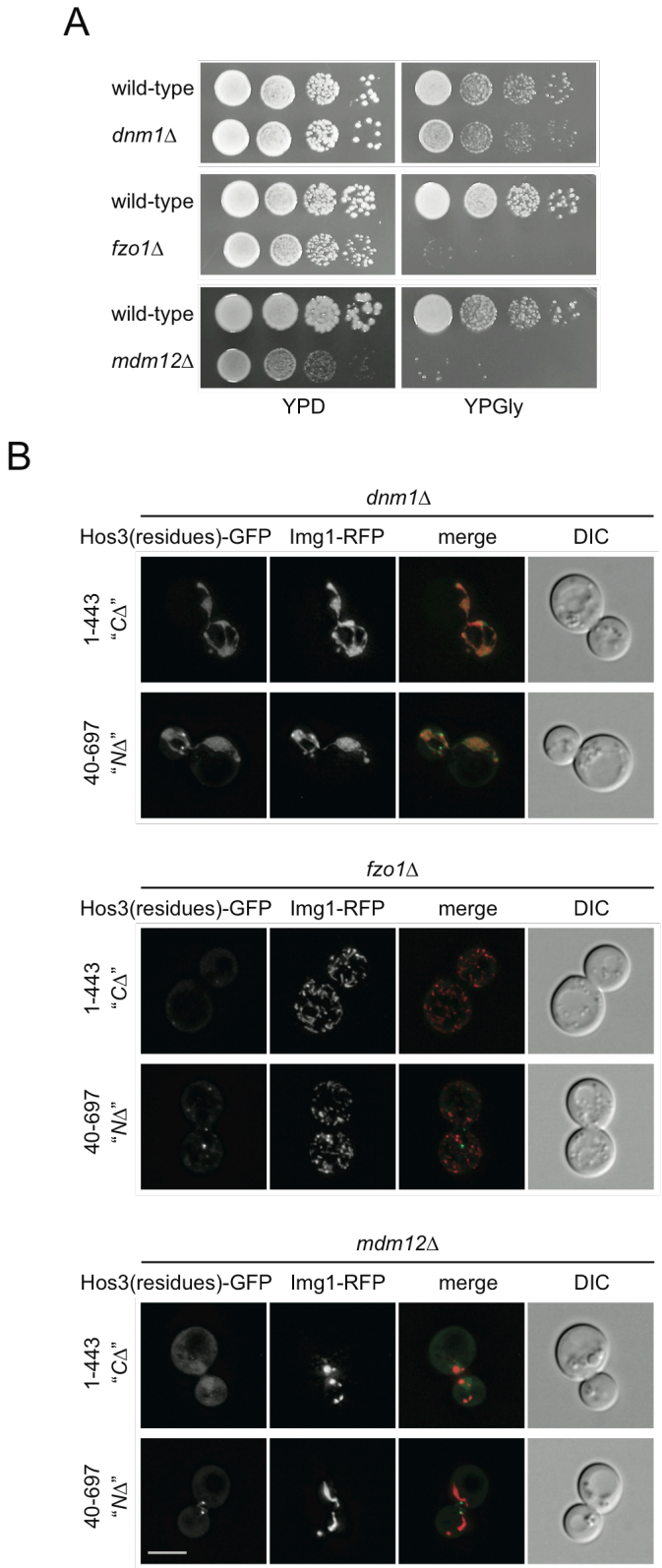
A
wild-type
dnm1Δ
wild-type
fzo1Δ
wild-type
mdm12Δ
YPD
YPGly
B
dnm1Δ
Hos3(residues)-GFP
Img1-RFP
merge
DIC
1-443 "CΔ"
40-697 "NΔ"
fzo1Δ
Hos3(residues)-GFP
Img1-RFP
merge
DIC
1-443 "CΔ"
40-697 "NΔ"
mdm12Δ
Hos3(residues)-GFP
Img1-RFP
merge
DIC
1-443 "CΔ"
40-697 "NΔ"

Figure 6.2. Localization of truncated Hos3 in mitochondria mutants

(A) Respiration capability of *dnm1*Δ, *fzo1*Δ, and *mdm12*Δ cells. Cells were grown to mid-log phase in YPD medium and assayed by 10-serial dilution onto YPD and YPGly plates for incubation at 30°C. Gly: glycerol.

(B) Truncated forms (*C*Δ, *N*Δ, and *N*Δ+*C*Δ) of Hos3-GFP (*CEN*) were imaged in *dnm1*Δ, *fzo1*Δ, and *mdm12*Δ cells coexpressing the mitochondria marker Img1-RFP (*CEN*). Scale bar, 5 μm.

REFERENCES

Ahn, S., Diaz, R. L., Grunstein, M., & Allis, C. D. (2006). Histone H2B deacetylation at lysine 11 is required for yeast apoptosis induced by phosphorylation of H2B at serine 10. *Molecular Cell, 24*(2), 211-220.

Bakin, R. E., & Jung, M. O. (2004). Cytoplasmic sequestration of HDAC7 from mitochondrial and nuclear compartments upon initiation of apoptosis. *Journal of Biological Chemistry, 279*(49), 51218-51225.

Berger, K. H., Sogo, L. F., & Yaffe, M. P. (1997). Mdm12p, a component required for mitochondrial inheritance that is conserved between budding and fission yeast. *The Journal of Cell Biology, 136*(3), 545-553.

Caydasi, A. K., Kurtulmus, B., Orrico, M. I. L., Hofmann, A., Ibrahim, B., & Pereira, G. (2010). Elm1 kinase activates the spindle position checkpoint kinase Kin4. *The Journal of Cell Biology, 190*(6), 975-989.

Chan, L. Y., & Amon, A. (2010). Spindle position is coordinated with cell-cycle progression through establishment of mitotic exit-activating and -inhibitory zones. *Molecular Cell, 39*(3), 444-454.

Cheng, J., Turkel, N., Hemati, N., Fuller, M. T., Hunt, A. J., & Yamashita, Y. M. (2008). Centrosome misorientation reduces stem cell division during ageing. *Nature, 456*(7222), 599-604.

Daum, J. R., Gomez-Ospina, N., Winey, M., & Burke, D. J. (2000). The spindle checkpoint of saccharomyces cerevisiae responds to separable microtubule-dependent events. *Current Biology, 10*(21), 1375-1378.

Hotz, M., Leisner, C., Chen, D., Manatschal, C., Wegleiter, T., Ouellet, J. et al. (2012). Spindle pole bodies exploit the mitotic exit network in metaphase to drive their age-dependent segregation. *Cell, 148*(5) 958-972.

Krogan, N.,J., Cagney, ,Gerard, Yu, ,Haiyuan, Zhong, ,Gouqing, Guo, ,Xinghua, Ignatchenko, ,Alexandr, et al. (2006). Global landscape of protein complexes in the yeast saccharomyces cerevisiae. *Nature, 440*(7084), 637-43.

Lee, J., Cook, J. R., Pollack, B. P., Kinzy, T. G., Norris, D., & Pestka, S. (2000). Hsl7p, the yeast homologue of human JBP1, is a protein methyltransferase. *Biochemical and Biophysical Research Communications, 274*(1), 105-111.

Li, R. (1999). Bifurcation of the mitotic checkpoint pathway in budding yeast. *Proceedings of the National Academy of Sciences, 96*(9), 4989-4994.

Lin, Y., Qi, Y., Lu, J., Pan, X., Yuan, D. S., Zhao, Y., et al. (2008). A comprehensive synthetic genetic interaction network governing yeast histone acetylation and deacetylation. *Genes & Development, 22*(15), 2062-2074.

Michishita, E., Park, J. Y., Burneskis, J. M., Barrett, J. C., & Horikawa, I. (2005). Evolutionarily conserved and nonconserved cellular localizations and functions of human SIRT proteins. *Molecular Biology of the Cell, 16*(10), 4623-4635.

Moore, J. K., Chudalayandi, P., Heil-Chapdelaine, R. A., & Cooper, J. A. (2010). The spindle position checkpoint is coordinated by the Elm1 kinase. *The Journal of Cell Biology, 191*(3), 493-503.

Okamoto, K., & Shaw, J. M. (2005). Mitochondrial morphology and dynamics in yeast and multicellular eukaryotes. *Annual Review of Genetics, 39*(1), 503-536.

Onyango, P., Celic, I., McCaffery, J. M., Boeke, J. D., & Feinberg, A. P. (2002). SIRT3, a human SIR2 homologue, is an NAD- dependent deacetylase localized to mitochondria. *Proceedings of the National Academy of Sciences, 99*(21), 13653-13658.

Otsuga, D., Keegan, B. R., Brisch, E., Thatcher, J. W., Hermann, G. J., Bleazard, W., et al. (1998). The dynamin-related GTPase, Dnm1p, controls mitochondrial morphology in yeast. *The Journal of Cell Biology, 143*(2), 333-349.

Pellman, D. (2007). Cell biology: Aneuploidy and cancer. *Nature, 446*(7131), 38-39.

Pereira, G., Höfken, T., Grindlay, J., Manson, C., & Schiebel, E. (2000). The Bub2p spindle checkpoint links nuclear migration with mitotic exit. *Molecular Cell, 6*(1), 1-10.

Pereira, G., & Schiebel, E. (2001). The role of the yeast spindle pole body and the mammalian centrosome in regulating late mitotic events. *Current Opinion in Cell Biology, 13*(6), 762-769.

Pereira, G., & Schiebel, E. (2005). Kin4 kinase delays mitotic exit in response to spindle alignment defects. *Molecular Cell, 19*(2), 209-221.

Pereira, G., & Yamashita, Y. M. (2011). Fly meets yeast: Checking the correct orientation of cell division [Abstract]. *Trends in Cell Biology, 21*(9) 526-533.

Rajagopalan, H., & Lengauer, C. (2004). Aneuploidy and cancer. *Nature, 432*(7015), 338-341.

Rapaport, D., Brunner, M., Neupert, W., & Westermann, B. (1998). Fzo1p is a mitochondrial outer membrane protein essential for the biogenesis of functional mitochondria in saccharomyces cerevisiae. *Journal of Biological Chemistry, 273*(32), 20150-20155.

Rehling, P., Brandner, K., & Pfanner, N. (2004). Mitochondrial import and the twin-pore translocase. *Nature Reviews. Molecular Cell Biology, 5*(7), 519-530.

Sen, S. (2000). Aneuploidy and cancer. *Current Opinion in Oncology, 12*(1)

Sheltzer, J. M., Blank, H. M., Pfau, S. J., Tange, Y., George, B. M., Humpton, T. J., et al. (2011). Aneuploidy drives genomic instability in yeast. *Science, 333*(6045), 1026-1030.

Yamashita, Y. M., Mahowald, A. P., Perlin, J. R., & Fuller, M. T. (2007). Asymmetric inheritance of mother versus daughter centrosome in stem cell division. *Science, 315*(5811), 518-521.